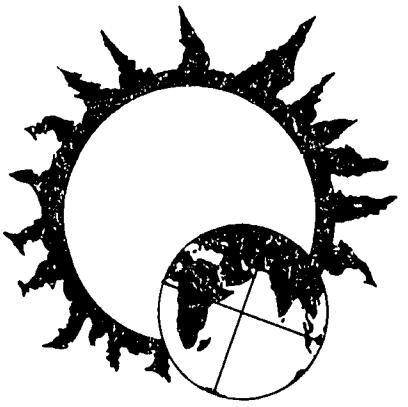

Training in Alternative Energy Technologies

A Cooperative Program of the
U.S. Agency for International Development
and the University of Florida

University of Florida

Gainesville, Florida

WIND ENERGY UTILIZATION

IN THE

DEVELOPING COUNTRIES

A report to the Office of Energy,
Bureau for Science and Technology,
US Agency for International Development
Washington, D.C.

December 1984

Martin Bush, Ph.D.
Associate in Engineering
Department of Mechanical Engineering
University of Florida
Gainesville, Florida 32611

Preface

The Training in Alternative Energy Technologies (TAET) program at the University of Florida, ran for nearly five years--from late 1979 until June 1984. The training program was sponsored by the Office of Energy of the US Agency for International Development (USAID). The purpose of the TAET program was to train technical personnel from the developing countries in the theory and application of the renewable energy technologies: solar energy, hydropower, biomass energy, wind power, and geothermal energy. A total of 286 participants from 54 developing countries attended the nine training session that were organized by the University.

The TAET curriculum was designed to meet the following specific objectives:

1. To acquaint the participants with the alternative energy technologies.

2. To provide the participants with sufficient knowledge to assess the natural renewable energy resources of the participant's country and to determine the best possible technological options to utilize these resources so that the participant can provide input in establishing realistic national alternative energy programs for the participant's country.

3. To provide technically trained people with the knowledge to select among technological options and to identify their most appropriate applications.

The training program consisted of lectures, seminars, demonstrations, laboratory work, and field trips--activities designed to explain the theory, illustrate the practice, demonstrate the operation and maintenance of the alternative energy systems, and to provide detailed training for the program participants.

As part of that effort, a number of technical notebooks and laboratory manuals were written by the program faculty at the University of Florida. All of the written material and other documentation was collected, and reorganized at the end of the training program in June 1984. This manual on wind energy utilization in the developing countries makes available most of the material on wind energy conversion systems that was presented to the TAET participants during the course of the training program.

TABLE OF CONTENTS

Topic	Page
Introduction	1
Wind resources	6
Basic principles	8
The Betz coefficient	14
Wind machine characteristics	16
Wind speed frequency distributions	18
Wind duration curves	25
Energy conversion	28
Conversion efficiency	43
Rotor configurations	45
Savonius rotor	45
Multibladed horizontal axis rotors	48
Darrieus wind machines	52
Lift and drag	55
Rotor design	59
Water pumping	64
Electric power generation	72
Wind system economics	76
References	82
Bibliography	85
Appendices	
List of manufacturers	88
Performance summary sheets	92
Wind resource climatology	116
Effect of site wind characteristics on energy production	131
The performance of simple horizontal axis wind-turbines for the direct drive of water pumps	155

Introduction

Wind power technology is one of the very oldest of the renewable energy technologies. The first windmills are mentioned in the late seventh century. The earliest systems were primitive devices consisting of a vertical rotating shaft turning a millstone. Attached to the shaft were simple wings or paddles probably constructed of woven matting. The device was positioned inside a circular wall with a large opening facing the prevailing wind in such a way that the wind impinged on only one side of the windmill blades. Mills of this type, called panemones, were certainly constructed on the plains of Persia which are swept by steady winds. These early vertical-axis systems were soon joined by horizontal-axis designs with as many as ten cloth sails.

In Asia and China, in the tenth century, windmills came into use for irrigation and drainage. By the thirteenth century the technology was in evidence across Europe from Portugal to Holland and beyond. At this time the windmill in Europe was used almost exclusively for the grinding and milling of grain (hence its name). Only in Holland, at a later time, was the technology used to pump water--an application in which there remains considerable interest particularly in the developing countries.

The Dutch refined wind technology in important ways. They invented a rudimentary airfoil; they created the spoiler and the airbrake and improved the overall efficiency of the machines. By the nineteenth century thousands of metal-bladed machines were grinding grain, milling paper, and processing timber.

The first windmills in the United States were modeled on the European machines. But by the middle of the nineteenth century Daniel Halliday had begun to experiment with the design that developed into the familiar multi-bladed water-pumping machine still to be seen across the American plains. More than six million small multibladed windmills have been built and used in the United States to pump water. It is estimated that over 150,000 are still in operation. These systems were the first wind mills to be massproduced. Factories in the US and Germany exported them to South America, Africa, Australia, Japan, and to nearly all the European countries.

Although literally millions of wind machines were in operation during the early part of the twentieth century, it was the development and evolution of the aeroplane wing and propellor that stimulated the development of the modern highspeed machines. At the same time it was recognized that the high rotational speeds of the new rotors was ideal for driving an electrical generator.

The first wind-electric systems were built in the early 1920's using discarded or home-made aeroplane propellors, automobile generators, and sheet-metal fins. Wherever the old water pumpers were in use, innovators constructed these sometimes primitive systems to charge batteries that powered electric lights and the first electric appliances and radios.

During the 1930's small wind machines that generated electricity came onto the market. Between 1930 and 1960, thousands of wind-powered electric generators were sold and installed in many countries. Production faltered in the 1960's after the Rural Electrification Administration succeeded in supplying most American farms and rural homes with inexpensive electricity from a central power station and transmission system.

The first really large machine that generated electricity from the wind was the 1.25 MWe Smith-Putnam machine located on Grandpa's knob in Vermont. Operational in 1941 and supplying power to the Vermont grid system, the project was considered a success, but mechanical problems, including blade failure, eventually shut down the machine.

However, the qualified success of the Putnam machine had not gone unnoticed, and in the late 1940's and 50's a number of large machines were built in England, France, Denmark, and Germany. This research and development effort gradually petered out, however, since no wind machine could generate electrical power that was competitive with the cheap electricity of the time.

By 1970 the utilization of wind energy was minimal. As electrical distribution systems reached out across the rural areas of the U.S. and Europe, the old water pumpers fell into disrepair and the market for the small wind-electric machines diminished until only a couple of companies were still manufacturing machines for the very remote areas.

The picture has now changed dramatically. Research and development work is underway in many countries. Wind farms--clusters of small wind machines generating electrical power in synchronicity--are springing up in the Western areas of the U.S., while the old wind-electric machines are being renovated and pressed back into service. At the same time, water pumping technology has come under renewed development and the new machines are cheaper and more efficient.

Wind power is a technology that should be of considerable interest in the developing countries, many of which have excellent wind resources. Used to pump water, wind machines have an immediate role in agriculture--the principal economic activity in the rural areas of the developing countries. In the early part of this century, when many developing countries were European colonies, a good number of water-pumping wind machines were erected in the developing countries by Europeans familiar with the technology. Diesel engine pumps eventually displaced the wind machines in times when petroleum fuels were cheap, and diesel engines were considered more reliable. The situation has now come full circle: diesel fuel is expensive, particularly in the rural areas, the engines themselves are difficult and costly to maintain and keep in operation, and energy planners and technologists are once again contemplating the new water pumping wind machines and considering their role in agricultural production and rural development.

Wind energy conversion systems (WECS) come in a wide variety of shapes, sizes, and configurations. Many of the different types of wind machines are shown diagrammatically in the sketches below and on the next page [1].

HORIZONTAL-AXIS WIND MACHINES

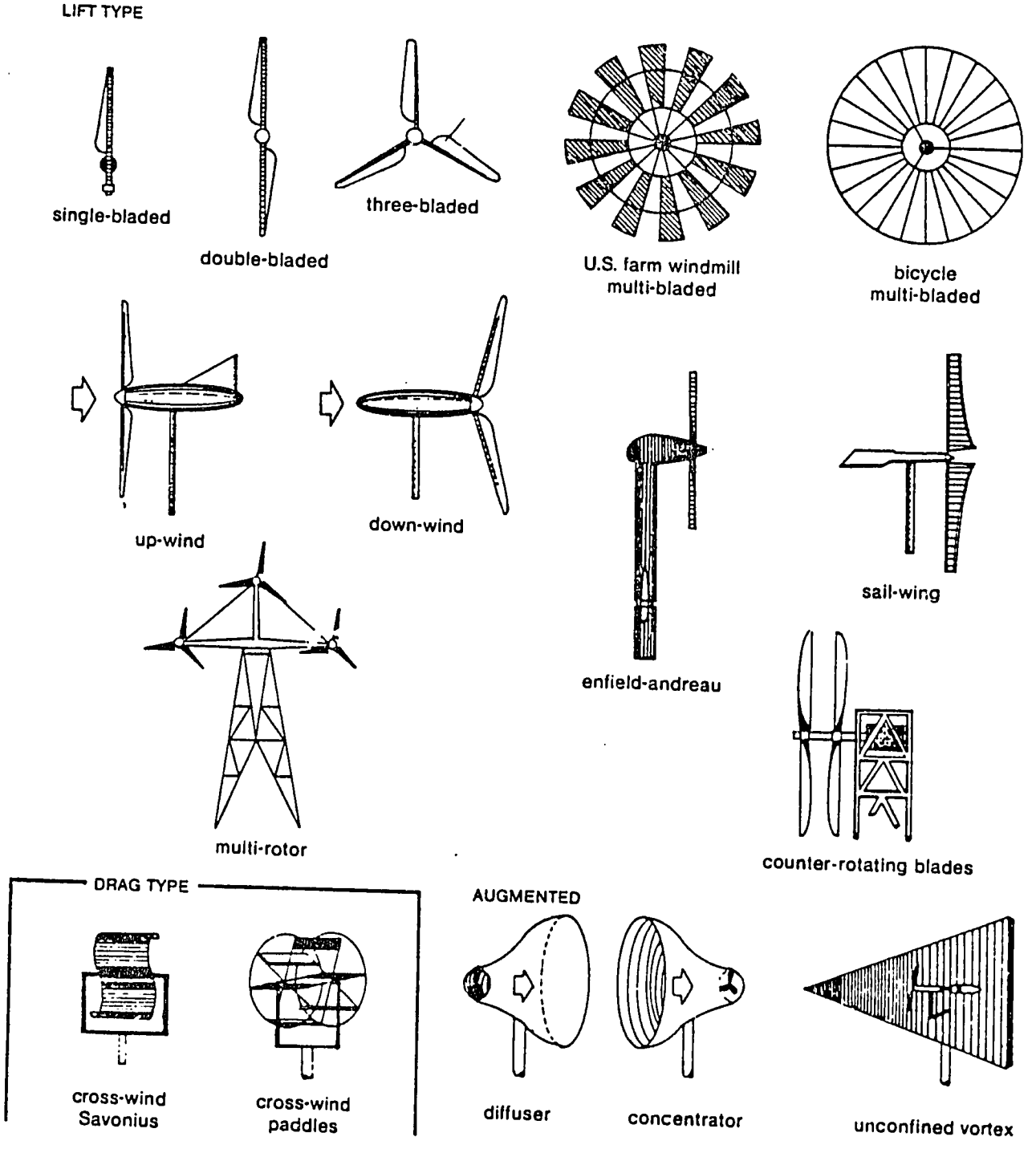

VERTICAL-AXIS WIND MACHINES

PRIMARILY DRAG TYPE

Savonius

multi-bladed Savonius

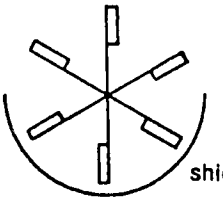

shield plates

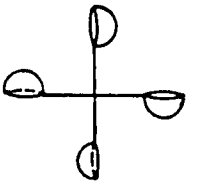

cupped

LIFT TYPE

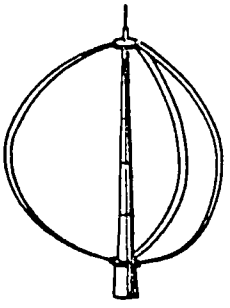

Darrieus (egg beater)

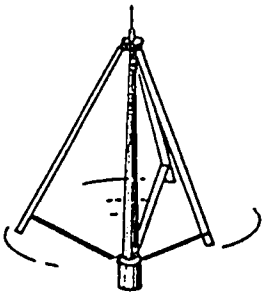

Darrieus

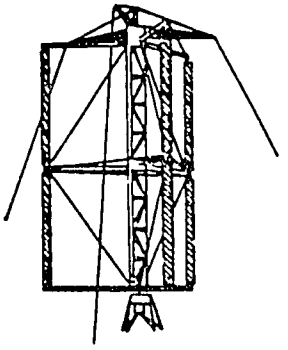

giromill

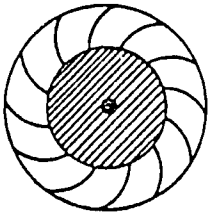

turbine

COMBINATIONS

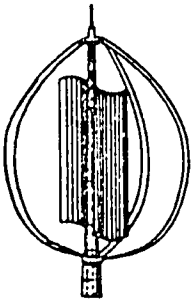

Savonius-Darrieus

Savonius

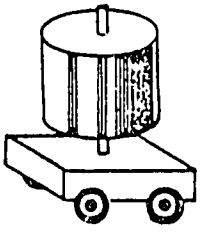

magnus

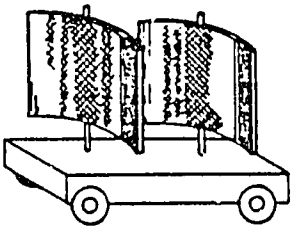

airfoil

AUGMENTED

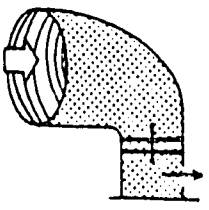

deflector

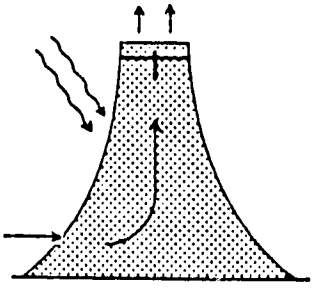

sunlight

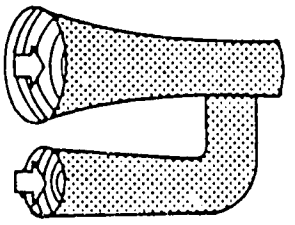

venturi

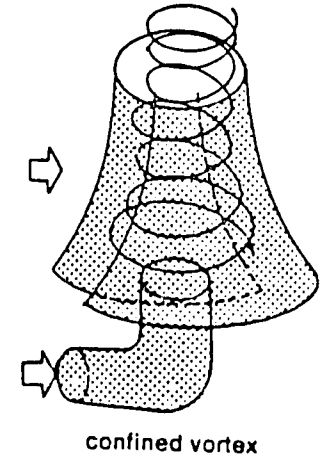

confined vortex

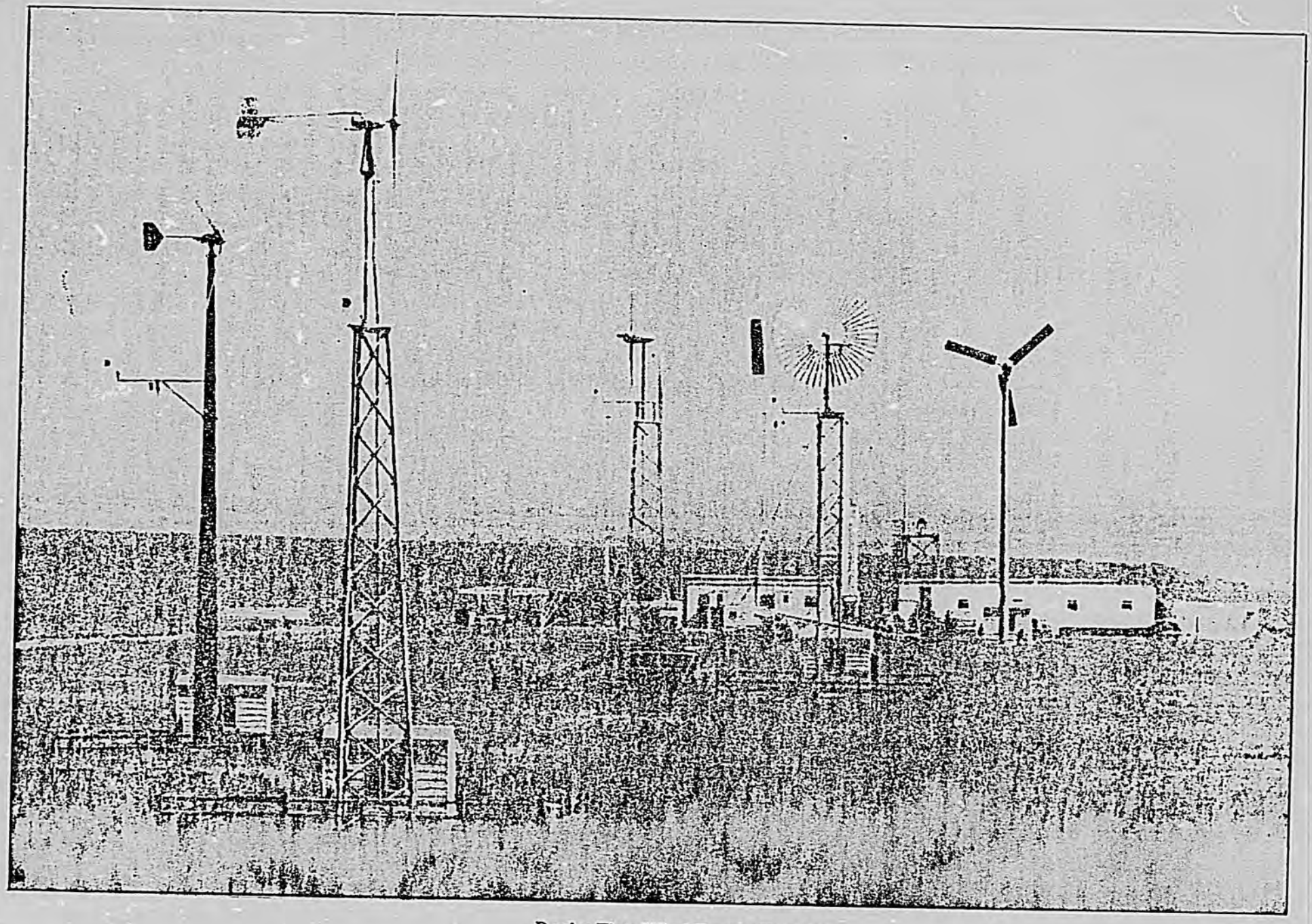

Rocky Flats Wind Energy Test Site

Wind Resources

The power in the wind is enormous: an estimated 20 million GW is theoretically available for extraction by wind turbines [8]. The problem is to determine to what extent, and in which locations, this potential source of power can be used economically. The database on mean annual windspeeds for sites in the developing countries is poor. However, some general remarks concerning wind resources can be made.

Africa: The African continent straddles the tropical and equatorial zones of the globe. Only in the extreme south does it touch the wind regime of the temperate westerlies. Nevertheless, the potential for wind energy utilization in Africa is promising. Very favorable sites can be found along the coasts of Tunisia, Algeria, Morocco, and Western Sahara. It is probable that good sites exist along the whole length of the coast running from Egypt round to Senegal, and along the western and southwestern coasts of southern Africa. Good sites are likely to be found on the Red Sea coast and along the eastern coastal edge of Somalia. All these coastal sites posses wind regimes which, particularly in the summer, are reinforced to a great extent by strong insolation. During the warmer months the wind blows with fairly steady daily regularity.

Inland regions are less favorable but possible good sites exist in a number of regions such as the upland areas running from the Sudan south into Tanzania.

Asia: The continent of Asia stretches from the equator to the polar seas. The main features of the circulation from the point of view of steady wind flow are the outflow from the Siberian anticyclone in winter and the influx of the monsoon across the equator into India and South East Asia in summer. Much of the continent falls under regimes of light and variable winds, particularly during the transition seasons.

Persistent strong winds may blow along the Pacific coast of the continent in winter. Constant north-east trade winds blow in winter around the subtropical Pacific anticyclone across the Philippine Islands and neighboring seas.

In summer there are persistent northerly winds along the Arctic coast. South-easterly winds along the North Pacific coast blow around the Pacific anticyclone which has shifted northwards following the sun. The Indian SW summer monsoon is stronger than the NE winter monsoon. For instance, the mean windspeed for Bombay during the height of the former season is 6.3 m/s compared with only half that value in the winter months.

A number of areas appear favorable for the utilization of wind energy. Good sites should exist in India, Pakistan, Bangladesh and along the western edge of the Malay peninsula. The southern Indonesian islands should also possess favorable sites.

South and Central America: The South American continent extends from the northern tropics deep into the strong westerly belt of the Southern Ocean. General westerly winds are observed in all seasons south of latitude 40° S. In all seasons east and north-east winds prevail along the coast of Brazil from 10° S up to the Equator. The north-east trade winds of the northern hemisphere are observed to the north; these are stronger and more persistent than in the latter half of the southern hemisphere summer when the doldrum belt is further south.

Along the coasts of Peru and Chile strong SW winds blow around the Pacific subtropical anticyclone. The gradient is intensified in summer by the sharp temperature contrast between the cold ocean current and the hotter inland areas.

Light and variable winds exist over much of the central part of the continent but sites offering good wind energy potential may be found in many coastal regions, particularly along the west coast.

The Caribbean islands possess many favorable sites, particularly on the eastern coasts of the islands in the Antilles chain.

Basic Principles

Wind is a fluid in motion; its energy is kinetic. The power in the wind, P_W, is therefore given by

$$P_W = 1/2\ \dot{m}\ V^2 \quad \text{Watts} \qquad (1)$$

where $\dot{m}$ = air mass flow rate, kg/s
V = air speed, m/s

This expression is usually rewritten as

$$P_W = 1/2\ \rho\ AV^3 \quad \text{Watts} \qquad (2)$$

Where ρ = air density, kg/m^3
A = flow area, m^2

The density of air varies with both temperature and pressure. At 20°C and atmospheric pressure the density of air is 1.2 kg/m^3. Since the air pressure decreases with increasing altitude the temperature corrected density should also be corrected for altitude. The density of dry air at atmospheric pressure is tabulated below.

Density of Dry Air at Atmospheric Pressure

Temperature °C	Density kg/m^3	Temperature °C	Density Kg/m^3
0	1.29	20	1.20
5	1.27	25	1.18
10	1.25	30	1.16
15	1.23	35	1.15

The correction factor for variation in altitude, C_A, is shown below. This factor should be multiplied by the density at atmospheric pressure to determine the correct air density.

Altitude Correction Factor, C_A

Altitude, ft	C_A	Altitude, ft	C_A
0	1	5000	0.832
1000	0.964	6000	0.801
2000	0.930	7000	0.772
2500	0.912	8000	0.743
3000	0.895	9000	0.715
4000	0.864	10000	0.688

It is important to note from Equation 2, that the power available in the wind varies as the cube of the wind speed. If the wind speed doubles the available power increases by a factor of eight. Small differences in average wind speed between potential wind sites can therefore make a great deal of difference in terms of power generation.

A rotor can extract power from the wind. At standstill the rotor clearly produces no power, and at very high rotational speeds the airflow is effectively blocked by the rotor and power output is minimal. In between these extremes there is a rotational speed where the power extracted from the wind is maximized. This relationship is shown in the figure below.

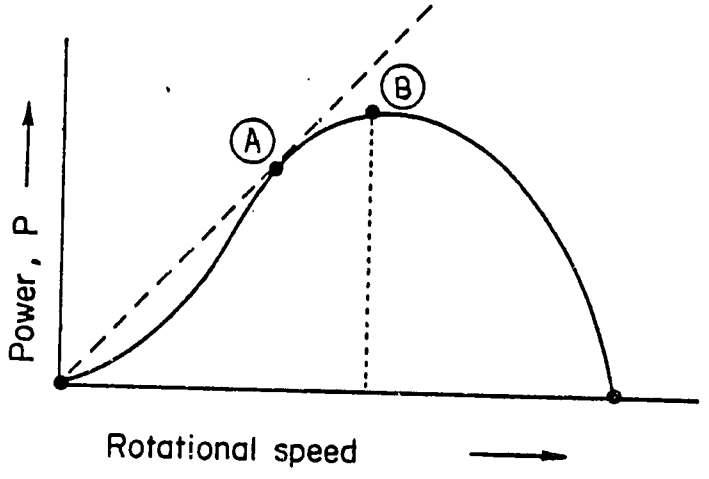

Fig. 1 The power produced by a wind rotor as a function of its rotational speed, at one given wind speed.

It is also important to consider the torque characteristics of a wind rotor. The power, P, is related to the torque, Q, and rotational speed, w, by the simple formula;

$$P = Q\,w \qquad \text{Watts} \qquad (3)$$

It follows that the torque, Q, is equal to the slope of the line from the origin to some point on the power curve. Where such a line is tangential to the curve marks the point where the rotor will produce maximum torque. This point is labelled A in Figure 1. Note that the rotational speed that generates maximum torque is always less than the speed for which the power extracted is a maximum, (B).

The simple relationship between power, torque, and speed enables one to construct the torque-speed curve shown below.

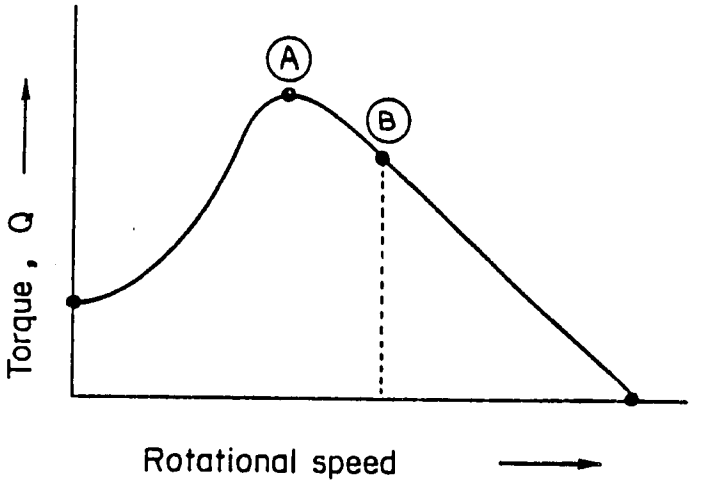

Fig. 2 The torque produced by a wind rotor as a function of its rotational speed at one given wind speed.

If the wind speed increases then both power and torque increase as shown in Figure 3.

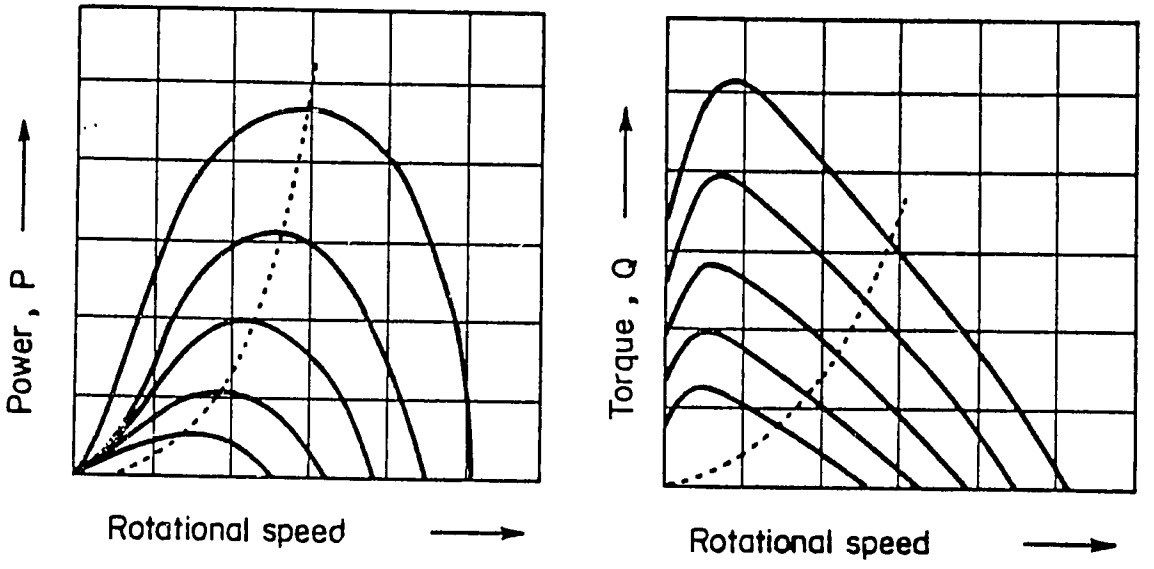

Fig. 3 The power and torque of a wind rotor as a function of rotational speed for different wind speeds.

These sets of curves are not very convenient to work with. It is possible, though, to work with a dimensionless set of parameters: the power coefficient, C_p; the torque coefficient, C_Q; and the tip speed ratio, λ.

These are defined as

$$C_p = P/\tfrac{1}{2}\rho AV^3 \tag{4}$$

$$C_Q = Q/\tfrac{1}{2}\rho AV^2R \tag{5}$$

$$\lambda = wR/V \tag{6}$$

In these expression V is the velocity of the upstream undisturbed air flow, and R is the radius of the swept area. Substituting these expressions in Equation 3 gives the simple relationship

$$C_p = C_Q\,\lambda \tag{7}$$

The advantage of these dimensionless coefficients is that they permit performance data for different kinds of wind systems operating under different conditions to be reduced to a common basis. For example, Figure 4 shows power-speed and torque-speed curves in dimensionless form, for a typical multibladed and two-bladed wind rotor. Immediately apparent are two essential differences between these kinds of rotors. Multibladed rotors develop maximum power at lower rotational speeds, and the torque generated, particularly the starting torque, is high. In contrast, the twin-bladed rotors are efficient at much higher rotational speeds, the torque produced by the rotor is low, and starting torque is very low indeed. For these reasons, multibladed rotors are generally used for pumping water, while the high speed machines with only two or three blades are more often used for generating electricity. Figure 5 shows power coefficient curves as a function of tip speed ratio for several classes of rotors. Note that, in addition to the distinctions mentioned above, high speed rotors are generally more efficient than the low speed multibladed turbines. However, this efficiency is accomplished at some cost: high speed rotors require sophisticated airfoils and more advanced technology. These machines are generally more expensive than the low-speed wind systems.

There is a limit to the amount of energy that can be extracted from the wind by a turbine. It can be shown that the power coefficient of a wind machine cannot exceed 59.3 percent. This figure is called the Betz Coefficient. The performance curve for the ideal wind turbine, shown in Figure 5 is asymptotic to this limit. The derivation of this coefficient is presented in the next section of the text.

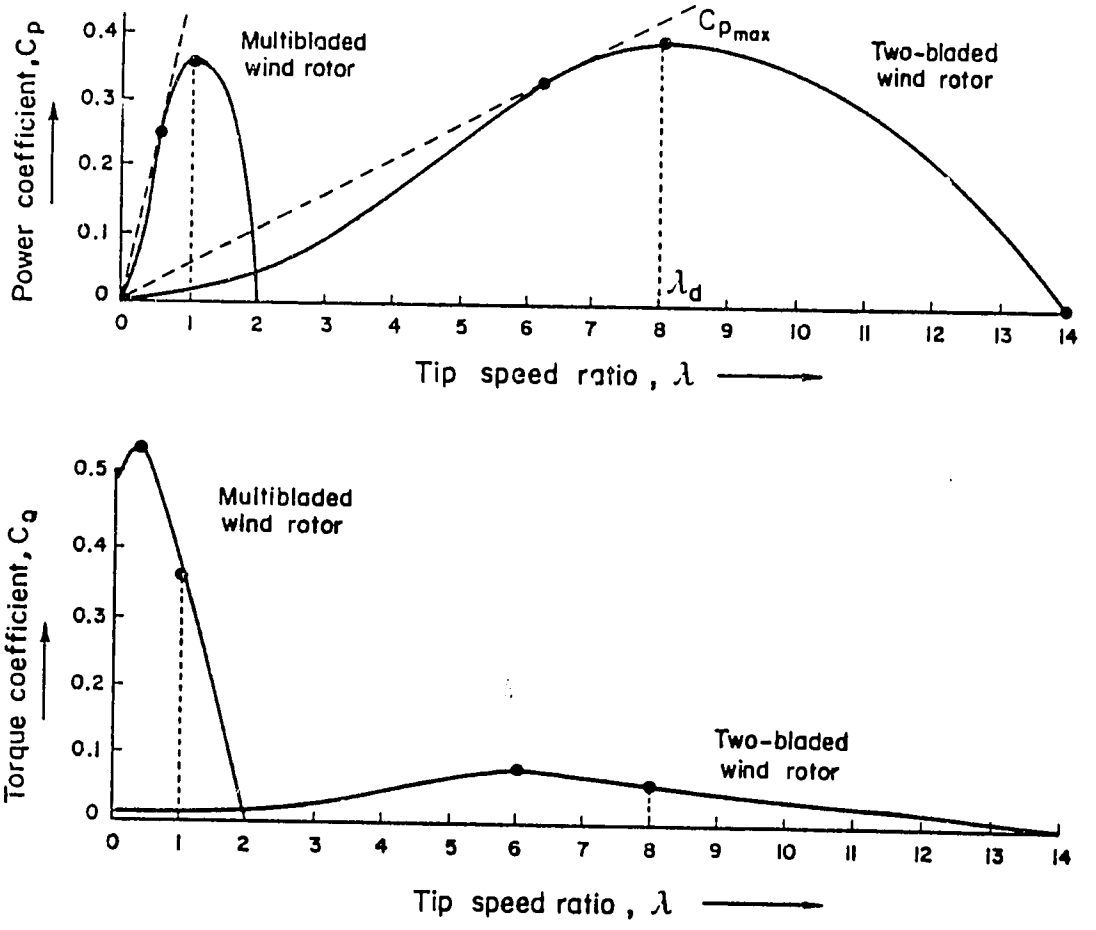

Fig. 4 Dimensionless power and torque curves of two wind rotors as a function of tip speed ratio.

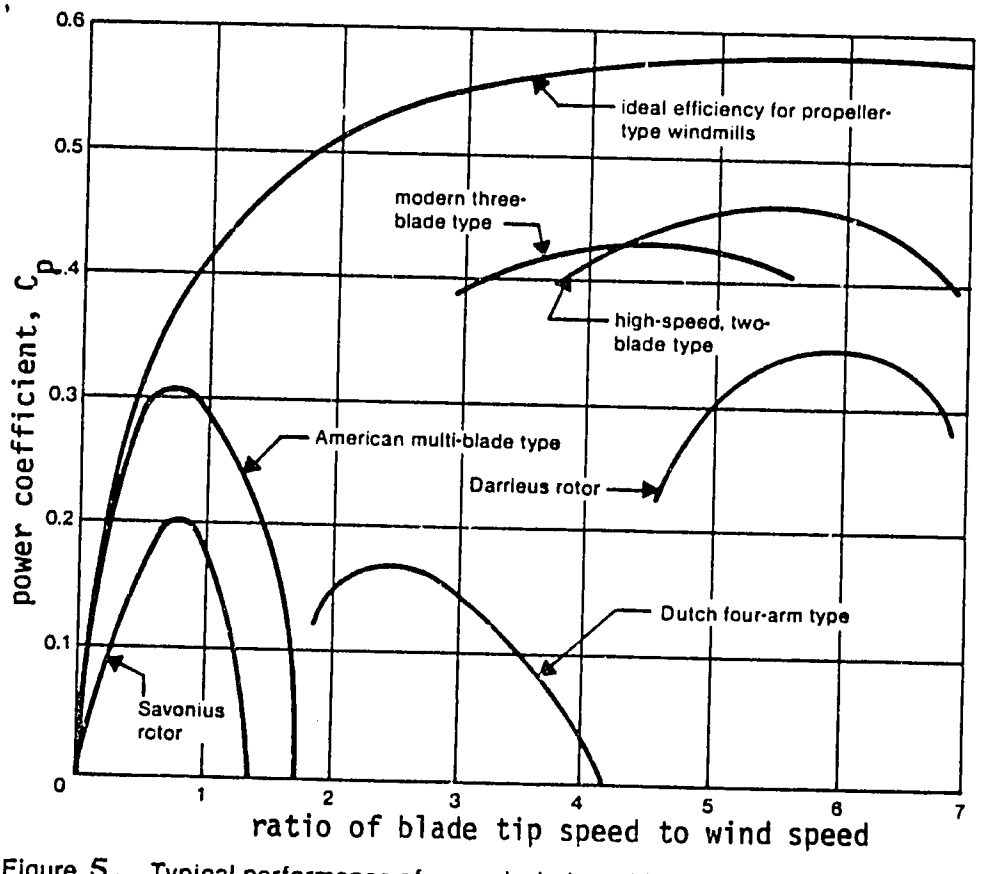

Figure 5. Typical performance of several wind machines.

Operating characteristics of major rotor types [22]

Rotor Type	Tip/Speed Ratio Range	C_p*	RPM	Torque	Typical Load
Propeller (lift) 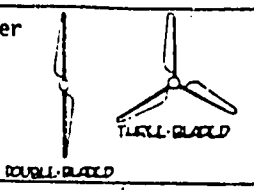	6 to 10 (up to 20)	0.42	High	Low	Electrical Generator
Darrieus (lift) 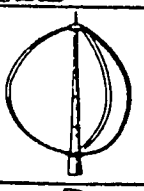	5 to 6	0.40	High	Low	Electrical Generator
Cyclogiro (lift) 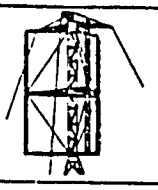	3 to 4	0.45	Moder-ate	Moder-ate	Electrical Generator or Pump
Chalk Multi-Blade (lift) 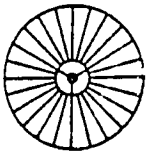	3 to 4	0.35	Moder-ate	Moder-ate	Electrical Generator or Pump
Sailwing (lift) 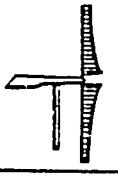	4	0.35	Moder-ate	Moder-ate	Electrical Generator or Pump
Fan-Type (drag) 	1	0.30	Low	High	Pump
Savonius (drag) 	1	0.15	Low	High	Pump
Dutch-Type (drag) 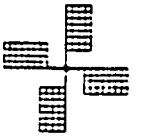	2 to 3	0.17	Low	High	Pump or Mill Stone

* C_P* is the maximum value of the power coefficient. Average power coefficients are lower.

The Betz Coefficient

The power developed when a force, F, acts on a translating body, or when a torque, Q, acts on a rotating body, is given by

$$P = FV = Q\omega$$

where V is the linear velocity and ω is the angular velocity in radians per second. The force, F, represents the component force in the direction of V.

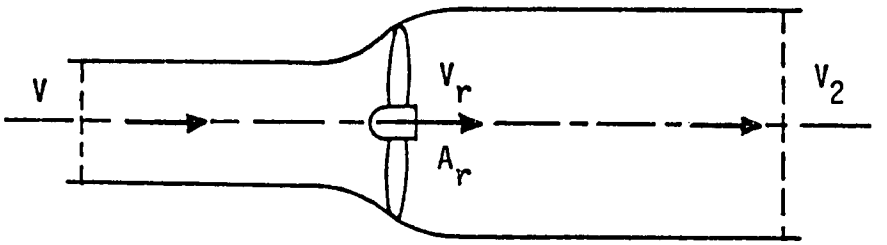

Figure 6. Airflow Through a Wind Turbine.

The force on the rotor, F, is equal to the change in momentum; so

$$F = \dot{m}(V - V_2) = \rho A_r V_r (V - V_2)$$

The power absorbed by the rotor is given by

$$P = FV_r = \rho A_r V_r^2 (V - V_2) \qquad (8)$$

However, the power absorbed can also be expressed as the difference in power of the fluid upstream and downstream of the rotor, i.e.,

$$P = \frac{1}{2}\dot{m}V^2 - \frac{1}{2}\dot{m}V_2^2$$

$$\text{or } P = \frac{1}{2}\rho A_r V_r (V^2 - V_2^2) \qquad (9)$$

Equations 8 and 9 are necessarily equivalent. It follows that we have

$$V_r(V - V_2) = \frac{1}{2}(V^2 - V_2^2) \tag{10}$$

or $$V_r = \frac{V + V_2}{2}$$

The force exerted on the rotor is therefore given by

$$F = \frac{1}{2}\rho A_r(V^2 - V_2^2) \tag{11}$$

and the power absorbed by the rotor as

$$P = \frac{1}{4}\rho A_r(V+V_2)^2(V-V_2) \tag{12}$$

or $$P = \frac{1}{4}\rho A_r(V^2-V_2^2)(V+V_2) \tag{13}$$

expanding Equations (12) or (13) gives

$$P = \frac{1}{4}\rho A_r(V^3 - VV_2^2 + V^2V_2 - V_2^3)$$

holding V constant and finding dP/dV_2 gives

$$\frac{dP}{dV_2} = \frac{1}{4}\rho A_r(-2VV_2 + V^2 - 3V_2^2)$$

for maximum power we have

$$(V + V_2)(V - 3V_2) = 0$$

so $$V_2 = -V \text{ or } V/3$$

with $V_2 = V/3$ we have from equation 13

$$P_{max} = \frac{1}{4}\rho A_r(V^2 - V^2/9)(V + V/3)$$

$$= \frac{1}{4}\rho A_r V^3 (1 - 1/9)(1 + 1/3)$$

so $$P_{max} = \frac{8}{27}\rho A_r V^3$$

Since the power in the wind is given by

$$P_w = \frac{1}{2} \rho A_r V^3$$

it follows that the highest fraction of the wind power that can be extracted by a rotor is given by

$$P_{max}/P_w = 16/27 = 0.593$$

This figure was derived by Carl Betz in 1927 and is called the Betz limit or Betz coefficient. In practice this limit is never acheived since the Betz coefficient represents the maximum power output of an ideal wind rotor with an infinite number of zero drag blades.

Wind Machine Characteristics

All wind energy machines exhibit certain fundamental operating characteristics which are related to the speed of the wind. At low wind speeds the rotor hardly turns, until the wind speed reaches a level called the cut-in speed. Since the energy in the wind is proportional to the cube of the windspeed, there is little energy in the wind at low speeds. As windspeeds increase above the cut-in speed, the rotor extracts increasing amounts of power until, at the rated windspeed, the system produces its rated output power.

At windspeeds above the rated windspeed, most systems produce roughly constant power by using some kind of governor, brake, or other form of speed control device, until at high wind speeds the rotor is braked or turned out of the wind to prevent damage to the system. The windspeed at which the system is shut down is called the cut-out or furling windspeed.

These characteristics are shown schematically in figure 7 which shows the power produced by two different wind machines as a function of wind speed. Machine A is rated at 2 kW at a windspeed of 25 mph; machine B is rated at 1 kW at a windspeed of 15 mph. Both machines cut in at about 8 mph. Machine A cuts out at 70 mph; machine B at 60 mph. Figure 8 shows the power output from a real 1 kW machine. The rated windspeed for this machine, a Sencendaugh Model 1000, is 9.8 m/s. Note that the power output from this machine varies considerably between its rated windspeed and its cut-out speed.

In assessing the energy produced by a wind system, therefore, it is essential to have available performance curves similar to the one shown for the Sencenbaugh machine.

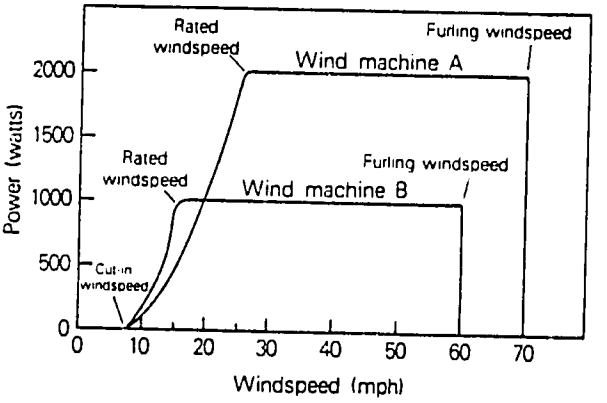

Figure 7. Output power for two typical wind machines. A rotor produces its maximum power at windspeeds between the rated and furling windspeeds.

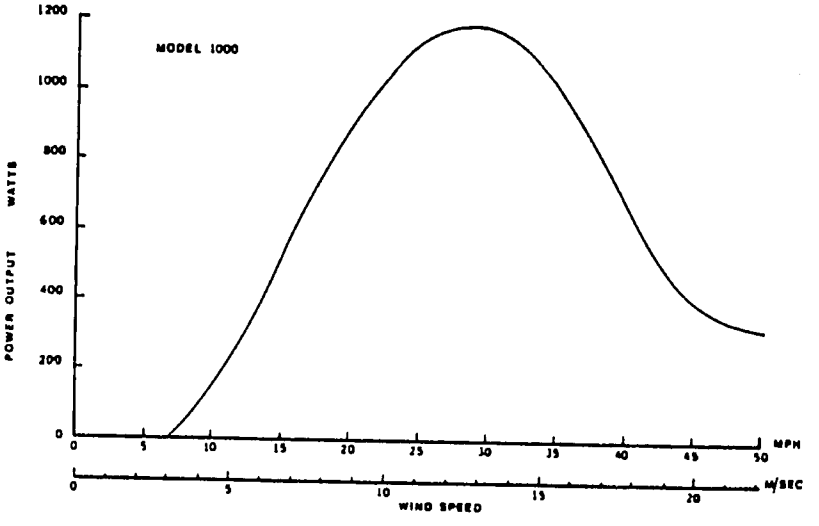

Figure 8. Output Power as a Function of Windspeed for a Commercial 1 kW Wind Machine.

Windspeed Frequency Distributions

In order to estimate the amount of energy available from a wind machine it is necessary to know, not only the power output of the machine as a function of windspeed, the subject of the preceeding discussion, but the windspeed distribution: the frequency distribution of wind speed at the proposed site of the wind machine.

If the real frequency distribution of wind speed at the site is known, the average output of the turbine, $\overline{P}$, may be computed from

$$\overline{P} = \int_0^\infty T_p(V) \cdot f(V)\, dV \qquad (14)$$

where $T_p(V)$= the machine power output as a function of windspeed

$f(V)$ = the frequency distribution of the wind speed

V = the wind speed at the rotor hub.

Figure 9 indicates schematically the way machine performance curves and wind frequency distributions are combined to produce an estimate of the energy available from the wind system.

Figure 9(a) shows an idealized machine performance curve similar to Figure 7. Point A is the cut-in windspeed, B is the rated windspeed and point C is the cut-out windspeed. Figure 9(b) shows a windspeed frequency distribution. This figure can be used to estimate the time the wind blows at a particular speed. This estimate, combined with a performance curve, is then used to estimate the energy extracted by the turbine as a function of the wind speed.

The problem with this approach to the estimation of the amount of energy available from the wind system is that the wind speed frequency distribution is not usually available. If it is, then the calculation is straightforward and reasonably accurate. However, the distribution curve can only be defined by monitoring windspeeds at a proposed site with sophisticated instruments over the course of, ideally, several years. Detailed data of this kind, however, is seldom available.

The next approach is to approximate the windspeed distribution. If only one statistic is known - the annual mean windspeed - it is possible to make a reasonably good guess at the frequency distribution. A frequency distribution often used is the Rayleigh distribution and it may be expressed as

$$f(V) = \frac{\pi}{2} \cdot \frac{V}{\overline{V}^2} \exp\left[- \pi V^2 / 4\overline{V}^2 \right] \qquad (15)$$

where $f(V)$ = frequency distribution of the windspeed

V = wind speed

$\overline{V}$ = mean wind speed

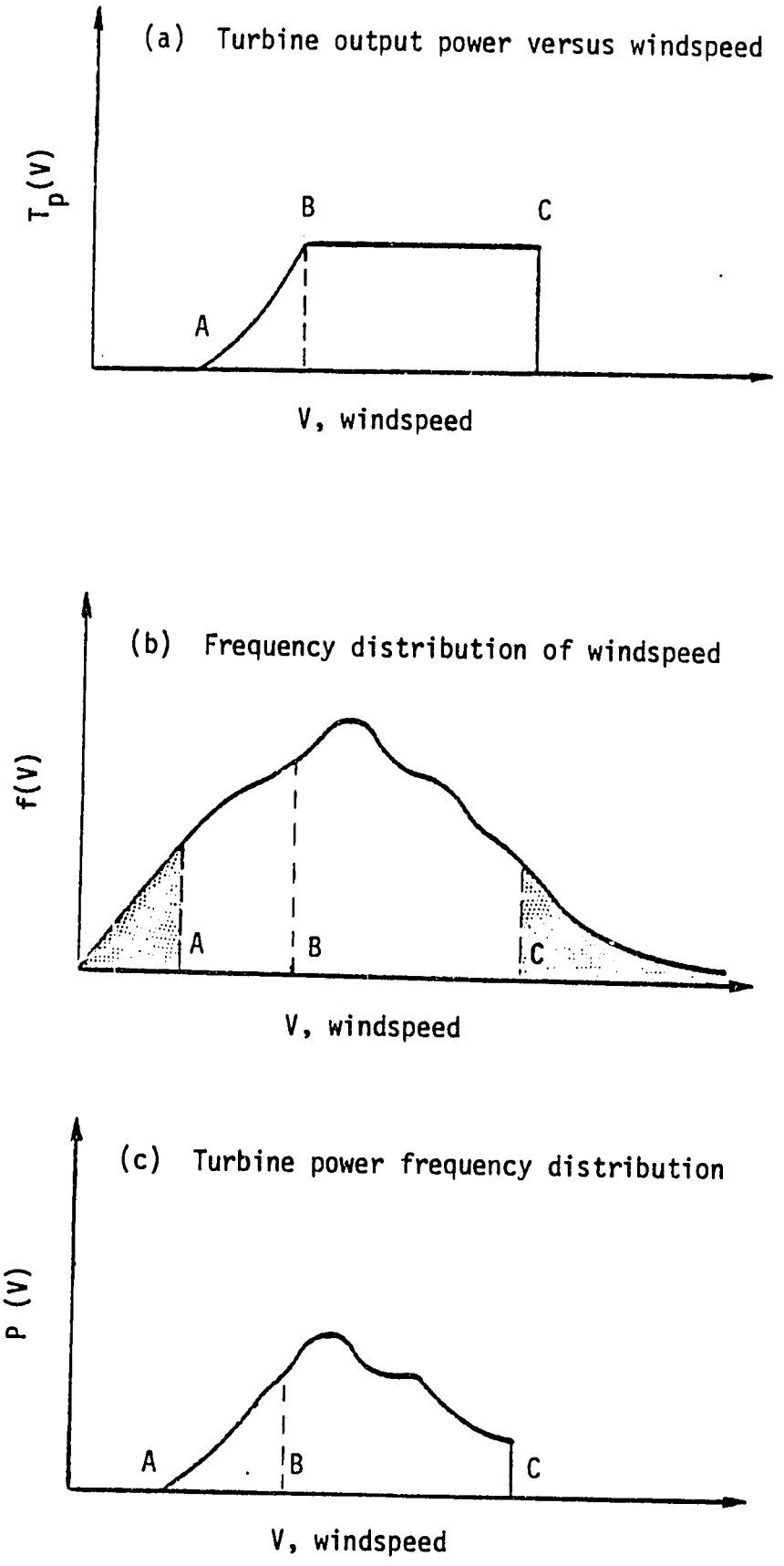

Figure 9. Interaction of wind turbine characteristics and wind frequency distribution to give wind turbine power frequency distribution. [13]

Generally, the Rayleigh distribution is a better approximation to the actual windspeed frequency distribution at the higher mean windspeeds. It should not be used where the mean windspeed is less than 4 m/s.

The Weibull function is another possible frequency distribution function. This is expressed as

$$f(V) = \left(\frac{k}{c}\right) \left(\frac{V}{c}\right)^{k-1} \exp\left[- \left(\frac{V}{c}\right)^{k} \right] \qquad (16)$$

The Weibull distribution has two adjustable parameters, c and k, and can be made to fit a wide range of observed winspeed frequency distributions, more accurately than the Rayleigh. The Rayleigh is actually a Weibull distribution with k= 2. The disadvantage of the Weibull from a wind assessment point of view is that its use requires a knowledge of both the mean wind speed and the standard deviation of the speed about the mean. These statistics are not known unless one has available an observed windspeed frequency distribution, in which case the actual recorded data should be the data used to assess the site.

Figure 10 compares two analytical frequency distributions with two observed ones. Curves 1 and 2 are the Rayleigh and Weibull distributions respectively for a site where the winds blows at a fairly constant speed. Curve 3 is an actual distribution based on one year's data from a site east of Puerto Rico, and curve 4 is an actual distribution from a site where the wind shows a bimodal distribution.

In order to show how energy production depends on the windspeed distribution, the annual average power output was computed for two small wind machines, using the frequency distributions shown in Figure 10. The performance characteristics for the wind turbines are shown in Figure 11. Both machines are rated 1.2 kW, but at different windspeeds. Furthermore, the profiles are noticeably different. The calculated average power outputs are shown in Figures 12 and 13. The graphs show that machine performance characteristics have a pronounced effect on average power output. The output of machine B is much larger, since that mahine produces power at its rated output over a wider range of windspeeds than machine A.

The graphs also indicate that estimates of average energy production are not overly sensitive to the form of the distribution function. Over most of the windspeed range shown, the average power output estimated from the Rayleigh distribution (the solid line) differs by no more than ±15% from estimates based on the actual distribution and the Weibull function. This is a reasonable level of accuracy and suggests that the use of the Rayleigh distribution, which is extremely simple to employ, is a quick and useful way to estimate wind site potential.

A further characteristic indicated by the curves is that the sensitivity of power production estimates to the windspeed distribution depends very much on the performance characteristics of the wind machine.

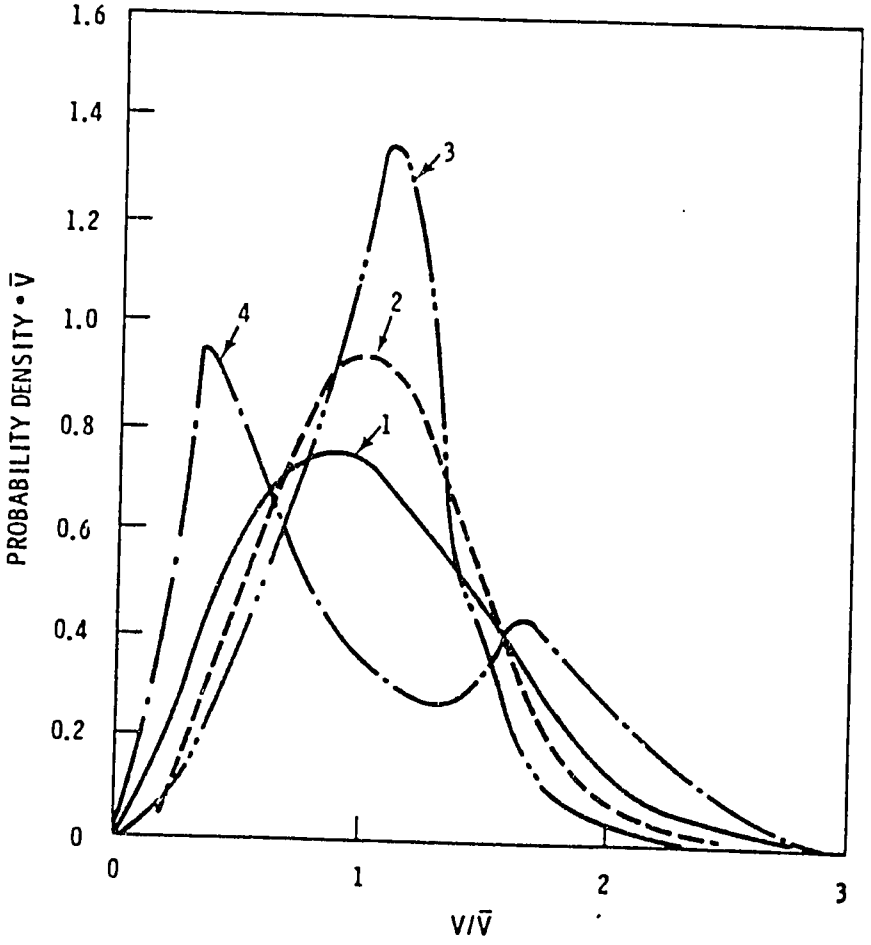

Figure 10. Some windspeed probability density functions. Curve 1 is the Rayleigh distribution and Curve 2 is a Weibull. Curves 3 and 4 are observed distributions. Curve 2 is actually a Weibull fit to Curve 3

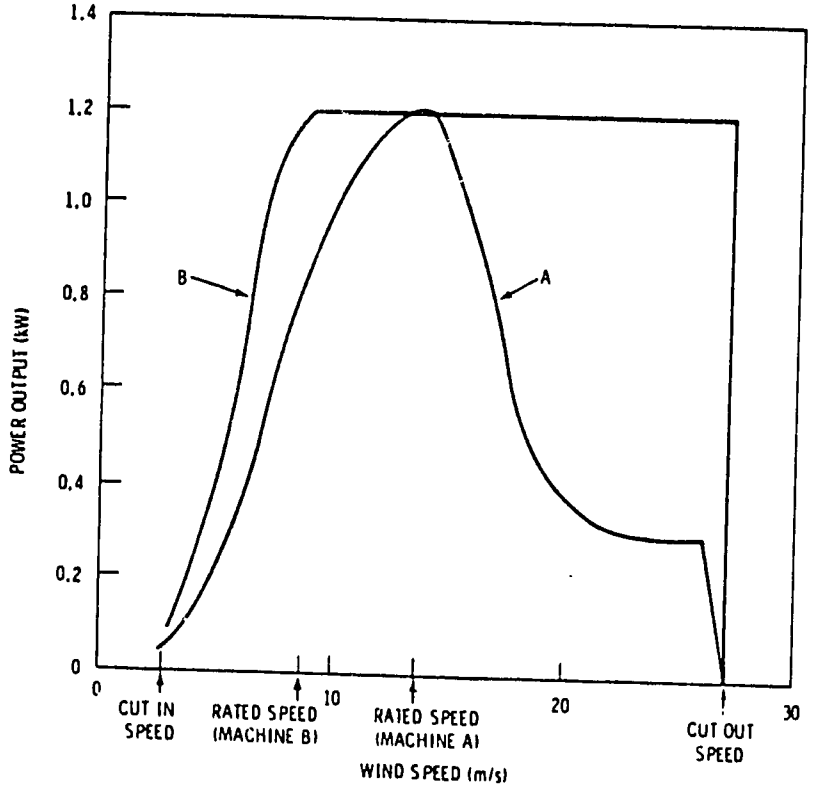

Figure 11. Steady-state performance characteristics for two small wind turbines

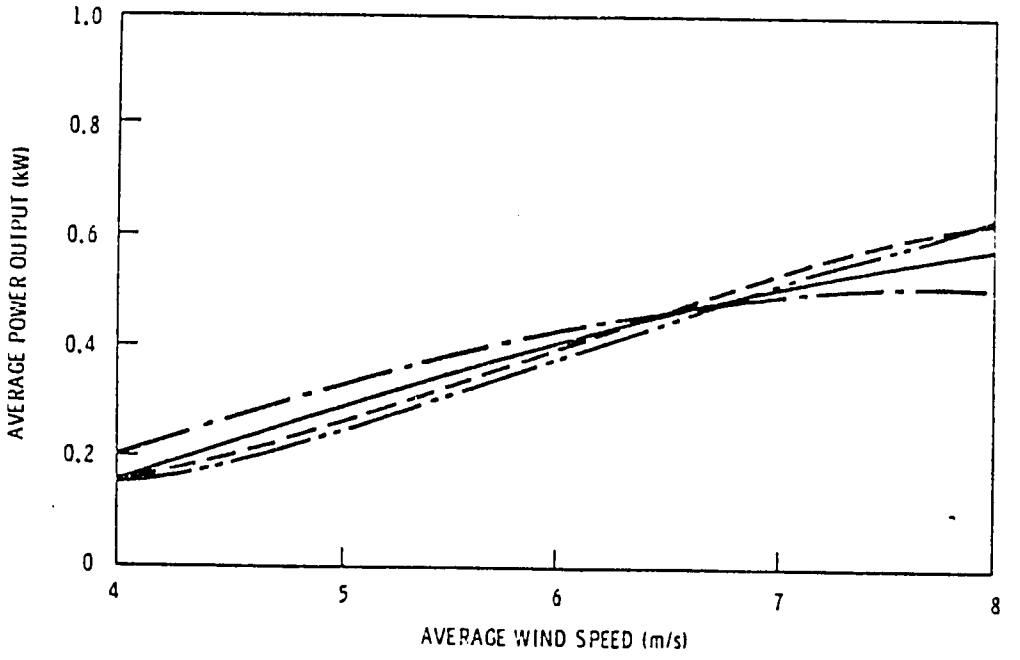

Fig. 12 Average Power Output for Machine A as a Function of Average Wind Speed. Four Possible wind speed probability density functions (PDFs) are showr. Each line corresponds to the PDF that is plotted with the same type of line in Figure 10

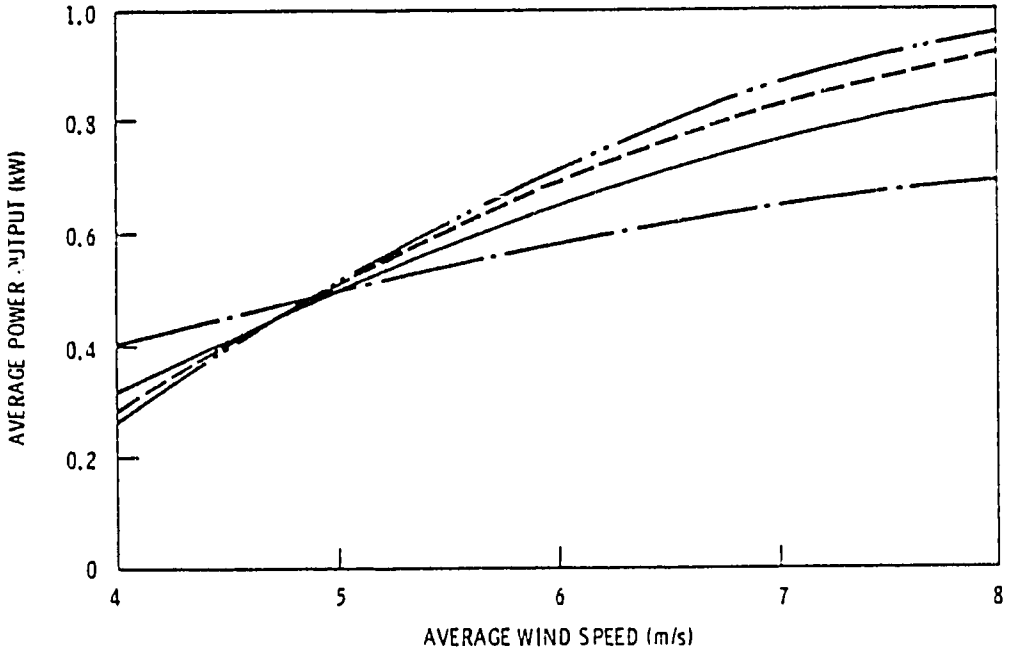

Fig. 13 Average Power Output for Machine B as a Function of Average Wind Speed. Four possible wind speed probability density functions (PDFs) are shown. Each line corresponds to the PDF that is plotted with the same type of line in Figure 10

The average production of machine B is relatively independent of the windspeed distribution because of its flat performance curve between windspeeds of 8.5 to 27 m/s. The cutout speed is an important machine parameter - the higher the cutout speed the less sensitive the power production estimates are to the form of the distributions function.

Windspeed distribution functions can be used to determine energy distribution curves. The energy in the wind is the power in the wind, P_W, at a particular windspeed multiplied by the time the wind blows at that windspeed, as either measured or predicted by the use of a frequency distribution function such as the Rayleigh.

Since	P_W	$= 1/2\ \rho AV^3$	Watts
and	$t(V)$	$= 8760\ f(V)$	hrs/yr
then	$E(V)$	$= P_W t/1000$	kWh/yr

The graphs below show Rayleigh windspeed distribution curves, and energy distribution curves for two sites with available windspeeds of 10 mph and 14 mph.

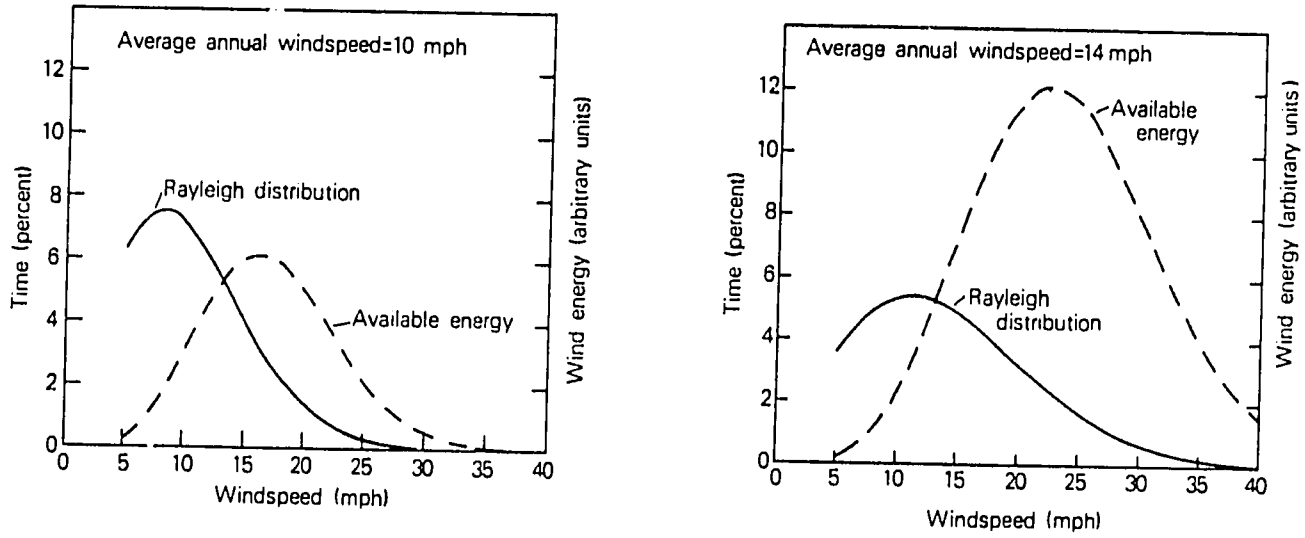

Figure 14. Rayleigh Windspeed Distributions for Sites with 10 mph and 14 mph Winds. The Available Wind Energy is far greater at the windier Site. [3]

It is important to note the following points:

1. The most frequent windspeed--the peak of the frequency distribution--occurs at a windspeed below the mean. If V_f is the most frequent windspeed and $\overline{V}$ is the mean, it can be shown for a Rayleigh frequency distribution that

$$V_f = 0.8\overline{V}$$

2. The peak of the energy curve occurs at a windspeed considerably higher than the mean windspeed. For a Rayleigh frequency distribution it can be shown that

$$V_{Emax} = 1.6\overline{V}$$

The relationship between the peak of the energy curve and the mean windspeed is especially important since it permits a quick calculation of the windspeed at which the maximum energy is available in the wind, knowing only one statistic - the mean annual windspeed. Wind machines need to be matched to the windspeed characteristics of the site. The rated windspeed and the cut-out windspeed of the machine should span the range of windspeeds where the energy in the wind reaches its maximum value. Generally, the rated windspeed of a wind turbine should lie within about 20 percent of the mean windspeed at the site if the energy produced by the machine is to be maximized.

Measuring the Wind

A wide range of instruments is available for use in measuring windspeed. A simple device will measure only one statistic--the average windspeed--but a great deal of preliminary design work and economic assessment can be based on just this one statistic. Simple aremometers and windrun counters cost about $100 - $150. More sophisticated systems that generate the full windspeed frequency distribution cost approximately $2000 - $3000. Measuring the full distribution makes possible a more accurate evaluation of the energy that could be produced at the site. But year-to-year variations can be significant, so the prediction of wind machine output can never be precise.

It seems sensible to assess a site initially with the use of a cheap portable instrument that will indicate average windspeeds. The instrument should be read each month so that strong seasonal variations in windspeeds show up early in the site assessment.

Wind Duration Curves

A useful way to organize wind velocity data is to construct a wind duration curve. This curve shows the number of hours that the windspeed at a site exceeds a particular value. For example, consider the wind speed data below for a site off the coast of Alaska.

SPEED / DIR.	1-3	4-6	7-10	11-16	17-21	22-27	28-33	34-40	41-47	48-55	≧56	%	MEAN WIND SPEED
N	.1	.3	1.3	1.1	1.0	.5	.2	.1	.0	.0	.1	4.8	15.8
NNE	.2	.1	.5	.7	.9	.8	.6	.1		.0	.0	3.8	19.8
NE	.2	.1	.6	.8	1.2	.8	.7	.1	.0	.1		4.5	19.4
ENE	.1	.1	.3	.8	1.3	1.5	1.2	1.0	.3	.2	.9	7.7	30.0
E	.2	.4	1.1	1.9	1.5	1.0	.9	1.0	1.0	.3	.2	9.5	23.7
ESE	.1	.1	.5	1.0	1.3	1.3	1.1	.8	.8	.7	.1	7.9	27.4
SE	.1	.3	.6	.7	1.1	1.6	1.3	.9	.4	.3	.1	7.6	25.1
SSE	.0	.2	.3	.2	.3	.4	.4	.7	.5	.6	.3	3.9	32.1
S	.3	.3	.6	.9	1.0	.7	.7	.8	.5	.4	.2	6.4	24.9
SSW	.1	.1	.5	.6	.4	.7	.7	.3	.0	.2	.2	3.7	24.9
SW	.1	.2	.6	1.2	.9	1.1	.9	.5	.3	.2	.2	6.3	23.9
WSW	.0	.2	.8	.9	1.1	1.1	.9	.6	.3	.2	.0	6.1	23.0
W	.2	.3	.7	.9	1.3	1.4	.9	.4	.1	.1		6.3	20.7
WNW	.2	.3	.5	1.1	1.0	1.1	.7	.6	.2	.1		6.0	21.3
NW	.3	.4	1.7	1.9	1.4	1.4	.7	.6	.2	.0		8.7	18.1
NNW	.0	.2	.8	1.7	1.5	1.1	.4	.2	.0	.1		6.0	18.6
VARBL													
CALM												.9	
	2.3	3.7	11.4	16.4	17.3	16.6	12.2	8.7	4.8	3.7	2.1	100.0	23.0

TOTAL NUMBER OF OBSERVATIONS 5146

The wind duration curve is a cumulative frequency diagram. Starting at the highest windspeed group, it is a simple matter to record the time that the wind blows at this level: 2.1 percent of the time. Multiplying by the number of hours in a year, 8760, gives 184 hours - the time that the wind blows at 56 mph or greater. One then works downward through the lower windspeed ranges summing the hours computed. The tabulated data is shown overleaf. The wind duration curve is plotted through the points marking the accumulated hourly totals, and the lowest point of the speed range pertaining to that total.

range mph	frequency %	time hrs	cumulative hrs
>56	2.1	184	184
48-55	3.7	324	508
41-47	4.8	420	928
34-40	8.7	762	1690
28-33	12.2	1069	2759
22-27	16.6	1454	4213
17-21	17.3	1515	5728
11-16	16.4	1437	7165
7-10	11.4	999	8164
4-6	3.7	324	8488
1-3	2.3	201	8689
Calm	0.8	71	8760

The wind duration curve is shown in Figure 15. For a Rayleigh distrubution, the wind duration curve for a mean windspeed, $\overline{V}$, can be expressed as

$$t_D = \exp\left[- \pi V^2/4 \overline{V}^2\right] \tag{17}$$

where t_D is the fraction of the time that the wind speed is greater than V. If $\overline{V}$ is mean annual windspeed, then t_D is multiplied by 8760 hours to give a wind duration curve similar to the one shown in Figure 15.

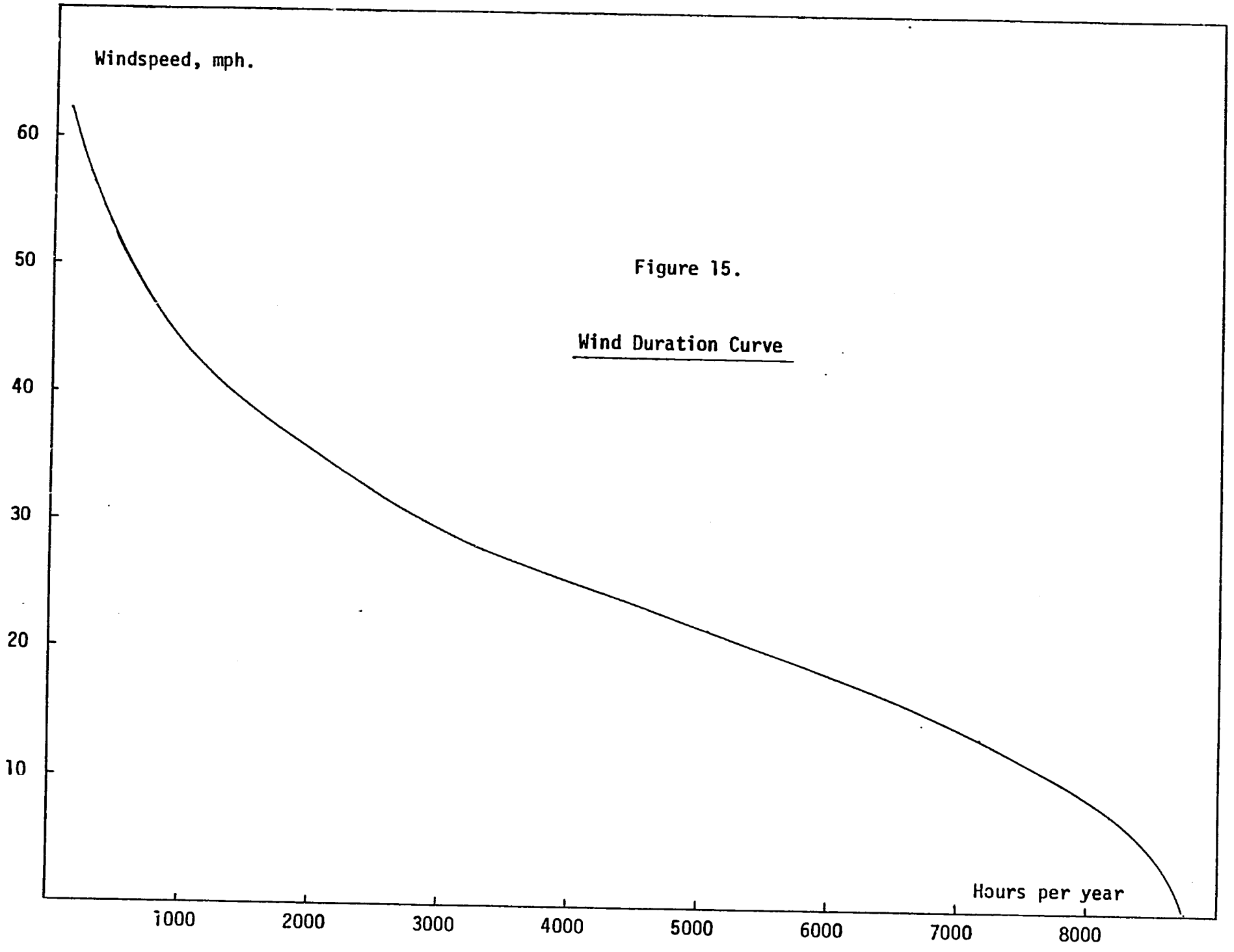

Figure 15.

Wind Duration Curve

Energy Conversion

Knowing both the site windspeed frequency distribution and the output characteristics of the wind machine under review, it is now possible to estimate the amount of energy available from the machine. Consider the graphs shown below. Figure 16 is a wind duration curve for a site (average windspeed 12.5 mph) where two machines, A and B, are being considered for installation. The performance curves for these machines are shown in Figure 17. Both machines are rated 1 kW but at different wind speeds. Machine A has a rated speed of 32 mph, machine B has a rated speed of 20 mph. Machine B also cuts in earlier than machine A.

To estimate the energy extracted by each machine we proceed as follows. Divide the abscissa of Figure 16 into 20-hour divisions and read off the average wind speed for each 20-hour period. From Figure 17, one then estimates the average power produced during this period. The average power generation multiplied by 20 gives the energy produced in watt-hours from each machine. Table 1 shows the results of this sequence of calculations.

What can be clearly seen is that Machine B produces more than twice as much energy as machine A. Even though both machines are nominally 1 kW, the difference in their rated windspeeds makes a great deal of difference to the amount of energy each machine is capable of extracting from the wind.

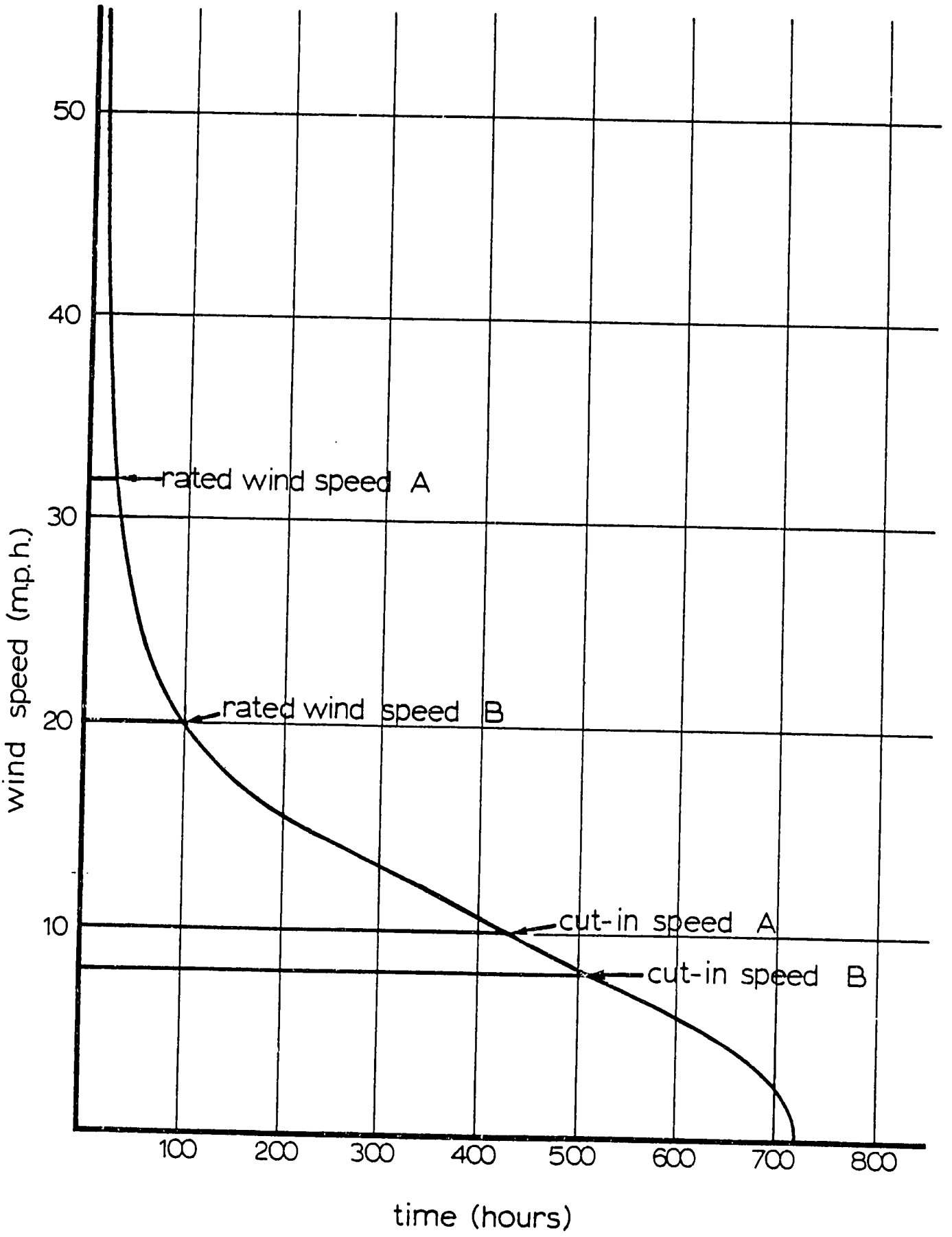

Figure 16. Example wind duration curve [1]

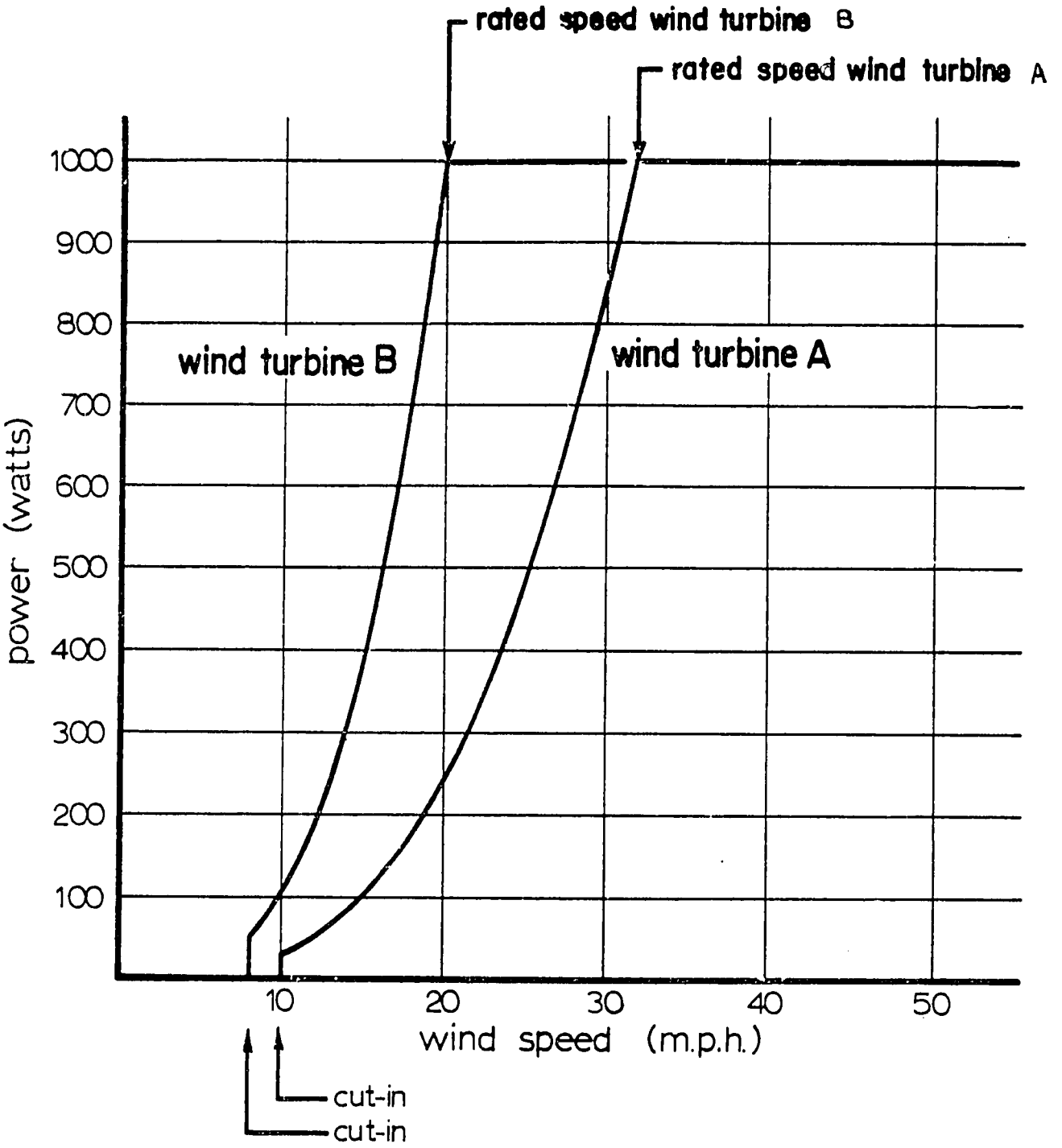

Figure 17. Power curves for two wind turbine generators [1]

Table 1. Energy extracted per month from the wind distribution shown in Figure 16 by wind turbines A and B.

		WIND TURBINE A		WIND TURBINE B	
No.	V mph	Power watts	Watts × 20 Hrs.	Power	Watts × 20 Hrs.
1	40	1000	20,000	1000	20,000
2	35	1000	20,000	1000	20,000
3	26	650	13,000	1000	20,000
4	22	320	6,400	1000	20,000
5	20	250	5,000	1000	20,000
6	19	238	4,760	950	19,000
7	17.5	162	3,240	650	13,000
8	17	150	3,000	600	12,000
9	16.5	138	2,760	550	11,000
10	16	125	2,500	500	10,000
11	15.5	113	2,260	450	9,000
12	15	100	2,000	400	8,000
13	14.5	90	1,800	360	7,200
14	14	80	1,600	320	6,400
15	13.5	70	1,400	280	5,600
16	13	60	1,200	240	4,800
17	12.5	50	1,000	200	4,000
18	12	45	900	180	3,600
19	11.5	40	800	160	3,200
20	11	35	700	140	2,800
21	10.5	30	600	120	2,400
22	10	25	500	100	2,000
23	9.5	0	0	95	1,800
24	9	0	0	87	1,740
25	8.5	0		70	1,400
26	8			50	1,000
27	7.5			0	0
28	7				
29	6.5				
30	6				
31	5.5				
32	5				
33	4.5				
34	4				
35	3.5				
36	2				
Total watt hours			95,420 = 95.4 kWh		229,940 = 229.9 kWh

This graphical procedure, however, can be a little tedious. Fortunately, there is a quick way to estimate the energy extracted by a wind machine.

Assume a Rayleigh distribution of windspeed

$$f(V) = \frac{\pi V}{2\bar{V}^2} \exp(- V^2\pi/4\bar{V}^2) \tag{18}$$

It is useful to define a parameter, a, by

$$a = -\pi/4\bar{V}^2 \tag{19}$$

so that Equation 18 can be written as

$$f(V) = - 2aV\exp(aV^2) \tag{20}$$

It is then necessary to model the performance of the turbine. The idealized turbine has a power output curve as shown in Figure 9(a). The turbine cuts in at a windspeed V_i (point A); reaches its rated power, P_r, at a windspeed of V_r (point B); and cuts out at a windspeed of V_o (point C).

We assume that the power output between windspeeds V_i and V_r (the curve from A to B) can be adequately represented by a quadratic function:

$$P = AV^2 + B \tag{21}$$

and it can be shown that

$$A = \frac{Pr}{V_r^2 - V_i^2} \tag{22}$$

and $$B = - AV_i^2 \tag{23}$$

The power produced by the turbine can therefore be expressed as

$$\left.\begin{array}{ll} P = 0 & V < V_i \\ P = AV^2 + B & V_i \leq V < V_r \\ P = P_r & V \geq V_r \end{array}\right\} \tag{24}$$

The average power generated between windspeeds V_i and V_r is given by

$$P_1 = \int_{V_i}^{V_r} (AV^2 + B)\, f(V) dV \tag{25}$$

and the average power generated between windspeeds V_r and V_o is given by

$$P_2 = \int_{V_r}^{V_o} P_r\, f(V)\, dV \tag{26}$$

On substitution of Equation 20, Equations 25 and 26 become

$$P_1 = -2a\int_{V_i}^{V_r} (AV^3 e^{aV^2} + BVe^{aV^2})\, dV \tag{27}$$

and

$$P_2 = -2aP_r \int_{V_r}^{V_o} Ve^{aV^2} dV \tag{28}$$

These integrals can be solved analytically since it is known that

$$\int xe^{ax^2} dx = \frac{e^{ax^2}}{2a}$$

and

$$\int x^3 e^{ax^2} dx = \frac{e^{ax^2}}{2a^2}(ax^2 - 1)$$

Therefore, we have

$$P_1 = -2aA\left[\frac{e^{aV^2}}{2a^2}(aV^2 - 1)\right]_{V_i}^{V_r} - 2aB\left[\frac{e^{aV^2}}{2a}\right]_{V_i}^{V_r}$$

and

$$P_2 = -2aP_r\left[\frac{e^{aV^2}}{2a}\right]_{V_r}^{V_o}$$

On substitution of Equations 22 and 23, the above equations finally reduce to

$$P_1 = P_r \left[\frac{e^{aV_r^2} - e^{aV_i^2}}{a(V_r^2 - V_i^2)} - e^{aV_r^2} \right] \tag{29}$$

and

$$P_2 = P_r \left[(e^{aV_r^2} - e^{aV_o^2}) \right] \tag{30}$$

The average power generated between windspeeds V_i and V_o, $\overline{P}$, is the sum of P_1 and P_2; thus

$$\overline{P} = P_r \left[\frac{e^{aV_r^2} - e^{aV_i^2}}{a(V_r^2 - V_i^2)} - e^{aV_o^2} \right] \tag{31}$$

Finally, introducing

$$A = a\ (V_r^2 - V_i^2) \tag{32}$$

$$B = \exp \left[a\ (V_o^2 - V_i^2) \right] \tag{33}$$

$$C = \exp\ (aV_i^2) \tag{34}$$

We have

$$\overline{P} = P_r\ C \left[\frac{e^A - 1}{A} - B \right] \quad \text{Watts} \tag{35}$$

This equation permits the average power of the wind machine to be quickly estimated. For example, consider again, wind machines A and B, the power output curves of which were shown in Figure 17. For Machine A we have

$$V_i = 10 \text{ mph}$$

$$V_r = 32 \text{ mph}$$

$$V_o = 50 \text{ mph}$$

$$P_r = 1 \text{ kW}$$

and $\overline{V}$ is given as 12.5 mph. So from Equation 19 we find

$$a = -\pi/4 \ (12.5)^2 = -0.00503$$

and from Equations 32-34

$$A = -4.6445$$

$$B \simeq 0$$

$$C = 0.6049$$

So from Equation 35 we can estimate the average power output of this machine as

$$\overline{P} = 1 \times 0.6049 \left(\frac{\exp(-4.6445) - 1}{-4.6445}\right)$$

$$= 0.129 \text{ kW}$$

So over a month of 720 hours the energy generated by this turbine should be about 720 x 0.129 = 93 kWh, a figure close to that calculated in Table 1.

For Machine B we have

V_i = 8 mph

V_r = 20 mph

V_o = 50 mph

P_r = 1 kW

Proceeding as before with the same mean windspeed we find

A = -1.6889

B ≃ 0

C = 0.7249

So from Equation 35 we find

$$\overline{P} = 1 \times 0.7249 \left(\frac{\exp(-1.6889) - 1}{-1.6889}\right)$$

$$= 0.350 \text{ kW}$$

Over the same month we would therefore expect to generate 720 x 0.35 = 252 kWh of electrical energy.

This estimate is nearly 10 percent higher than the figure calculated by the graphical procedure shown previously. But this arithmetical approach is simple, lends itself easily to the use of a calculator or computer, and is particularly useful when one wants to compare the energy output from a number of wind machines under consideration for erection at a specific site.

Consider 3 wind machines with the following characteristics

Machine:	A	B	C
Cut-in windspeed (V_i, m/s)	3.1	4.5	2.7
Rated windspeed (V_r, m/s)	11.2	9.8	9.0
Cut-out windspeed (V_o, m/s)	13.4	17.9	40.0
Rated power (P_r, kW)	2.0	1.5	1.0

It is interesting to take a look at how these wind turbines might operate at different windspeeds. Using Equation 35 once again for each machine, with a mean annual windspeed, $\overline{V}$, ranged between 4 and 12 m/s, we can compute the amount of energy generated annually by each machine at each windspeed. These data are tabulated below.

Mean annual windspeed	Energy generated annually, kWh/yr		
m/s	A	B	C
4	1913	1275	1647
5	3403	2651	2712
6	4824	4120	3716
7	5841	5425	4573
8	6376	6425	5271
9	6517	7079	5831
10	6392	7415	6273
11	6109	7496	6615
12	5745	7393	6867

The data can be plotted in the form of a graph as shown in Figure 18. What is important to note is that although Machine A is rated at 2 kW (at a windspeed of 11.2 m/s) and might therefore be considered the most productive of the 3 machines, this is not necessarily the case. Machine A generates more

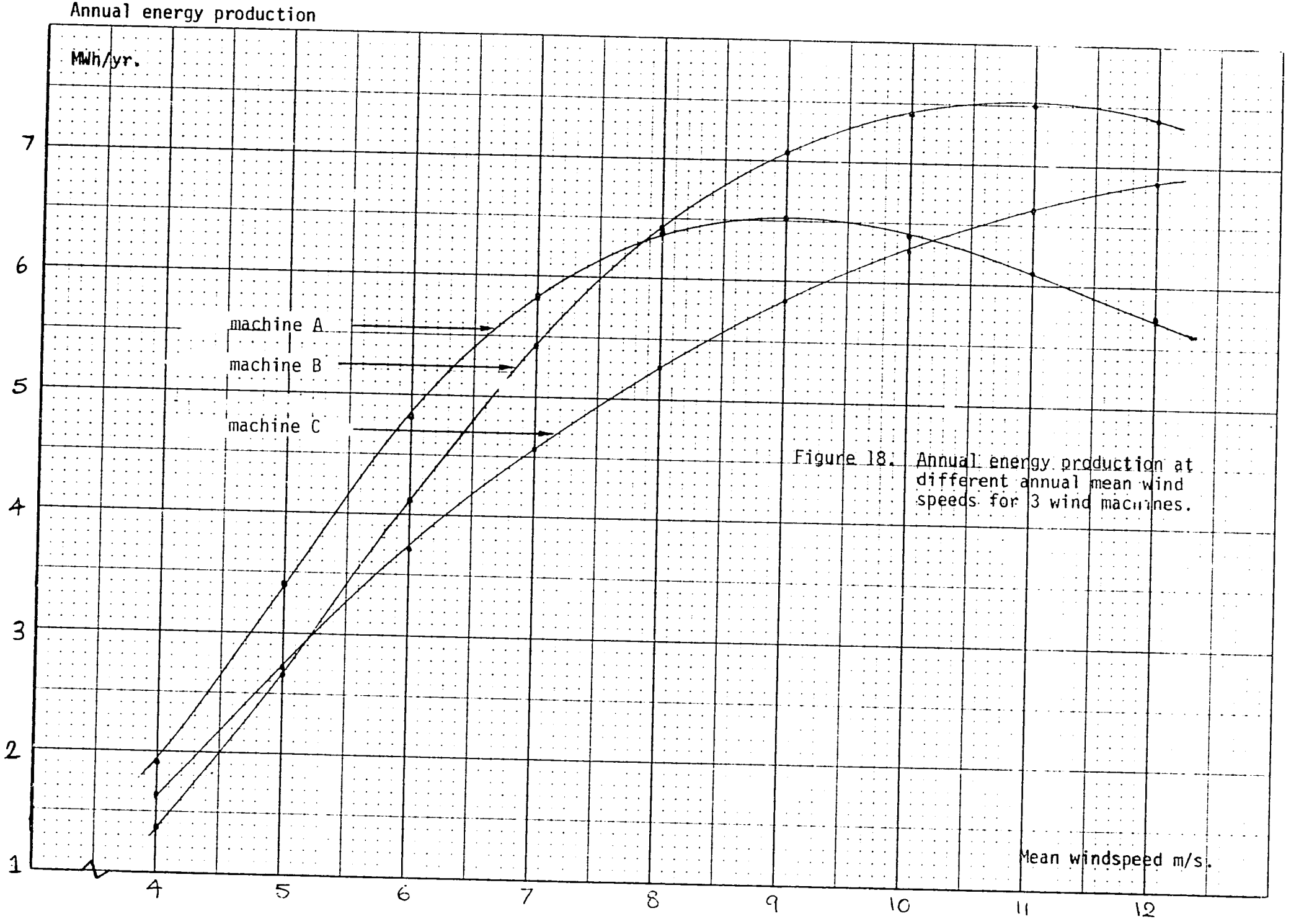

Figure 18. Annual energy production at different annual mean wind speeds for 3 wind machines.

power at mean annual windspeeds up to about 8 m/s. At higher mean windspeeds Machine A produces lesser amounts of power because of its low cut-out windspeed; it does not function well at the higher windspeeds. When comparing the performance of wind turbines, therefore, it is critically important to know more about the machine than just its rated power. One needs to estimate how much energy is produced by the machine, and for this exercise one requires the cut-in and cut-out windspeeds, the windspeed at which the turbine produces its rated power, and the mean annual windspeed of the site.

We can take this exercise a step further and ask what is the cost of energy produced. Assume that the installed cost of each machine is $2000/kW. The capital cost, K, is therefore given by

$$K = 2000 \times P_r$$

Capital charges are given as K multiplied by a Capital Recovery Factor (CRF) which is a function of the interest rate on the loan, i, and the time preiod, t, over which the loan is to be repaid. The Capital Recovery Factor is defined as

$$CRF(i, t) = \frac{i}{1 - (1 + i)^{-t}}$$

where i is expressed as a fraction, and t is in years. If operation and maintenance is 10 percent of K, we estimate annual charges, A, at

$$A = K \times CRF(i, t) + 0.1 \times K \quad \$/yr$$

and the cost of energy produced by the turbine as

$$\text{Energy cost} = \frac{K \times (0.1 + CRF(i, t)}{8760 \times \overline{p}} \quad \$/kWh$$

where $\overline{p}$, the average power output, is given by Equation 35.

This analytical procedure generates, for 3 machines, the data tabulated overleaf.

Mean annual windspeed	Energy costs, ¢/kWh		
m/s	A	B	C
4	76	86	44
5	43	41	27
6	30	26	20
7	25	20	16
8	23	17	14
9	22	15	12
10	23	15	12
11	24	15	11
12	25	15	11

The data are shown in Figure 19. Again, one can see how much the cost of energy is dependant both upon the operating characteristics of the wind machine and the wind characteristics of the site.

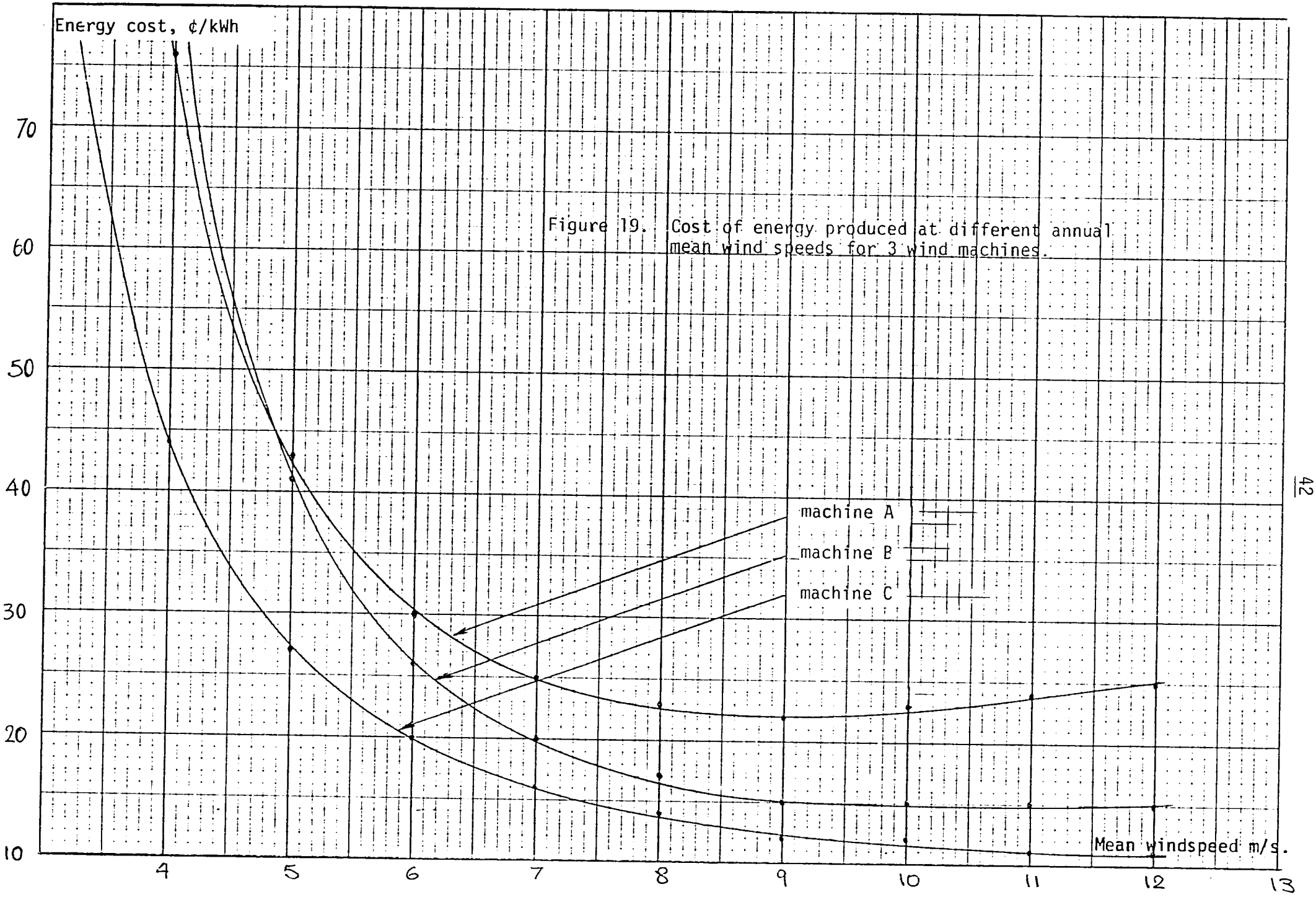

Figure 19. Cost of energy produced at different annual mean wind speeds for 3 wind machines.

Conversion Efficiency

It should be stressed that the power coefficient of a wind turbine defined by Equation 4, is frequently changing while the turbine is in operation. This occurs because the power in the wind varies with the cube of the windspeed, whereas the power generated by the rotor depends on the characteristics of the machine--as shown for example, in Figures 7 and 8, and also in the power curves given for the turbines documented in Appendix 1. The average conversion efficiency, i.e. the ratio of the long-term energy output of the turbine to the energy available in the wind over the same period, is a figure significantly less than the power coefficient maxima shown in Figure 5.

Assuming a Rayleigh distribution of windspeeds, the average power in the wind, $\overline{P}_W$, is given by

$$\overline{P}_W = \int_0^\infty P_W(V) f(V) dV \tag{36}$$

Where $P_W = \frac{1}{2}\rho A V^3$ Watts

and f(V) is the Rayleigh frequency distribution given by Equation 15. This integral can be solved analytically to give

$$\overline{P}_W = 0.955\ \rho A \overline{V}^3 \text{ Watts} \tag{37}$$

So the average power in the wind is 91 percent higher than the instantaneous power in the wind at the mean wind speed. The average power generated by the turbine, $\overline{P}$, is given by Equation 35; the mean efficiency of the machine, $\overline{\eta}$, is the ratio of the two figures:

$$\overline{\eta} = \overline{P}/\overline{P}_W \tag{38}$$

Defined in this way, efficiences are quite low--less than 20 percent for wind electric systems, less than 10 percent for wind pumping machines.

However, the real question that one would like to answer is: Given a site with a mean windspeed $\overline{V}$, how much energy can one expect to be produced by a typical wind machine? It is possible to make a rough guess at the answer to this question even if no information is available on the machine characteristics. It is only necessary to estimate V_i, V_o, and V_r for the hypothetical machine. As a rule of thumb, we will use

$$V_i = 0.4\ V_r$$

$$V_r = 0.9\overline{V}$$

and $$V_o = 2\ V_r$$

and then apply Equation 35 as before. For instance, with V = 8 m/s the procedure outlined above leads to $\bar{P}/Pr = 0.621$. So a 1 kW machine would average 621 Watts over the year giving an energy output of 5440 kWh/yr.

The area swept by the turbine can also be estimated. At the rated windspeed, wind turbines usually give their best performance, i.e. the instantaneous efficiency--which is the power coefficient C_p--is at its maximum value. This value can be estimated from Figure 5; let this value be C_{pmax}. It follows that

$$C_{pmax} = \frac{P_r}{\frac{1}{2} \rho A V_r^3} \tag{39}$$

$$\text{or} \quad A = \frac{P_r}{\frac{1}{2} \rho A V_r^3 C_{pmax}} \tag{40}$$

If the work required from the machine, W KWh/yr, is specified, the appropriate machine is determined as follows. Knowing the site mean annual windspeed, $\bar{V}$, and estimating V_i, V_r, and V_o, for a well-matched machine using the guidelines above, calculate $\bar{P}/P_r$. The energy produced by the machine, therefore, is 8760 $\bar{P}$ kWh/yr per rated kilowatt, so the rated power, P_r, is found from

$$P_r = W/8760\bar{P} \tag{41}$$

It should be stressed that this approach only gives an approximate value for annual energy production. Once a machine has been specified, the measured power output characteristics and the site windspeed frequency distribution should be used to find a more precise estimate of the amount of energy produced by the wind system.

Rotor Configurations

There are basically four common types of wind machine: the Savonius rotor, the Darrieus rotor, both vertical axis configurations; multibladed low-speed rotors like the U.S. farm windmills, and high-speed propellor-type rotors, both horizontal-axis configurations. These rotors have different aerodynamic and power characteristics and a particular rotor configuration can be selected that is well-suited for the mechanical task at hand. Savonius rotors and the multibladed high-solidity rotors are low-speed rotors that have a high starting torque and are appropriate for mechanical work such as pumping water or milling and grinding grain. The vertical-axis Darrieus and the propellor-type rotors spin much faster and have little or no starting torque. Their high rotational speeds make these rotor types appropriate for driving electric generators.

Savonius Rotor

The Savonius rotor is an extremely simple and robust wind energy conversion system. Sometimes called the S-rotor because of its dinstinctive shape, it looks rather like an oil drum that has been cut in half along its length and the halves separated sideways. More often than not, this is exactly how it is built. Figures 20 and 21 show a couple of typical configurations.

The advantages of the Savonius rotor include its simplicity and ease of construction, and its high starting torque which permits it to start up under load. However, it suffers from rather low efficiency (a coefficient of performance of about 10-20 per cent), and difficulties with overspeed control.

Savonius rotors come in all shapes and sizes. Figure 22 shows some of the more common design configurations. The more simple two-vane design seems to work as well as the multivane types. The aspect ratio, the ratio of vane height to rotor diameter, has an effect on the torque produced. Higher aspect ratio rotors (taller and slimmer) will generally run at higher rotational speeds and lower torque than those systems with a low aspect ratio.

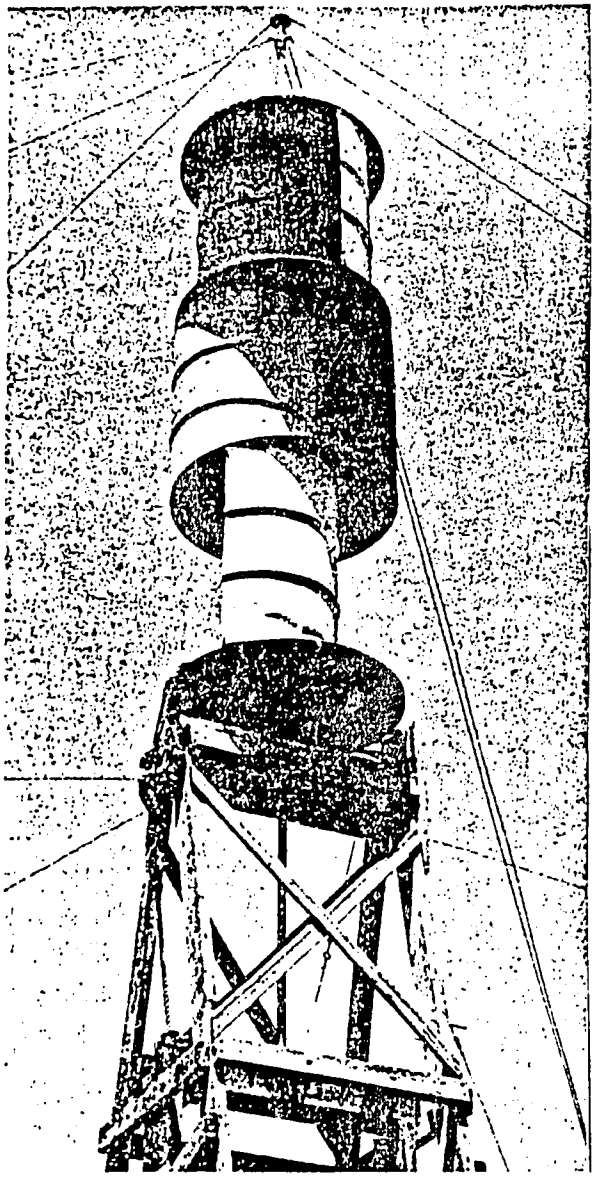

A low-technology Savonius rotor. Easily fabricated from surplus oil drums, this drag-type machine offers only limited power.

Figure 20

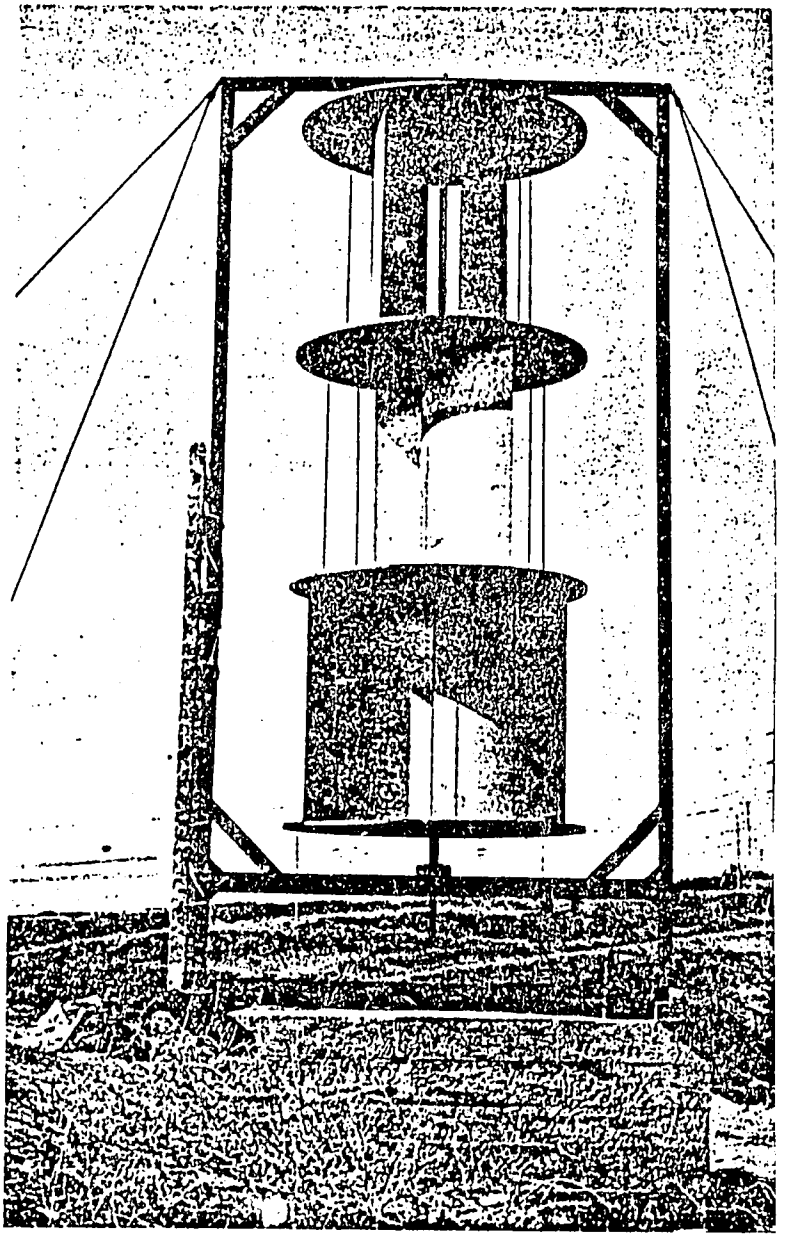

A three-tiered Savonius rotor designed to generate electricity.

Figure 21

Reference 3.

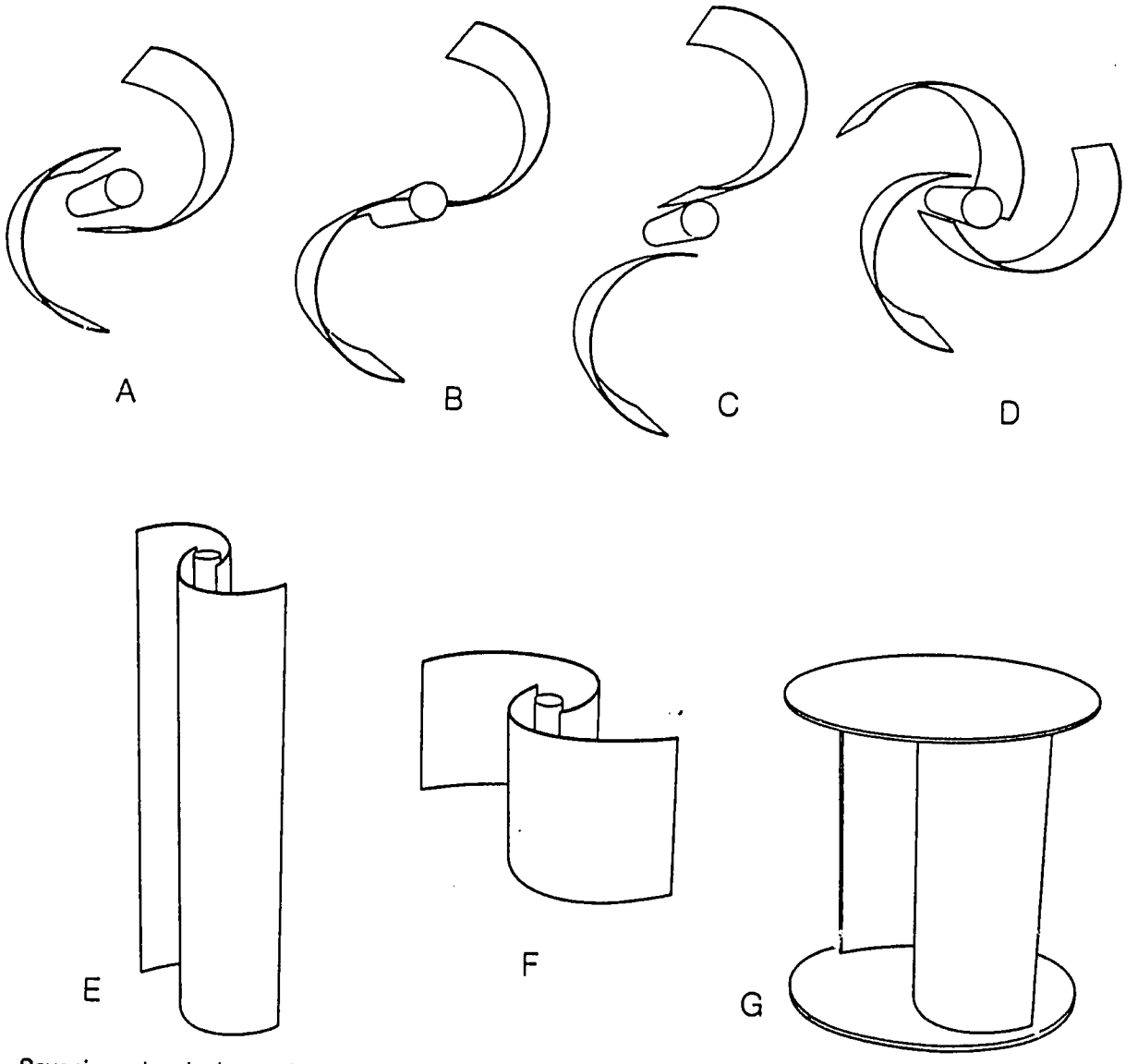

Savonius rotor design options include the intervane gap, number of vanes, aspect ratio, and tip plates. Option E has a much higher aspect ratio than F, and the tip plates in option G improve the rotor performance at low rpm.

Figure 22 [3]

Multibladed Horizontal Axis Rotors

The multibladed horizontal axis rotor is by far the most common wind energy conversion system. In the United States the old farm windmills can still be seen in operation doing what they do best: pumping water. The desirable features of the multiblade rotor are:

- High starting torque
- Simple design and construction
- Simple control requirements
- Durability

Among its disadvantages are:

- Poor compatability with high rpm loads
- High rotor drag load on the tower

The basic components of the American farm windmill are shown in Figure 23. Multibladed rotors are high-solidity low-speed rotors. Their optimal tip speed ratio is about 1 at which point their efficiency may be as high as 30 per cent, but 15-20 per cent is more realistic.

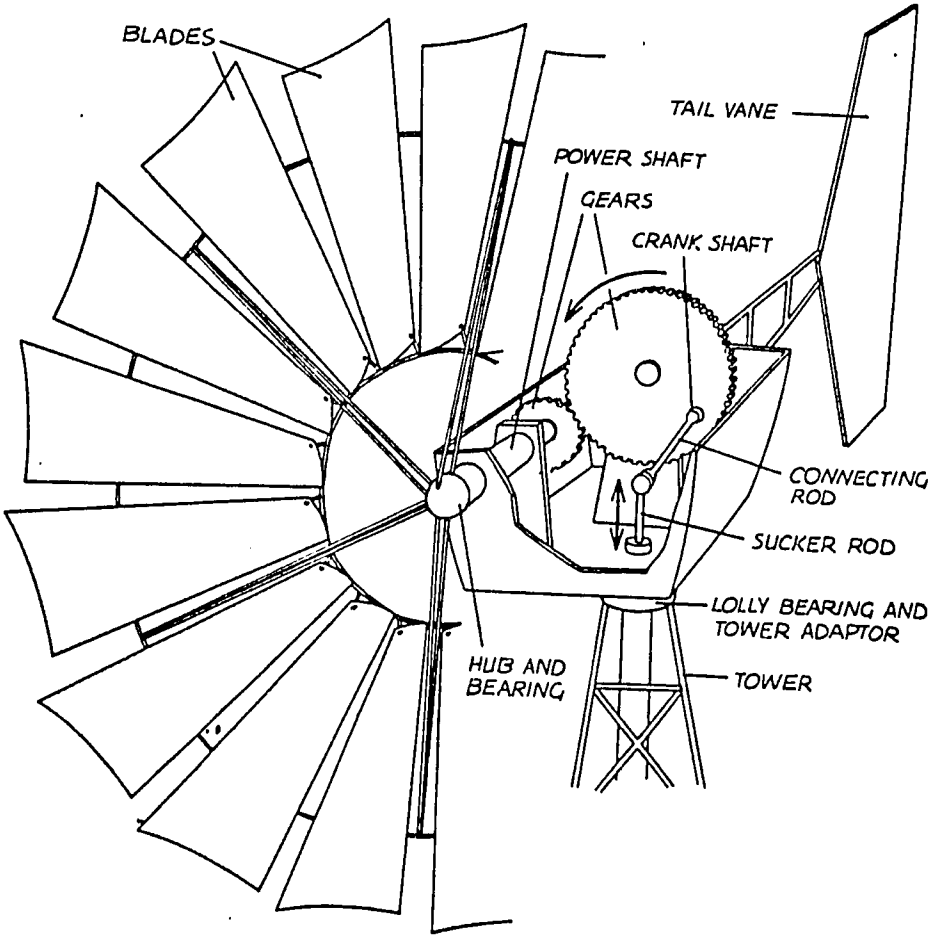

Figure 23.
Components of an American Farm windmill. Gears and crankshaft convert rotary power into the up-down motion of the sucker rod. [3]

Many kinds of multivane wind turbines suitable for pumping water have now come into use in the rural areas of many developing countries. Figure 24 shows a design offered by VITA which uses a recycled automobile axle as a transmission system. The design has flat blades.

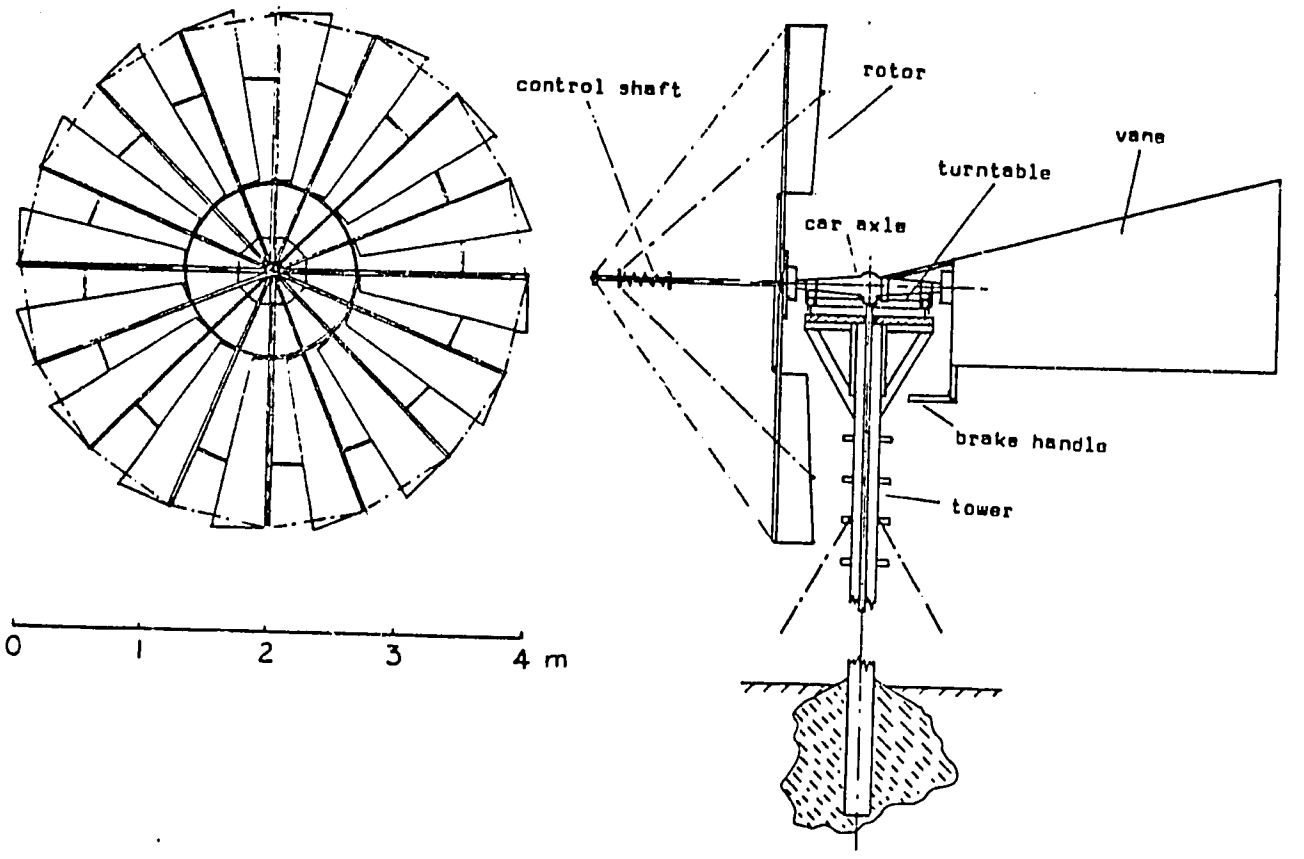

Figure 24. Windmill design suggested by VITA [9]

Perhaps the most simple type of horizontal axis windmills are the sail windmills. This type of windwheel has 4-12 radial arms to which are attached triangular sails. These machines are common on the islands of the Aegean and in other parts of the Mediterranean. The mountain plateau of Lasithi in Crete boasts so many sail windmills that it has come to be known as the "Valley of 10,000 Windmills".

A feature of these windwheels is the forward extension of the axial shaft to provide an attachment for wire stays bracing the radial arms. Stays also extend from tip to tip of the arms. The stays brace the windwheel and generally stiffen the structure. One side of each sail is attached along the rotor arm while the opposed corner is attached at a point along the circumferential bracing in the manner shown below

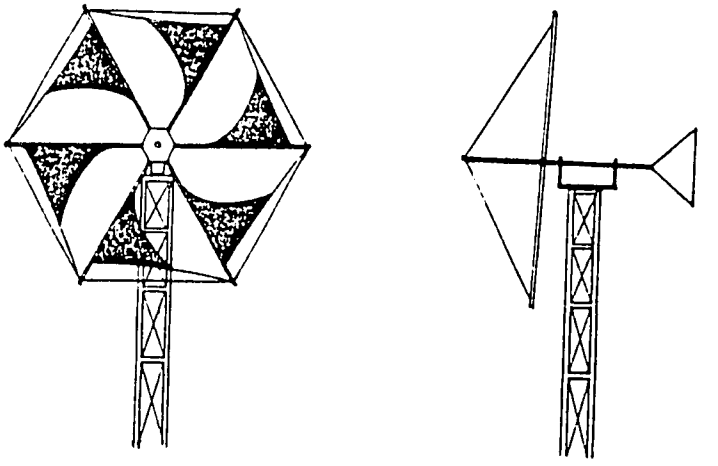

Figure 25 Configuration of a typical sail wind turbine. [15]

In the traditional Cretan design, the circumferential bracing is commonly made of chain, and the setting of the sails is effected by engaging a hook, attached to the corner of the sail, with an appropriate link in the chain. When the wind is strong, and reefing is required, the sails are wound around the poles so as to reduce their area.

The sail mill has many advantages. It has great strength, the aerodynamic surface is self-forming and flexible, and it shows a high degree of self-regulation. It is also a simple and inexpensive machine.

It is interesting to note that the traditional Cretan windwheel design has been successfully used in Africa. The American Presbyterian Mission at Omo Station in Ethiopia has introduced a water pumping version of the sail wind turbine to the local people with great success. The windwheel is used to pump water from the River Omo and irrigate small plots of land along the banks of the river. The project is interesting because the people involved compared a modified Cretan windwheel with a Savonious rotor with respect to their ability to pump water. The sail windmills were found to be superior. The first wind systems used were imported U.S. multibladed farm windmills, (Dempsters), but these proved too expensive a proposition for the local Geleb farmers. The locally fabricated sail wind rotors were produced for about one third the cost of the Dempster water pumpers and were built almost entirely of locally available materials. [11]

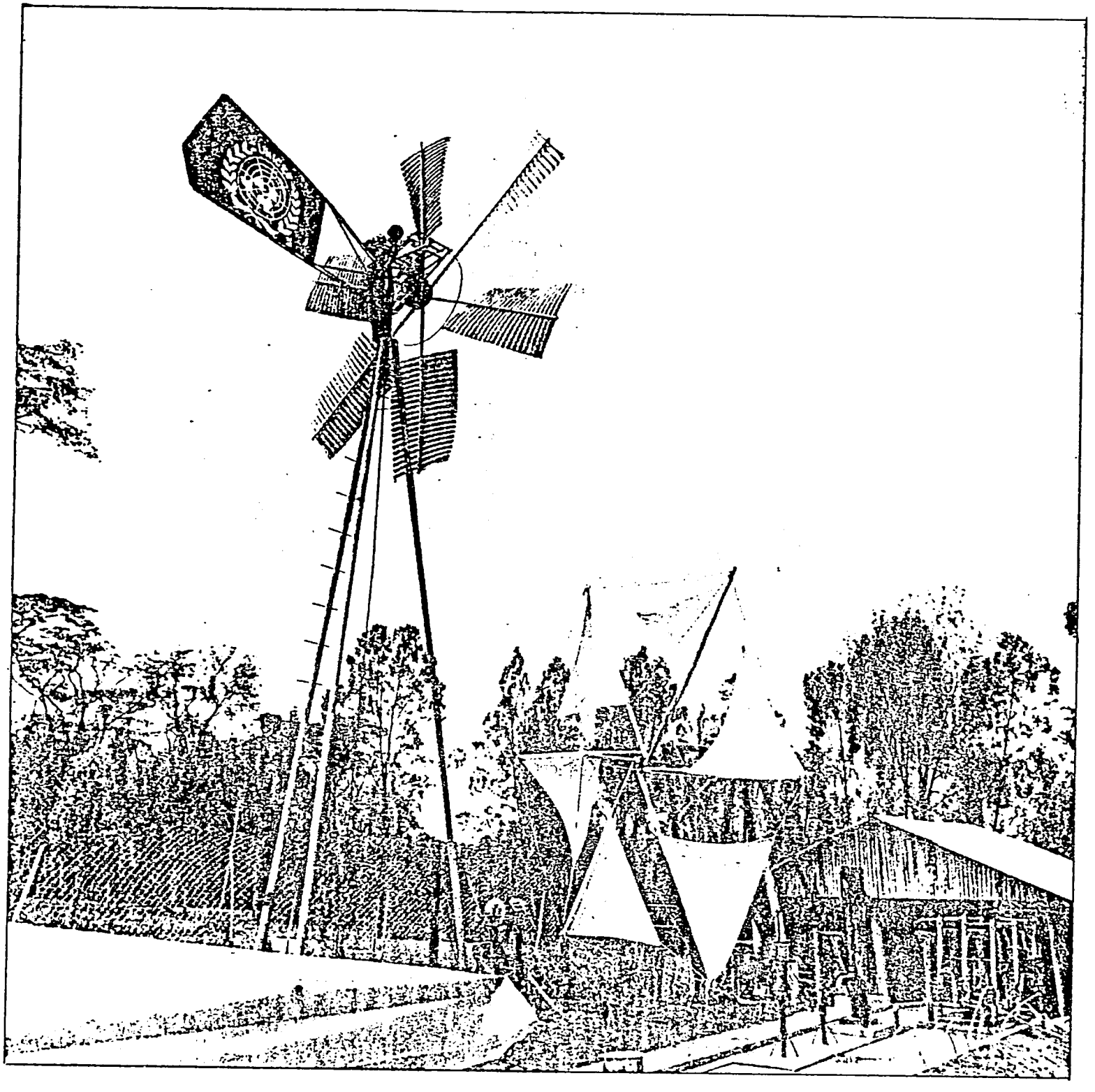

The Arusa windmill and a sail cloth windmill at the UNICEF village technology unit display in Nairobi, Kenya.

Darrieus Rotor

In 1925, G. J. Darrieus applied for a U.S. patent for a wind energy conversion system designed to generate electrical power. Figure 15 shows the basic system configuration. Each blade is a symmetrical airfoil and is curved in the shape that a perfectly flexible cable of uniform density and cross-section would assume if rotated about a vertical axis. The blade shape is called a troposkien. The advantage of this unusual shape is that rotation does not cause the blade to bend and thus the stresses will be only tension.

The Darrieus rotor exhibits some rather unusual aerodynamic characteristics. At low rotational speeds the airfoil is stalled over an appreciable portion of a revolution. The rotor therefore produces almost no torque at low rotational speeds. The Darrieus rotor must therefore be provided with a starting system. This can be an electric motor that disengages when the rotor gains speed or, more simply, one or more small Savonius rotors mounted on the main rotor shaft. Since the Savonius develops maximum torque at start-up it is a useful complement to the more sophisticated and efficient Darrieus rotor.

One version of the Darrieus rotor uses straight blades held parallel to the vertical axis of rotation. Such a machine is sometimes called a cyclogiro or a giromill. The straight bladed Darrieus has the advantage that the blades can be easily hinged. By changing the blade pitch the low-speed stall region can be reduced.

The performance of a Darrieus rotor is very sensitive to tip speed ratio. At low rotational speeds the blade is stalled, at high speeds torque falls off rapidly. The optimal tip speed ratio is about 6 at which point the rotor efficiency is about 35 per cent.

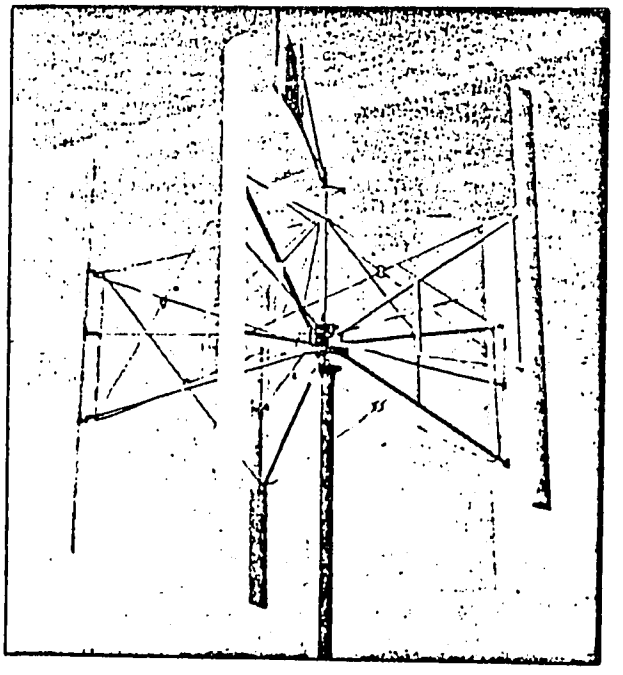

Figure 26 A straight-bladed Darrieus rotor. The pitch angle of the blades is changed automatically.

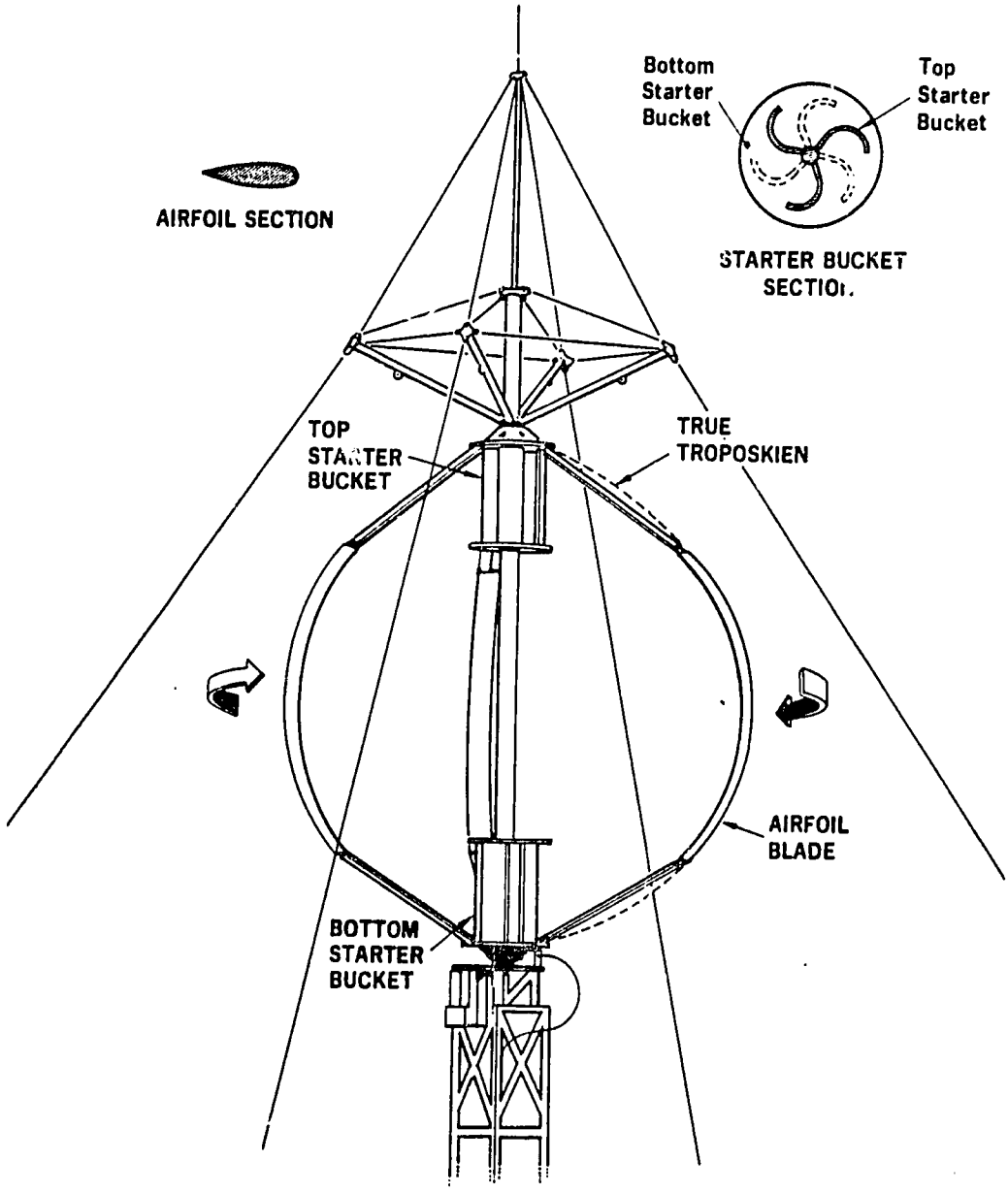

Figure 27. Darrieus vertical axis wind turbine

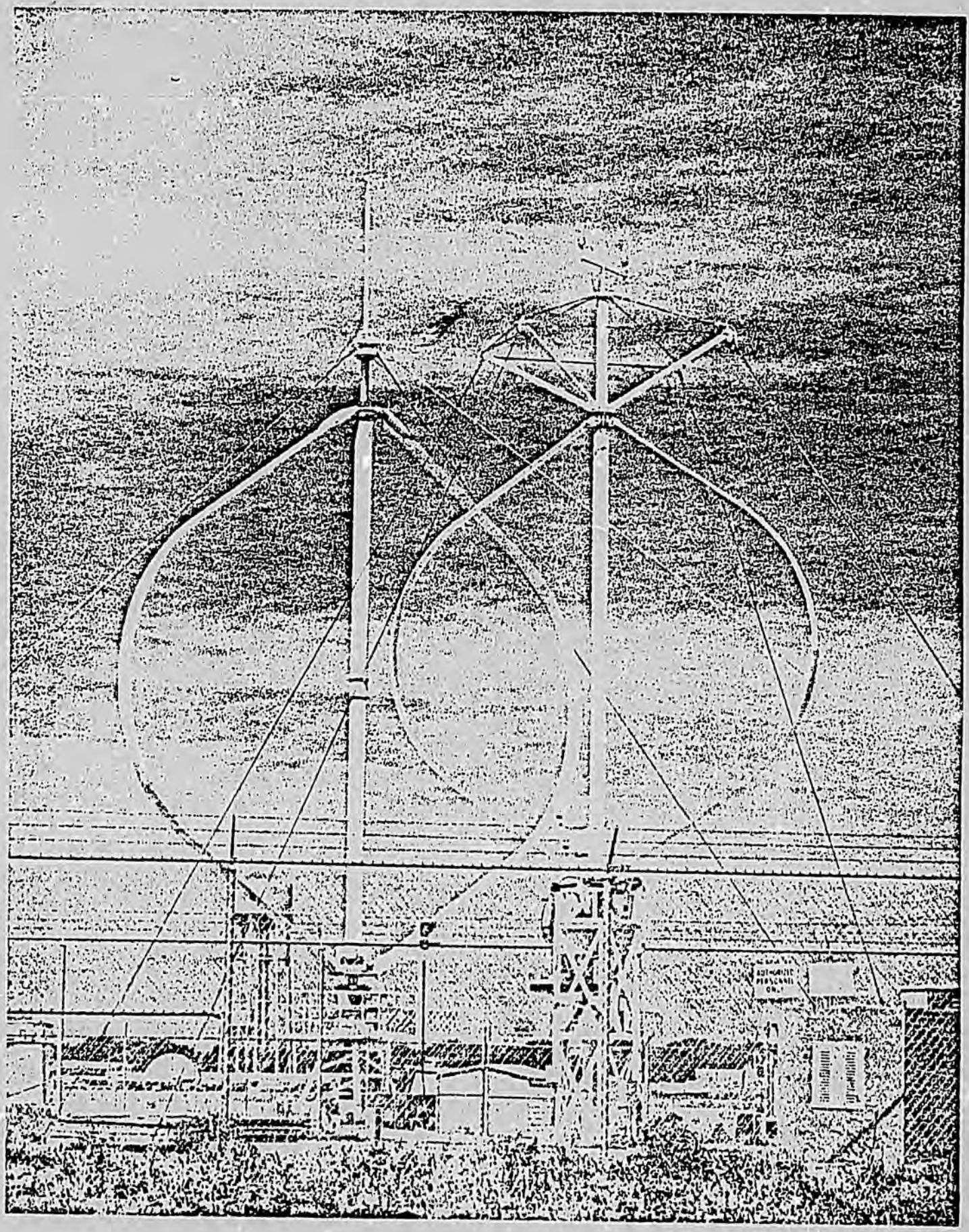

Figure 28. 5 m and 17 m Darrieus Turbines

Lift and Drag

Wind machines use a combination of lift and drag forces to convert the kinetic energy in the wind into a torque applied at the axis of the rotor. The drag force on an airfoil occurs in a direction parallel to the relative wind. The lift force acts in a direction perpendicular to the relative wind. The forces are shown in the diagram below.

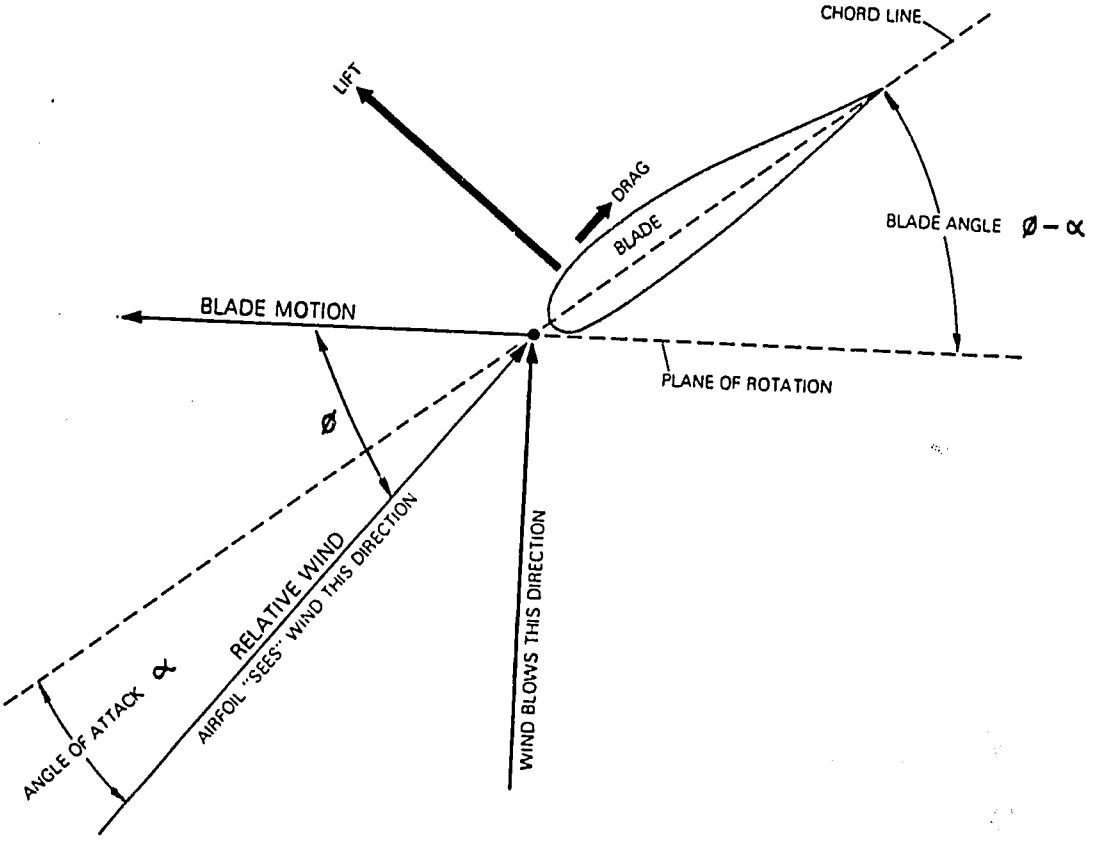

Figure 29 Vector diagram of the airflow at a single rotor blade. The driving force on a horizontal axis wind turbine is the forward component, L sin ∅ of the lift, reduced by the backward component, D cos ∅ of the drag. Airfoils with a high lift-to-drag ratio are therefore more efficient.

The principal attribute of the airfoil is the ability to produce a high lift while incurring only a small drag. Airfoils characteristically have a blunt nose and a finely tapering tail. They can be symmetrical or cambered as shown below.

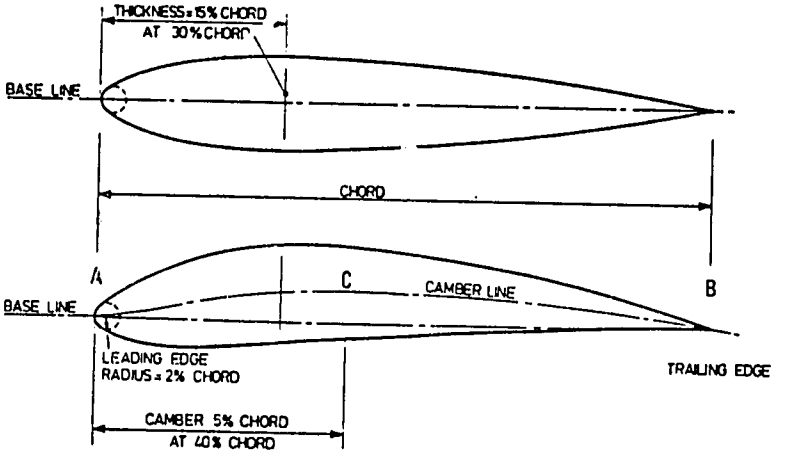

Figure 30. Geometry of symmetrical and cambered airfoils [15].

The airfoils above illustrate the characteristic features of (1) the nose radius, (2) the position and magnitude of the point of maximum thickness, and (3) the angle of the trailing edge. These parameters are usually expressed in terms of the chord length. The upper airfoil is symmetrical; it will produce no lift until the airflow makes an angle with the chord line as depicted in Figure 29. This angle is called the angle of attack. Symmetrical airfoils, used on boats for rudder and keels, are essential for lift-dominated vertical axis wind turbines like the Darrieus rotor. If the airfoil is to develop lift at zero angle of attack, then it must be cambered as shown by the lower airfoil in the figure above.

The airfoil properties of interest to the wind system designer are, of course, the lift and the drag, and sometimes the turning moment which the flow exerts on the airfoil. Typical curves of lift and drag, plotted against the angle of attack for a low-speed airfoil are shown in Figure 31 together with the ratio of the forces, called the lift to drag ratio or L/D ratio.

As the angle of attack is increased, the lift increases at a faster rate than the drag does until the blade stalls: the angle of attack at which the lift falls dramatically and drag rapidly increases.

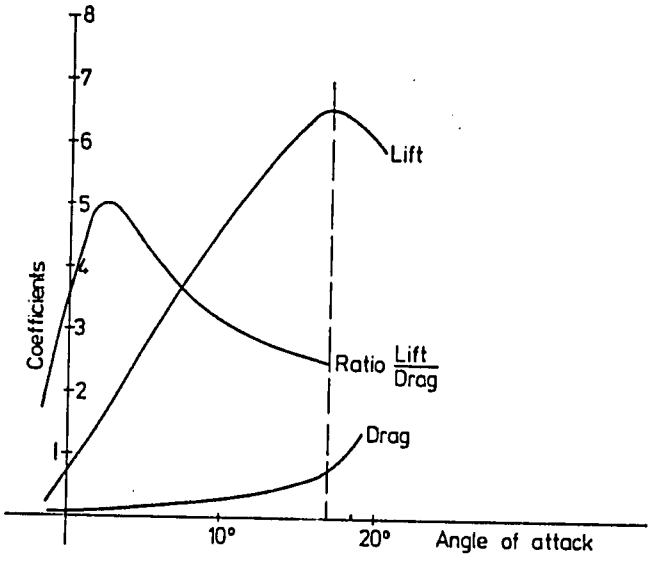

Figure 31. Properties of an airfoil [15]

The forces on the blade due to lift and drag may be calculated from

$$\text{Lift} = 1/2\ C_L \rho S V^2 \qquad \text{Newtons}$$

$$\text{Drag} = 1/2\ C_D \rho S V^2 \qquad \text{Newtons}$$

where C_L and C_D are the dimensionless coefficients of lift and drag respectively.

also ρ = air density, kg/m^3
s = blade surface area, m^2
V = airspeed, m/s

Generally, the higher the blade L/D ratio, the faster the rotor will spin, and the greater will be the coefficient of performance. But high L/D ratios arise only from sophisticated blade design which generally means an expensive rotor. We find, therefore, in windmill blade design the usual trade-offs between complexity, sophistication, performance, and cost. The table below shows how these trade-offs are usually resolved for different applications for typical horizontal axis wind systems.

Wind Machine	Design TSR	Blades	Blade Type	Blade L/D
Water pumper	1	6-20	Flat Plate	10
	1	6-20	Curved Plate	20-40
	1	4-10	Sail wing	10-25
Small wind-electric	3-4	4-6	Simple airfoil	10-50
	4-6	2-4	Twisted airfoil	20-100
	3-5	3-6	Sail wing	20-35
Large wind-electric	5-15	1-3	Twisted airfoil	20-100

The values of the lift and drag coefficients, C_L and C_D, vary with Reynolds number, but their general relationship, both with the angle of attack of the airfoil, and to each other is similar to the graphs shown below. A plot of C_L against C_D is called a polar-plot.

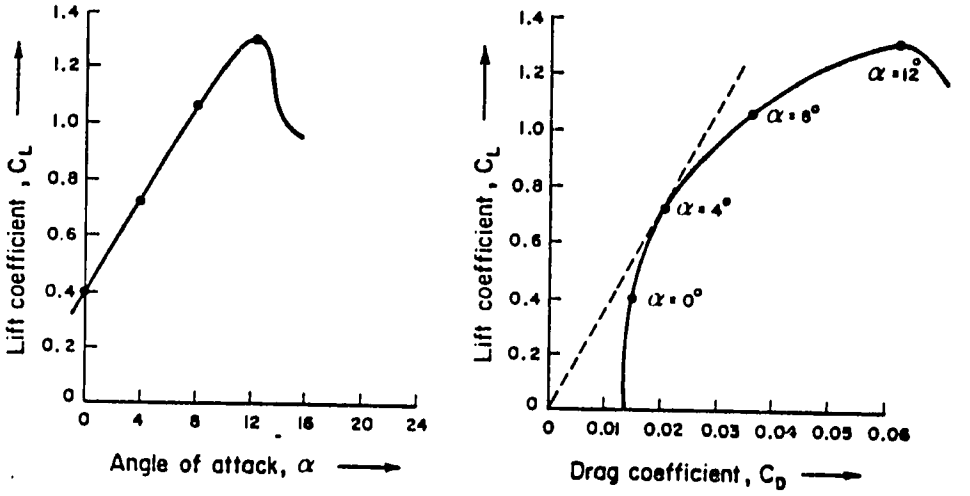

Figure 32. The lift and drag coefficients of a given airfoil [21]

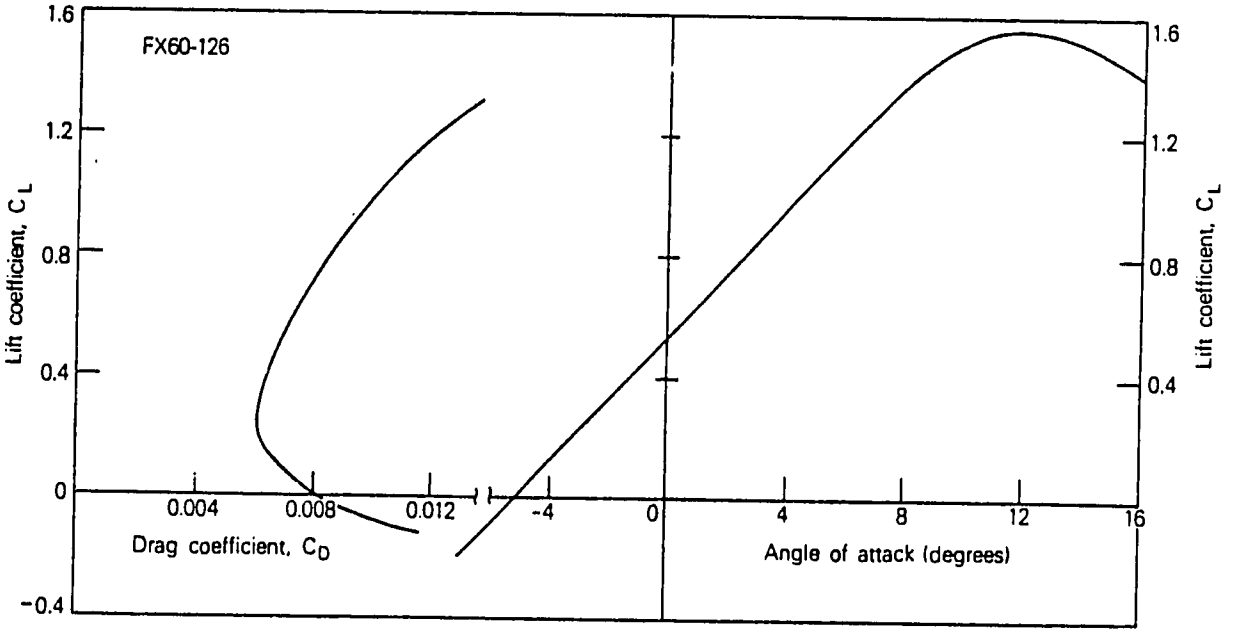

Figure 33. Drag polar plot for the FX60-126 airfoil [3]

The line from the origin tangential to the C_L -C_D curve marks the point on the curve where the lift/drag ratio is maximized. In the first of the graphs shown, this occurs at an angle of attack of 4 degrees. The values of α and C_L at maximum C_L/C_D ratios are important design parameters.

The values of these parameters for some common airfoils are given below in Table 2 [21].

Table 2

Typical values of the drag-lift ratio C_D/C_L and of α and C_L for a number of airfoils. The curvature of the curved plate profile is defined as the ratio of its projected thickness and its chord.

	C_D/C_L	α	C_L
Flat plate	0.1	5°	0.8
Curved plate (10 % curvature)	0.02	3°	1.25
Curved plate with tube on concave side	0.03	4°	1.1
Curved plate with tube on convex side	0.2	14°	1.25
Airfoil NACA 4411	0.01	4°	0.8

Rotor Design

The design of the rotor basically consists in finding the value of the chord, c, and the blade angle, $\phi - \alpha$, at a number of positions along the blade. We will use the following nomenclature

B	= number of blades
R	= radius of the swept area
C_{Ld}	= design lift coefficient
α_d	= angle of attack at design point
λ_d	= design tip speed ratio
β	= blade, or setting, angle
ϕ	= wind angle
c	= chord length
λ_r	= speed ratio at radius

A number of these parameters must be set before the rotor can be designed. Consideration of the average power required from the rotor, and the task for which the power is employed, leads to the selection of R, λ_d, and B. Then selection of an appropriate airfoil leads to the definition of C_{Ld} and α_d.

The type of load also sets λ_d: Water-pumping wind systems employ low-speed high-torque rotors with a design top speed ratio of between 1 and 2; electrical generating machines spin faster: small machines have $4 < \lambda_d < 6$, larger machines $6 < \lambda_d < 15$.

The number of blades is roughly related to the design tip speed ratio as follows:

λ_d	B	Machine Type
1	6-20	Water pumping
2	4-12	Water pumping
3	3-6	Small wind-electric
4	2-4	Small wind-electric
5-8	2-3	Large wind-electric
8-15	1-2	Large wind-electric

The airfoil parameters, C_{Ld} and α_d can be taken from Table 2 for simple flat and curved blades. For more sophisticated airfoils reference must be made to charts showing lift and drag coefficient at different angles of attack. The idea is to find the angle of attack at which the lift to drag ratio is highest. This angle sets α_d. The lift coefficient at this angle of attack is C_{Ld}.

The preliminary procedures outlined above set R, λ_d, B, C_{Ld} and α_d. The following formulae are then used

$$\lambda_r = \lambda_d \cdot \frac{r}{R} \tag{42}$$

$$\phi = \frac{2}{3} \arctan \frac{1}{\lambda_r} \tag{43}$$

$$C = \frac{8\pi r}{BC_{Ld}} .(1-\cos\phi) \tag{44}$$

$$\beta = \phi - \alpha_d \tag{45}$$

These formulae are used at different positions along the blade.

Example 1

A rotor is to be designed to drive a reciprocating pump. The diameter of the rotor is 2.74 meters. The rotor is to have six curved blades. At the design point $\alpha_d = 4°$ and $C_{Ld} = 1.1$. The rotor is to be designed for a tip speed ratio of 2 .

Solution

We first design the blades to have a constant lift coefficient along the length of the blades. The chord will therefore change. The procedure consists of calculating the chord, c, the blade angle β, at a number of positions along the blade. For example, take a point at 25 percent of the blade length at r = 0.343 meters. From Equation 37 the speed ratio at this position is given by

$$\lambda_r = 2 \cdot \frac{0.342}{1.37} = 0.5$$

then $$\phi = \frac{2}{3} \arctan \frac{1}{0.5} = 42.3°$$

then $$c = \frac{8\pi \times 0.3425}{6 \times 1.1} \cdot (1 - \cos 42.3)$$

$$= 0.339 \text{ metres}$$

and $$\beta = 42.3 - 4 = 38.3°$$

We therefore arrive at the figures tabulated below.

Position	r(m)	λ_r	ϕ	α_d	β	c(m)
1	0.3425	0.5	42.3°	4°	38.3°	0.339
2	0.685	1.0	30.0°	4°	26.0°	0.347
3	1.0275	1.5	22.5°	4°	18.5°	0.297
4	1.37	2	17.7°	4°	13.7°	0.247

It is apparent from these data that both the chord and the blade angle vary along the blade. Such a blade is difficult to fabricate, and it is common practice to design a more simple blade that approximates the blade shape calculated above without unduly sacrificing aerodynamic performance. One approach is to design a blade with a constant chord.

In this design procedure Equation 44has to be restructured as

$$C_{Ld} = \frac{8\pi r}{Bc} (1-\cos \phi)$$

Then, knowing the lift coefficient, C_L, as a function of the angle of attack, α, this angle is then determined at each position along the blade.

For example, suppose we wish to design a rotor with six constant chord blades with c= 0.324. The blades will be curved, with a 10% curvature. We need to know how the lift coefficient varies with the angle of attack.

Assume the graph below is applicable.

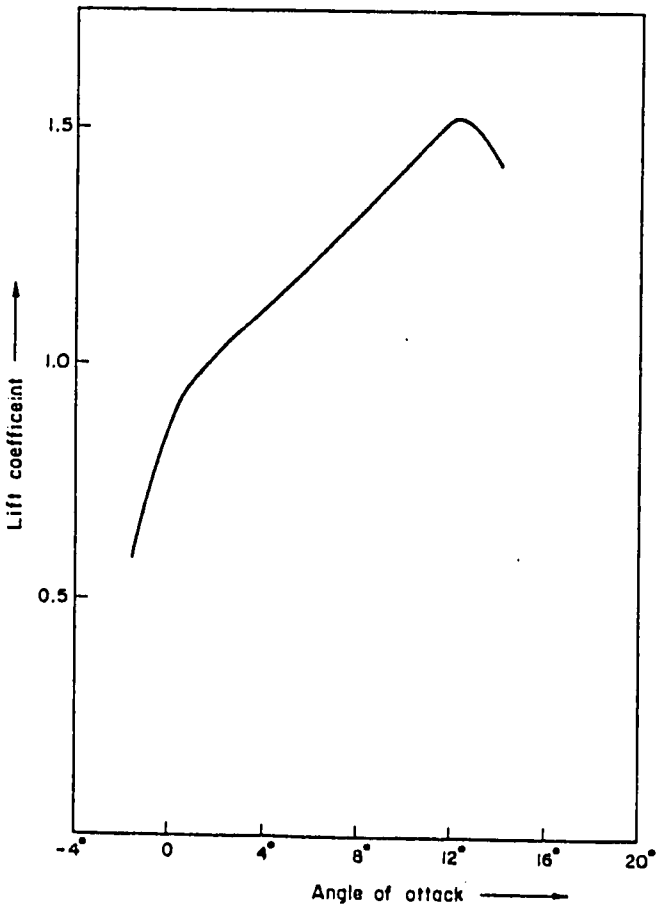

Figure 34. Lift coefficient as a function of angle of attack [21]

The calculation proceeds as follows. Assume the first position is again at r = 0.3425 metres. As before, λ_r, = 0.5 and ϕ = 42.3°. But now we compute the lift coefficient from

$$C_L = \frac{8\pi \times 0.3425}{6 \times 0.324} \cdot (1 - \cos 42.3)$$

$$= 1.15$$

From the graph above we estimate α as 4.5°. Following this procedure for the other blade positions, we arrive at the data tabulated below.

Position	r(m)	λ_r	ϕ	c(m)	C_L	α
1	0.3425	0.5	42.3°	0.324	1.15	4.5°
2	0.685	1.0	30.0°	0.324	1.19	5.3°
3	1.0275	1.5	22.5°	0.324	1.01	1.7°
4	1.37	2	17.7°	0.324	0.84	0°

Since it is difficult to manufacture a curved blade with a non-linear twist it is convenient to twist the blades so that the blade angle is about right at both ends and varies linearly between. So one might, for example, set blade angles of 38°, 31°, 24°, and 17°, for the positions indicated in the above table.

Water Pumping

There are two principal tasks for which wind machines are designed: pumping water and generating electricity. Each task requires a different type of wind machine. The water-pumping system must develop a high torque at start-up. Low speed multibladed rotors operating at tip speed ratios of about 1 are used. Figure 35 shows a typical wind driven water pumping system of the kind still common in the U.S.

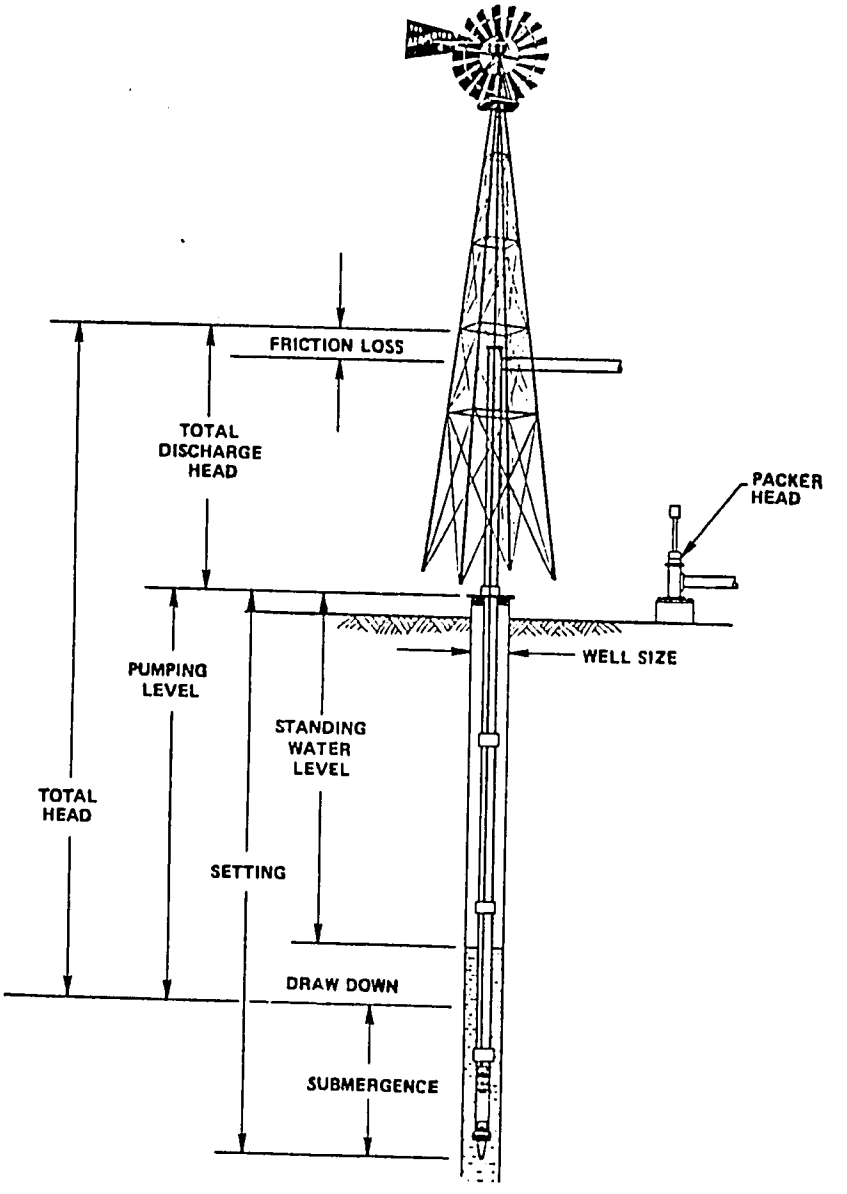

Figure 35 Typical water pumping wind system [7]

Irrigation methods fall into two categories: surface irrigation and well irrigation. In surface irrigation, water is led from rivers, lakes, tanks, etc. to the land to be irrigated by means of gravity flow or low-lift irrigation pumps. Well irrigation utilizes ground water resources by tapping underground aquifers through the construction of shallow open wells or deep tube wells.

Designing a water-pumping wind system is relatively straightforward. The first calculation is to determine how much water needs to be supplied, and how much power is required to pump the water from its point of supply to its point of use. Table 4 shows water requirements for rural communities and should be applicable to developing countries; Table 5 shows water requirements for farm animals based on U.S. experience.

TABLE 4.

Approximate water requirement for various purposes

Use	*Daily requirement*
Domestic	
minimum for survival	5 l/person
water carried home from distant communal supply	10 l/person
water carried home from nearby communal supply	30 l/person
one tap in each house	50 l/person
multiple tap connections	200 l/person
Livestock	
cattle	35 l/head
horses, mules and donkeys	20 l/head
sheep and goats	5 l/head
poultry	25 l/100
pigs	15 l/head
Irrigation	
including conveyance and field application losses	5 to 10 mm or 50 to 100 m^3/ha

The power, P, required to pump water is given by

$$P = \dot{m}gH \quad \text{Watts}$$

where $\dot{m}$ = mass flow, kg/s
g = acceleration due to gravity, 9.81 m/s^2
H = total head, metres

In this expression, the total head must also include friction losses in the piping system.

TABLE 5. Water Requirements for Farm Animals

Effect of External Temperature on Water Consumption

Water Consumption of Hogs
(Pounds per Hog per Hour)

Temperature (°F.)	*75-125 lb. hogs*	*275-380 lb. hogs*	*Pregnant Sows*
50	0.2	0.5	0.95
60	0.25	0.5	0.85
70	0.30	0.65	0.80
80	0.30	0.85	0.95
90	0.35	0.85	0.90
100	0.60	0.85	0.80

Water Consumption of Dairy Cows
(Gallons per Day per Cow)

Temperature	*Lactating Jerseys*	*Lactating Holsteins*	*Dry Holsteins*
50	11.4	18.7	10.4
50-70	12.8	21.7	11.5
75-85	14.7	21.2	12.3
90-100	20.1	19.9	10.7

Water Consumption of Hens
(Milliter per Bird per Day)

Temperature	*White Leghorn*	*Rhode Island Red*
70	286	294
80	272	321
90	350	408
100	392	371
70	222	216
70	246	286

Water Consumption of Sheep
(Pounds of Water per Day)

On range or dry pasture	5-13
On range (salty feeds)	17
On rations of hay and grain or hay, roots and grains	0.3-6
On good pasture	Little (if any)

Water Consumption of Pigs
(Pounds of Water per Day)

Conditions	
Body Weight—30 lbs	5-10
Body Weight—60-80 lbs	7
Body Weight—75-125 lbs	16
Body Weight—200-380 lbs	12-30
Pregnant Sows	30-38
Lactating Sows	40-50

Water Consumption of Chickens
(Gallons per 100 Birds per Day)

Conditions	
1-3 weeks of age	0.4-2.0
3-6 weeks of age	1.4-3.0
6-10 weeks of age	3.0-4.0
9-13 weeks of age	4.0-5.0
Pullets	3.0-4.0
Nonlaying hens	5.0
Laying Hens (moderate temperatures)	5.0-7.5
Laying Hens (temperature 90°F)	9.0

Water Consumption of Growing Turkeys
(Gallons per 100 Birds per Week)

Conditions	
1-3 weeks of age	8- 18
4-7 weeks of age	26- 59
9-13 weeks of age	62-100
15- 19 weeks of age	117-118
21-26 weeks of age	95-105

Water Consumption of Cattle

Class of Cattle	*Conditions*	*Pounds per Day*
Holstein calves (liquid milk or dried milk and water supplied)	4 weeks of age	10-12
	8 weeks of age	13
	12 weeks of age	18-20
	16 weeks of age	25-28
	20 weeks of age	32-36
	26 weeks of age	33-48
Dairy Heifers	Pregnant	60-70
Steers	Maintenance ration	35
	Fattening ration	70
Range Cattle		35-70
Jersey Cows	Milk Production 5-30 lbs/day	60-102
Holstein Cows	Milk Production 20-50 lbs/day	65-182
	Milk Production 80 lbs/day	190
	Dry	90

SOURCE: Water, *Yearbook of Agriculture*, U.S. Department of Agriculture *1955*.

Some interesting results from the field are presented by Fraenkel [11] in the chart shown below. The 16 ft. diameter four bladed sailwing rotors driving twin pumps clearly perform much better than the other systems. The vertical axis Savonius rotors are notably inefficient.

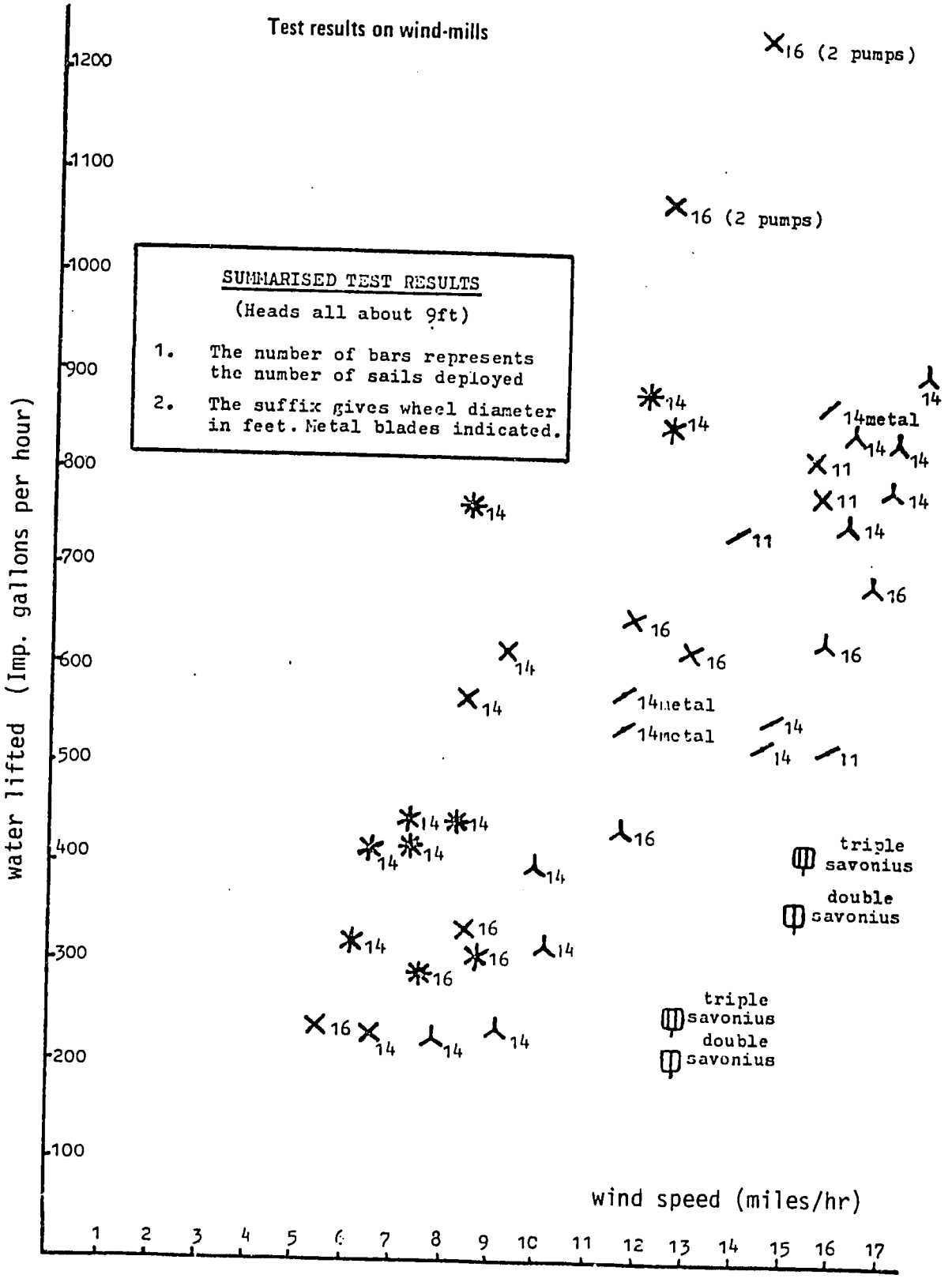

WATER-PUMPING WIND SYSTEMS (1)

NAME	TYPE	Diam. m.	OUTPUT			Power (2) Output, W	C_p (3)	V_i m/s	V_r m/s	V_o m/s	NOTES
			head, m	L/hr	V m/s						
Heller-Aller Co. Model: Baker, 6 ft.	Multibladed, horizontal axis, upwind	1.83	7.6	1325	6.7	27.5	0.06	3.1	6.7	11.2	(4)
			22.9	606		37.7	0.08				
			30.5	568		47.2	0.10				
			38.1	454		47.2	0.10				
Heller-Aller Co. Model: Baker, 8 ft.	Multibladed, horizontal axis, upwind	2.44	7.6	3407	6.7	70.7	0.08	3.1	6.7	11.2	(4)
			22.9	1325		82.5	0.10				
			30.5	908		94.3	0.11				
			38.1	833		103.7	0.12				
Heller-Aller Co. Model: Baker, 10 ft.	Multibladed, horizontal axis, upwind	3.05	7.6	4731	6.7	98.2	0.07	3.1	6.7	11.2	(4)
			22.9	1798		112.0	0.09				
			45.7	1060		132.0	0.10				
			76.2	814		169.0	0.13				
Heller-Aller Co. Model: Baker, 12 ft.	Multibladed, horizontal axis, upwind	3.66	7.6	9084	6.7	188.6	0.10	3.1	6.7	11.2	(4)
			22.9	4258		265.2	0.15				
			45.7	1987		247.6	0.14				
			91.4	757		188.6	0.10				
Dempster Industries Model: 6 ft.	Multibladed, horizontal axis	1.83	7.9	1976	6.7	42.7	0.09	2.2	6.7	22.4	$525, not including tower (4)
			11.9	1310		42.4	0.09				
			18.9	780		40.2	0.09				
			36.6	435		43.4	0.09				
Dempster Industries Model, 8 ft.	Multibladed, horizontal axis	2.44	11.3	2952	6.7	90.7	0.11	2.2	6.7	22.4	$760, not including tower (4)
			16.8	2139		97.7	0.12				
			27.1	1151		85.1	0.10				
			52.4	655		93.5	0.11				
Dempster Industries Model: 10 ft.	Multibladed, horizontal axis	3.05	17.4	2403	6.7	113.8	0.09	2.2	6.7	22.4	$1275, not including tower (4)
			26.2	1582		113.0	0.09				
			41.8	939		106.8	0.08				
			78.0	530		112.7	0.09				
Dempster Industries Model: 12 ft.	Multibladed, horizontal axis	3.66	25.3	3111	6.7	214.5	0.12	2.2	6.7	22.4	$2178, not including tower (4)
			38.1	2059		213.8	0.12				
			73.2	984		196.2	0.11				
			118.3	681		219.6	0.12				
Dempster Industries Model: 14 ft.	Multibladed, horizontal axis, upwind	4.27	37.8	2672	6.7	275.2	0.11	2.2	6.7	22.4	$3291, not including tower (4)
			57.0	1760		273.4	0.11				
			91.4	1045		260.3	0.10				
			176.8	602		289.9	0.11				

NAME	TYPE	Diam. m.	OUTPUT			Power (2) Output, W	C_p (3)	V_i m/s	V_r m/s	V_o m/s	NOTES
			head, m	L/hr	V m/s						
Aeromotor Model: 702-6	Multibladed, horizontal axis, upwind	1.83	5.2	3407	6.7	48.1	0.10	4.0	6.7	12.5	(4)
			8.2	2157		48.4	0.10				
			19.8	852		46.0	0.10				
			39.6	397		42.9	0.09				
Aeromotor Model: 702-8	Multibladed, horizontal axis, upwind	2.44	5.2	7097	6.7	100.2	0.12	4.0	6.7	12.5	(4)
			9.1	3974		99.0	0.12				
			24.4	1457		96.8	0.12				
			56.4	568		87.2	0.10				
Aeromotor Model: 702-10	Multibladed, horizontal axis, upwind	3.05	4.3	12,491	6.7	145.2	0.11	4.0	6.7	12.5	(4)
			14.0	3974		151.8	0.12				
			36.6	1457		145.2	0.11				
			85.3	568		132.0	0.10				
Aeromotor Model: 702-12	Multibladed, horizontal axis, upwind	3.66	6.7	12,491	6.7	228.2	0.13	4.0	6.7	12.5	(4)
			20.7	3974		224.5	0.12				
			54.9	1457		217.9	0.12				
			128.0	568		198.1	0.11				
Aeromotor Model: 702-14	Multibladed, horizontal axis, upwind	4.27	9.4	12,491	6.7	321.6	0.12	4.0	6.7	12.5	(4)
			29.9	3974		323.5	0.13				
			79.2	1457		314.7	0.12				
			182.9	568		282.9	0.11				
Aeromotor Model: 702-16	Multibladed, horizontal axis.	4.88	15.2	12,491	6.7	518.7	0.15	4.0	6.7	12.5	(4)
			48.8	3974		528.1	0.16				
			129.5	1457		514.4	0.15				
			304.8	568		471.6	0.14				
Sherman's Madural	Sailwing, HA, cretan-type	10.0	2.88 MJ over 12-hr period		2.8	66.7	0.07		2.2		Cost: RS 5480 (5, 6)
Voltas, Bombay	Multibladed, HA	6.0	5-6	10,000	4.2	149.9	0.12				(6)
			5-6	18,000	5.6	269.8	0.09				
Poghil (Sri Amm Chettiar)	Sailwing, HA, cretan-type	3.8	9	1500	4.2	36.8	0.07	2.8	5.6	12.5	Cost: Rs 3000 (7)
			9	1750	5.6	42.9	0.04				
Merin Ltd. Model: Mujahid	Multibladed, HA, upwind	3.05									Cost: Rs 15,000 + Rs 5000 for pump (8)
Merin Ltd. Model: Tawana	Multibladed, HA, upwind	6.1									Cost: Rs 60,000 + Rs 7000 for pump (8)
NAL Bangalore Model WP-2	Multibladed, HA, upwind	4.9	3.0	13,500	4.4	110.4	0.11	2.2	4.4	13.3	(9)
			7.6	6700		138.8	0.14				
			15.2	3400		140.8	0.15				
			30.4	1800		149.1	0.15				

NOTES 1. The amount of water pumped by a turbine depends not only on the size of the machine and its efficiency, but also on the total dynamic head which increases with decreasing pipe diameter and increased flow. The figures given are therefore only approximate. V_i = cut-in windspeed; V_r = rated windspeed; V_o = cut-out windspeed.

2. Power output is hydraulic power output, i.e. the power delivered to the water calculated as mass flow (kg/s) x gravity (9.81 m/s^2) x head (m).

3. Power coefficient defined here is the ratio of hydraulic power output to the power in the wind at the indicated windspeed.

4. Data is from Hunt, reference 7; costs are circa 1980.

5. Sails and spars replaced every 2 years for Rs 990; beams and poles replaced every 5 - 10 years for Rs 500; lifetime 10 - 15 years.

6. From Jagadeesh, reference 25.

7. From Geethaguru, reference 17.

8. From Merin brochure: Merin Ltd, Dada Chambers, M.A. Jinnah Rd., Karachi, Pakistan.

9. From Tewari, reference 27.

Example 2

A wind system is required to irrigate 4 hectares of land at a rate of 100 mm per month. A source of water is available that can provide water at a maximum rate of 6000 liters per hour. The total dynamic head is about 6.6 meters. The mean windspeed over the season when the irrigation is required is 6 m/s.

Solution

The amount of water to be supplied is given by 4 x 10,000 m^2 x 100 mm = 4000 m^3/month. Assuming a 31 day month, the average flow of water, $\dot{m}$, is

$$\dot{m} = \frac{4000 \times 1000}{31 \times 24 \times 3600} = 1.49 \text{ kg/s}$$

The water must be lifted against a head of 6.6 meters. The power required is therefore

$$P = 1.49 \times 9.81 \times 6.6 = 96.5 \text{ Watts}$$

It can be seen from the preceeding table showing the operating characteristics of several water-pumping wind systems, that most of the multibladed U.S. machines are designed to operate in 6 - 7 m/s winds. We assume we can obtain a machine with the following characteristics:

V_i = 3 m/s
V_r = 6 m/s
V_o = 22 m/s

The site windspeed, $\bar{V}$, is 6 m/s. Using Equations 32-35 we can find $\bar{P}/P_r$ = 0.621. So a machine rated at P_r = 1 kW will deliver, on the average, 621 Watts under this wind regime. The machine needed here therefore should be rated at 96.5/0.621 = 155 Watts at a windspeed of 6 m/s. At its rated windspeed the machine will have a power coefficient of about 0.1. The area of the turbine is found from Equation 40 as:

$$A = \frac{155}{0.6 \times 6^3 \times 0.1} = 11.96 \text{ m}^2$$

This is a rotor with a diameter of 3.9 meters.

If one had to select a machine from a manufacturer it is necessary to check that the machine will perform the intended task. For instance, consider the NAL machine--the WP-2--listed in the table. It appears to be large enough, with a 4.9 meter diameter rotor; it is reasonably efficient. But it is rated at a windspeed of 4.4 m/s. How much water will this machine pump if the mean windspeed is 6 m/s?

We have, for the WP-2, V_i = 2.2 m/s, V_r = 4.4 m/s, and V_o = 13.3 m/s. Using the same equations as before we find $\bar{P}/P_r$ = 0.75. From the table of data for the WP-2 it appears that P_r is about 140 Watts. So it would be expected that the WP-2 would deliver about 105 Watts over the season, which is enough to supply the necessary amount of water.

Electric Power Generation

Wind electric systems are generally low-solidity designs that operate at high tip speed ratios. Some of the early wind turbines used direct-drive generators where the generator armature turned at the same speed as the rotor. However, low speed generators, although robust and durable, are heavy and expensive. Modern wind electric systems usually have a gear system designed to gear up the rotor speed to a higher level. This permits the use of a smaller, lighter, less costly generator, but this saving is offset by the cost and maintenance requirements of the transmission system.

Generators installed in wind electric systems can produce either direct current (DC) or alternating current (AC). Alternating current is generated in an AC generator or alternator. The frequency of the generated current is governed by the rotational speed of the generator. To produce a constant frequency output the wind turbine must therefore spin at a constant speed even when the wind velocity is changing. This is accomplished by automatically altering the pitch of the blades; however, this is an expensive mechanism for small wind-electric systems.

Generators used to produce AC power at the same frequency as the utility supply are called synchronous generators. This type of system increases the complexity of the blade control mechanism and thus the cost of the wind machine. On very large wind turbines, synchronous generators are a practical concept. Generators that produce a constant frequency output under variable speed conditions are under development. These generators are called field modulated generators.

Generation of direct current, in the past, usually involved generation of AC inside the generator, then conversion to direct current by means of brushes and a commutator. The method commonly used now is to rectify the AC output of an alternator to direct current. This technique eliminates the need for brushes and a commutator and takes advantage of the superior low-speed characteristics of alternators. The three basic generator configurations are shown schematically in the figure below.

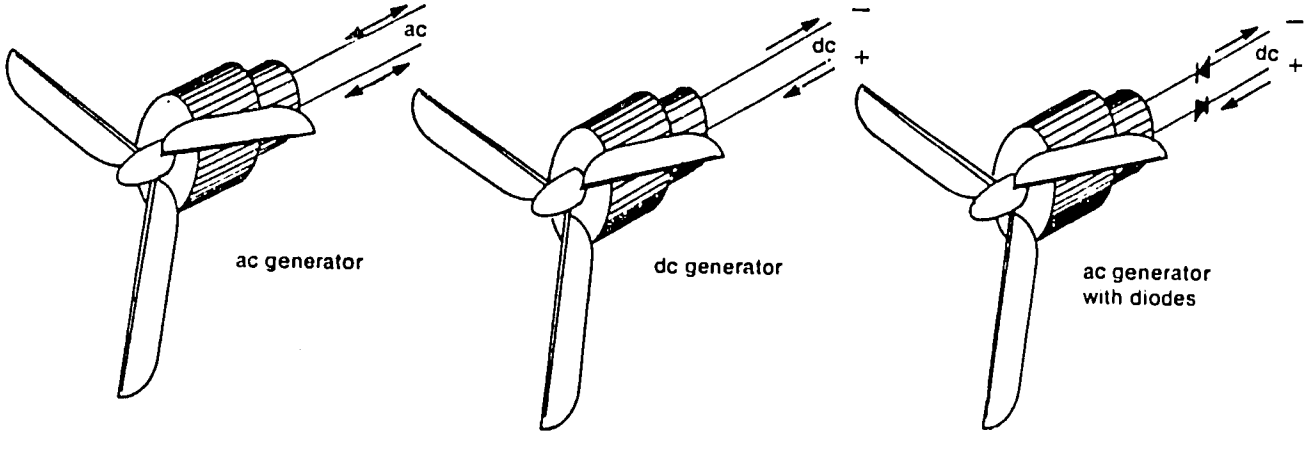

Figure 36 Three types of generators [2]

WIND ELECTRIC SYSTEMS (1)

NAME	TYPE (2)	Diameter meter	Rated Power, kW	Rated windspeed, m/s	Cut in m/s	Cut out m/s	Cost (3)
Aero Power Systems SL 1500	3 blades, HA, upwind	3.66	1.5	10.7	3.6	45	$3,000
Aerowatt S.A. 300 FP7	2 blades, HA, upwind	3.26	1.125	7.0	3.0	22.4	$7,400
Aerowatt S.A. 4100 FP7	2 blades, HA upwind	9.36	4.1	7.2	1.5	24.6	$35,350
Altos BWP-8B	multibladed, HA, upwind	2.32	1.5	12.5	4.5	33.5	
Altos BWP-12A	multibladed, HA, upwind	3.51	2.2	12.5	3.6	26.9	
American Wind Turbine SST-12	multibladed, HA, upwind	3.51	0.9	8.9	3.6	15.6	$1,496
American Wind Turbine SST-16	multibladed, HA, upwind	4.66	1.8	8.9	3.6	17.9	$2,420
Astral-Wilcon AW 8-C	3 blades, HA, upwind	7.92	8.0	9.8	3.6	22.4	$7,900
Astral-Wilcon 2.5 kW	3 blades, HA, upwind	4.57	2.5	13.4	4.0	13.4	$1,989
Dakota BC-4	3 blades, HA, upwind	4.27	4.0	12.1	3.8	none	$7,350
Dunlite Model M Standard	3 blades, HA upwind	3.96	2.0	11.2	4.3	35.8	$6,350
Dynergy 5-meter	3 blades, VA	4.57	3.3	10.7	4.5	35.8	$6,975
Elektro G.m.b.h. WV05	2 blades, HA, upwind	2.50	0.5	8.9	3.1	22.4	$3,871(4)
Elektro G.m.b.h. WVG 50G	3 blades, HA, upwind	5.00	6.0	13.4	3.1	22.4	$14,874
Enertech Corp. Model 1500	3 blades, HA, downwind	4.02	1.5	9.8	4.0	17.9	$2,900
Jacobs Model 45	3 blades, HA, upwind	4.27	1.8	10.3	3.1	44.7	$1,800
Kedco, Inc. Model 1200	3 blades, HA, downwind	3.66	1.2	9.4	3.1	31.3	$2,300
Kedco, Inc. Model 1610	3 blades, HA, downwind	4.88	2.0	9.8	4.5	26.8	$3,195

NAME	TYPE (2)	Diameter meter	Rated Power, kW	Rated windspeed, m/s	Cut in m/s	Cut out m/s	Cost (3)
North Wind Model 2 kW	3 blades, HA, upwind	4.15	2.0	9.8	3.6	none	$3,500
North Wind Model 3 kW	3 blades, HA, upwind	4.15	3.0	11.2	3.6	none	$4,600
Pinson Energy Corp. C2E3	3 blades, VA, cycloturbine	4.75	2.2	10.0	3.6	22.4	$4,500(4)
Sencenbaugh Model 1000-14	3 blades, HA, upwind	3.66	1.0	10.3	3.1	26.8	$2,950
Skyhawk Model IV	3 blades, HA, upwind	4.57	4.0	10.3	3.4	40.2	$4,795
Storm Master Model 10	3 blades, HA, downwind	10.0	18.0	10.7	3.8	none	$18,000
Whirlwind Power Co. Model A	2 blades, HA, downwind	3.05	2.0	11.2	4.5	22.4	$2,995
Zephyr Model 647 VLS-PM	3 blades, HA, downwind	6.10	15.0	13.4	3.6	20.1	$25,000

Notes:
1. Data from V. Daniel Hunt, "Windpower", (reference 7); for more information on the machines in this table see text.
2. HA: horizontal axis; VA: vertical axis.
3. All costs are circa 1980.
4. Not including tower.

Output Regulation

Generally, three methods are used for regulating or controlling the electric output of the generator:

1. Voltage regulators are used on field wound units to control the strength of the field, which in turn controls the output voltage.

2. Voltage controllers may be used on permanent magnet units to adjust voltage levels according to the output of the generator and the needs of the system.

3. No regulation at all. The output of the permanent magnet generator is used as is, while that of the wound field is fed back to the field either directly, or through a resistor to give a variablestrength field according to the strength of the generator output.

Figure 37 is a schematic wiring diagram for a simple DC system with a back up generator. The upper load monitor senses situations when the wind system generates more power than the batteries and loads A and B can accomodate, and responds by switching in load C. This load could be a resistance heater heating water, another battery bank, or any load that can take the excess power. The other load monitor is coupled to an automatic starting system for the auxiliary generator. When this monitor senses a low-voltage condition, which could occur during periods of light winds and heavy energy demand, the monitor starts up the generator to supply the load and to charge the batteries.

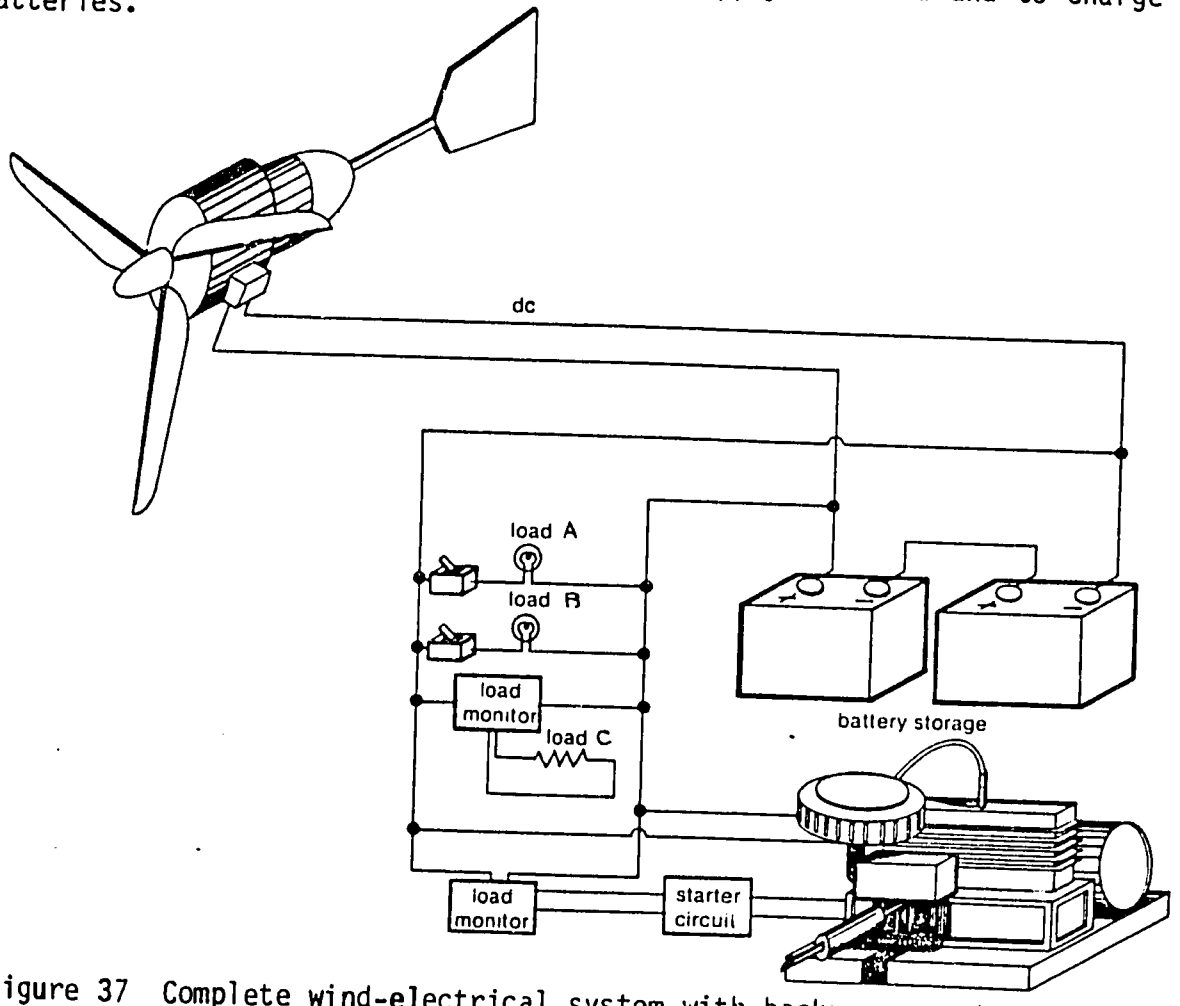

Figure 37 Complete wind-electrical system with backup generator

Wind System Economics

The economics of wind energy conversion systems are absolutely dependent on the wind speed characteristics of the intended site. This means that it is impossible to generalize about the cost of electricity, or of pumped water, produced by a wind turbine; the economist or planner must know the average windspeed at the site before he can make any estimate of these costs.

The approach to take, in order to estimate energy costs, has already been introduced in the earlier section on energy conversion (p 28 - 42). We demonstrate the technique again in this section for some commercially-available wind machines in operation in the US.

Wind Electric Machines

Overleaf is shown two photographs of wind turbines operating in the Altamont Pass area of California. This area, just east of San Francisco, enjoys high mean annual wind speeds of about 15 mph. The turbines in the righthand picture are manufactured by US Windpower in San Francisco. The characteristics of the model 56-50 are as follows:

Cut-in windspeed	8 mph
Rated power	50 kW
Rated windspeed	22 mph
Cut-out windspeed	40 mph

The cost of the machine is about $100,000, including sitework, and maintenance is estimated at $2000 per year.

In the absence of any detailed wind speed frequency data for the site, we assume a Rayleigh distribution of windspeed about the mean ($\overline{V}$ = 15 mph) and therefore proceed as outlined earlier.

Using Equations 19, and 32 - 35 we find

$$a = -\pi/4\overline{V}^2 = -0.0034907$$

$$A = a(22^2 - 8^2) = -1.46608$$

$$B = \exp[a(40^2 - 8^2)] = 0.004693$$

$$C = \exp[a(8^2)] = 0.7998$$

$$\text{so } \overline{P} = 50 \times 0.7998 \left[\frac{\exp(-1.46608) - 1}{-1.46608} - 0.004693\right]$$

$$= 20.793 \text{ kW}$$

So the energy produced each year may be estimated as 8760 x 20.793 = 182,147 kWh/yr.

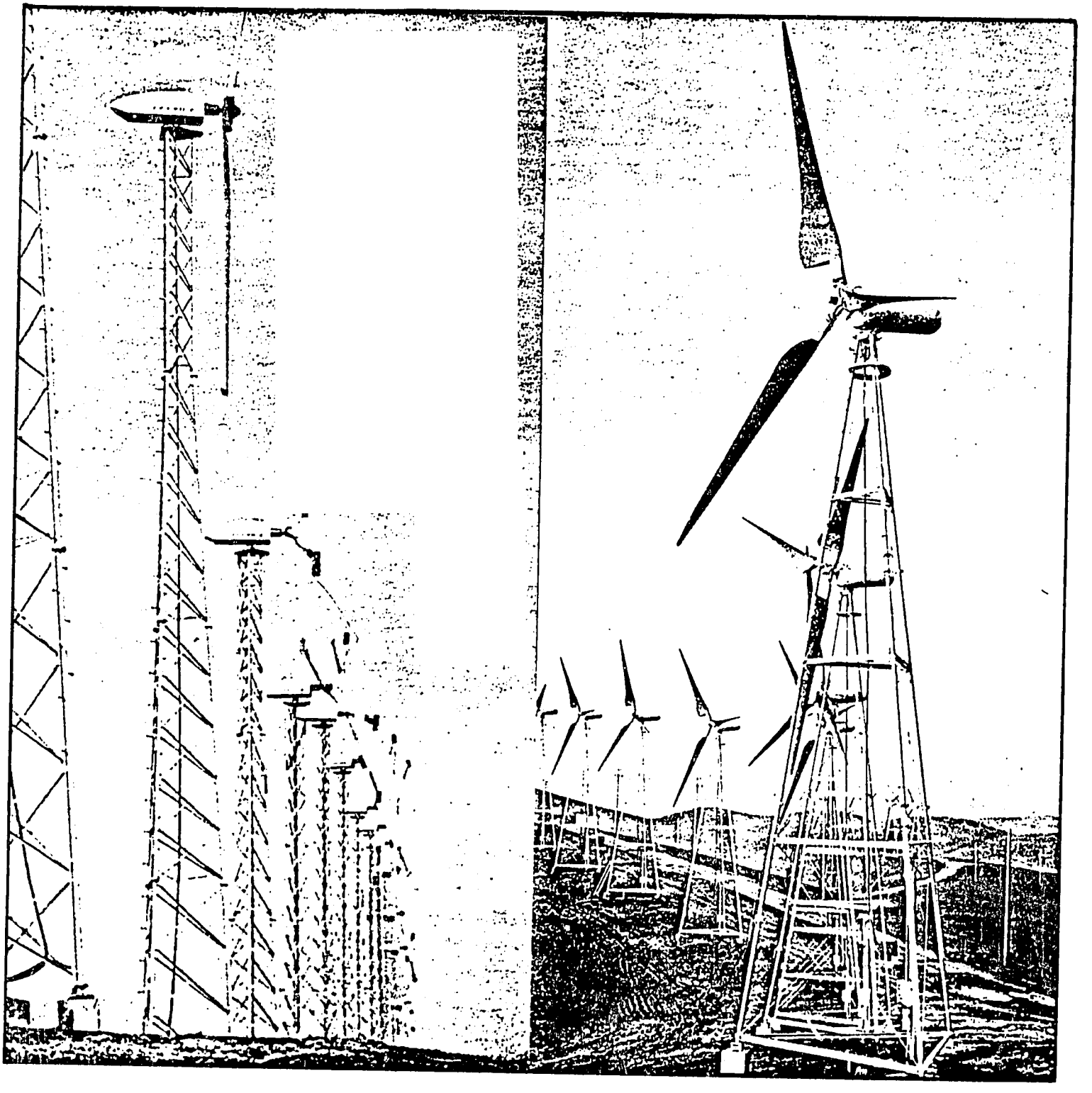

The windfarms of California: at the beginning of 1984, over 3400 wind turbines were in operation, with a rated power of 225 MW. Above left: ESI 80/200 machines, rated at 200 kW (at a windspeed of 25 mph); above right: US Windpower 56-50 machines, rated at 50 kW at a windspeed of 22 mph.

Assume that we finance the system with a 10-year loan at 12 percent interest; then a capital recovery factor (CRF) is given by

$$CRF\ (i,\ t) = \frac{0.12}{1 - (1 + 0.12)^{-10}} = 0.177$$

So annual charges are \$100,000 x 0.177 plus maintenance charges of \$2000 giving a yearly expenditure of \$19,700. The cost of energy is therefore:

$$\frac{19,700}{182,147} = 0.108\ \$/kWh$$

So the estimated cost of electrical energy production is approximately 11¢/kWh.

In the US, this cost would not be competitive with more conventional electric power technologies, but generous federal and state subsidies and tax credits make California windfarms an attractive proposition to many investors.

As another example, again using data from a real machine operating in California, consider the Mod-2 wind machine located in Solano County. This large two-bladed machine has been generating powersince April 1982. Technical data is shown below.

Rated capacity	2.5 MW
Rotor rotational speed	17.5 rpm
Rotor tip speed	190 mph
Generator speed	1800 rpm
Cut-in wind speed	14 mph
Cut-out wind speed	60 mph
Rated wind speed	20 mph
Tower height	200 feet
Rotor length tip-to-tip	300 feet
Rotor weight	94 tons
Total weight	314 tons

The cost of the turbine was \$6.7 million; the mean annual windspeed at the site is estimated as 20 mph. Following the analytical procedure outlined previously, we have

$$a = -0.00196$$

$$A = -0.40055$$

$$B = 0.001251$$

$$C = 0.6805$$

The annual energy production is therefore given by

$$8760 \times 2500 \times 0.6805 \left[\frac{\exp(-0.40055) - 1}{-0.40055} - 0.0125\right]$$

$$= 12.2612 \times 10^6\ kWh/yr$$

Assuming the same financial arrangements as for the previous example, and operation and maintenance costs of 2% of capital costs, annual expenditures would be 134,000 + 0.177 x 6.7 x 10^6 = 1.3199 million dollars a year. Energy costs would therefore be given by

$$\frac{1.3199 \times 10^6}{12.2612 \times 10^6} = 0.108 \text{ \$/kWh}$$

coincidentally, exactly the same as the cost of energy from the smaller machine.

Only a few of these large machines have been built and put into operation in the US. The hope is that if a sufficient number of these big machines are purchased, the price will drop to about a million dollars per machine. This would drop the cost of power generation to perhaps 2.5¢/kWh, a cost which would be fully competitive with conventional electric power technologies.

Water-Pumping Machines

The analysis of water-pumpers is essentially the same as the analysis of wind-electric machines, except that there is usually less data available on machine performance. But the table on page 68 gives operating data that can be used to estimate the cost of pumping water using wind machines.

Take for example the 12 ft. Dempster machine. For a range of mean windspeed it is possible to estimate the average power produced by this wind machine using the data in the table, and substituting these values in Equation 35, taking the rated power as about 210 Watts.

The cost of the Dempster is about $2200 (1980). Using a capital recovery factor of 0.2638 (10 percent over five years), and assuming $100 per year for routine maintenance, annual expenses for the first five years are 2200 x 0.2638 + 100 = $680/yr. Dividing this figure by the amount of hydraulic energy delivered by the pump at each mean windspeed gives the cost of pumping water. The table below gives the calculated data.

Table 8. Cost of Hydraulic Energy from Wind Machine

mean windspeed $\bar{V}$, m/s	hydraulic energy delivered kWh/yr	energy cost $/kWh
3	335	2.03
4	635	1.07
5	899	0.76
6	1034	0.66
7	1256	0.54
8	1366	0.50
9	1440	0.47
10	1484	0.46

The actual quantity of water pumped will depend on the head, H meters. The flow can be found from:

$$\text{flow} = \frac{\text{energy delivered (kWh/yr)}}{8.76 \times g \times H} \quad \text{kg/s}$$

where g is 9.81 m/s^2. The cost of water, in terms of so many dollars per cubic meter, therefore depends on the characteristics of the water resource at the site.

Water-pumping wind machines must be able to compete economically with small diesel engine pumps, if wind machines are to have a role in irrigation in the rural areas of developing countries. As an example, consider the following diesel engine pump, the characteristics of which are listed below.

Engine:	single cylinder air-cooled diesel
Rated power:	3 kW
Cost:	$1200
Fuel consumption:	0.42 liter/hr per kW
Lube oil:	0.008 liter/hr per kW
Pump efficiency:	30 percent
Maintenance:	3¢ per hour of operation

The engine will deliver 3 kW x 0.3 = 0.9 kW of hydraulic power. If E is the hydraulic energy required annually (kWh/yr), then the number of hours of operation, h, is simply

$$h = E/0.9 \quad \text{hr/yr}$$

As before, we assume a capital recovery factor based on 5 years and 10 percent interest; so CRF (0.1, 5) = 0.2638. Annual costs therefore consist of 4 component expenses:

	$/yr
Capital charges (1200 x 0.2638	317
Fuel costs (C_F, $/liter)	(0.42 x 3) x h x C_F
Lube costs (C_L, $/liter)	(0.008 x 3) x h x C_L
Maintenance	0.03 x h

The cost of lube oil is taken to be twice the cost of diesel fuel; so $C_L = 2\ C_F$. So an equation can be developed for the cost of hydraulic energy, C_E ($/kWh):

$$C_E = 317 + (1.308\ C_F + 0.03) \times h \quad \$/kWh$$

Table 9 below shows the results of this calculation for a range of energy requirements and for a range of diesel fuel costs.

Hydraulic energy, kWh/yr	Operating time, hr/yr	Cost of hydraulic energy, $/kWh, at different fuel costs (¢/liter) 40	50	80
500	556	1.25	1.54	1.83
1000	1111	0.93	1.22	1.51
1500	1667	0.83	1.12	1.41
2000	2222	0.77	1.06	1.35
2500	2778	0.74	1.03	1.32

This analysis clearly suggests that in any area of irrigation where there are mean windspeeds of 5 m/s or above, wind powered pumps will be cheaper than diesel engine pumps. With windspeeds below 5 m/s a detailed analysis will be necessary to determine which option appears more favorable.

However, there are additional considerations that favor the wind machines as a water-pumping technology. First of all, diesel fuel is more expensive in the rural areas of many developing countries; it is also impossible to obtain from time to time. And its price is likely to rise in the future. Secondly, there is evidence that locally built wind machines can probably be constructed less expensively than the American Dempster machine used in the example above. For instance, locally fabricated sail windmills in Ethiopia cost less than half the price of an imported 8 ft. diameter Dempster machine, and also pumped more water [11].

References

1. Park, J., and Schwind, D., "Wind Power for Farms, Homes, and Small Industry", NTIS:RFP-2841/1270/78/4, September 1978.

2. Home Wind Power, U.S.D.O.E., Garden Way Publishing, Charlotte, Vermont, 1981.

3. Park, J., "The Wind Power Book", Cheshire Books, Palo Alto, California, 1981.

4. Wegley, H.L., "A Siting Handbook for Small Wind Energy Conversion Systems", Battelle Pacific Northwest Laboratories, NTIS:PNL-2521, May 1978.

5. Eldridge, F.R., "Wind Machines", 2nd ed., Van Nostrand Reinhold Co., 1980.

6. Golding, E.W., "The Generation of Electricity by Wind Power", E.F.N. Spon, New York, 1955.

7. Hunt, V.D., "Windpower", Van Nostrand Reinhold Co., 1981.

8. Wind Power, Proceedings of the U.N. Conference on New Sources of Energy, Vol. 7, Rome, August 1961.

9. Bossell, Hartmut, "Low-cost Windmill for Developing Nations", VITA, 1970.

10. Kozlowski, J.A., "Savonius Rotor Construction", VITA, 1977.

11. Fraenkel, P., "Food From Windmills", Intermediate Technology Publications Ltd., London, 1975.

12. Wegley, H.L., "A Siting Handbook for Small Wind Energy Conversion Systems", Battelle Pacific Northwest Labs., PNL-2521, 1978. Available from NTIS.

13. Cliff, W.C., "The Effect of Generalized Wind Characteristics on Annual Power Estimates from Wind Turbine Generators", Pacific Northwest Laboratories, PNL-2436, 1977. Available from NTIS.

14. "Wind Machines", National Science Foundation, 1975. Available from U.S. Government Printing Office, Stock number 038-000-00272-4.

15. Calvert, N.G., "Windpower Principles", Charles Griffin and Co., London, 1981.

16. Tewari, S.K., "Economics of Wind Energy Use for Irrigation in India", Science, 202:481 (1978).

17. Geethaguru, V., "Poghil-A Low Cost Windmill for Water Pumping", Sri A.M.M. Murugappa Chettiar Research Centre, Monograph No. 10, Madras, India, 1980.

References

1. Park, J., and Schwind, D., "Wind Power for Farms, Homes, and Small Industry", NTIS:RFP-2841/1270/78/4, September 1978.

2. Home Wind Power, U.S.D.O.E., Garden Way Publishing, Charlotte, Vermont, 1981.

3. Park, J., "The Wind Power Book", Cheshire Books, Palo Alto, California, 1981.

4. Wegley, H.L., "A Siting Handbook for Small Wind Energy Conversion Systems", Battelle Pacific Northwest Laboratories, NTIS:PNL-2521, May 1978.

5. Eldridge, F.R., "Wind Machines", 2nd ed., Van Nostrand Reinhold Co., 1980.

6. Golding, E.W., "The Generation of Electricity by Wind Power", E.F.N. Spon, New York, 1955.

7. Hunt, V.D., "Windpower: A Handbook on Wind Energy Conversion Systems", Van Nostrand Reinhold Co., New York, 1981.

8. Wind Power, Proceedings of the U.N. Conference on New Sources of Energy, Vol. 7, Rome, August 1961.

9. Bossell, Hartmut, "Low-cost Windmill for Developing Nations", VITA, 1970.

10. Kozlowski, J.A., "Savonius Rotor Construction", VITA, 1977.

11. Fraenkel, P., "Food From Windmills", Intermediate Technology Publications Ltd., London, 1975.

12. Wegley, H.L., "A Siting Handbook for Small Wind Energy Conversion Systems", Battelle Pacific Northwest Labs., PNL-2521, 1978. Available from NTIS.

13. Cliff, W.C., "The Effect of Generalized Wind Characteristics on Annual Power Estimates from Wind Turbine Generators", Pacific Northwest Laboratories, PNL-2436, 1977. Available from NTIS.

14. "Wind Machines", National Science Foundation, 1975. Available from U.S. Government Printing Office, Stock number 038-000-00272-4.

15. Calvert, N.G., "Windpower Principles", Charles Griffin and Co., London, 1981.

16. Tewari, S.K., "Economics of Wind Energy Use for Irrigation in India", Science, 202:481 (1978).

17. Geethaguru, V., "Poghil-A Low Cost Windmill for Water Pumping", Sri A.M.M. Murugappa Chettiar Research Centre, Monograph No. 10, Madras, India, 1980.

18. Stanley, D., "The Arusha Windmill: A Construction Manual", VITA, 1977.

19. Van der Elst, W.J., "The Aerodynamics of Axial Flow Wind Power Turbines", MEW/2720, Mechanical Engineering Research Institute, Pretoria, 1979.

20. Le Gourieres, D., "Wind Power Plants: Theory and Design", Pergamon Press, New York, 1982.

21. Jansen, N.A.M., et. al., "Wind Rotor Design", Renewable Energy Review Journal, 4 (1): 1982.

22. "Meteorological Aspects of the Utilization of Wind as an Energy Source", World Meteorological Organization, Technical Note NO. 175, WMO, Geneva, Switzerland, 1981.

23. Mikhail, A., "Wind Power for Developing Nations", Solar Energy Research Institute, SERI/TR-762-966, July, 1981.

24. Hirshberg, Gary, "Water Pumping Windmill Handbook", New Alchemy Institute; published by Brick House Publishing Co., Andover, Massachusetts, 1982.

25. Jagadeesh, A., "Windmills for Irrigation in India", Renewable Sources of Energy Journal, Vol. 1, No. 2, (1983).

26. Malhotra, K.S. and Kaur M., "Black Level Planning in Energy Management: Case Study of a Rural Section in Rajasthan, India", Renewable Sources of Energy Journal, Vol. 1, No. 3, (1983).

27. Tewari, S.K., "A Review of Efforts Made in India for Wind Power Utilization", in Proceedings of the meeting of the Expert Working Group on the Use of Solar and Wind Energy, Energy Resources Development Series No. 16, UN, New York, 1976.

28. Mubayi, V. et alia, "Irrigation in Less Developed Countries", Brookhaven National Laboratory, Upton, New York, 1979.

WIND ENERGY BIBLIOGRAPHY

1. **Wind Power Plants - Theory and Design**, by Desire Le Gourieres, University of Dakar. Published by Pergamon Press, Elmsford, New York; 285 p, 1982.

2. **The Wind Power Book**, by Jack Park. Published by Cheshire Books, Palo Alto, California; 253 p, 1981.

3. **Windpower: A Handbook on Wind Energy Conversion Systems**, by V. Daniel Hunt. Published by Van Nostrand Reinhold Co., New York; 610 p, 1981.

4. **The Wind Cyclopedia**, prepared by the Power Company-Midwest Inc. Available from Wind Cyclopedia, PO Box 221; Genesee Depot, Wisconsin 53127; 204 p, 1980.

5. **Wind Machines**, 2nd edition, by Frank Eldridge, MITRE Corporation. Published by Van Nostrand Reinhold Co., New York; 214 p, 1980.

6. **Commercial Applications of Wind Power**, by Paul Vosburgh. Published by Van Nostrand Reinhold Co., New York; 279 p, 1983.

7. **Winds and Wind System Performance**, by C.G. Justus, Georgia Institute of Technology. Published by The Franklin Institute Press, Philadelphia, Pennsylvania; 120 p, 1978.

8. **Wind Power for Developing Nations**, by Amir Mikhail, Solar Energy Research Institute. Available from NTIS (DE81 025792), Springfield, Virginia; 320 p, July 1981.

9. **Meteorological Aspects of the Utilization of Wind as an Energy Source.** Technical Note No. 175, World Meteorological Organization. Available from the WMO, Geneva, Switzerland; 180 p, 1981.

10. **Wind Energy Information Directory**, prepared by the Solar Energy Research Institute. Available from the US Government Printing Office (S/N 061-000-00350-9), Washington, D.C.; 28 p, 1980.

11. **Brochures of Wind Turbine Manufacturers**, prepared by the Alternative Energy Institute. Available from this institute at: West Texas State University, Box 248, Canyon, Texas; May 1984.

12. **Wind Power for Farms, Homes, and Small Industry**, by Jack Park and Dick Swind. Available from NTIS (RFP-2841/1270/78/4), Springfield, Virginia; 1978. This text was later republished as: "Home Wind Power"; available from Garden Way Publishing, Charlotte, Vermont; 203 p, 1981.

13. **Wind Power**, Vol. 7 of the proceedings of the UN Conference on New Sources of Energy, Rome, 1961. Available from the United Nations, New York; (E/F.63.I.41), 408 p, 1964.

14. **Rural Electric Wind Energy**, proceedings of the workshop held in Boulder, Colorado, June 1982. Available from NTIS (DE83004406), Springfield, Virginia; 320 p, 1983.

15. **Aerodynamic Performance of Wind Turbines**, by Robert Wilson et. al. Available from NTIS (PB 259089), Springfield, Virginia; 164 p, June 1976.

16. **The Effect of Generalized Wind Characteristics on Annual Power Estimates from Wind Turbine Generators**, by William Cliff, Battelle Pacific Northwest Laboratories. Available from NTIS (PNL-2436), Springfield, Virginia; 48 p, October 1977.

17. **Food from Windmills**, by Peter Fraenkel, ITGD. Available from Intermediate Technology Publications, King St., London, England; 75 p, 1975.

18. **Literature Survey: Horizontal Axis Fast Running Wind-Turbines for Developing Countries**, by W. Jansen, (SWD 76-2). Available from SWD, Amersfoort, The Netherlands; 43 p, 1976.

19. **Horizontal Axis Fast Running Wind-Turbines for Developing Countries**, by W. Jansen, (SWD 76-3). Available from SWD, Amersfoort, The Netherlands; 91 p, 1976.

20. **Rotor Design for Horizontal Axis Windmills**, by W. Jansen and P. Smulders; (SWD 77-1). Available from SWD, Amersfoort, The Netherlands; 52 p, 1977.

21. **Construction Manual for a Cretan Windmill**, by N. Van de Ven; (SWD 77-4). Available from SWD, Amersfoort, The Netherlands; 59 p, 1977.

22. **Performance Characteristics of Some Sail and Steel-Bladed Windrotors**, by Th. A.H. Dekker, (SWD 77-5). Available from SWD, Amersfoort, The Netherlands; 60 p, 1977.

23. **Savonius Rotors for Water Pumping**, by E.H. Lysen et. al., (SWD 78-2). Available from SWD, Amersfoort, The Netherlands; 42 p, 1978.

24. **Matching of Wind Rotors to Low Power Electrical Generators**, by H.J. Hengeveld et. al., (SWD 78-3). Available from SWD, Amersfoort, The Netherlands; 85 p, 1978.

25. **Catalogue of Windmachines**, by L. Van der Stelt, (SWD 79-1). Available from SWD, Amersfoort, The Netherlands; 41 p, 1979.

26. **Darrieus Wind Turbine and Pump Performance for Low-Lift Irrigation Pumping**, by L. Hagen an M. Sharif, US Department of Agriculture. Available from NTIS (DE82016270), Springfield, Virginia; 51 p, 1981.

27. **Electric Utility Value Determination for Wind Energy**, Vol. I - A Methodology, Vol. II - A User's Guide, by David Percival and James Harper, Solar Energy Research Institute. Available from NTIS (SERI/TR-732-604), Springfield, Virginia; 1981.

28. **Water Pumping Windmill Book**, by Gary Hirshberg. A New Alchemy publication available from Brick House Publishing Co., Massachusetts; 141 p, 1982.

29. **Wind Energy: How To Use It**, by Paul Gipe. Available from Mother Earth News, Hendersonville, North Carolina; 400 p.

30. **How to Build a Cretan Sail Windpump**, by R.E. Mann. Available from ITDG publications, New York; 80 p, 1979.

31. **Wind Industry News Digest** (journal), published twice monthly by Alternative Sources of Energy, Inc., 107 S. Central Ave., Milaca, Minnesota 56353.

32. **Your Wind Driven Generator**, by Benjamin Wolff. Published by Van Nostrand Reinhold, New York; 208 p, 1984.

33. **A Siting Handbook for Small Wind Energy Conversion Systems**, by H. Wegley et. al., Battelle Memorial Institute, Pacific Northwest Laboratories. Available from the National Technical Information Serivce, (PNL-2521), Springfield, Virginia; 1978.

34. **A Siting Handbook for Large Wind Energy Systems**, by T. Hiester and W. Pennell, Battelle Memorial Institute, Pacific Northwest Laboratories. Available from the National Technical Information Service, Springfield, Virginia; 514 p, 1981.

35. **Windletter**. The newsletter of the American Wind Energy Association (AWEA). The AWEA also publishes the proceedings of the annual conferences they organize. Contact: AWEA, Washington, D.C.

36. **Windpower Principles: Their Application on a Small Scale**, by N.G. Calvert, University of Liverpool. Published by Charles Griffin and Co., Crendon House, High Wycombe, Buckinghamshire HP13 6LE, England; 122 p, 1979.

37. **Savonius Rotor Construction**, by Jozef Kozlowski. Published by VITA, Arlington, Virginia; 53 p, 1977.

38. **The Generation of Electricity by Wind Power**, by E.W. Golding. Published by E & F.N. Spon Ltd., 11 New Fetter Lane, London EC4P 4EE, England; 338 p, 1976.

39. **Introduction to Wind Turbine Engineering**, by Andrze Wortman. Published by Butterworth Publishers, 80 Montvale Ave., Stoneham, Massachusetts 02180; 130 p, 1984.

List of Manufacturers

Water Pumping Wind Systems

Aeromotor, Division of the
Valley Pump Group
P.O. Box 1364
Conway, Arkansas 72032

Agro-Aids
27 Shrungar Shopping Centre
Mahatma Ghandi Road
Bangalore 560001
India

Bowjon
2829 Burton Avenue
Burbank, California 91504

S.A. Bruno
Route du Mans
Bonchamps-les-Laval
53210 Agentre
France

Dempster Industries, Inc.
P.O. Box 848
Beatrice, Nebraska 68310

Eoliennes Humblot
8 Rue d'Alger
Coussey
88300 Neufchateau
France

ETS Poncelet & Cie
BP No. 1
10380 Plancy L'Abbage
France

Heller-Aller Co.
P.O. Box 29
Napoleon, Ohio 43545

M.B.P. (S.A.) PTY Ltd
P.O. Box 2047
Adelaide
South Australia 5001

Reymill Steel Products
Sta. Rosa
Neuva Ecija
Philippines

Sidney Williams & Co. (Pty) Ltd
P.O. Box 22
Dulwich Hill
New South Wales
Australia 2203

Southern Steel Works Ltd
Ballyhale
Co. Kilkenny
Ireland

Sparco (Denmark)
c/o Enertech Corp.
P.O. Box 420
Norwich, Vermont 05055

Tai U Sa Industrial Factory
No. 5g/15 M007
2 Pracharaj 2 Road
Dusit
Bangkok
Thailand

Toowoomba Foundry Pty Ltd
259 Ruthven Street
Toowoomba
Australia 4350

Verdun Co.
P.O. Box 1481
Hutchison, Kansas 67501

Wakes & Lamb Ltd.
Millgate Works
Newark-on-Trent
Notts NG24 4XB
England

Wind Baron Corp.
3702 W. Lower Buckeye Road
Phoenix, Arizona 85009

Water Pumping Wind Systems (continued)

Maquinas Agricolas Fortuna Ltda
Divisao International
Rua Joao Adolfo, 118
conj. 710/711
CED 01050
Sao Paulo
Brazil

Windpumpen-Zentrale
Leutthoern 31
D 2330 Eckernfoerde
West Germany

Wyatt Brothers Ltd
Wayland Works
Whitchurch
Salop ST13 1RS
England

Large Wind Electric Turbines

Bendix Corporation
2582 South Tejon Street
Englewood, Colorado 80110

Boeing Engineering &
Construction
P.O. Box 3703, MS 9A-65
Seattle, Washington 98124

Bosman
Waterbeheersing En
Milieverbetering B.V.
Steegjesdijk 4
Postbus 3518
3364 Piershil (Z-H)
Netherlands

Carter Wind Systems
Route 1, Box 405A
Burkburnett, Texas 76354

DAF Indal
3570 Hawkestone Road
Mississauga, Ontario
Canada L5C 2V8

Energy Sciences Inc.
P.O. Box 3009
Boulder, Colorado 80303

Fayette Manufacturing
P.O. Box 1149
Tracy, California 95376

General Electric
Advanced Energy Programs Dept.
P.O. Box 527
King of Prussia, Penn. 19406

Hamilton Standard
Division of United Technologies
Windsor Locks, Connecticut 06096

Westinghouse Electric Corp.
Advanced Energy Systems Divison
P.O. Box 10864
Pittsburg, Pennsylvania 15236

WECS-Tech Corp.
1505 Mahalo Place
Compton, California 90220

Wind Power Systems
8630 Production Avenue
San Diego, California 92121

Windtech, Inc.
P.O. Box 837
Glastonbury, Connecticut 06033

WTG Energy Systems, Inc.
251 Elm Street
Buffalo, New York 14203

Small Wind Electric Turbines

Aeolian Energy, Inc.
R.D. #4
Ligonier, Pennsylvania 15658

Aerolite
550 Russells Mills
P.O. Box 576
S. Dartmouth, Massachusetts 02748

Aerowatt Company
37 Rue Chanzy
75011 Paris
France

Alsthom-Neypric
Techniques des Fluides
B.P. 75
38041 Genoble Cedex
France

Altos - The Alternate Current
Horizon Industris
3700 Havana, #212
Denver, Colorado 80239

American Energy Savers
912 St. Paul Rd.
Box 1421
Grand Island, Nebraska 68802

Astral Wilcon, Inc.
P.O. Box 291
Millbury, Massachusetts 01527

Bergey Windpower Co.
2001 Priestly
Norman, Oklahoma 73069

Bircher Machine, Inc.
P.O. Box 97
Kanopolis, Kansas 67454

Carter Wind Systems
Rt. 1, Box 405A
Burkburnett, Texas 76354

DAF Indal
3750 Hawkestone Road
Mississauga, Ontario
Canada L5C 2V8

Jacobs Wind Electric Co.
2720 Fernbrook Lane
Minneapolis, Minnesota 55441

Lubing Maschinenfabrik
D-2347 Barnstorf
Postfach 110
German Federal Republic

Millville Hawaii Windmills
3028 Ualena Street
Honolulu, Hawaii 96819

Neah Energie Systeme Gmbh
Muhlenstr 11
D-53 Bonn
W. Germany

North Wind Power, Inc.
P.O. Box 556
Moretown, Vermont 05660

PM Wind Power, Inc.
P.O. Box 89
Mentor, Ohio 44060

Product Development Institute
4445 Talmadge Road
Toledo, Ohio 43623

Sancken Wind Electric
4160 Skylark
Kingman, Arizona 86401

Sencenbaugh Wind Electric
P.O. Box 11174
Palo Alto, California 94306

SWX Corp.
17914 E. Warren Avenue
Detroit, Michigan 48224

Thermax Corp.
One Mill Street
Burlington, Vermont 05401

Trimble Windmills
Crimple Grange
Beckwithshaw
Harrogate
North Yorkshire HG3 1QU
England

Small Wind Electric Turbines (continued)

Davey Dunlite
P.O. Box 120
Oakleigh
Melbourne
Australia 3166

Dunlite
c/o Enertech Corp.
P.O. Box 420
Norwich, Vermont 05055

Enag SA
Route de Pont-l'abbe
F 29000 Quimper
Finistere
France

Energy Sciences, Inc.
900 28th Street
P.O. Box 3009
Boulder, Colorado 80303

Enertech Corp.
P.O. Box 420
Norwich, Vermont 05055

Elektro Gmbh
St. Gallerstrasse 27
8400 Winterthur
Switzerland

Fayette Manufacturing
P.O. Box 1149
Tracy, California 95376

Forces Motrices
Neuchateloises S.A.
Rue Pourtales 13
CH-2000
Neuchatel
Switzerland

Hummingbird Windpower
Power Group International
12306 Rip Van Winkle
Houston, Texas 77024

U.S. Windpower
500 Samsome Street, #205
San Francisco, California 94111

WESCO
Iroko House
Bolney Avenue
Peacehaven
Sussex BN9 8HQ
England

WECS-Tech Corp.
1505 Mahalo Place
Compton, California 90220

WhirlWind PowerCo.
207 1/2 E. Superior
Duluth, Minnesota 55802

Winco
Division of Dyna Technology, Inc.
7850 Metro Parkway
Minneapolis, Minnesota 55410

Wind Power Systems, Inc.
8630 Production Avenue
San Diego, California 92121

Windtech, Inc.
P.O. Box 837
Glastonbury, Connecticut 06033

Windworks, Inc.
Rt. 3, Box 44A
Mukwonago, Wisconsin 53149

Winpower Corp.
P.O. Box 99
Newton, Iowa 50208

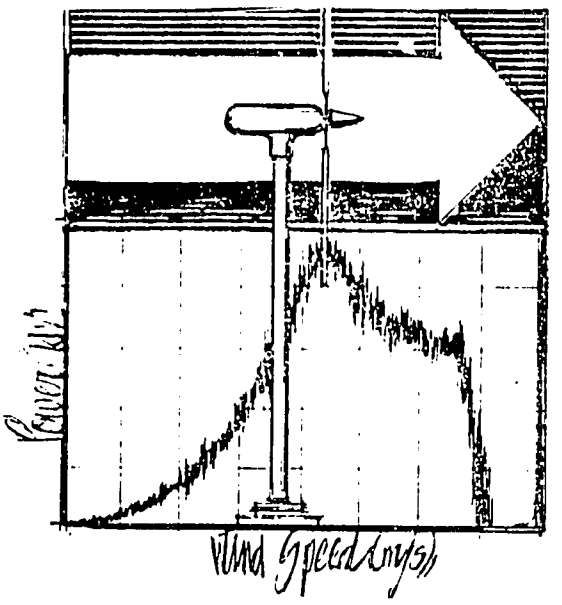

ROCKY FLATS

Performance Summary Sheets

Rocky Flats Wind Systems Program
P. O. Box 464
Golden, CO 80401

PERFORMANCE SUMMARIES, produced by the Rocky Flats Wind Systems Program, are intended to aid manufacturers and prospective consumers evaluate small wind energy conversion system (SWECS) performance. Information for these reports is gathered through atmospheric and/or controlled velocity tests. While normal test periods for machines average two years, the data reported in performance sheets may reflect the results from a shorter period. Information supplied by the PERFORMANCE SUMMARIES includes machine design specifications, methods of testing, and the results of those tests (see explanation on reverse side). Periodic updates are performed to reflect additional or changed information

The data contained in these sheets are collected and processed by the Small Wind Systems Test Center (WSTC) at the U.S. Department of Energy's (DOE) Rocky Flats Plant near Golden, Colorado. Operated by Rockwell International as part of the Federal Wind Energy Program, the WSTC provides data gathered from atmospheric and controlled velocity testing of SWECS to manufacturers, researchers, and others interested in wind energy conversion.

Commercially available SWECS, commercial prototypes, and prototype machines developed by private businesses under DOE contract are installed for a test period of approximately two years to compile data on machine performance in a variety of wind and weather conditions. To provide more immediate results, some are tested under controlled velocity conditions. Controlled velocity test (CVT) data are gathered while the SWECS is mounted on a rail car (pushed by a locomotive) with the same instrumentation package used during atmospheric tests. The CVT data can provide information on the SWECS power output over specific wind speeds, but cannot predict a system's ability to withstand the varying conditions present during atmospheric testing.

How to Use Performance Summary Sheets

MANUFACTURER'S SPECIFICATIONS

(See U.S. CONTACT for available options)

DESIGN OUTPUT:

The power output at which the wind machine is rated and the lowest wind speed at which this output is predicted.

ROTOR SPEED CONTROL:

Method used to prevent excessive rotational speed. Protects the SWECS from sustaining structural damage resulting from high winds (wind speeds exceeding design conditions).

OPERATING WIND SPEEDS:

Cut-in wind speed:
Cut-out wind speed:

Cut-in is the wind speed at which the SWECS begins producing power. Cut-out is the speed at which the SWECS is no longer expected to produce power.

ROTOR CONFIGURATION:

Describes the size of the rotor, its physical configuration, and the construction materials.

GENERATOR/TRANSMISSION:

Describes the mechanism which produces the power, the type of power (ac/dc; voltage), and the transmission (if any) used to increase shaft rpm to meet generator requirements.

MACHINE DESCRIPTION:

General description and design characteristics

U.S. CONTACT:

For cost information and other details.

ROCKY FLATS PERFORMANCE DATA

MEASURED CHARACTERISTICS:

Cut-in wind speed...
Cut-out wind speed..
Survived wind speed.
Output @ ___ .....

Represents synopsis of the test results for key characteristics. Unless otherwise noted, all data are valid at sea level. Survived wind speed is the highest wind speed experienced during testing without damage or failure.

POWER CURVE:

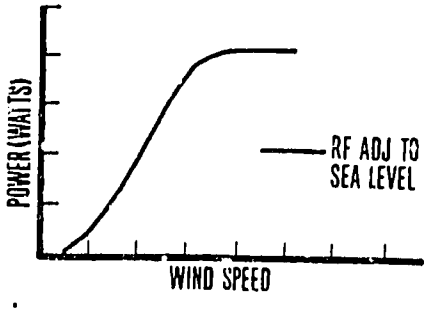

Wind speed vs. power output. The machine performance is represented by a power curve on a graph where the horizontal axis represents the wind speed and the vertical axis represents the generated power. To determine power output at a specific wind speed, first locate the desired wind speed along the horizontal axis. Next, trace vertically until the power curve is intersected.

ESTIMATED ANNUAL ENERGY PRODUCTION:

Predicted annual energy production at sites with annual wind speeds of 8, 10, 12, 14, and 16 mph.

SUMMARY:

Defines testing method, duration, and results to date.

Rocky Flats Performance Summary

AERO POWER SL1000

DECEMBER 1980

MANUFACTURER'S SPECIFICATIONS

(See U.S. CONTACT for available options)

DESIGN OUTPUT:

1.0 kW @ 9 m/s (20 mph)

ROTOR SPEED CONTROL:

Mechanical, centrifugally advanced to feather.

OPERATING WIND SPEEDS:

CUT-IN: 2.7 m/s (6 mph)

CUT-OUT: None; machine operates at all wind speeds.

ROTOR CONFIGURATION:

ROTOR DIAMETER: 3.05 m (10 ft)

ROTOR TYPE: Horizontal axis, variable pitch, upwind.

NUMBER OF BLADES: 3

MATERIAL: Aircraft spruce, stainless steel leading edge.

GENERATOR/TRANSMISSION:

OUTPUT: 14.5 volts, 3Ø rectified to dc.

GEARBOX: 3:1 ratio.

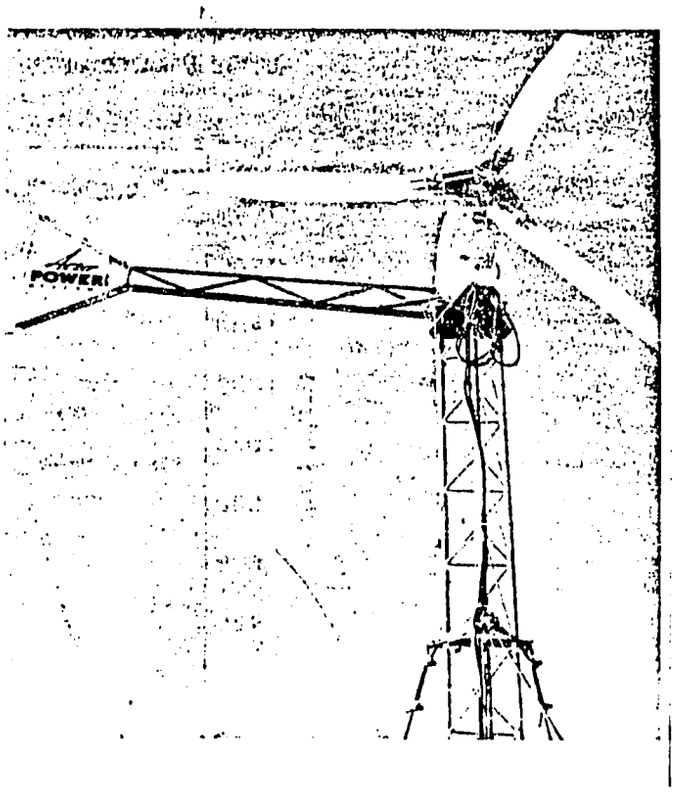

MACHINE DESCRIPTION:

The Aero Power SL1000 is a 3-bladed, upwind machine. The machine utilizes the centrifugal force imposed on the hub to control the blade pitch, which in turn controls the rotational speed. The machine is designed primarily to charge batteries and is adaptable as a 117 Vac, 60 hz power source with the use of an inverter.

U.S. CONTACT:

AERO POWER SYSTEMS, INC.
2398 FOURTH STREET
BERKELEY, CALIFORNIA 94710

(415) 848-2710
MARIO V. AGNELLO

This PERFORMANCE SUMMARY was prepared and published by the Rockwell International Corporation Energy Systems Group, Rocky Flats Plant, Wind Systems Program, P.O. Box 464, Golden, CO 80401
for the
U.S. Department of Energy, Office of Solar Power Applications
Federal Wind Energy Program

Contract DE-AC04-76DP03533

ROCKY FLATS PERFORMANCE DATA

Aero Power SL1000

MEASURED CHARACTERISTICS
(ADJUSTED TO SEA LEVEL)

CUT-IN WIND SPEED.....4 m/s (9 mph)
CUT-OUT WIND SPEED.....None
SURVIVAL WIND SPEED.....Not Available
OUTPUT @ 9 m/s (20 mph).....649 Watts
OUTPUT @ 11.2 m/s (25 mph).....984 Watts
NOISE @ RATED OUTPUT.....Not Available

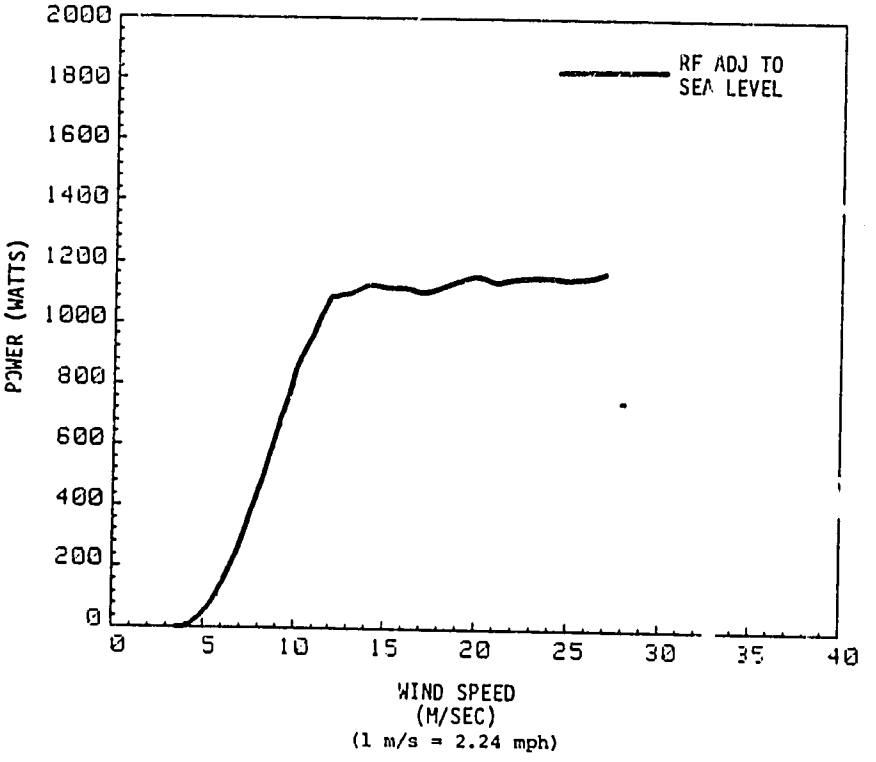

ESTIMATED ANNUAL ENERGY PRODUCTION
(USING A RAYLEIGH WIND DISTRIBUTION)

AVERAGE WIND VELOCITY (m/s)	(mph)	ANNUAL ENERGY OUTPUT (kWh)
3.58	8	440
4.47	10	1040
5.36	12	1820
6.26	14	2660
7.15	16	3490

NOTE: *The annual energy output is based on the measured Rocky Flats power curve for this machine. The power curve is superimposed on a Rayleigh velocity duration curve to generate a power duration curve which is then integrated over time to obtain energy. Energy output will vary at specific sites due to variations in wind characteristics and other factors.*

SUMMARY

Performance data presented above were collected during Controlled Velocity Testing (CVT) of the Aero Power SL1000 at the Department of Transportation rail site in Pueblo, Colorado. Due to the fact that this version of the SL1000 has not yet been tested under natural (atmospheric) conditions at the Small Wind Systems Test Center, no survivability data are available. However, an earlier version of the SL1000 was tested at Rocky Flats from January 1979 through May 1979 and survived winds in excess of 35.8 m/s (80 mph) without incurring structural damage.

12/80 dlm

Rocky Flats Performance Summary

AUGUST 1980

ALTOS Model 8B

MANUFACTURER'S SPECIFICATIONS

(See U.S. CONTACT for available options)

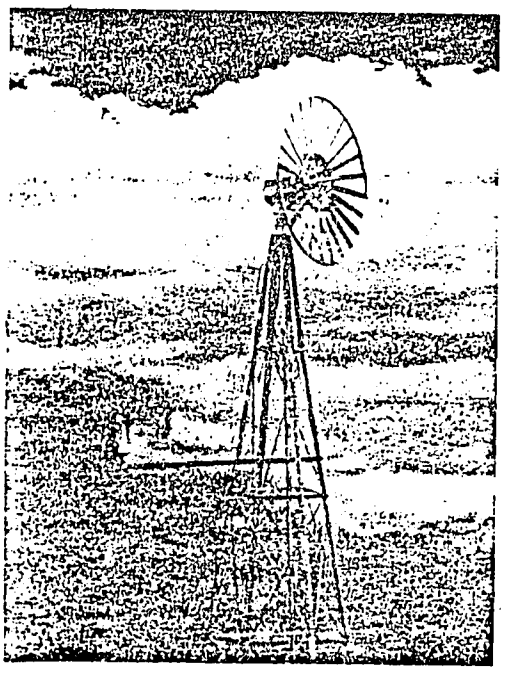

DESIGN OUTPUT:

1.5 kW @ 12.5 m/s (28 mph)

ROTOR SPEED CONTROL:

Mechanical; foldable tail; automatic or manual.

OPERATING WIND SPEEDS:

CUT-IN: 4.5 m/s (10 mph)

CUT-OUT: 33.5 m/s (75 mph)

ROTOR CONFIGURATION:

ROTOR DIAMETER: 2.4 m (8 ft)

ROTOR TYPE: Horizontal axis, upwind, bicycle/multibladed, fixed pitch.

NUMBER OF BLADES: 24

MATERIAL: Aluminum, 5052

GENERATOR/TRANSMISSION:

OUTPUT: Rectified to 24 Vdc, 0-70 amps, trickle draw.

GEARBOX: 11:1 ratio

MACHINE DESCRIPTION:

The Altos (formerly Amerenalt) is a light weight machine manufactured by Altos Corporation, Boulder, Colorado. The main generator housing is welded steel. The alternator is coupled through a 11:1 cycloidal gearbox and is driven by a multibladed rotor 2.4 m in diameter. The rotor is constructed of formed aluminum Clark Y airfoils supported by stainless steel spokes and inner and outer rims.

Rotor overspeed control is provided by utilizing increasing wind pressure on the rotor to swing the rotor and alternator assembly (which is offset from the tail assembly) out of the oncoming wind. During this operation, the tail remains parallel to the wind stream. As the wind decreases, a return spring causes the tail to reopen with respect to the rotor and alternator. This brings the rotor back into the wind stream.

U.S. CONTACT:

ALTOS: THE ALTERNATE CURRENT
P.O BOX 905
BOULDER, CO 80302

(303) 442-0885
EDWARD GITLIN

This PERFORMANCE SUMMARY was prepared and published by the Rockwell International Corporation, Energy Systems Group, Rocky Flats Plant, Wind Systems Program, P.O. Box 464, Golden, Co 80401 for the U.S. Department of Energy, Office of Solar Power Applications Federal Wind Energy Program Contract DE-AC04-76DP03533

ROCKY FLATS PERFORMANCE DATA

ALTOS Model 8B

MEASURED CHARACTERISTICS
(ADJUSTED TO SEA LEVEL)

CUT-IN WIND SPEED.....4 m/s (9 mph)
CUT-OUT WIND SPEED.....Not available
SURVIVED WIND SPEED.....42 m/s (94 mph)
OUTPUT @ 9 m/s (20 mph).....393 Watts
OUTPUT @ 12.5 m/s (28 mph).....393 Watts
NOISE @ RATED OUTPUT.....Not available

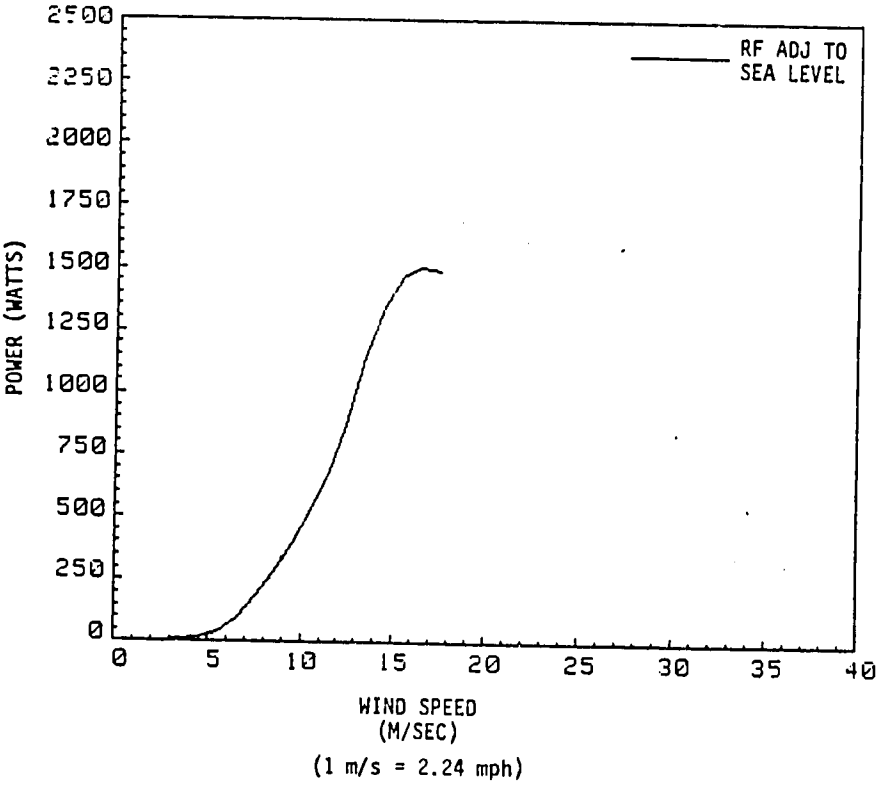

(1 m/s = 2.24 mph)

ESTIMATED ANNUAL ENERGY PRODUCTION
(USING A RAYLEIGH WIND DISTRIBUTION)

AVERAGE WIND VELOCITY (m/s)	(mph)	ANNUAL ENERGY OUTPUT (kWh)
3.58	8	240
4.47	10	560
5.36	12	1050
6.26	14	1690
7.15	16	2390

NOTE: *The annual energy output is based on the measured Rocky Flats power curve for this machine. The power curve is superimposed on a Rayleigh velocity duration curve to generate a power duration curve which is then integrated over time to obtain energy. Energy output will vary at specific sites due to variations in wind characteristics and other factors.*

SUMMARY

The Altos Model 8B WTG survived wind speed in excess of 36 (80 mph) while undergoing atmospheric testing at the WSTC. Although the machine experienced three failures, the failures appeared to be more related to manufacturing problems than design deficiencies. During atmospheric and controlled velocity testing (CVT), the machine did not achieve its rated output. A tail over-travel problem continually hampered performance of the Altos and contributed to the machine's inability to produce rated output. This over-travel problem was not resolved by the manufacturer during the test period at Rocky Flats.

Rocky Flats Performance Summary

AMERICAN WIND TURBINE AWP-16

OCTOBER 1980

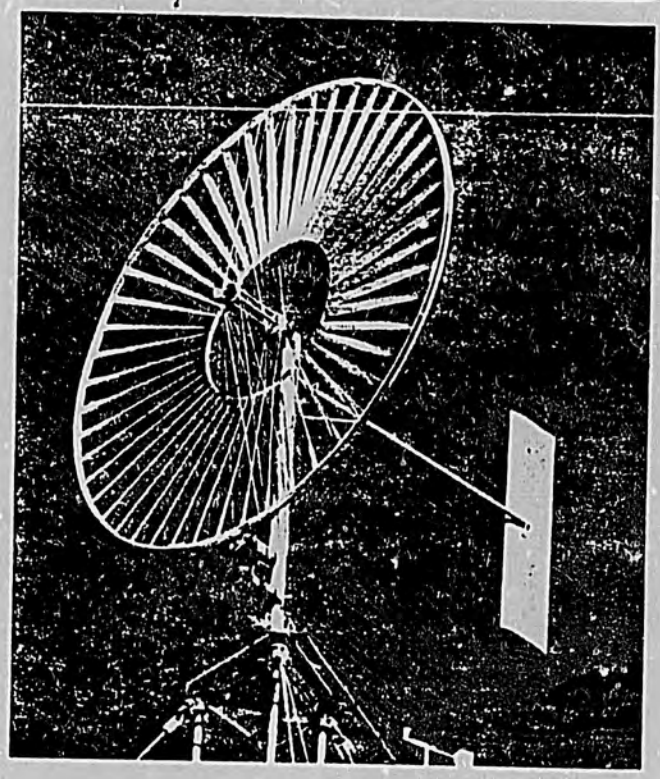

MANUFACTURER'S SPECIFICATIONS

DESIGN OUTPUT:

2.0 kW @ 9 m/s (20 mph)

ROTOR SPEED CONTROL:

Mechanical, foldable tail.

OPERATING WIND SPEEDS:

CUT-IN: 4.5 m/s (10 mph)

CUT-OUT: 15.7 m/s (35 mph)

ROTOR CONFIGURATION:

ROTOR DIAMETER: 4.7 m (15.3 ft)

ROTOR TYPE: Horizontal axis, bicycle type, fixed pitch, upwind

NUMBER OF BLADES: 48

MATERIAL: Aluminum

GENERATOR/TRANSMISSION:

OUTPUT: 220 Vac, 3Ø, variable frequency, permanent magnet generator

GEARBOX: Belt-drive; 30:1 ratio

MACHINE DESCRIPTION:

The AWT is a lightweight machine manufactured by American Wind Turbine Co., Stillwater, Oklahoma, and is designed for use with an electric water pump. The alternator is rim-belt driven by a multibladed rotor, 4.5 m in diameter, with a 30:1 ratio. The rotor is constructed of formed aluminum airfoils supported by stainless steel spokes and inner and outer rims.

Rotor overspeed control is achieved by utilizing increasing wind pressure on the rotor to gradually swing the rotor and alternator assembly out of the oncoming wind. The return spring aligns the tail as the wind speed decreases.

This PERFORMANCE SUMMARY was prepared and published by the Rockwell International Corporation, Energy Systems Group, Rocky Flats Plant, Wind Systems Program, P.O. Box 494, Golden, CO 80401
for the
U.S. Department of Energy, Office of Solar Power Applications
Federal Wind Energy Program

Contract DE-AC04-76DP03533

10/80 dlm

ROCKY FLATS PERFORMANCE DATA

American Wind Turbine AWP-16

MEASURED CHARACTERISTICS
(ADJUSTED TO SEA LEVEL)

CUT-IN WIND SPEED.....5 m/s (11 mph)
CUT-OUT WIND SPEED.....NOT AVAILABLE
SURVIVAL WIND SPEED.....44.7 m/s (100 mph)
OUTPUT @ 9 m/s (20 mph).....470 Watts
OUTPUT @ 12 m/s (27 mph).....925 Watts
NOISE @ RATED OUTPUT.....NOT AVAILABLE

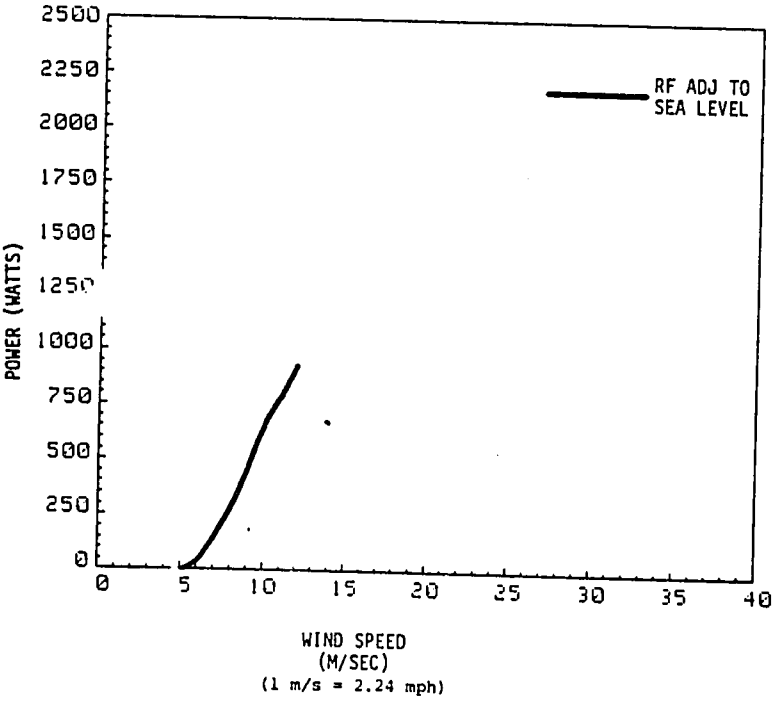

ESTIMATED ANNUAL ENERGY PRODUCTION
(USING A RAYLEIGH WIND DISTRIBUTION)

AVERAGE WIND VELOCITY (m/s)	(mph)	ANNUAL ENERGY OUTPUT (kWh)
3.58	8	190
4.47	10	560
5.36	12	1050
6.26	14	1490
7.15	16	1800

NOTE: *The annual energy output is based on the measured Rocky Flats power curve for this machine. The power curve is superimposed on a Rayleigh velocity duration curve to generate a power duration curve which is then integrated over time to obtain energy. Energy output will vary at specific sites due to variations in wind characteristics and other factors.*

SUMMARY

While undergoing atmospheric testing at Rocky Flats, the American Wind Turbine AWP-16 substantiated the manufacturer's survival wind speed of 44.7 m/s (100 mph). The one major failure occurred when winds reached speeds of 53 m/s (119 mph). However, the machine was unable to produce the manufacturer rated output during the test period. It is believed two factors contributed significantly to this low power output. The first factor was the use of a manufacturer specified resistive load, rather than a submersible pump motor which the machine was designed to power. The second factor was the high start-up torque of the variable frequency, permanent magnet generator.

Rocky Flats Performance Summary

Jay Carter Model 25

MARCH 1981

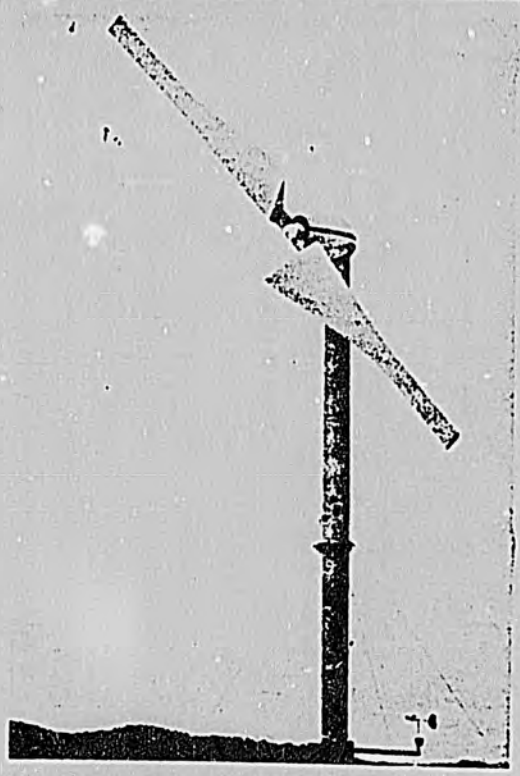

MANUFACTURER'S SPECIFICATIONS

(See U.S. CONTACT for available options)

DESIGN OUTPUT:

25 kW @ 11.6 m/s (26 mph)

ROTOR SPEED CONTROL:

Mechanical, blade feathering activated by centrifugal force, causing each blade to pitch to stall.

OPERATING WIND SPEEDS:

CUT-IN: 3.6 m/s (7.5 mph)

CUT-OUT: None

ROTOR CONFIGURATION:

ROTOR DIAMETER: 9.75 m (32 ft)

ROTOR TYPE: Horizontal axis, fixed pitch, downwind.

NUMBER OF BLADES: 2

MATERIAL: Fiberglass and PVC foam.

GENERATOR/TRANSMISSION:

OUTPUT: 220 Vac, 60 cycle, 3Ø induction generator.

GEARBOX: Double reduction, helical, 15:1.

MACHINE DESCRIPTION:

The Jay Carter Model 25 is a 2-bladed, horizontal axis, downwind machine. When the unit is generating power, the blades are designed to automatically stall in high winds. Should an overspeed condition occur by unloading of the generator during a power outage, centrufugal loads on weights mounted in the trailing edge of the blade cuff cause each blade to pitch into a highly stalled configuration, thereby causing the rotor to slowly stop. When wind speeds decrease, a hydraulic snubber slowly returns the blades to their original pitch setting and allows the rotor to resume normal operation. In addition, a self-adjusting mechanical brake can also be used to stop the rotor at any wind speed. The brake can be manually activated from the base of the tower, or automatically activated by a vibration monitor. Each Model 25 is marketed with a specifically designed tower. Manufacturer installation is required for the system.

U.S. CONTACT:

JAY CARTER ENTERPRISES, INC.
P.O. BOX 684
BURKBURNETT, TEXAS 76354

(817) 569-2238
JAY CARTER

This PERFORMANCE SUMMARY was prepared and published by the Rockwell International Corporation, Energy Systems Group, Rocky Flats Plant, Wind Systems Program, P.O. Box 464, Golden, CO 80401
for the
U.S. Department of Energy, Office of Solar Power Applications
Federal Wind Energy Program

Contract DE-AC04-76DP03533

02/81 dlm

ROCKY FLATS PERFORMANCE DATA

Jay Carter Model 25

MEASURED CHARACTERISTICS*
(ADJUSTED TO SEA LEVEL)

CUT-IN WIND SPEED.....4 m/s (9 mph)
CUT-OUT WIND SPEED.....NONE
SURVIVED WIND SPEED.....40.2 m/s (90 mph)
OUTPUT @ 9 m/s (20 mph).....10.3 kW
OUTPUT @ 11.6 m/s (26 mph).....19 kW
NOISE @ RATED OUTPUT.....NOT AVAILABLE

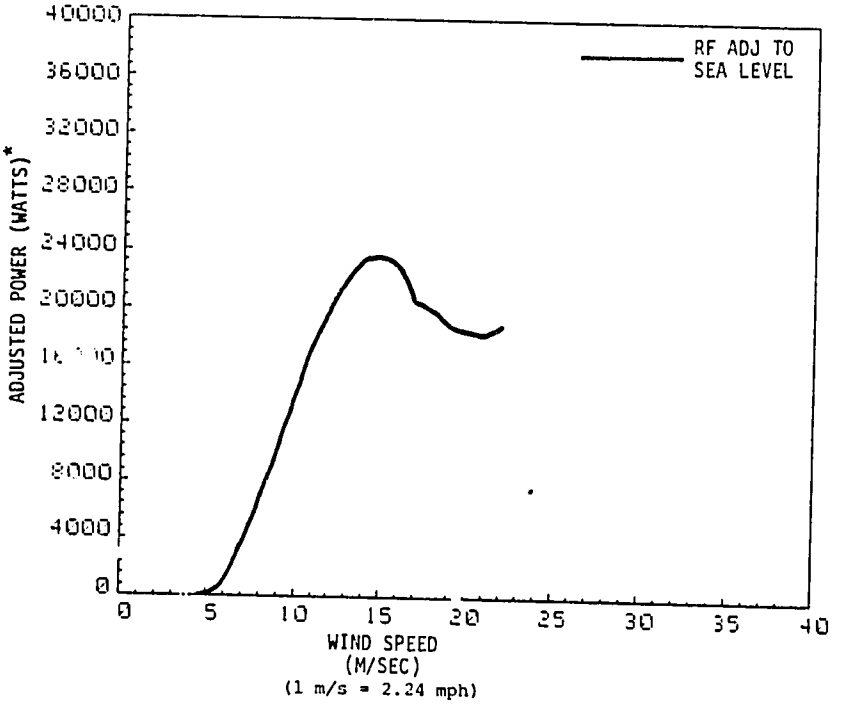

ESTIMATED ANNUAL ENERGY PRODUCTION
(USING A RAYLEIGH WIND DISTRIBUTION)

AVERAGE WIND VELOCITY (m/s)	(mph)	ANNUAL ENERGY OUTPUT* (kWh)
3.58	8	4840
4.47	10	13,870
5.36	12	27,130
6.26	14	42,640
7.15	16	58,430

NOTE: *The annual energy output is based on the measured Rocky Flats power curve for this machine. The power curve is superimposed on a Rayleigh velocity duration curve which is then integrated over time to obtain energy. Energy output will vary at specific sites due to variations in wind characteristics and other factors.*

* The above data were gathered on a machine with a 31 ft. rotor diameter rather than the 32 ft. diameter standard on Model 25's. In addition, wind speeds used in RF data were gathered at an anemometer height of 56 ft. (hub height), while the manufacturer data (see DESIGN OUTPUT) were based on wind speeds measured at 30 ft.

SUMMARY

The Jay Carter Model 25 has operated satisfactorily in winds of 40.2 m/s (90 mph) while undergoing atmospheric testing at Rocky Flats (RF). Although performance data generated at RF do not agree with manufacturer data, it is important to note that the machine tested at RF has a 31 ft. rotor diameter, while the standard Model 25 has a rotor diameter of 32 ft. The rotor diameter of the test machine was shortened to 31 ft. by the manufacturer as a result of damage suffered through the use of an incorrect manufacturer-installed tower section. Subsequent tower redesign has eliminated the possibility of this problem re-occurring. To help compensate for the lower air density at the Rocky Flats Wind Systems Test Center, the initial blade pitch angle of the test machine was changed from -1 degree to 0 degrees. All RF data were adjusted to reflect temperature and barometric pressure differential between Rocky Flats and sea level standard day conditions.

AUGUST 1980

Rocky Flats Performance Summary

DUNLITE Model 81/002550

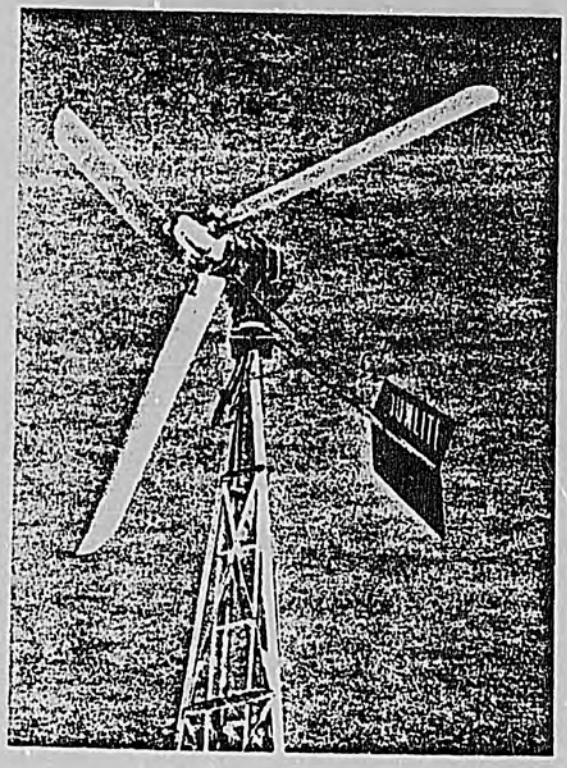

MANUFACTURER'S SPECIFICATIONS

(See U.S. CONTACT for available options)

DESIGN OUTPUT:

2.0 kW @ 11 m/s (25 mph)

ROTOR SPEED CONTROL:

Mechanical, blade feathering activated by centrifugal forces on flyballs.

OPERATING WIND SPEEDS:

CUT-IN: 3.6 m/s (8 mph)

CUT-OUT: NONE

ROTOR CONFIGURATION:

ROTOR DIAMETER: 4.1 m (13.5 ft)

ROTOR TYPE: Horizontal axis, upwind variable pitch

NUMBER OF BLADES: 3

MATERIAL: Galvanized Sheet Steel

GENERATOR/TRANSMISSION:

OUTPUT: 110 Vdc, 3Ø, brushless alternator with built-in rectifier

GEARBOX: Single-stage; 5:1 ratio

MACHINE DESCRIPTION:

The Dunlite is manufactured by Dunlite Electrical Company, a division of Pye Industrial Sales, Australia, and is distributed in the United States. The alternator is coupled through a 5:1 helical gearbox and is driven by a 3-bladed propeller 4.10 m in diameter. The blades are made from galvanized steel sheets.

Propeller overspeed control is provided by the automatic feathering action of the blades. As speed increases, the centrifugal force on the governor weight on each of the blades overcomes the tension of a central spring and shock absorber unit and moves the blade to a coarser pitch. As the wind speed decreases, the propeller speed will slow, thus reducing the centrifugal force on the governor weights. This allows the central spring to return the blades to maximum speed position.

U.S. CONTACT:

DUNLITE ELECTRICAL PRODUCTS, CO.
C/O ENERTECH CORPORATION
P.O. BOX 420
NORWICH, VERMONT 05055
(802) 649-1145

This PERFORMANCE SUMMARY was prepared and published by the Rockwell International Corporation Energy Systems Group, Rocky Flats Plant, Wind Systems Program, P.O. Box 464, Golden, CO 80401 for the U.S. Department of Energy, Office of Solar Power Applications Federal Wind Energy Program

Contract DE-AC04-76DP03533

08/80 dlm

ROCKY FLATS PERFORMANCE DATA

DUNLITE Model 81/002550

MEASURED CHARACTERISTICS
(ADJUSTED TO SEA LEVEL)

CUT-IN WIND SPEED.....4 m/s (9 mph)
CUT-OUT WIND SPEED.....NONE
SURVIVED WIND SPEED.....36 m/s (80 mph)
OUTPUT @ 9 m/s (20 mph).....1.1 kW
OUTPUT @ 11 m/s (22 mph).....1.9 kW
NOISE @ RATED OUTPUT (at base of tower).....55 dBA

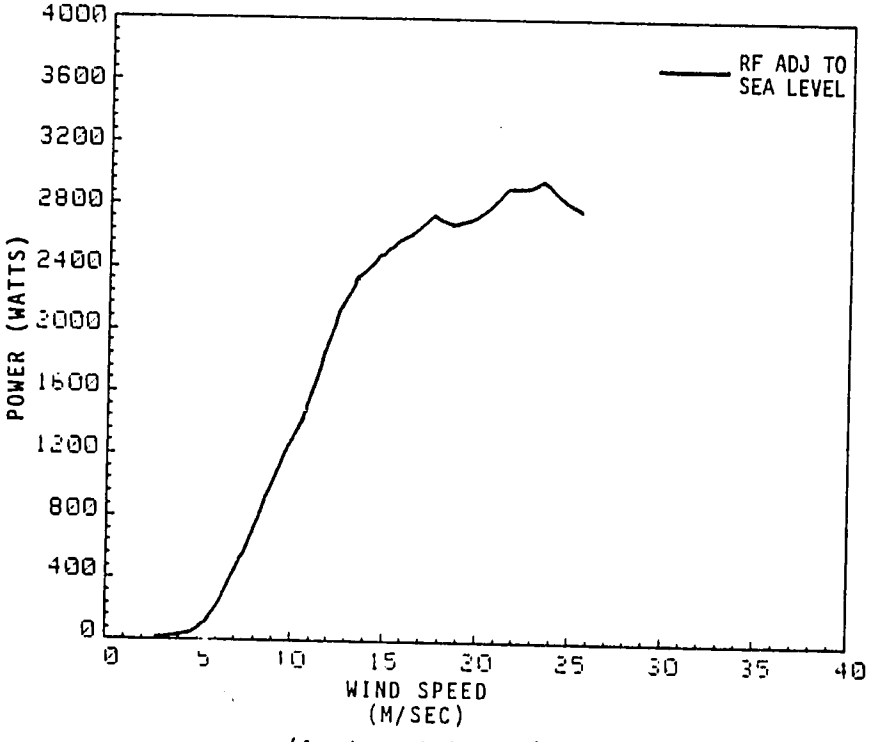

(1 m/s = 2.24 mph)

ESTIMATED ANNUAL ENERGY PRODUCTION
(USING A RAYLEIGH WIND DISTRIBUTION)

AVERAGE WIND VELOCITY (m/s)	(mph)	ANNUAL ENERGY OUTPUT (kWh)
3.58	8	720
4.47	10	1680
5.36	12	3000
6.26	14	4540
7.15	16	6200

NOTE: *The annual energy output is based on the measured Rocky Flats power curve for this machine. The power curve is superimposed on a Rayleigh velocity duration curve to generate a power duration curve which is then integrated over time to obtain energy. Energy output will vary at specific sites due to variations in wind characteristics and other factors.*

SUMMARY

The Dunlite Model 81/002550 WTG has met all manufacturer claims of performance and reliability. The machine operated satisfactorily in winds up to the manufacturer rated survival speed of 35.8 m/s (80 mph). In addition, the Dunlite operated in winds exceeding 22.5 m/s (50 mph) for eight hours without incurring damage. Damage to the machine occurred when wind speeds exceeded 40.2 m/s (90 mph). If winds of this velocity are expected, the manufacturer offers a high speed model designed to withstand winds of 49.5 m/s (110 mph). Testing of the Dunlite indicated that the machine is capable of producing its rated output of 2 kW at 11 m/s (25 mph).

Rocky Flats Performance Summary

ENERTECH 1500

DECEMBER 1980

MANUFACTURER'S SPECIFICATIONS

(See U.S. CONTACT for available options)

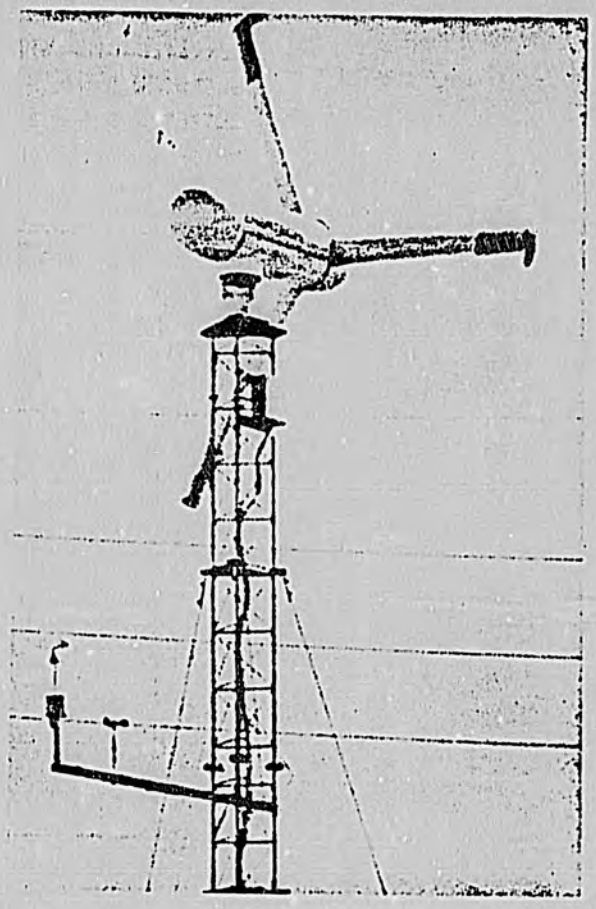

DESIGN OUTPUT:

1.5 kW @ 9.8 m/s (22 mph)

ROTOR SPEED CONTROL:

1. Aerodynamic brake applied when anemometer senses wind speed of 17.9 m/s (40 mph) for more than 30 seconds.
2. Brake actuated when utility power fails.
3. Centrifugal backup switch actuates brake if overspeed occurs.
4. Blade tip brakes.

OPERATING WIND SPEEDS:

CUT-IN: 4.5 m/s (10 mph)

SHUT DOWN: 30-second average of 17.9 m/s (40 mph)

ROTOR CONFIGURATION:

ROTOR DIAMETER: 4 m (13 ft.)

ROTOR TYPE: Horizontal-axis, fixed-pitch, downwind.

NUMBER OF BLADES: 3

MATERIAL: Wood, painted finish.

GENERATOR/TRANSMISSION:

OUTPUT: 115 Vac, 1Ø, induction generator

GEARBOX: Two-stage; 11.4:1 ratio

MACHINE DESCRIPTION:

The Enertech 1500 is a horizontal axis, downwind machine rated at 1500 watts in a 9.8 m/s (22 mph) wind. The unit is equipped with an induction generator, which produces sine-wave, 60 hz, 115 Vac within its range of operating speeds (1800 to 1950 rpm). The blades are locked until a cup anemometer, which is supplied with the machine, senses winds which average 4.5 m/s (10 mph) for 30 seconds. When this event occurs, the brake is released and the blades accelerate to 1800 rpm in a 4-5 second time span. Similarly, when winds of at least 17.9 m/s (40 mph) are sensed for at least 30 seconds, the brake is energized, bringing the rotor to a stop. The brake is also energized when utility power fails so that the generator cannot backfeed a dead utility line.

U.S. CONTACT:

ENERTECH CORPORATION
P.O. BOX 420
NORWICH, VERMONT 05055
(802) 649-1145

This PERFORMANCE SUMMARY was prepared and published by the Rockwell International Corporation Energy Systems Group, Rocky Flats Plant, Wind Systems Program, P.O. Box 464, Golden, CO 80401 for the U.S. Department of Energy, Office of Solar Power Applications Federal Wind Energy Program

Contract DE-AC04-76DP03533

ROCKY FLATS PERFORMANCE DATA

Enertech 1500

MEASURED CHARACTERISTICS
(ADJUSTED TO SEA LEVEL)

CUT-IN WIND SPEED.....4.2 m/s (9.5 mph)
SHUT DOWN SPEED....30-second average of 26.8 m/s (60 mph)
SURVIVED WIND SPEED.....44.7 m/s (100 mph)
OUTPUT @ 9 m/s (20 mph).....695 Watts
OUTPUT @ 9.8 m/s (22 mph).....1095 Watts
NOISE @ RATED OUTPUT.....Not Available

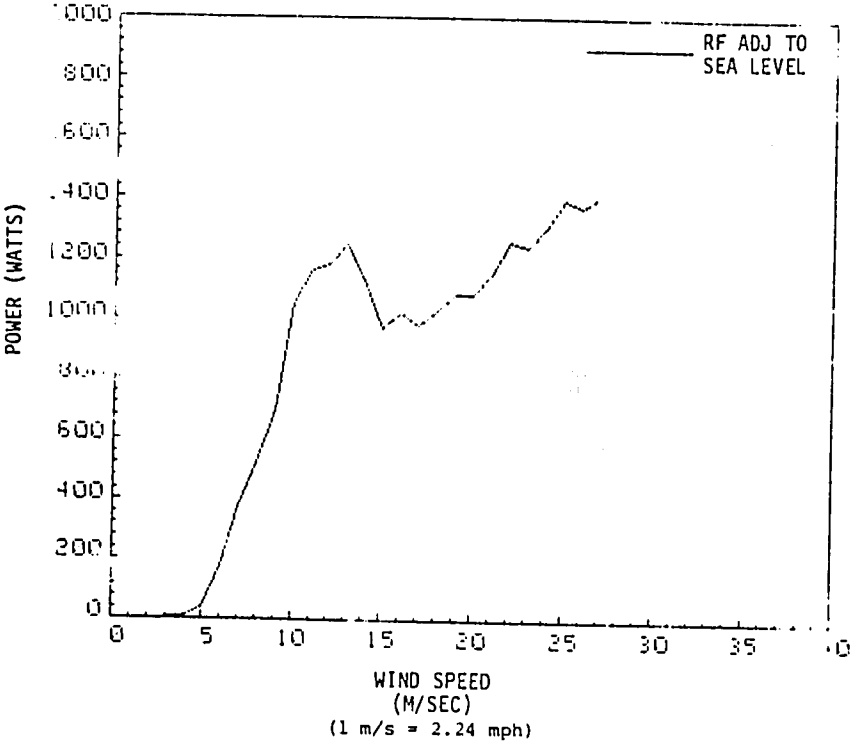

ESTIMATED ANNUAL ENERGY PRODUCTION
(USING A RAYLEIGH WIND DISTRIBUTION)

AVERAGE WIND VELOCITY (m/s)	(mph)	ANNUAL ENERGY OUTPUT (kWh)
3.58	8	528
4.47	10	1225
5.36	12	2115
6.26	14	3048
7.15	16	3920

NOTE: *The annual energy output is based on the measured Rocky Flats power curve for this machine. The power curve is superimposed on a Rayleigh velocity duration curve to generate a power duration curve which is then integrated over time to obtain energy. Energy output will vary at specific sites due to variations in wind characteristics and other factors.*

SUMMARY

Performance data presented above were generated by Controlled Velocity Testing (CVT) of the Enertech 1500 at the Department of Transportation rail facility in Pueblo, Colorado and are in close agreement with data generated by testing under natural (atmospheric) conditions at Rocky Flats. It is important to note, however, that RF performance data are for a machine with blade tip brakes; while manufacturer specifications contained in this Performance Summary Sheet are for an earlier model without the tip brakes. Up to this point in its atmospheric testing program, the Enertech 1500 has survived wind speeds of 44.7 m/s (100 mph).

AUGUST 1980

Rocky Flats Performance Summary

KEDCO Model 1200

MANUFACTURER'S SPECIFICATIONS

(See U.S. CONTACT for available options)

DESIGN OUTPUT:

1.2 kW @ 10 m/s (22 mph)

ROTOR SPEED CONTROL:

Mechanical, blade feathering activated by centrifugal forces on fly-weight.

OPERATING WIND SPEEDS:

CUT-IN: 3.1 m/s (7 mph)

CUT-OUT: 31 m/s (70 mph)

ROTOR CONFIGURATION:

ROTOR DIAMETER: 3.66 m (12 ft)

ROTOR TYPE: Horizontal axis, downwind, variable-pitch

NUMBER OF BLADES: 3

MATERIAL: 2024-T3 Aluminum

GENERATOR/TRANSMISSION:

OUTPUT: 14.4 Vac alterator rectified to dc field windings

GEARBOX: 8.76:1 ratio

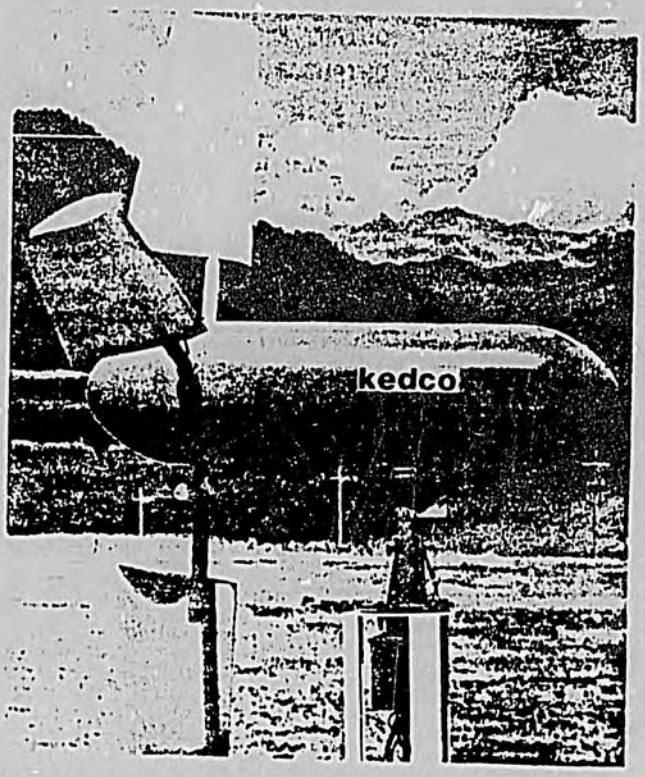

MACHINE DESCRIPTION:

The Model 1200 is a downwind, 3-bladed machine of aluminum construction utilizing aerospace bonding, welding, and riveting techniques. The alternator is a standard industrial model, 12 Vdc rated at 85 A maximum (24 Vdc optional). This model is designed for battery charging and direct electrical applications.

The governor assembly is blade rpm limiting, using a fly-weight/speeder compression spring to feather the blades. Blade feathering devices are mounted on the hub control shaft. The governor assembly will limit the blades to approximately 300 rpm maximum. A vibration monitor initiates feathering of the wind generator when any harmful vibration such as overspeed, a damaged blade, or loading due to ice triggers the monitor arm. The monitor arm can be activated by vibration or manually by cable. Once the vibration problem has been remedied, the blades can be returned (reset) to the generating position manually by the cable.

The carriage which supports the drive train pivots on the yaw column to allow the wind machine to remain aimed into the wind. A tapered bearing supports the weight of the wind electric generator while a plastic seal acts as a bearing to hold the assembly level.

U.S. CONTACT:

KEDCO, INC.
9016 AVIATION BOULEVARD
INGLEWOOD, CA 90301

(213) 776-6636
WIND PROGRAM MANAGER

This PERFORMANCE SUMMARY was prepared and published by the Rockwell International Corporation, Energy Systems Group, Rocky Flats Plant, Wind Systems Program, P.O. Box 464, Golden, CO 80401 for the U.S. Department of Energy, Office of Solar Power Applications Federal Wind Energy Program

Contract DE-AC04-76DP03533

ROCKY FLATS PERFORMANCE DATA

KEDCO Model 1200

MEASURED CHARACTERISTICS
(ADJUSTED TO SEA LEVEL)

CUT-IN WIND SPEED.....5 m/s (11 mph)
CUT-OUT WIND SPEED.....Not available
SURVIVAL WIND SPEED.....Not available
OUTPUT @ 9 m/s (20 mph).....550 Watts
OUTPUT @ 10 m/s (22 mph).....750 Watts
NOISE @ RATED OUTPUT.....Not Available

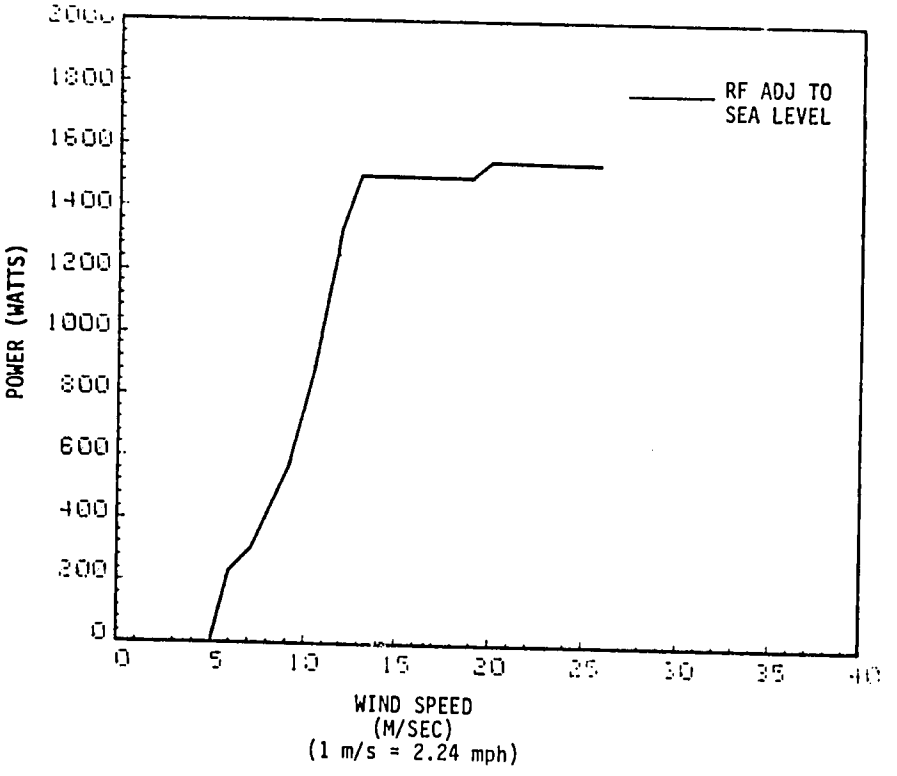

ESTIMATED ANNUAL ENERGY PRODUCTION
(USING A RAYLEIGH WIND DISTRIBUTION)

AVERAGE WIND VELOCITY (m/s)	(mph)	ANNUAL ENERGY OUTPUT (kWh)
3.58	8	430
4.47	10	1030
5.36	12	1850
6.26	14	2810
7.15	16	3810

NOTE: *The annual energy output is based on the measured Rocky Flats power curve for this machine. The power curve is superimposed on a Rayleigh velocity duration curve to generate a power duration curve which is then integrated over time to obtain energy. Energy output will vary at specific sites due to variations in wind characteristics and other factors.*

SUMMARY

Due to problems with the manufacturer's control box and the feathering mechanism, significant amounts of long term data were never generated by atmospheric testing of the Kedco 1200. Therefore, to produce performance data, a decision was made to suspend atmospheric testing of the machine and transport it to the Department of Transportation rail facility in Pueblo, Colorado for controlled velocity testing (CVT). Prior to the start of CVT, a new control box was installed on the Kedco. The control box performed flawlessly during the tests. Also, the feathering mechanism was manually adjusted during CVT, thereby eliminating problems encountered during atmospheric testing. It is felt that the CVT data presented above are reflective of the true performance of the Kedco and would be in close agreement with data obtained from atmospheric testing.

08/80 dlm

Rocky Flats Performance Summary

MEHRKAM 440

FEBRUARY 1982

MANUFACTURER'S SPECIFICATIONS

(See U.S. CONTACT for available options)

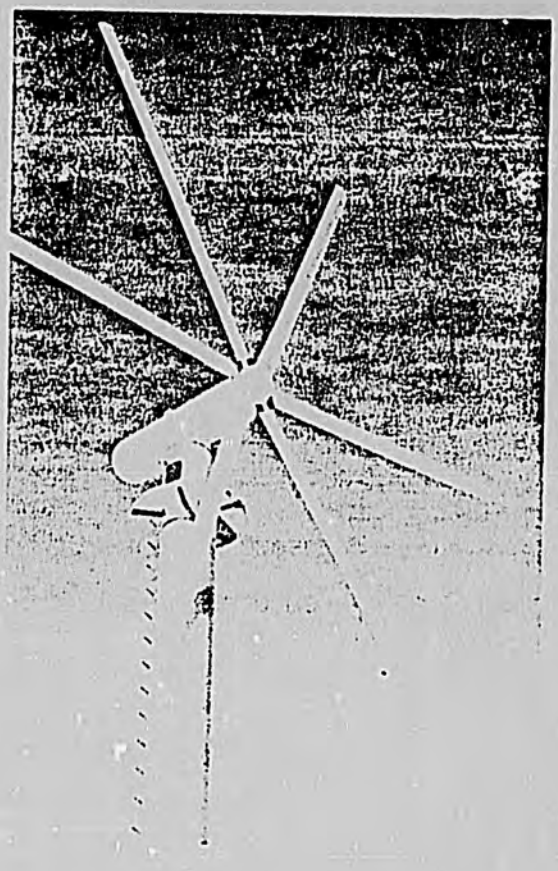

DESIGN OUTPUT:

40 kW @ 12.1 m/s (27 mph)

ROTOR SPEED CONTROL:

Three (3) heavy duty friction brakes activated by control sensor or manual operation.

OPERATING WIND SPEEDS:

CUT-IN: 2.2 m/s (5 mph)

CUT-OUT: 17.9 m/s (40 mph)

ROTOR CONFIGURATION:

ROTOR DIAMETER: 11.28 m (37 ft)

ROTOR TYPE: Horizontal axis, fixed pitch, downwind.

NUMBER OF BLADES: 6

MATERIAL: Aluminum (pop riveted sheet)

GENERATOR/TRANSMISSION:

OUTPUT: 480 Vac, 60 cycle, 3Ø induction generator

GEARBOX: Ratio 24.85:1

MACHINE DESCRIPTION:

The Mehrkam 440 tested at Rocky Flats was a 6-bladed, horizontal-axis, downwind machine. The unit was free in yaw with a mechanical system for orientation into the wind (if needed). An anemometer and high gust detection device was used in the test machine to trigger three (3) brakes to the rotor low and high speed shafts for shutdown in winds above 17.9 m/s (40 mph). These brakes were also designed to actuate when rotor overspeed, excessive vibration, or utility power loss was detected.

U.S. CONTACT:

MEHRKAM ENERGY DEVELOPMENT COMPANY
179 EAST ROAD #2
HAMBURG, PA 19526

(215) 562-8856
HELENA MEHRKAM OR KAREN VOTYAS

This PERFORMANCE SUMMARY was prepared and published by the Rockwell International Corporation, Energy Systems Group, Rocky Flats Plant, Wind Systems Program, P.O. Box 464, Golden, CO 80402
for the
U.S. Department of Energy, Wind Energy Technology Division
Federal Wind Energy Program

Contract DE-AC04-76DP03533

ROCKY FLATS PERFORMANCE DATA

MEHRKAM 440

MEASURED CHARACTERISTICS
(ADJUSTED TO SEA LEVEL)

CUT-IN WIND SPEED.....4 m/s (9 mph)
CUT-OUT WIND SPEED.....17.9 m/s (40 mph)
SURVIVED WIND SPEED*.....44.7 m/s (100 mph)
OUTPUT @ 9 m/s (20 mph).....3540 Watts
OUTPUT @ 12.1 m/s (27 mph).....5660 Watts
NOISE @ RATED OUTPUT.....Not Available

* See SUMMARY below

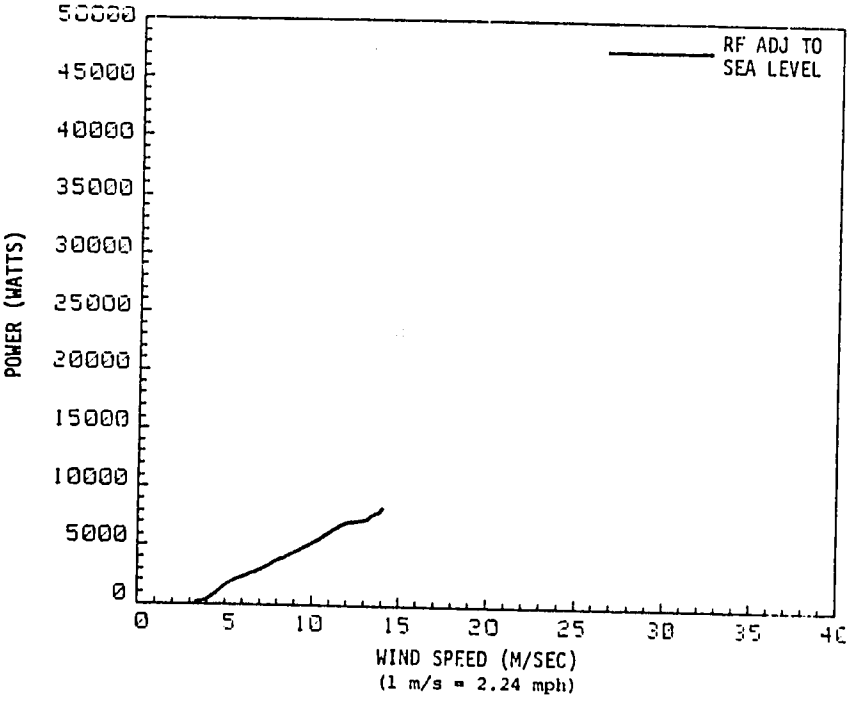

ESTIMATED ANNUAL ENERGY PRODUCTION
(USING A RAYLEIGH WIND DISTRIBUTION)

AVERAGE WIND VELOCITY (m/s)	(mph)	ANNUAL ENERGY OUTPUT (kWh)
3.58	8	6410
4.47	10	11350
5.36	12	16480
6.26	14	21120
7.15	16	24560

NOTE: *The annual energy output is based on the measured Rocky Flats power curve for this machine. The power curve is superimposed on a Rayleigh velocity duration curve which is then integrated over time to obtain energy. Energy output will vary at specific sites due to variations in wind characteristics and other factors.*

SUMMARY

While undergoing atmospheric testing at the Wind Systems Test Center, the Mehrkam 440 experienced wind speeds of 44.7 m/s (100 mph) while in a total shutdown mode. However, while in this mode fatigue cracks occured at the junction of the blade support spars and hub ends of all six blades. Due to the significant differences between Rocky Flats test data and manufacturer's predicted machine performance, the machine was removed from the tower to undergo dynamometer testing and aerodynamic rotor analysis to determine the cause for the disparity. These analyses indicated that the torque required for the unit to generate 40 kW could only be obtained at wind speeds of at least 26.8 m/s (60 mph) and with a blade pitch angle that would prohibit rotor startup in moderate winds. During these tests, a short developed in the rotor brake control system. Based upon these findings and manufacturer unavailability to perform necessary repairs, further testing was suspended.

Rocky Flats Performance Summary

PINSON C2E1

OCTOBER 1981

MANUFACTURER'S SPECIFICATIONS

(See U.S. CONTACT for available options)

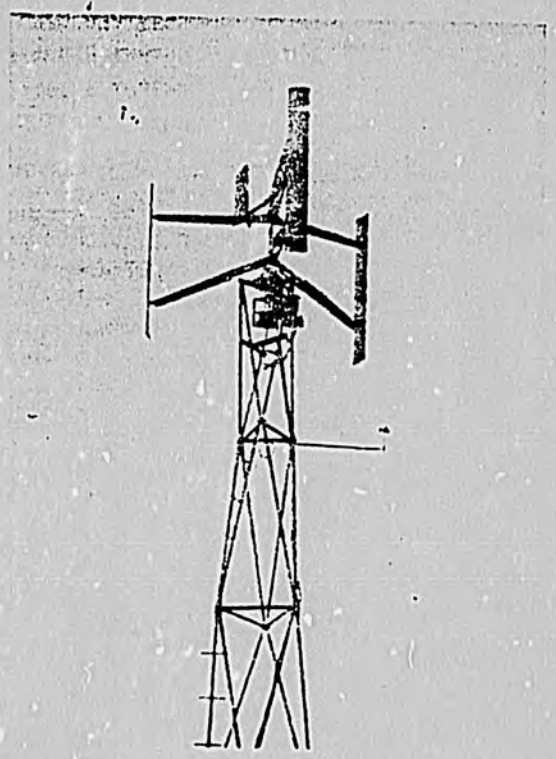

DESIGN OUTPUT:

2.0 kW @ 10.7 m/s (24 mph)

ROTOR SPEED CONTROL:

Mechanical, centrifugally activated force balance adjusts blade angles.

OPERATING WIND SPEEDS:

CUT-IN: 3.1 m/s (7 mph)

CUT-OUT: 17.9 m/s (40 mph)

ROTOR CONFIGURATION:

ROTOR DIAMETER: 3.66 m (12 ft)

ROTOR TYPE: Vertical axis, Vertically straight-bladed, variable pitch.

NUMBER OF BLADES: 3

MATERIAL: 6061-T6 aluminum

GENERATOR/TRANSMISSION:

OUTPUT: 240 Vac, 16 A, internal excitation alternator.

GEARBOX: 2 stage timing belt. Ratio 8.57:1

MACHINE DESCRIPTION:

The C2E is a vertical axis, vertically straight-bladed wind machine with cyclically pitched blades. It is similar in aerodynamic operation to a design patented in 1931 by G.J.M. Darrieus. The cycloturbine differs from this classic eggbeater rotor in that its blades do not remain at a fixed "flat" angle, but follow a preset schedule of angle, allowing more favorable use of aerodynamic force on the blades. The amount and timing of pitch change is determined by a cam device mounted atop the main shaft, actuating the blades via pull rods. A tail vane affixed to the cam programs correct operation relative to the wind direction. The overspeed control system is a mechanical, centrifugally activated force balance. When the centrifugal force reaches a specified amount, a tilt box is tripped, which drives the blades to a feathered condition.

U.S. CONTACT:

PINSON ENERGY CORPORATION
P.O. BOX 7
MARSTON MILLS, MA 02648

(617) 477-2913
HERMAN DREES

This PERFORMANCE SUMMARY was prepared and published by the Rockwell International Corporation Energy Systems Group, Rocky Flats Plant, Wind Systems Program, P.O. Box 464, Golden, CO 80401 for the U.S. Department of Energy, Office of Solar Power Applications Federal Wind Energy Program

Contract DE-AC04-76DP03533

10/81 dlm

ROCKY FLATS PERFORMANCE DATA

Pinson C2E1

MEASURED CHARACTERISTICS
(ADJUSTED TO SEA LEVEL)

CUT-IN WIND SPEED.....4 m/s (9 mph)
CUT-OUT WIND SPEED.....22 m/s (49 mph)
SURVIVED WIND SPEED.....52.7 m/s (117 mph)
OUTPUT @ 9 m/s (20 mph).....938 Watts
OUTPUT @ 10.7 m/s (24 mph).....1669 Watts
NOISE @ RATED OUTPUT.....Not Available

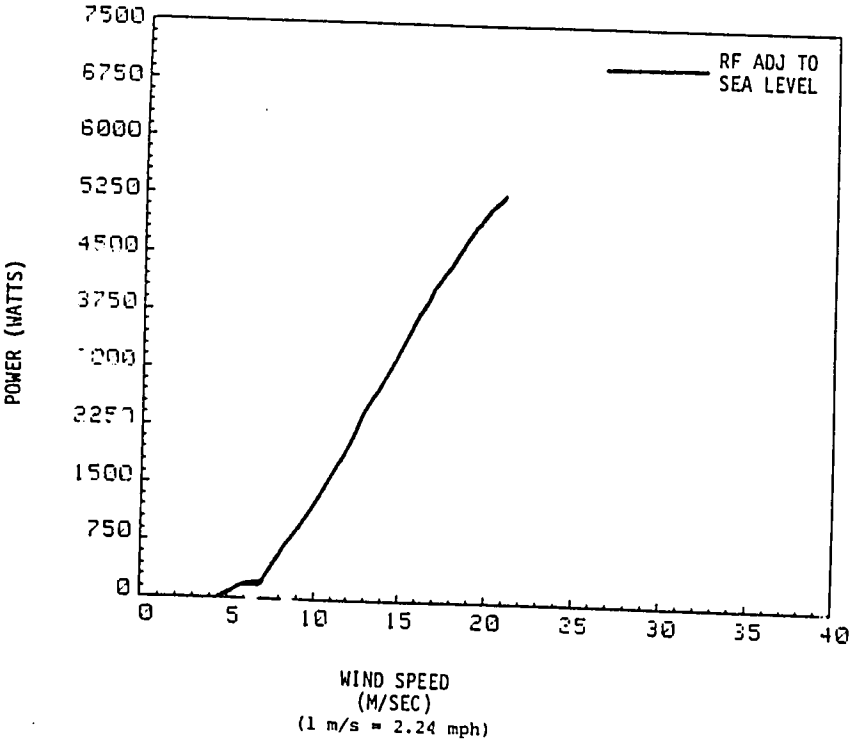

ESTIMATED ANNUAL ENERGY PRODUCTION
(USING A RAYLEIGH WIND DISTRIBUTION)

AVERAGE WIND VELOCITY (m/s)	(mph)	ANNUAL ENERGY OUTPUT (kWh)
3.58	8	690
4.47	10	1540
5.36	12	2820
6.26	14	4500
7.15	16	6450

NOTE: *The annual energy output is based on the measured Rocky Flats power curve for this machine. The power curve is superimposed on a Rayleigh velocity duration curve which is then integrated over time to obtain energy. Energy output will vary at specific sites due to variations in wind characteristics and other factors.*

SUMMARY

While undergoing atmospheric testing at Rocky Flats, the Pinson C2E1 was mounted on a Rohn SSV tower with an octahedron extension. Following a windstorm that produced speeds of 42 m/s (94 mph), cracks were observed on the C2E1 hub plates and blade skins. The machine feathered normally during this windstorm and no conclusive data exist linking the high wind speeds and the cracks. A subsequent investigation revealed that machine/tower interaction was at least partially responsible for these cracks. Consequently, the Rohn SSV was replaced with octahedron sections and the hub plates redesigned. Following this change, the C2E1 underwent limited atmospheric testing and survived wind speeds of 52.7 m/s (117 mph) without incurring structural damage. However, performance during these tests was sparse and inconclusive. As a result, performance data presented above were generated during controlled velocity testing at the Department of Transportation rail facility in Pueblo, Colorado. The maximum output presented above may be attributed to the fact that the auto-pitch control was not attached during these tests and, therefore, the machine did not feather as designed.

Rocky Flats Performance Summary

AUGUST 1980

SENCENBAUGH Model 1000-14

MANUFACTURER'S SPECIFICATIONS

(See U.S. CONTACT for available options)

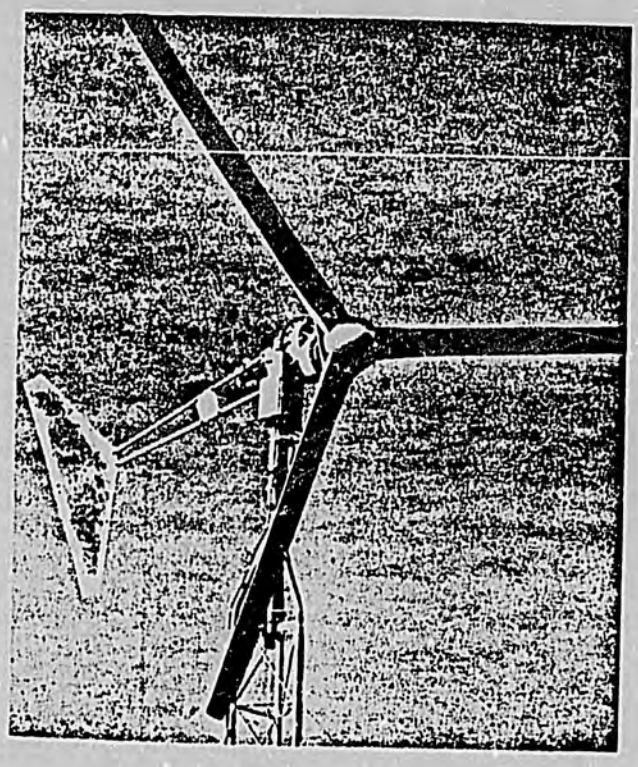

DESIGN OUTPUT:

1.0 kW @ 10.3 m/s (23 mph)

ROTOR SPEED CONTROL:

Mechanical, rotor turns edgewise to wind, activated by excessive thrust load.

OPERATING WIND SPEEDS:

CUT-IN: 2.7 m/s (6 mph)

CUT-OUT: 27 m/s (60 mph)

ROTOR CONFIGURATION:

ROTOR DIAMETER: 3.65 m (12 ft)

ROTOR TYPE: Horizontal axis, upwind, fixed-pitch.

NUMBER OF BLADES: 3

MATERIAL: Wood (Sitka spruce), bonded copper leading edge, epoxy finish.

GENERATOR/TRANSMISSION:

OUTPUT: 3-Ø, 6-pole alternator, rect. to dc.

GEARBOX: Helical, 3:1 ratio

MACHINE DESCRIPTION:

The Sencenbaugh is a lightweight machine manufactured by Sencenbaugh Wind Electric, Palo Alto, California. The blades are manufactured from Sitka spruce, with a bonded copper leading edge and a polyurethane finish. The main generator casting is 356T6 aluminum alloy. The alternator is coupled through a 3:1 helical gearbox, and is driven by a 3-bladed propeller 3.65 m in diameter. Overspeed control is provided by using the increasing wind pressure of the propeller (and the resultant propeller thrust) to swing the alternator assembly (which is offset from the bearing support column) out of the oncoming wind. The foldable tail automatically reopens as wind speed decreases due to gravitational forces on the tail assembly. Tail offset and inclination with respect to the rotor may be varied, thus changing the cut-in speed of the machine.

U.S. CONTACT:

SENCENBAUGH WIND ELECTRIC
P.O. BOX 11174
PALO ALTO, CALIFORNIA 94306

(415) 964-1593
JIM SENCENBAUGH

This PERFORMANCE SUMMARY was prepared and published by the Rockwell International Corporation, Energy Systems Group, Rocky Flats Plant, Wind Systems Program, P.O. Box 464, Golden, CO 80401 for the U.S. Department of Energy, Office of Solar Power Applications Federal Wind Energy Program

Contract DE-AC04-76DP03533

SENCENBAUGH 1000-14

MEASURED CHARACTERISTICS
(ADJUSTED TO SEA LEVEL)

CUT-IN WIND SPEED.....3 m/s (7 mph)
CUT-OUT WIND SPEED.....Not available
SURVIVAL WIND SPEED.....52.5 m/s (117 mph)
OUTPUT @ 9 m/s (20 mph).....780 Watts
OUTPUT @ 10.3 m/s (23 mph).....820 Watts
NOISE @ RATED OUTPUT.....Not available

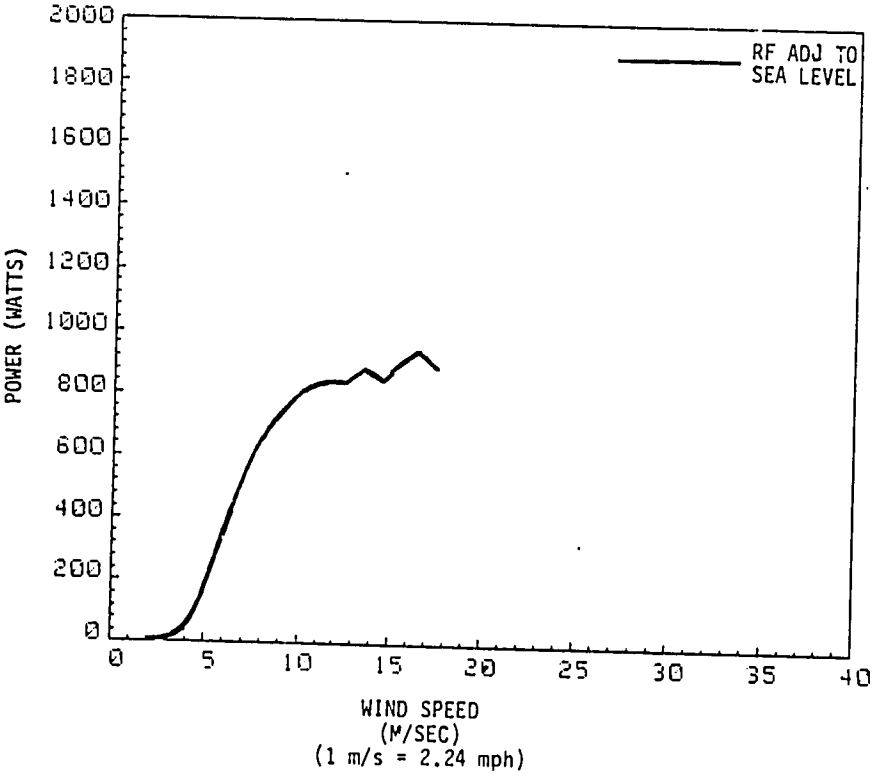

ESTIMATED ANNUAL ENERGY PRODUCTION
(USING A RAYLEIGH WIND DISTRIBUTION)

AVERAGE WIND VELOCITY (m/s)	(mph)	ANNUAL ENERGY OUTPUT (kWh)
3.58	8	960
4.47	10	1750
5.36	12	2550
6.26	14	3270
7.15	16	3860

NOTE: *The annual energy output is based on the measured Rocky Flats power curve for this machine. The power curve is superimposed on a Rayleigh velocity duration curve to generate a power duration curve which is then integrated over time to obtain energy. Energy output will vary at specific sites due to variations in wind characteristics and other factors.*

SUMMARY

The Sencenbaugh Model 1000-14 WTG met or exceeded all manufacturer claims of survivability while undergoing atmospheric testing at Rocky Flats. The machine operated satisfactorily in wind speeds exceeding 52.5 m/s (117 mph). In addition, the Sencenbaugh operated in winds exceeding 22.5 m/s (50 mph) for 17 hours without incurring damage. However, performance data generated by atmospheric testing of the machine did not agree with manufacturer performance data over the entire wind speed range. It should be noted that the machine tested at Rocky Flats was tested under a variety of tail assembly adjustments. It is believed that the operational characteristics of the tail design contributed to the machine's inability to reach rated output.

Rocky Flats Performance Summary

WHIRLWIND A120

DECEMBER 1980

MANUFACTURER'S SPECIFICATIONS

(See U.S. CONTACT for available options)

DESIGN OUTPUT:

2.0 kW @ 11.2 m/s (25 mph)

ROTOR SPEED CONTROL:

Electromagnetic; actuated by wind sensor for wind gusts above 13.4 m/s (30 mph); manually activated for maintenance and in anticipation of high winds; will hold propeller shut down in winds up to 80 mph.

OPERATING WIND SPEEDS:

CUT-IN: 3.1 m/s (7 mph)

CUT-OUT: 13.4 m/s (30 mph)

ROTOR CONFIGURATION:

ROTOR DIAMETER: 3.05 m (10 ft)

ROTOR TYPE: Horizontal axis, fixed pitch, downwind.

NUMBER OF BLADES: 2

MATERIAL: Wood, polyurethane finish.

GENERATOR/TRANSMISSION:

OUTPUT: 3Ø, alternator; permanent magnet type; 18 pole.

GEARBOX: Direct-drive.

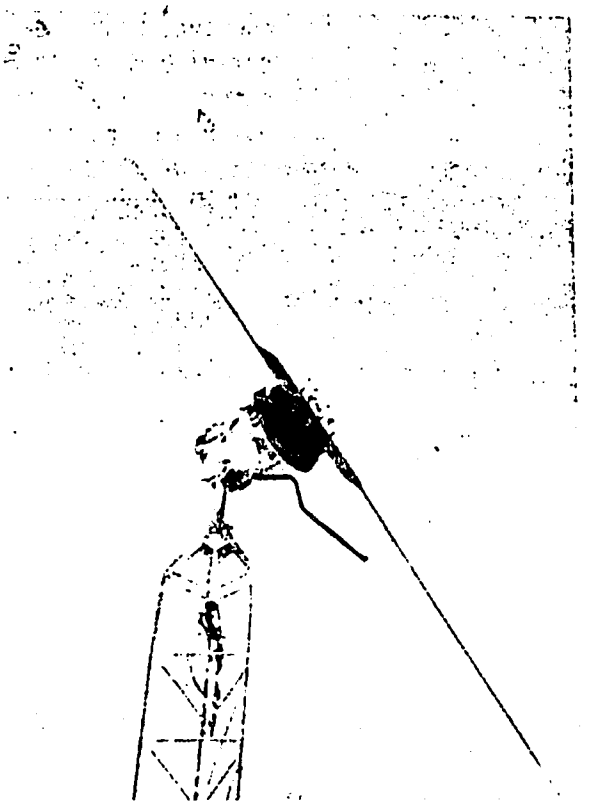

MACHINE DESCRIPTION:

The Whirlwind is a horizontal axis, downwind machine with a two-bladed, fixed-pitch propeller-type rotor. It is rated at 2 kW in an 11.2 m/s (25 mph) wind. The 3 phase alternator is self-excited and produces variable frequency ac. The control box accepts the output of the generator and produces four distinct load types. These are: 1) 90-110 V, 500 watts (W) of regulated ac (40-130 Hz); 2) battery 2,000 W (17 amps) at 120 Vdc; 3) system heater (space heater) 2,000 W ac; 4) auxiliary heater (optional) 2,000 W ac.

The control box has a "priority" switch which allocates the power from the wind generator. In the automatic position of the priority switch, the control box will first send power to the regulated ac load, second to the battery, third to the auxiliary heater, and lastly, to the system heater. The switch can also be set to send power only to the auxiliary heater or only to the battery. When power is directed to the auxiliary heater only, power will be redirected to the system heater when the heating requirements of the auxiliary heater are (thermostatically) satisfied.

U.S. CONTACT:

WHIRLWIND POWER COMPANY
2458 W. 29th AVENUE
DENVER, COLORADO 80211

(303) 477-6436
ELLIOTT BAYLY

This PERFORMANCE SUMMARY was prepared and published by the Rockwell International Corporation Energy Systems Group, Rocky Flats Plant, Wind Systems Program, P.O. Box 464, Golden, CO 80401
for the
U.S. Department of Energy, Office of Solar Power Applications
Federal Wind Energy Program

Contract DE-AC04-76DP03533

ROCKY FLATS PERFORMANCE DATA

Whirlwind A120

MEASURED CHARACTERISTICS
(ADJUSTED TO SEA LEVEL)

CUT-IN WIND SPEED.....5 m/s (11 mph)
CUT-OUT WIND SPEED.....14 m/s (31 mph)
SURVIVAL WIND SPEED.....35.8 m/s (80 mph)
OUTPUT @ 9 m/s (20 mph).....1088 Watts
OUTPUT @ 11.2 m/s (25 mph).....1.8 kW
NOISE @ RATED OUTPUT.....NOT AVAILABLE

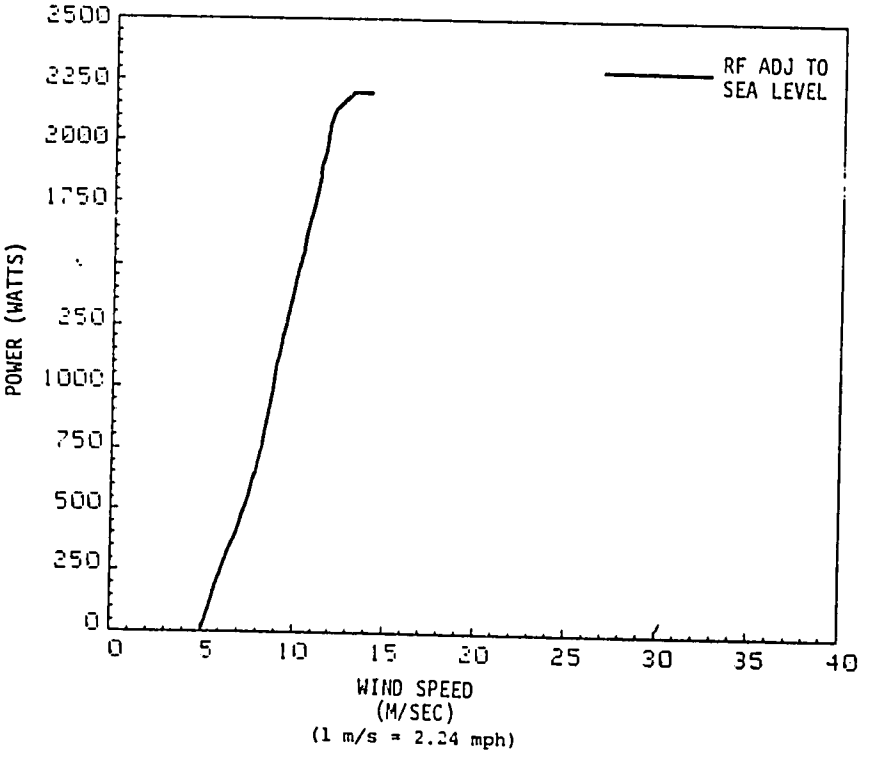

ESTIMATED ANNUAL ENERGY PRODUCTION
(USING A RAYLEIGH WIND DISTRIBUTION)

AVERAGE WIND VELOCITY (m/s)	(mph)	ANNUAL ENERGY OUTPUT (kWh)
3.58	8	590
4.47	10	1580
5.36	12	2900
6.26	14	4250
7.15	16	5360

NOTE: *The annual energy output is based on the measured Rocky Flats power curve for this machine. The power curve is superimposed on a Rayleigh velocity duration curve which is then integrated over time to obtain energy. Energy output will vary at specific sites due to variations in wind characteristics and other factors.*

SUMMARY

During atmospheric testing at Rocky Flats, the Whirlwind A120 met manufacturer survivability claims by experiencing wind speeds of 35.8 m/s (80 mph) without incurring structural damage. The one major machine failure occurred when the rotor oversped during winds of approximately 22.4 m/s (50 mph) thereby creating excessive heat which destroyed the generator. All A120's now marketed include a "sidewheel" yaw mechanism that is designed to prevent failures of this nature. However, Rocky Flats testing of the A120 was concluded prior to the addition of this feature. Rocky Flats performance data are in close agreement with manufacturer-produced data and indicate the A120 is capable of producing its rated output.

12/80 dlm

EXPLORATORY PHASE

WIND RESOURCE CLIMATOLOGY

H. L. Wegley, D. L. Elliott and W. R. Barchet
Pacific Northwest Laboratory

Establishment of a wind resource climatology for a region or nation can be divided into three phases:

1) identification of all available wind data sources
2) use of supplemental information for data-sparse areas, and
3) synthesis and presentation of the wind data to show spatial and temporal variations of wind energy.

1.1 DATA SOURCES AND QUALITY

Most countries have a climatological data center that can provide the majority of wind data for a wind resource analysis. Data available at a climatic center may be digitized on magnetic tape, exist in wind summaries, or be simply a collection of unsummarized weather logs. Digitized data can be easily processed to produce summaries providing there is access to computing facilities. Unsummarized wind data can be summarized by hand or it can be entered into a data storage system for processing. However, both of these approaches can be time consuming and costly. An alternative is to screen the data to infer or estimate the wind characteristics. (Suggested screening procedures will be discussed later in this section.)

Sources of data other than those available at national climatic centers should also be investigated. These sources might include wind data from offshore platforms, ships, or lighthouses. Routinely gathered, or experimental, air pollution wind data may be available from industrial or other sites. Universities with programs in the atmospheric sciences or agriculture may have wind data. Rawinsonde or pibal measurements may also be a useful source of data. Their application is described in Section 1.2.1.

Once all wind data sources have been identified, the data should be stratified according to quality. Stratification by quality, though often subjective, will help to ensure that only the highest quality data available are used in each region analyzed. As the wind data become more sparse, lower quality data will become useful in describing the wind characteristics of a region.

Wind data quality depends upon factors, such as:

- the size of speed classes in available wind summaries
- the sampling (observation) rate
- the averaging interval of the observation
- the accuracy of the observational equipment or technique
- changes in height and exposure of anemometry
- format of the data used
- knowledge and experience of the observer
- wind speed sample size.

High quality data will contain many observations per day, which have an averaging interval close to the WECS response time to the wind. The data will be collected by either accurate anemometry (which is properly maintained) or by a knowledgeable observer. Height and exposure changes of the anemometry should be documented. The best data will contain five or more years at a constant height and exposure.

Screening of unsummarized wind data by the above criteria may eliminate data from the analysis or place data in a lower-quality category so they would only be used in data-sparse regions. If unsummarized data are to be used, selected periods can be scanned visually. By visually scanning and categorizing the seasonal and annual wind speeds, the need for more detailed analysis of unsummarized data can be determined. If a site appears to have moderate or strong winds or appears to be an anomaly in a region, then more detailed visual scanning can be performed on at least one year of the unsummarized wind records to estimate the most frequent wind speeds, prevailing direction, frequency and direction of the higher wind speeds (those capable of driving a WECS), and the persistence of the winds.

1.2 INTERPOLATION IN DATA-SPARSE AREAS

In data-sparse regions, an objective interpolation among wind locations may not provide a reliable wind resource analysis. Quite often the data-sparse regions are in areas of complex terrain, and certain indirect indicators of wind energy, such as 1) meteorological and topographical indicators, 2) vegetation features and 3) eolian landforms[(a)] may aid the analysis of the wind resource.

1.2.1 Meteorological and Topographical Indicators of Wind

Some meteorological and topographical features indicative of high wind energy are:

- corridors of frequent and strong pressure gradients
- long, sloping valleys parallel to prevailing winds
- high elevation plains and plateaus in areas of strong geostrophic winds
- plains and valleys with persistent downslope winds associated with strong pressure gradients
- exposed ridge crests and mountain summits in areas of strong geostrophic winds
- exposed coastal sites in areas of strong geostrophic winds or thermal gradients.

Low wind power areas are often associated with:

- valleys perpendicular to the prevailing wind
- small and/or sheltered basins
- short and/or very narrow valleys or canyons
- areas of high surface roughness.

Figure 1.1 illustrates many of the indicators of both high and low wind energy potential as they have been applied to the Rocky Mountains of the United States.

(a) Numerical or physical modeling discussed in Section 3.2 of "Selecting Sites for Wind Machines" may also provide insight into the wind resource in data-sparse areas.

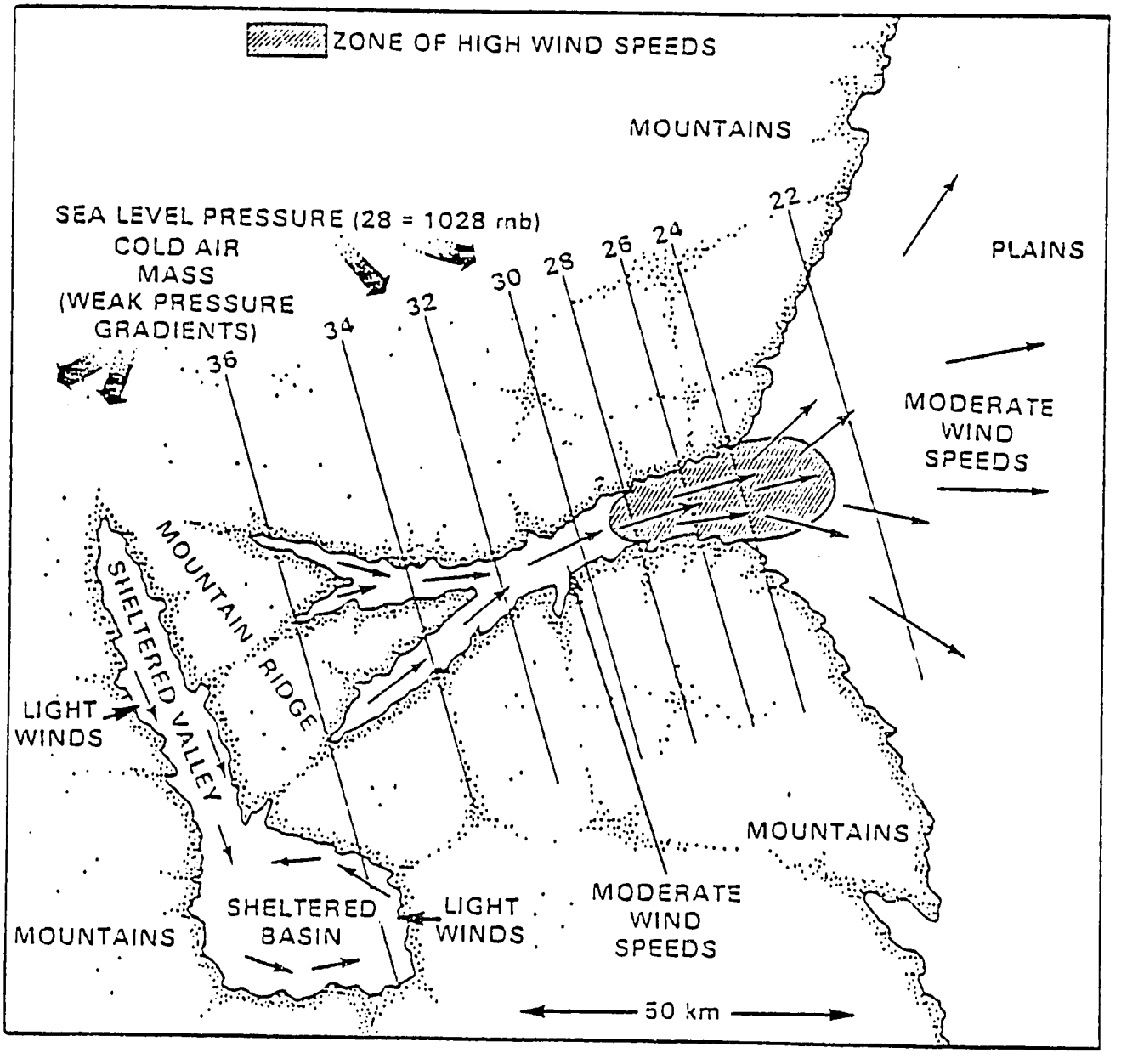

FIGURE 1.1. Frequent Winter Condition in the Northern Rocky Mountains Resulting in Strong Corridor Winds (Elliott 1979)

In mountainous areas, rawinsonde data can be used to infer high wind energy potential on exposed ridge crests. Rules-of-thumb that have been used for estimating wind power in exposed mountainous locations from free-air observations are:

- the 10-meter wind power is equal to one-third of the free-air wind power
- the 50-meter win ower is equal to two-thirds of the free-air wind power.

Any available wind data in such locations can be used to augment or refine these estimates.

The 1/3 and 2/3 wind power rules-of-thumb are based upon median values obtained when correlating mountain-top and free-air wind speeds, then converting the mean wind speeds to wind power density using a Rayleigh distribution. Seasonal climatologies for 850 mb, 700 mb, and 500 mb constant pressure levels can be used in a linear interpolation scheme to estimate the free-air wind speed for a mountain peak. An alternate procedure is to develop mean seasonal wind profiles up to the height of the highest peaks from rawinsonde summaries for the region and to estimate the free-air speed at mountain-top level. The latter procedure is preferred in trade wind regimes to account for the wind speed maximum that generally is found between 900 mb and 850 mb.

1.2.2 Vegetation and Eolian Indicators of Wind

In remote forested areas, vegetation indicators may be useful in estimating wind energy potential. The flagging of trees is perhaps the most easily observed method of using vegetation to infer wind speed. (A flagged tree is one in which the growth of branches produces an asymmetrical crown.) Figure 1.2 depicts flagged trees from the side and top and numerically classifies the degree of flagging using the Griggs-Putnam Index. Different species of trees may be flagged to different extents by the same winds; however, classification of flagging by tree type has demonstrated that this method can be used to obtain rough estimates of the annual average wind speed. Some results of using the Griggs-Putnam Index to estimate the average annual winds are shown in Figure 1.3. The mean speed prediction error for this technique is $\pm$15% of the true mean wind speed.

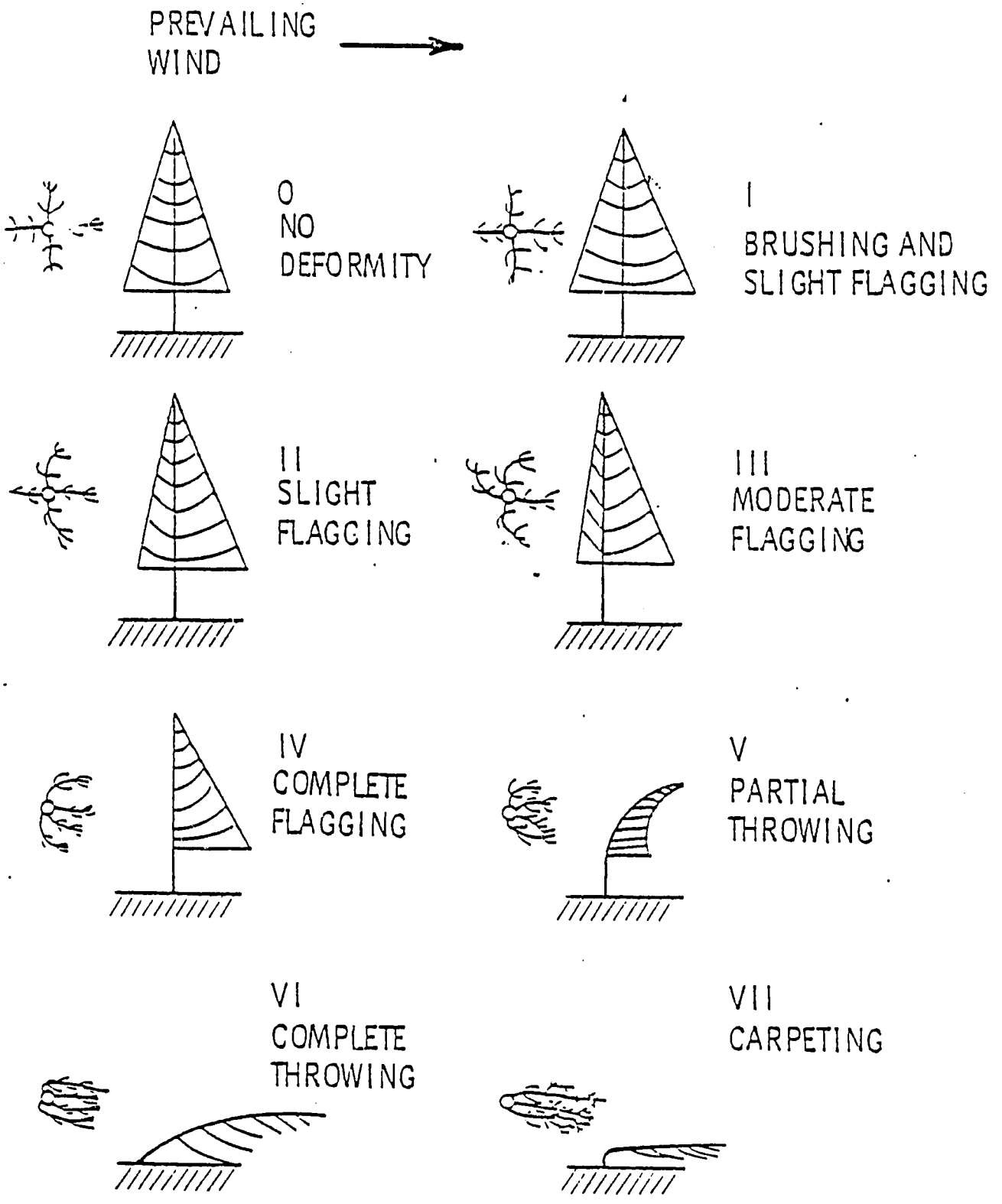

FIGURE 1.2. Classification of Tree Flagging by the Griggs-Putnam Index (Hewson et al. 1979)

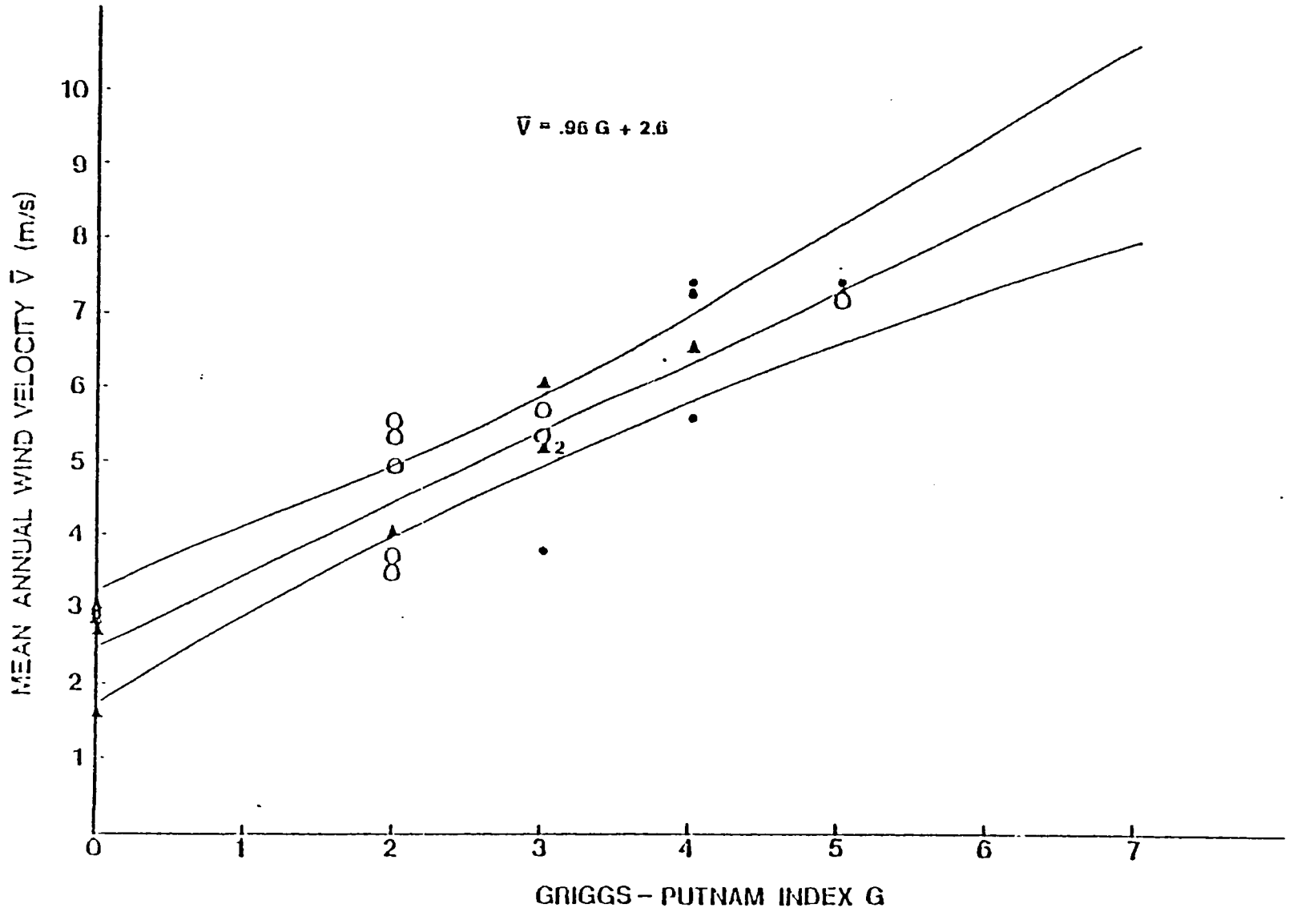

FIGURE 1.3. The Relationship Between the Griggs-Putnam Index and Mean Annual Wind Speed for a Data Set Containing Both Douglas-Fir and Ponderosa Pine. The 99% estimation limits are given for the regression equation. Hewson et al. 1979)

The deformation ratio shown in Figure 1.4 ranks second to the Griggs-Putnam Index in accuracy. Linear regression of the deformation ratio with mean wind speed produced the results shown in Figure 1.5. These results represent approximately a ±18% mean error in estimating annual average winds.

When using vegetative indicators of wind, there are certain drawbacks which must be considered. The degree of flagging is a species-dependent phenomenon and may be biased toward winds occurring during the growing season (spring and summer). Past or present growing conditions, diseases, trees that once grew nearby and ice storms may also cause deformation of the tree crown. Although trees provide only rough estimates of wind power potential, continued research in this area involving more species of trees and the analysis of large data samples should yield vegetation indicators that provide a useful means of estimating the wind resource in forested data-sparse areas.

Eolian landforms are another type of supplemental wind information that may be useful in data-sparse regions. Eolian indicators of wind are most likely to be present in sparsely vegetated arid and semi-arid lands. Surface features indicative of areas of strong wind are sand dunes, playas[(a)], and scour features produced by wind erosion. Mapping of such features from satellite imagery or aerial photography can be used to locate regions of possibly high wind energy potential. However, quantitative techniques for estimating wind speeds from an analysis of eolian landforms are still in the developmental stage.

1.3 SYNTHESIS AND PRESENTATION OF WIND RESOURCE DATA

A realistic goal of any wind resource analysis is to provide as completely as possible a description of the spatial and temporal variations in the available wind energy and to describe the analysis techniques employed to give the user an appreciation of the uncertainties in the analysis. Furthermore, the spatial variation of the resource is sensitive to the exposure of sites to the wind and to the height above the surface at which the resource is to be depicted.

(a) Playas are shallow desert basins where water gathers after rains and then evaporates.

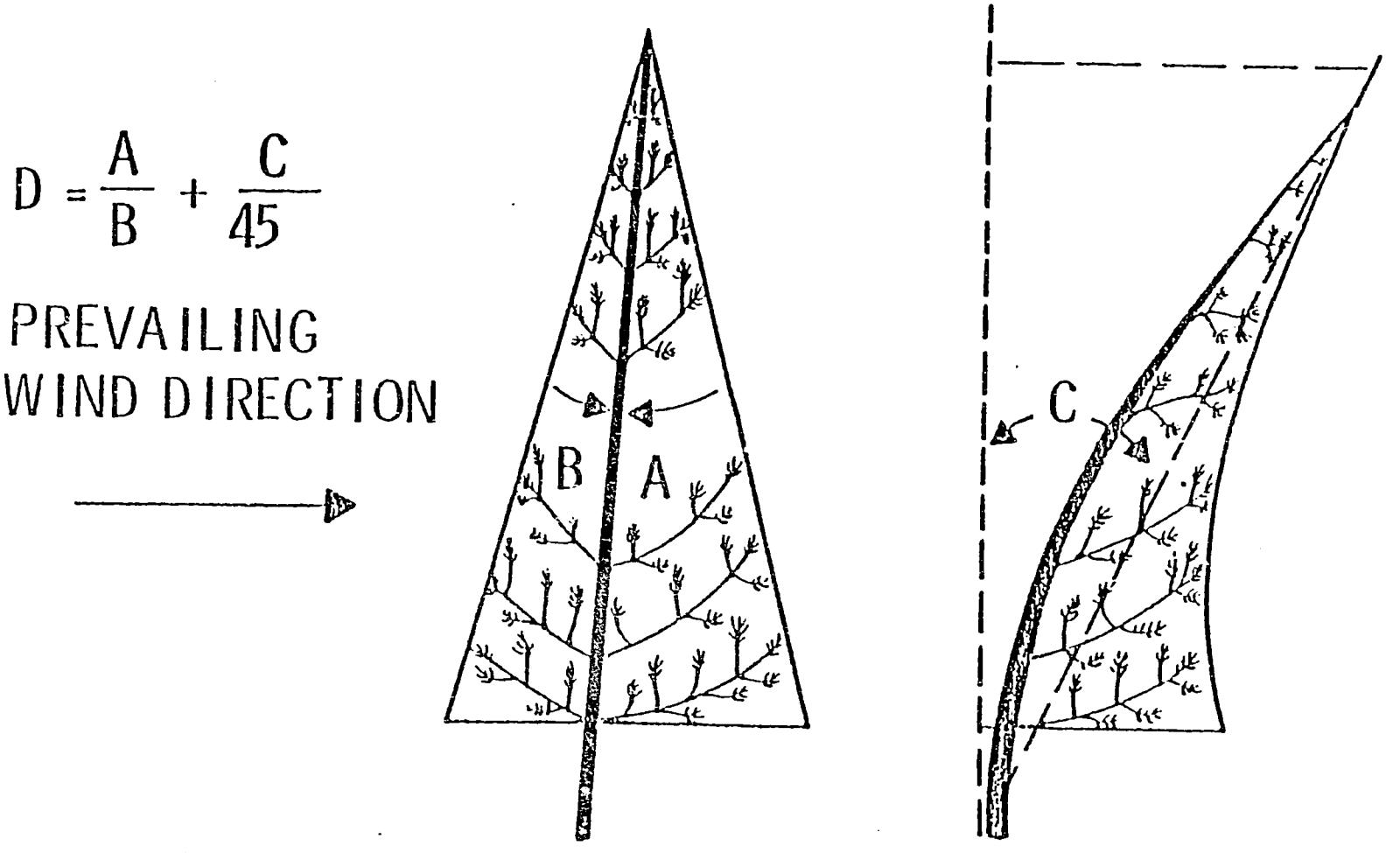

FIGURE 1.4. Classification of Tree Flagging by the Deformation Ratio (Hewson et al. 1979)

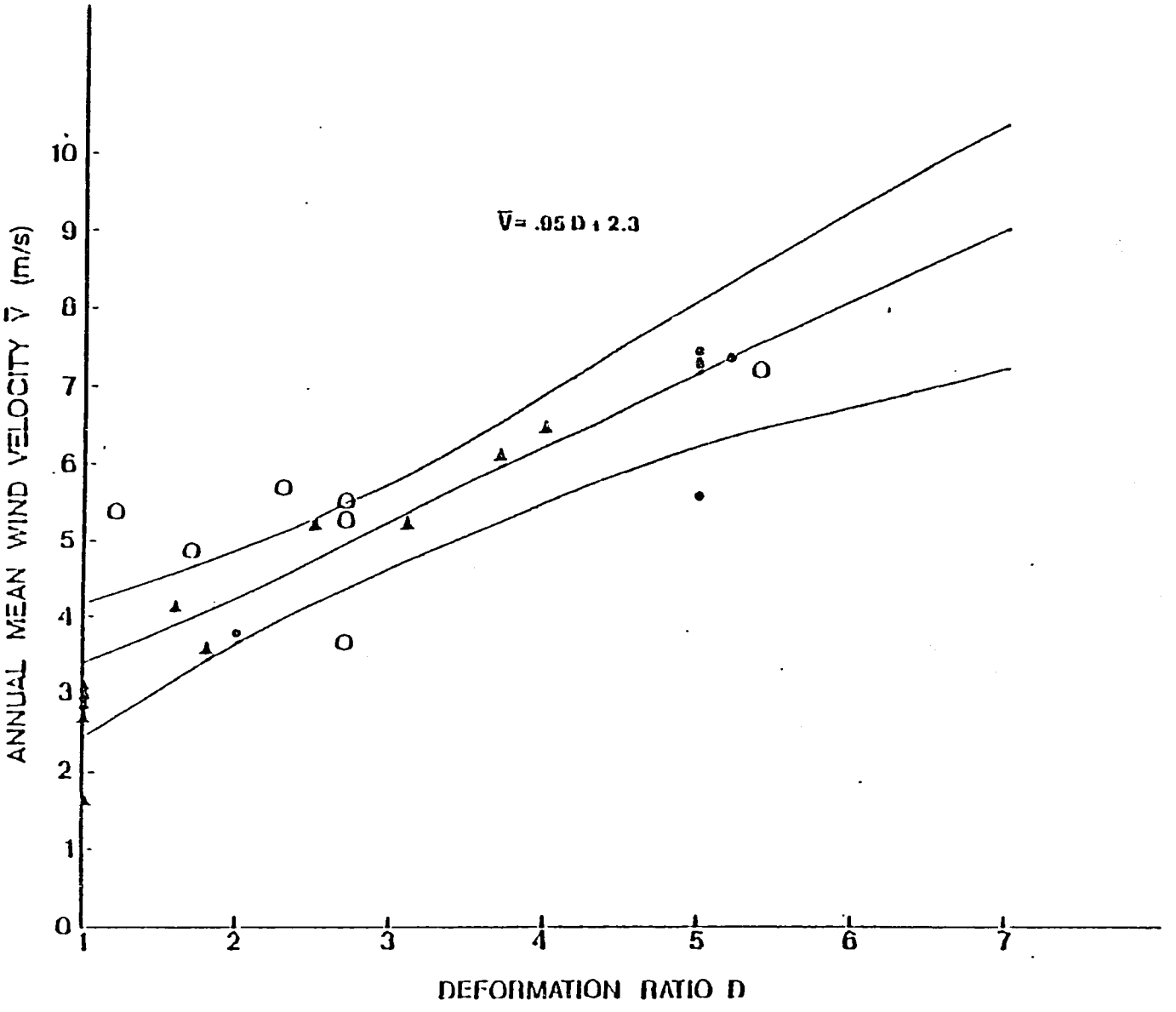

FIGURE 1.5. The Relationship Between the Deformation Ratio and Mean Annual Wind Speed for a Date Set Containing Both Douglas-Fir and Ponderosa Pine. The 99% estimation limits are given for the regression equation. (Hewson et al. 1979)

Adjustment of wind data to a standard reference height above the surface is a necessity for the proper intercomparison of the wind resource at various sites. An examination of long-term mean wind speeds at air terminal locations and at towers with multiple levels of anemometry indicates that a power-law extrapolation is generally adequate. This extrapolation is as shown:

$$\frac{\overline{V}_r}{\overline{V}_a} = \left(\frac{Z_r}{Z_a}\right)^{\alpha} \quad \text{or} \quad \frac{\overline{P}_r}{\overline{P}_a} = \left(\frac{Z_r}{Z_a}\right)^{3\alpha} \tag{1}$$

where

$\overline{V}_{a,r}$ and $\overline{P}_{a,r}$ = the mean wind speed ($\overline{V}$), or mean wind power density ($\overline{P}$), at the anemometer and reference levels respectively.

α = the power law exponent.

An α of 1/7 has been found to be widely applicable to low surface roughnesses and well-exposed sites (such as air terminals). Other techniques for vertical extrapolation include 1) power-law extrapolations where α is allowed to vary with surface roughness and stability, or 2) log-law extrapolation, where both the surface roughness(es) and the depth of the boundary layer are considered, or 3) power-law extrapolations in which α is given by an empirically determined function of the mean wind speed.

The selection of well-exposed sites as the reference exposure to present the resource appears optimum for wind energy purposes. Well-exposed sites include mountain summits, ridge crests, hill tops, and large upland clearings that are open to the prevailing wind (i.e., not sheltered by upwind topographical features or nearby obstructions).

The completed analysis of the wind resource represents a synthesis of wind data, information on the characteristics of the sites at which data were taken, indirect indicators of wind energy, and the meteorology and topography of the region. A combination of regional maps, as suggested below, plus selected individual station wind data provides a very effective presentation.

1) a map showing major cities and significant cultural and geographical features
2) a detailed topographical relief map
3) a map showing wind data locations as well as data or analysis techniques used in data-sparse areas
4) annual wind-power maps showing wind power for exposed locations at reference heights typical of both large and small WECS (see Figure 1.6)
5) a table relating wind power density to mean wind speed (see Table 1.1)
6) seasonal wind-power maps (in the same scale and format as the annual map)
7) maps for at least four times of the day showing the diurnal variation of wind power by season (where there is sufficient data).

TABLE 1.1. Classes of Wind Power Density at 10 m and 50 m[a] (Elliott and Barchet 1979)

Wind Power Class	10 m (33 ft) Wind Power Density, watts/m²	10 m (33 ft) Speed,[b] m/s (mph)	50 m (164 ft) Wind Power Density, watts/m²	50 m (164 ft) Speed,[b] m/s (mph)
1	0	0	0	0
2	100	4.4 (9.8)	200	5.6 (12.5)
3	150	5.1 (11.5)	300	6.4 (14.3)
4	200	5.6 (12.5)	400	7.0 (15.7)
5	250	6.0 (13.4)	500	7.5 (16.8)
6	300	6.4 (14.3)	600	8.0 (17.9)
7	400	7.0 (15.7)	800	8.8 (19.7)
	1000	9.4 (21.1)	2000	11.9 (26.6)

(a) Vertical extrapolation of wind speed based on the 1/7 power law
(b) Mean wind speed is based on Rayleigh speed distribution of equivalent mean wind power density. Wind speed is for standard sea-level conditions. To maintain the same power density, speed increases 5%/5000 ft (3%/1000 m) of elevation.

Some potential WECS users may consider WECS sites very near existing wind stations. As a result, graphs or tables of the following wind characteristics for selected stations should be included in the presentation of data:

1) interannual wind power and speed variation
2) monthly average wind power and speed
3) diurnal wind power and speed by season
4) joint wind speed and direction frequencies
5) wind speed and power duration.

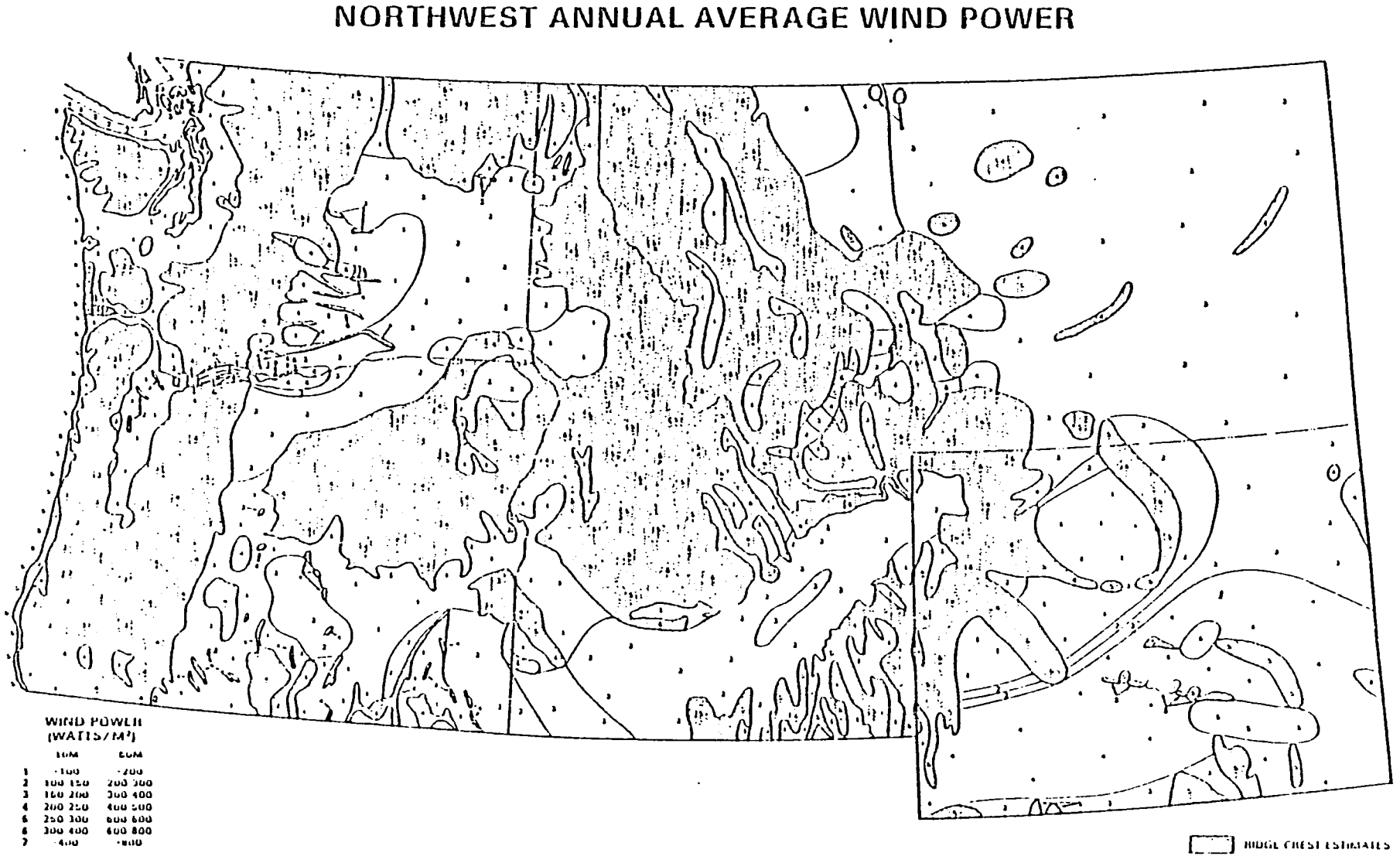

FIGURE 1.6. Northwestern United States Annual Average Wind Power (Elliott and Barchet 1979)

An atlas of the wind resource containing the suggested wind characteristics would serve a variety of users. It may provide the potential small WECS user with sufficient information to determine WECS feasibility for his intended application. The maps in such an atlas could be overlaid with maps of land availability, thus enabling utilities to locate areas for more intensive siting studies for large WECS. In a similar manner, the maps in the atlas could be overlaid with costs of electricity to define potential markets for WECS manufacturers. Such a wind energy atlas could provide the needed link between wind resource assessments and WECS siting methodologies.

REFERENCES

Elliott, D. L. June 1979. "Meteorological and Topographical Indicators of Wind Energy for Regional Assessments," Proceedings of the Conference on Wind Characteristics and Wind Energy Siting 1979, PNL-SA-7895, Pacific Northwest Laboratory, Richland, WA 99352.

Elliott, D. L. and W. R. Barchet. November 1979. Wind Energy Resource Atlas: The Northwest Region, PNL-3195, Vol. 1, Pacific Northwest Laboratory, Richland, WA 99352.

Hewson, E. W., J. E. Wade, and R. W. Baker. February 1979. Vegetation as an Indicator of High Wind Velocity. RLO/2227-T24-79/1, Oregon State University, Department of Atmospheric Sciences, Corvallis, Oregon.

Marrs, R. W. May 1978. Eolian Features as Indicators of High Wind Areas in the Pacific Northwest. RLO/2343-78/5, University of Wyoming, Laramie, Wyoming.

Wahl, E. W. 1966. Windspeed on Mountains. No. AF19(628)-3873, USAF-CRL, Bedford, Massachusetts.

EFFECT OF SITE WIND CHARACTERISTICS ON ENERGY PRODUCTION

William T. Pennell and Harry L. Wegley
Atmospheric Sciences Department
Pacific Northwest Laboratory
Richland, Washington

ABSTRACT

The effect of differences in wind characteristics on estimates of wind turbine performance has been examined. Net energy production over a given period can be estimated if both the performance characteristics of the turbine and the wind speed probability density function (PDF) are known. Simulations covering a range of PDFs and machine performance characteristics showed that reasonable estimates of net energy production can be made using simple, analytic PDFs. The analytic PDFs only require knowledge of the average wind speed at a site.

Some wind energy applications require knowledge of how temporal variations in turbine output interact with temporal variations in the load. The effect of variations in the diurnal modulation of wind speed on load matching was examined by simulating the energy transfer between a utility and a residence equipped with a small wind turbine generator. Turbine performance was simulated at six sites having a wide range of diurnal characteristics. The simulations showed that for a given turbine, a given average wind speed, and a residential-type load, large differences in diurnal characteristics had minimal effects on energy transfers between the house and the utility. This suggests that only approximate knowledge of the diurnal behavior of the wind speed is required when evaluating residential applications of wind turbine generators.

1. INTRODUCTION

A decision to purchase a wind machine will usually be based on its perceived economic value. Economic value is a strong function of the amount of energy a machine generates at a site, and the way this energy interacts with the load. Under some conditions, the value of a wind machine will only depend on the total energy produced over a given time period; that is, the machine must do a certain amount of work but there is no need to meet a power demand at a specific time. This condition could be met, for example, if the load serviced by a machine were always greater than or equal to the maximum output of the machine and if the cost of back-up power were constant. Under other conditions, however, economic value may depend on the temporal match between the load and machine output. An example of this condition is a small wind turbine connected to a residence that is supplied by a utility. Here, the match between the temporal characteristics of the load and the temporal characteristics of machine output could be very important to the economics of the installation, since the rates the utility charges for energy consumed and the credits it gives for excess energy produced could be a function of the time of day.

This paper examines two topics:

- wind data requirements for estimating the annual energy production of a wind turbine
- wind data requirements for examining the temporal match of load and turbine output.

The emphasis in the paper is on small, residential-size wind turbine generators, but some of the conclusions could apply to large machines, as well.

2. ESTIMATING ENERGY PRODUCTION

Energy production can be estimated by combining knowledge of site wind characteristics with information on machine performance. Usually, the only available performance information is a machine's steady-state performance function. This function gives the relationship between power output and wind speed when the machine is operated in an absolutely steady, homogeneous flow.

In reality, the performance of a machine will differ from that predicted by the steady-state performance characteristics, since the natural wind is unsteady and non-homogeneous and the response of the machine to the wind is fairly complicated. Some of the differences between actual performance and the performance predicted by the steady-state performance function can be illustrated if we assume that the power output at any time t can be expressed

$$p(t) = \int_0^\infty k(\tau)V(t-\tau)d\tau \qquad (1)$$

where $V(t)$ is some suitably weighted average of the wind through the rotor disk and $k(\tau)$ is the response function (or the impulse response) of the machine. Equation (1) assumes that a wind turbine behaves like a linear filter. Over most of a machine's performance envelope, this is probably a reasonable approximation as long as fluctuations in wind speed and direction are not too large. The response function $k(\tau)$, however, will be a function of wind speed.

When steady-state performance characteristics are used to estimate average power production, the average wind speed is determined for a given time interval (an hour or less) and the average power output is assumed to be defined by the steady-state performance function. The actual power output averaged over some time interval T is, however,

$$\bar{p}\left(t_1 + \frac{1}{2}T\right) = \frac{1}{T}\int_{t_1}^{t_1+T}\int_0^\infty k(\tau)V(t-\tau)d\tau dt \quad . \qquad (2)$$

Thus, average power output is a function of the temporal behavior of the wind through the rotor disk and the responsiveness of the machine. The variance between the actual average power and an estimate of the average power obtained by using steady-state performance characteristics usually increases as the length of the time interval increases. Variance between actual and predicted performance is also increased when wind information from a single height is used to represent flow through the entire rotor disk.

Estimates of energy production over long periods of time, such as a month, a season, or a year, can be made by summing time series of energy production estimates that are determined from time series of average wind speed and the machine's performance characteristics. Net energy production can also be computed if the probability density function (PDF) for wind speed is known at the site. The PDF gives the probability that the wind speed will fall within a given wind speed interval. At a given location, the exact form of the PDF will depend on the time interval over which the wind speed is averaged and the total period to which the PDF applies (i.e., a day, a month, a season or a year). Since an hour is the shortest time scale for conventional meteorological observations, it is the averaging time usually used to develop PDFs. Once the PDF is known, the average power output of a particular machine can be estimated as

$$\bar{p} = \int_0^\infty p(v)\ f(v)dv \tag{3}$$

where $p(v)$ is the steady-state performance function and $f(v)$ is the PDF.

The most obvious way to determine the PDF at a site is, of course, to collect the pertinent data and compute it. However, if this is not done, there are several analytic PDFs that can be used to estimate the wind characteristics at a site. The simplest is the Rayleigh distribution:

$$f(v) = \frac{\pi v}{2\bar{v}^2} \exp\left(-\frac{\pi v^2}{4\bar{v}^2}\right) \tag{4}$$

where $\bar{v}$ is the average wind speed over the period for which the PDF applies. All that is needed to determine the Rayleigh distribution for a site is the mean wind speed.

The Weibull function is another possible PDF:

$$f(V) = \left(\frac{k}{c}\right)\left(\frac{v}{c}\right)^{k-1} \exp\left[-\left(\frac{v}{c}\right)^k\right] \quad . \tag{5}$$

The Weibull distribution has two adjustable parameters (c and k) and can be made to fit a wide range of observed PDFs more accurately than the Rayleigh, which is actually a special case of the Weibull. A simple relationship exists between the Weibull parameters c and k in equation (5) and the first two moments of the probability distribution:

$$\bar{v} = \frac{c}{k}\,\Gamma\left(\frac{1}{k}\right) \tag{6}$$

and

$$\overline{v^2} = \frac{2c^2}{k}\,\Gamma\left(\frac{2}{k}\right) \tag{7}$$

Thus, the Weibull distribution can be estimated once the mean wind speed and the standard deviation of the wind speed about the long-term mean are known.

Figure 1 compares two analytic PDFs with two observed ones; all of the distributions have the same mean. Curve 1 is the Rayleigh function and Curve 2 is a Weibull density for a site where the wind tends to blow at a fairly constant speed (the standard deviation is small). Curve 3 is an observed PDF of hourly averaged wind speed, based on 12 months' measurement at an actual wind turbine site in the trade winds east of Puerto Rico. Curve 4 is the observed PDF after 12 months' measurement at a site displaying a double peaked (i.e., bimodal) distribution. The curves illustrated in Figure 1 should be fairly typical of the range of PDFs that might be experienced at typical sites.

Surprisingly, there is very little published information on how accurately energy production can be estimated given machine performance data and wind data in either a time series or a PDF format. Golding [1] describes a study by Juul [2] in which actual energy production from an operating machine was compared with computed energy production. Juul used a 13 kW, fixed-pitch machine with a rotor diameter of 8 m. Power was measured by a watt-hour meter and wind speed was measured at hub height on a nearby tower. Monthly energy production was compared with computed production using hourly averaged

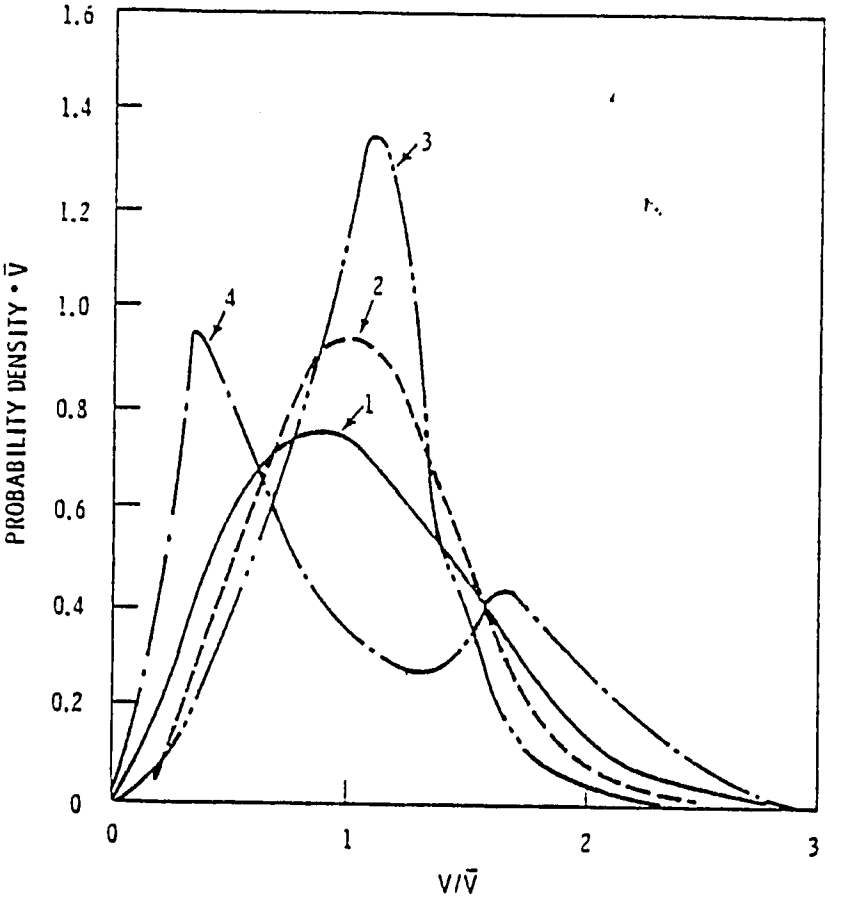

Fig. 1. Some Wind Speed Probability Density Functions. Curve 1 is the Rayleigh distribution and Curve 2 is a Weibull. Curves 3 and 4 are observed distributions.

winds. After eight months, computed energy production agreed to within 10 percent of the actual production. However, there was a great deal of scatter between computed and measured energy production on a monthly basis. Even for some of the windier months, the discrepancy between computed and measured output was 30 to 40 percent. It is not certain that 10 percent agreement between computed and measured performance would have been typical of other long-term averages.

3. EFFECTS OF SITE WIND CHARACTERISTICS ON ESTIMATES OF NET ENERGY PRODUCTION

The preceding section suggests that energy production estimates based on conventional procedures are imprecise. The accuracy of such estimates depends on many factors, some of which are unique to a given machine or a given site. Based on currently available information*, the authors would estimate the uncertainties in computations of average energy production based on the hourly averaged wind speed at hub height and steady-state performance characteristics to be between 10 and 30 percent. Given this fundamental uncertainty, how accurately must the wind behavior at a site be known? If estimates of the net energy production are all that is required, can these be obtained from analytic models of a site's PDF, for example, or must the actual wind behavior be measured?

In order to show how energy production estimates depend on wind behavior, the annual average power output was computed for two very different sets of wind turbine characteristics using the four PDFs shown in Figure 1. Steady-state performance characteristics for the two turbines are shown in Figure 2. The characteristics are modeled after manufacturer's performance information for two actual machines. These characteristics probably represent extremes in the shape of the performance function. The results are depicted in Figures 3 and 4 for a wind speed range that covers what would be expected at most potential sites. The figures show machine performance characteristics to have a pronounced effect on average power output. Although both machines have the same rated output, the average power output of Turbine B is much larger, since Turbine B produces its rated output over a wider wind speed range than Turbine A.

The figures also indicate that estimates of average energy production are not particularly sensitive to the form of the PDF. Results indicate that reasonable estimates can be made with limited wind data. For example, over most of the wind speed range shown in the figures, the average power output

*This information includes the previously cited study by Juul and experience with the NASA/Department of Energy 200 kW wind turbine at Clayton, New Mexico [3,4].

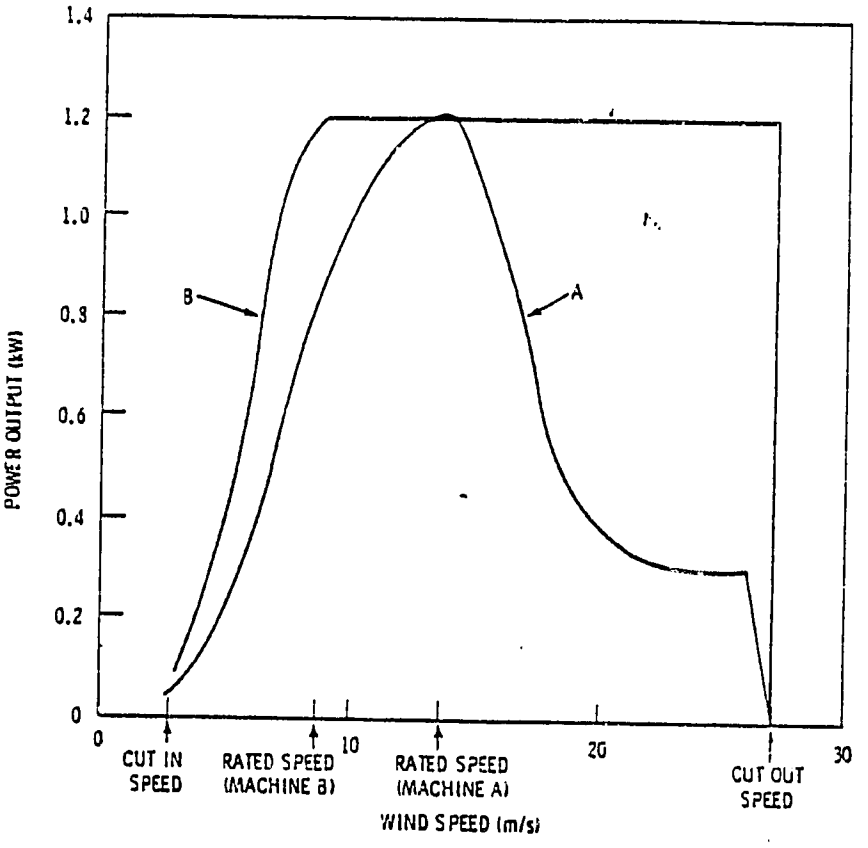

Fig. 2. Steady-State Performance Characteristics for Two Small Wind Turbines

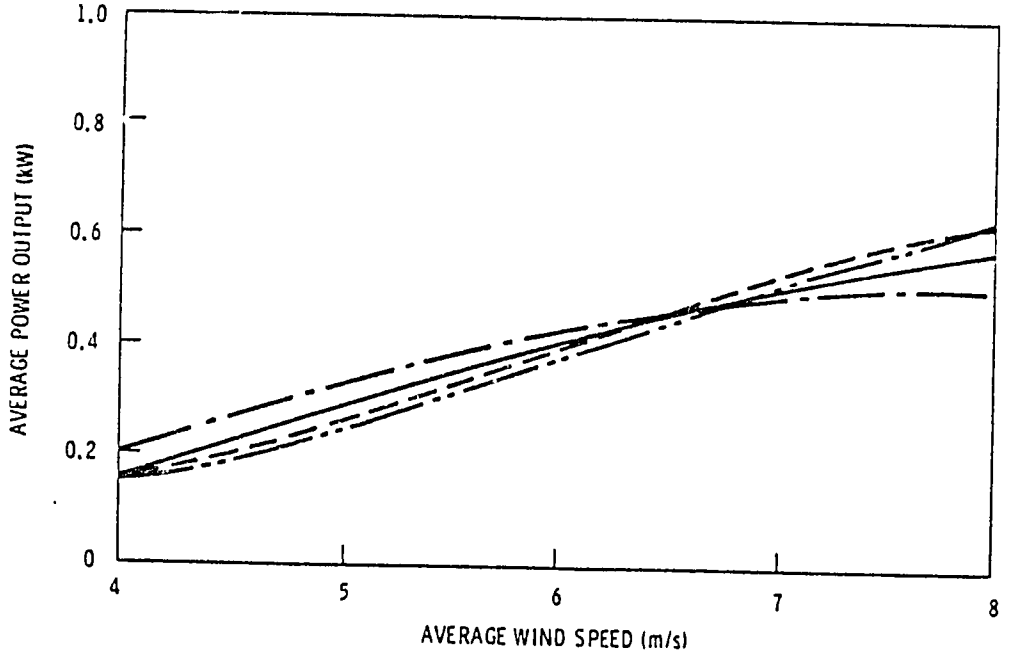

Fig. 3. Average Power Output for Machine A as a Function of Average Wind Speed. Four Possible wind speed probability density functions (PDFs) are shown. Each line corresponds to the PDF that is plotted with the same type of line in Figure 1.

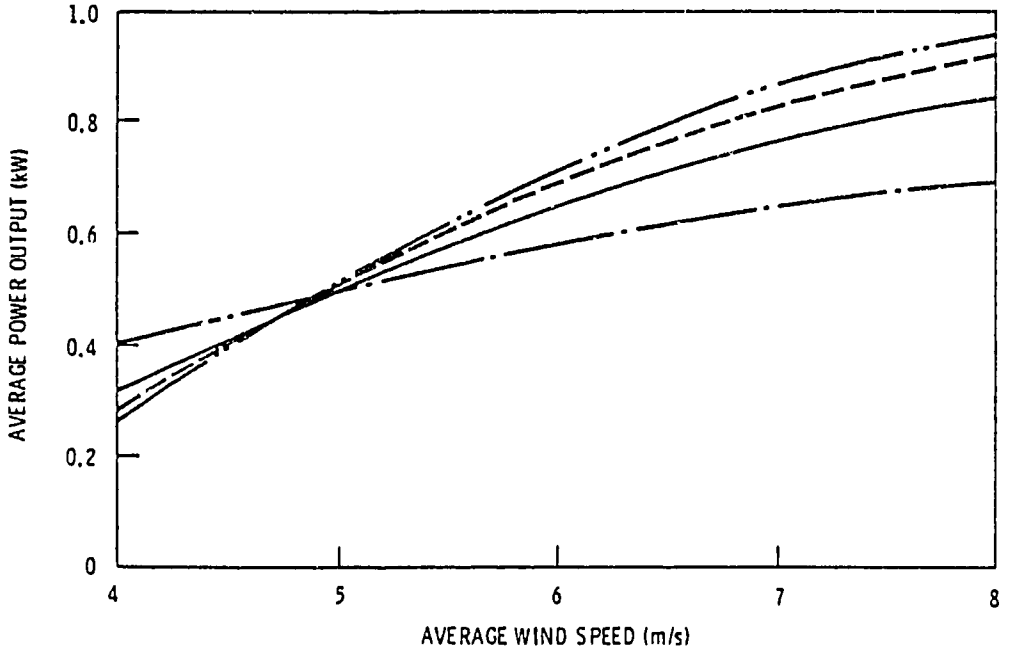

Fig. 4. Average Power Output for Machine B as a Function of Average Wind Speed. Four possible wind speed probability density functions (PDFs) are shown. Each line corresponds to the PDF that is plotted with the same type of line in Figure 1.

obtained by using a Rayleigh PDF differs by no more than ±15 percent from estimates obtained by using the other PDFs shown in Figure 1. Differences of this magnitude do not seem large when compared with the other uncertainties inherent in energy production estimates.

Differences between energy production estimates based on an observed PDF and a model PDF can be further reduced if a Weibull distribution is used.* However, using a Weibull distribution to fit the PDF at a site requires more knowledge of wind characteristics than fitting a Rayleigh function. Fortunately, there appear to be empirical relationships between mean wind speed and the two Weibull parameters. Cherry [5] has found the following empirical relationships predict the Weibull parameters at several sites in New Zealand with reasonable accuracy:

$$c \approx \frac{1.39\,\overline{v}}{(\overline{v} - 2)^{0.089}} \tag{8}$$

$$k \approx 1 + 0.48(\overline{v} - 2)^{0.51} \quad . \tag{9}$$

The general applicability of (8) and (9) is not yet known. Cherry is currently extending his analysis to sites in the United States, and the results should be published in the near future. Using a function such as the Weibull to estimate net energy production has certain additional advantages, however. By varying the c and k parameters through reasonable limits, uncertainties in energy production estimates due to uncertainties in the form of the PDF can be gauged.

*Curve 2 in Figure 1 is a Weibull fit to the Puerto Rico distribution (curve 3). The average power output curves in Figures 3 and 4, which correspond to curves 2 and 3 in Figure 1, show the effects that differences in these PDFs have on production estimates.

4. EFFECT OF DIURNAL WIND BEHAVIOR ON THE ENERGY CONSUMPTION OF A RESIDENCE

Wind speeds are usually a strong function of the season of the year and the time of day. At most sites, the wind is driven by pressure gradients associated with large weather systems. At temperate latitudes, the intensity and frequency of these weather systems are greatest in the winter and spring; thus these are the seasons of strongest winds.

The diurnal modulation of wind speed is a result of solar heating of the earth's surface. This heating causes wind speeds near the surface to be greatest in the afternoon. There is a simple explanation for this phenomenon. Surface heating generates turbulence, and this turbulence transports momentum from higher levels in the atmosphere to the ground. Since wind speed usually increases with height, the transport of momentum to the surface increases the wind speed there. The intensity of surface heating depends on the solar angle of incidence and on cloud cover; hence, diurnal modulation of the wind speed is greatest in summer and lowest in winter. A few hundred feet above the surface, however, the diurnal effect is reversed. At these elevations, surface-generated turbulence increases the effect of surface drag, and wind speeds tend to be higher at night than during the day.

To examine the importance of variations in the diurnal cycle on load matching, the net energy consumption of a typical residence equipped with a small wind turbine generator was simulated for a variety of wind conditions. Time series of hourly average wind speed, spanning a three-month period, were obtained at six locations. The locations exhibited a range of diurnal wind speed behavior. The wind data were converted to time series of average power output using the steady-state performance characteristics of two machines designed for residential use. The performance characteristics of the machines are shown in Figure 5.* To isolate the importance of the diurnal cycle, wind speeds at the six sites were adjusted by a constant amount so that the total energy production at each of the sites was approximately the same for a given machine. Because of differences in the performance characteristics of the

*In Figure 5, Turbine B is the same machine as that in Figure 2.

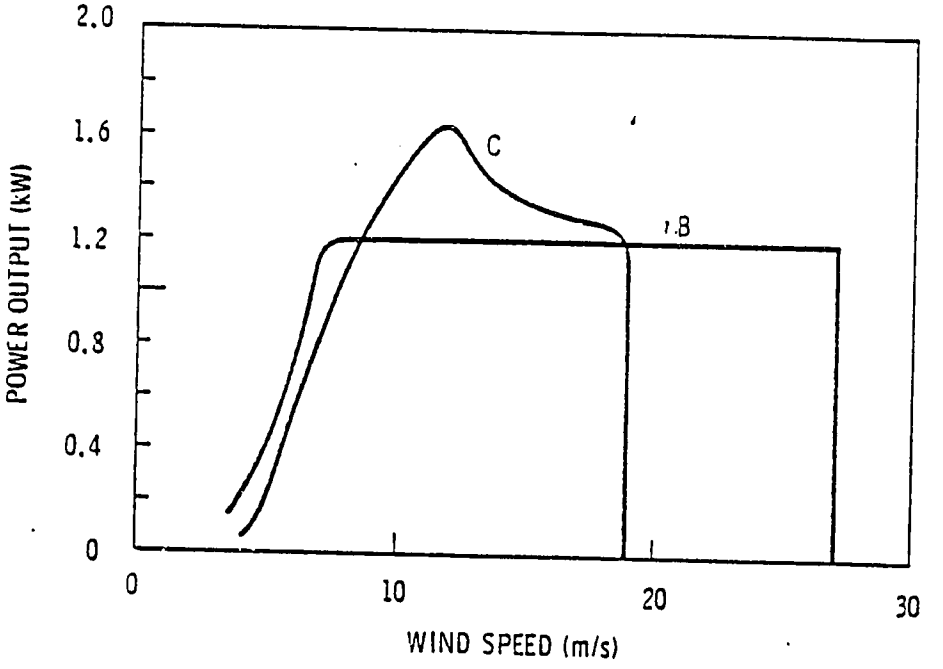

Fig. 5. Steady-State Performance Characteristics for Two Small Wind Turbines

two machines, the magnitude of the adjustment was a function of both the site and the machine.

Table 1 lists the sites used, indicates the time periods covered by the data and gives both the actual average wind speed and the adjusted average wind speed for each of the two machines. Since adjusted wind speeds were used in obtaining all of the following results, the sites will be identified by the lower case letters shown in Table 1.

The average diurnal cycle is shown for each of the sites in Figure 6. Sites a, b and c illustrate diurnal wind behavior typical of springtime on the Great Plains. Site d shows a diurnal behavior typical of winter. Site e shows a mean diurnal cycle for a "special" site where unique topography and meteorology combine to produce a localized wind resource. Site e also belies the usual rule that the wind never blows during the summer. The last site, f, is typical of an isolated high hill or ridge.

Table 1. Summary of Wind Data

Site	Actual Av. Wind Speed (m/s)	Adjusted Wind Speed Turbine C (m/s)	Adjusted Wind Speed Turbine B (m/s)
Russell, KS (a) March-May 1978	6.1	7.0	6.7
Huron, SD (b) April-June 1978	5.7	6.8	6.7
Amarillo, TX (c) March-May 1978	7.4	6.6	6.6
Montauk Pt., Long Island (d) January-March 1978	7.9	6.7	6.5
San Gorgonio Pass, CA (e) June-August 1977	8.0	6.4	6.2
Boone, NC (f) February-April 1977	7.4	7.1	6.7

Figure 7 depicts the diurnal behavior of average power output for Turbine C at each of the six sites. The figure shows that the estimated average power output follows the average hourly wind speed very closely, as is expected. But now we come to the central question: Do variations in the diurnal behavior of the magnitude shown in Figure 7 significantly affect the net energy consumption of a residence equipped with a small wind turbine generator? If they do, how accurately must this behavior be known? Are detailed wind measurements required, or can one estimate the effects by applying fairly crude models of wind behavior?

Figure 8 is the load that was used to simulate the electrical demand of a typical house. Figure 8 represents typical appliance and lighting loads only; it does not include water heating, space heating, or air conditioning. In conducting the simulations, the house was assumed to be connected to a utility system and to have no means of temporary energy storage. The energy flow between the utility and the house was computed for each hour of the simulation by subtracting the estimate of the turbine's energy production from the load. The results for Turbine C are summarized in Table 2.

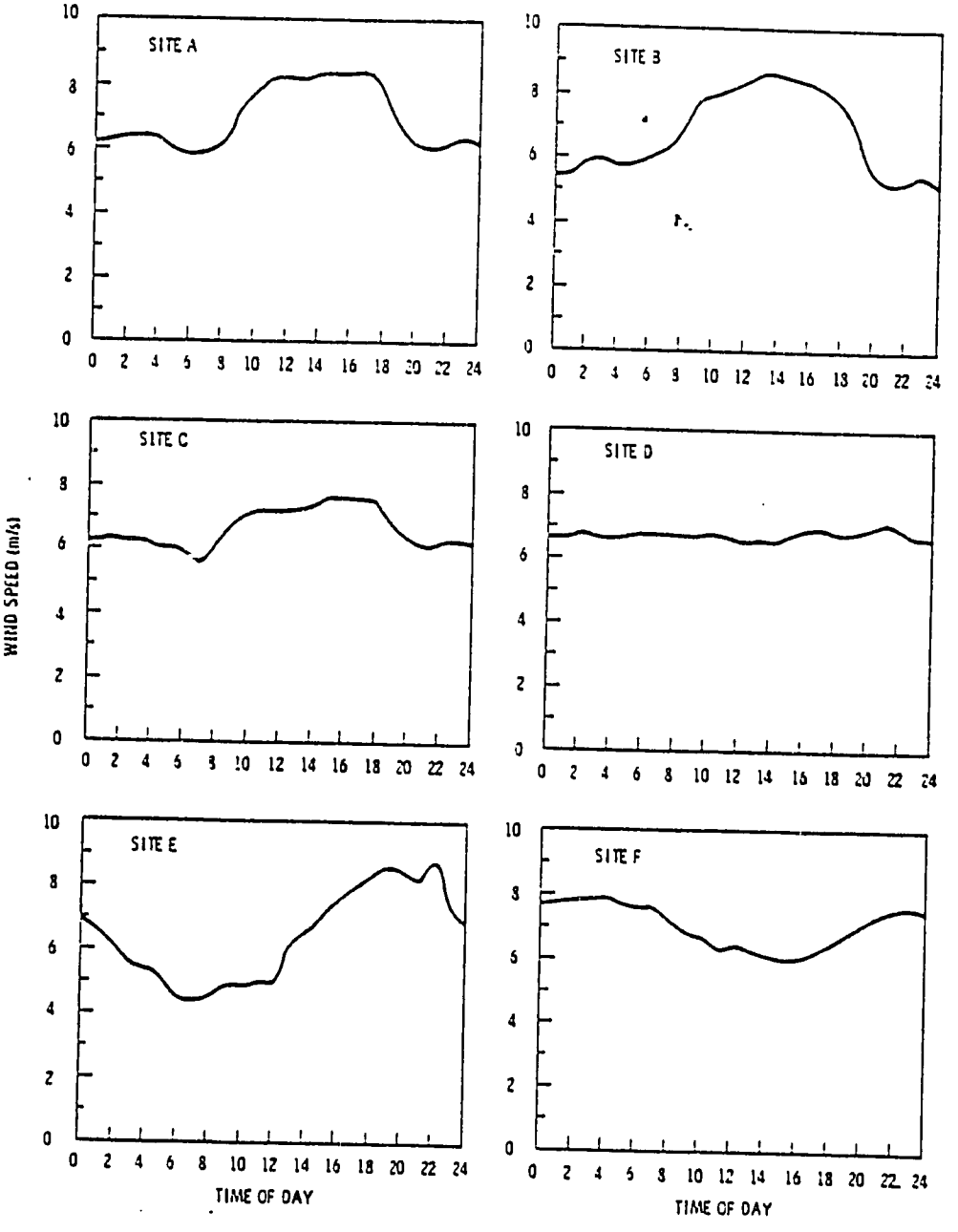

Fig. 6. Mean Diurnal Wind Speed Characteristics for the Sites Listed in Table 1. These are the diurnal characteristics for the adjusted winds used to drive Turbine C.

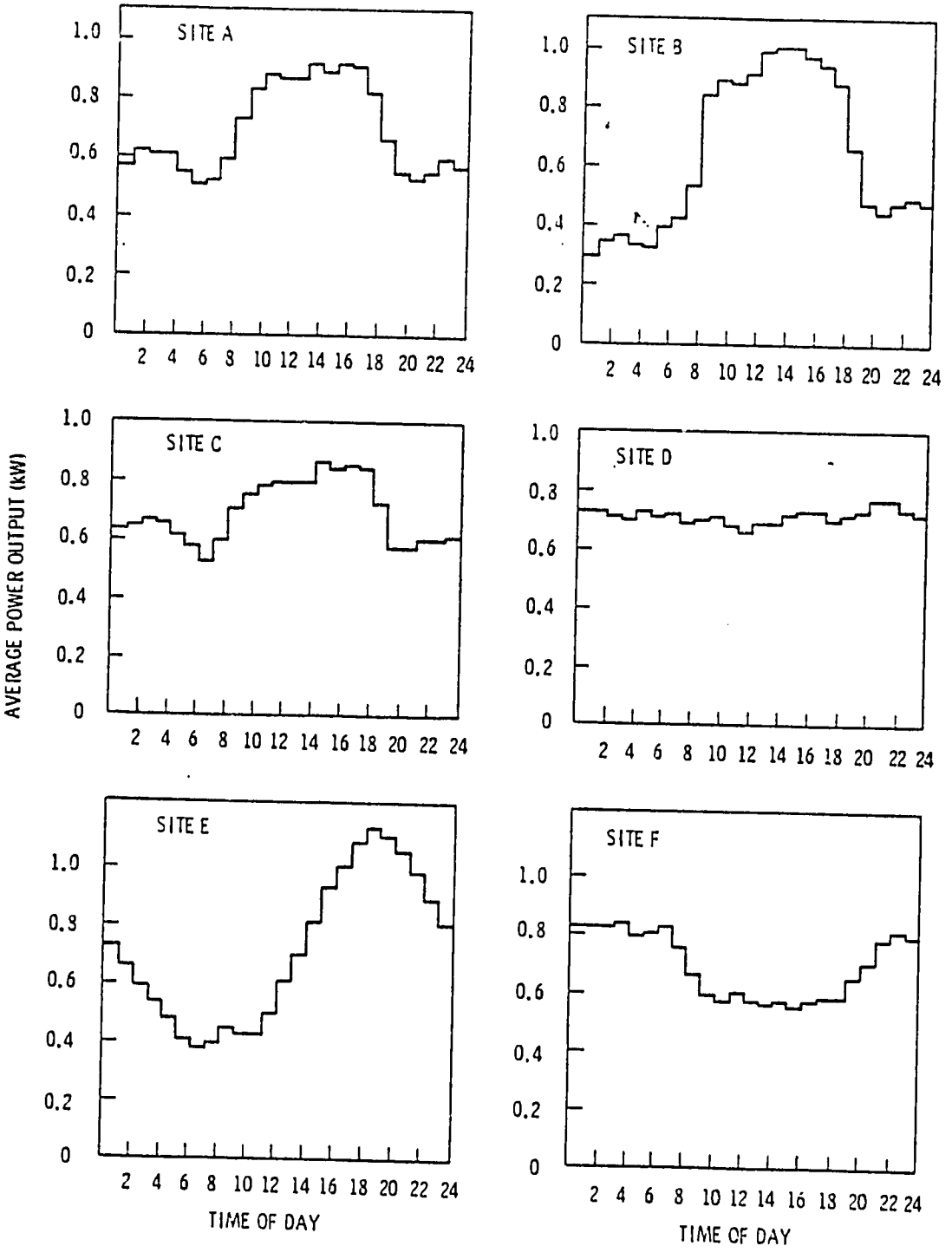

Fig. 7. Average Power Output for Machine C at the Sites Listed in Table 1

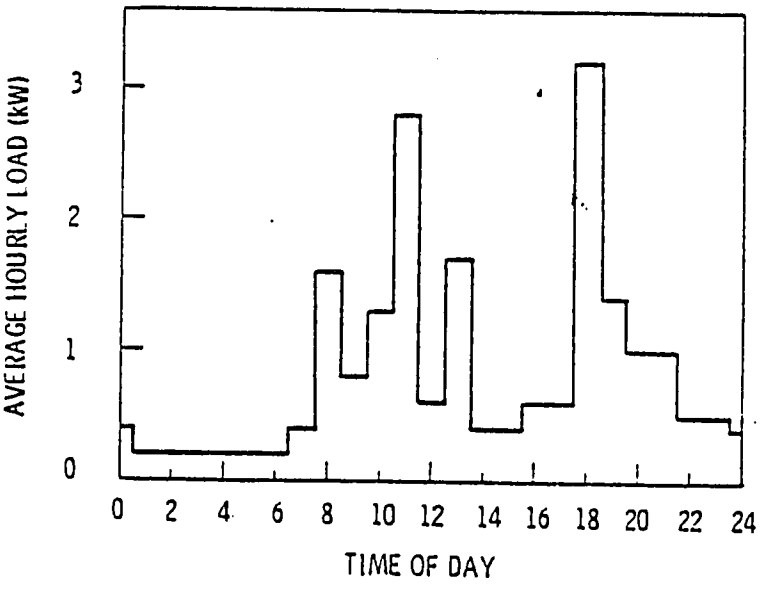

Fig. 8. Average Hourly Appliance Load for a Typical Residence. Source: "Application of Solar Technology to Today's Energy Needs, Volume 1," Office of Technology Assessment, June 1978.

Table 2. Effect of the Diurnal Behavior of the Wind on Estimated Energy Consumption for a Residence. All estimates are for a three-month period. (Turbine C)

Site	Total Energy Consumed* (kWh)	Total Energy Generated (kWh)	Energy Required from Utility (kWh)	Energy Supplied to Utility (kWh)
a	1590	1305	829	544
b	1586	1335	780	529
c	1589	1309	822	542
d	1584	1342	834	592
e	1591	1331	827	567
f	1595	1292	893	590
Average	1589	1319	831	561

*Variations in total energy consumption among the sites are due to slight differences in the length of the wind data records.

Table 2 shows that at each site the total energy produced by Turbine C equals about 80 percent of the electrical energy consumption. However, the simulated wind turbine reduced the amount of energy purchased from the utility by only about half. The balance was fed back to the utility.

Table 2 also shows the reductions in energy purchases are surprisingly independent of the mean characteristics of the diurnal wind speed cycle. For sites a through e, between 57 and 60 percent of the total energy generated goes directly to reducing energy purchases from the utility. Even at site f, which shows the poorest match between turbine output and load, 54 percent of the total energy production goes towards reducing energy purchases. There are two major reasons for this insensitivity to the diurnal behavior of the wind. The first is that all six locations are very good wind turbine sites. Even during the "off" hours, there is usually enough wind to generate power. The second is related to the nature of the load serviced by the machine. Although this load shows several large peaks (Figure 8), there is a fairly constant base load of about 0.6 to 0.8 kW from around 8:00 a.m. to about 9:00 p.m. This base load is also well matched to the average output of Turbine C over these hours (Figure 7).

Table 2 shows that the net energy flows between a utility and a residence served by a small wind turbine were not a strong function of the mean characteristics of the diurnal cycle. However, it does not follow that wind-generated electricity would have the same value in reducing the total utility bill at each site. The credit given a customer for excess energy will undoubtedly be a function of the time of day; in addition, a utility might charge a wind turbine customer a time-of-day rate for energy consumed.

A certain utility in the eastern United States is currently offering the following rate to customers with wind turbines: the rate charged for energy purchases is not a function of the time of day, but it does change with season. Credit for excess energy depends on the time of day in three broad classifications: on-peak (10 a.m. to 10 p.m.), off-peak (midnight to 7 a.m.), and intermediate (all remaining hours). The value of these credits also changes with season.

Table 3 summarizes the distribution of the surplus energy generated among the three time-of-day categories. Since these categories are so broad, only site f shows any significant difference.

Table 3. Effects of Diurnal Behavior of the Wind on Energy Flow to the Utility System. All estimates are for a three-month period. (Turbine C)

Site	On-Peak (10 a.m.-10 p.m.) (kWh)	Off-Peak (Midnight-7 a.m.) (kWh)	Intermediate (All Other Hours) (kWh)
a	240	260	44
b	245	244	40
c	222	282	38
d	206	338	48
e	257	263	47
f	159	331	100

The results shown in Table 3 could be different for a load showing a stronger diurnal dependence. They could also be a function of the performance characteristics of the wind turbine. To examine this possibility, the entire simulation was repeated using a hypothetical wind turbine with the performance characteristics of Turbine B. The results are summarized in Table 4. The table shows that although the energy generated by the turbine exceeded the electrical energy consumed by the residence, this excess energy did not go to further reducing energy purchases from the utility. It went to increasing the size of the surplus returned to the grid.

The distribution of this surplus among three broad time-of-day categories is shown in Table 5. At sites a, b, c and e, Turbine B supplies between 55 to 60 percent of its surplus generation during on-peak times. At these same sites, only about 45 percent of Turbine C's surplus is supplied during on-peak hours. Clearly, any differences in the value of the electricity produced by Turbine B over the value of the electricity produced by Turbine C would be governed by the utility's buy-back rates.

Table 4. Effect of the Diurnal Behavior of the Wind on Estimated Energy Consumption for a Residence. All estimates are for a three-month period. (Turbine B)

Site	Total Energy Consumed (kWh)	Total Energy Generated (kWh)	Energy Required from Utility (kWh)	Energy Supplied to Utility (kWh)
a	1590	1835	847	1092
b	1586	1861	792	1067
c	1589	1842	838	1091
d	1584	1850	873	1139
e	1591	1859	827	1095
f	1595	1823	956	1184
Average	1589	1845	856	1111

Table 5. Effects of Diurnal Behavior of the Wind on Energy Flow to the Utility System. All estimates are for a three-month period. (Turbine B)

Site	On-Peak (10 a.m.-10 p.m.) (kWh)	Off-Peak (Midnight-7 a.m.) (kWh)	Intermediate (All Other Hours) (kWh)
a	611	370	111
b	621	330	116
c	572	412	107
d	502	510	127
e	640	361	94
f	403	638	143

5. WIND DATA REQUIREMENTS FOR EXAMINING LOAD MATCHING

Understanding how a small wind turbine generator might affect energy consumption and utility bills requires knowledge of how the output of the wind turbine generator interacts with the load. In the previous section we showed that the effect of a small wind turbine on a residential-type load was not especially sensitive to the characteristics of the mean diurnal cycle. This suggests that only approximate knowledge of the diurnal characteristics of the wind is required.

If the PDF for wind speed were known for each hour of the day, one could determine how a given wind turbine would interact with a given load. For example, the average power output as a function of time of day is

$$\overline{p}(t,T) = \int_0^\infty p(v)\ f(v,t,T)dv \tag{10}$$

where $f(v,t,T)$ is the PDF at time t, and T is the time interval (such as an hour) over which the wind speed, v, is averaged. Since $f(v,t,T)dv$ is the probability of the wind speed falling between v and $v + dv$,

$$N \cdot T \int_{v_n}^{v_m} f(v,t,T)dv \tag{11}$$

is the length of time v falls in the interval (v_n,v_m). In expression (11), N is the number of days in the period (such as a month or a season) for which $f(v,t,T)$ applies. The energy produced by the wind turbine during the time the wind speed falls between v_n and v_m is

$$E(v_n,v_m,t) = N \cdot T \int_{v_n}^{v_m} p(v)f(v,t,T)dv \quad . \tag{12}$$

If the load serviced by the turbine, $\ell(t)$, is assumed to be only a function of time of day, a wind speed $v_\ell(t)$ can be defined where

$$p(v_\ell) = \ell(t) \quad . \tag{13}$$

The energy flow from the utility system to the house is then

$$E^{+}(t) = N \cdot T\left[\ell(t) - \int_{0}^{v_{\ell}} p(v) f(v,t,T)dv\right] \tag{14}$$

while the energy surplus delivered to the grid is

$$E^{-}(t) = N \cdot T\left[\ell(t) - \int_{v_{\ell}}^{\infty} p(v) f(v,t,T)dv\right] \quad . \tag{15}$$

The PDFs in Equations (10), (14) and (15) can be measured or they can be approximated by some analytic function, such as the Rayleigh or Weibull densities. There are several reasons for believing that a Rayleigh or Weibull function is an acceptably accurate approximation for f(v,t,T). First, the Rayleigh and Weibull distributions are conservative; they tend to underestimate the available wind power at low wind sites, while yielding good estimates at higher wind sites [6]. Second, the machine performance characteristic, $p(v)$ in Equations (10) through (15), is a strong filter. Convoluting $p(v)$ with f(v,t,T) reduces the significance of differences in the shape of the PDF. This effect is illustrated in Figures 3 and 4. Third, the nature of tne residential-type load and the buy-back provisions that utilities are beginning to offer residential customers moderate the need for precise load matching. Fourth, a probability density determined from a single month's or season's measurement is also only an estimate of the true, climatological PDF and will be in error by an unknown amount. Lastly, the reader should recognize that the methods used in modeling wind turbine output (average hub-height wind speeds and steady-state performance characteristics) are fairly crude. Results obtained by using these models should only be treated as approximate.

As a partial test of the hypothesis that analytic PDFs can be used to estimate energy flows in residential applications of small wind turbines, the average power output for each hour of the day was computed using the actual wind data and using Equation (10) with f(v,t,T) taken as a Rayleigh function [Equation (4)]. Both estimates of the average power output were compared at all six sites and for each of the two machines.

Figure 6 shows that the means of the hourly averaged wind speeds ranged from just over 4 m/s at site e to just under 9 m/s at site b. Examination of PDFs determined from the actual wind data showed that the observed PDFs for a given hour varied from near-Rayleigh in appearance to definitely bimodal. Estimates of average power output were again found to be fairly insensitive to the exact shape of the PDF, as expected. The average discrepancy between estimates based on the Rayleigh function and estimates based on the actual data was 8 percent with a standard deviation of 7 percent.

6. CONCLUSIONS

Intelligent use of wind turbines requires some knowledge of the amount of energy a wind turbine will produce at a particular site and of how the turbine will interact with the load to be serviced. If similar applications of wind energy have been made in the neighborhood, knowledge of the success or failure of these applications is the best information for making a decision on installing a wind turbine. If there is no experience with wind turbines in the vicinity, the performance of a turbine at the site must be estimated.

The usual method for simulating wind turbine performance uses information on the behavior of wind speed at a site and the steady-state performance characteristics of a machine to produce estimates of energy production. The wind speed information can be in the form of time series or probability density functions. The accuracy of these methods of simulation is still uncertain. It would be prudent to assume that any estimate of wind turbine energy production could be high by as much as 10 to 30 percent.

The amount of energy a wind turbine will produce in a given time period can be estimated if the wind speed PDF is known for that period. We have shown that estimates of the energy output of a turbine over a given period are not especially sensitive to the exact form of the wind speed PDF. Thus, estimates of energy output can be made if the actual PDF is approximated by a Rayleigh or a Weibull function. Since there are empirical relationships between the Weibull parameters and the mean wind speed, use of either of these functions only requires knowledge of the mean wind speed for the period in question.

Many potential applications of wind energy require knowledge of how the output of a wind turbine will interact with the load it services. Since many loads show considerable seasonal and diurnal variability, the seasonal and diurnal modulations of turbine energy production must be understood. Seasonal effects can be accounted for if the interaction of the turbine and the load are analyzed on a monthly or seasonal basis. The effects of the diurnal modulation of turbine energy output can be simulated if the PDF for wind speed is known as a function of the time of day.

In this paper we have shown that the energy transfer between a utility system and a residence equipped with a small wind turbine depends on the way the turbine output modifies the load. However, we showed that for selected wind turbine characteristics, estimates of this energy transfer were only slightly affected by differences in the temporal behavior of the wind speed at good wind turbine sites. On the basis of this relative insensitivity and because of the uncertainties inherent to simple models of wind turbine performance, we argue that simple analytic PDFs such as the Rayleigh or Weibull functions are acceptable approximations to the wind speed PDF for a given time of day. The Rayleigh function is particularly attractive since it only depends on the mean wind speed, and using it only requires knowledge of the monthly or seasonally averaged diurnal cycle. On the other hand, the Weibull function has the advantage of enabling one to test the sensitivity of his analysis to the form assumed for the PDF. In either case, the effect of a small wind turbine on a residential-type load could be estimated with knowledge of only a few, easily determined wind characteristics.

ACKNOWLEDGEMENTS

This article is an account of work performed for the U.S. Department of Energy under Contract DE-AC06-76RLO 1830.

REFERENCES

1. Golding, E.W. 1955. The Generation of Electricity by Wind Power. John Wiley & Sons, New York.

2. Juul, J. 1951. "Report of Results Obtained With the SEAS Experimental Wind Power Generator." Elektroteknikeren, 47, pp. 5-12 (in Danish, referenced in Golding, 1955).

3. Glasgow, J.C. and W.H. Robbins. 1979. "Utility Operational Experience on the NASA/DOE MOD-OA 200-kW Wind Turbine." In Proceedings of the Workshop on Economic and Operational Requirements and Status of Large Wind Systems. EPRI ER-1110-SR, Electric Power Research Institute, Palo Alto, California.

4. Robbins, W.H. and D.H. Baldwin. 1980. "Large Wind Turbines: A Utility Option for Generation of Electricity." 1980 Solar Program Review Meeting, Electric Power Research Institute, Palo Alto, California.

5. Cherry, N.J. 1980. "Wind Energy Resource Methodology." J. Industrial Aerodynamics, 5, 247-280.

6. Doran, J.C., J.A. Bates, P.J. Liddell and T.D. Fox. 1977. Accuracy of Wind Power Estimates. PNL-2442, Pacific Northwest Laboratory, Richland, Washington.

THE PERFORMANCE OF SIMPLE HORIZONTAL AXIS WIND-TURBINES FOR THE DIRECT DRIVE OF WATER PUMPS

J.A.C. Kentfield

Department of Mechanical Engineering
University of Calgary
Calgary, Alberta, Canada

ABSTRACT

Two turbine types were considered. Interest in both types, Cretian compliant-sail bladed machines and turbines with multiple flat slats as blades, has recently been revived, in developing nations, for water pumping applications. The work was based on wind-tunnel tests the results of which are presented in the form of power and torque coefficients versus velocity ratio. It was shown that a Cretian turbine can attain a maximum power coefficient of approximately 0.28 and also achieve a high starting torque. It was also found that optimised slatted wind-turbines are limited to maximum power coefficients of 0.19 to 0.23 depending upon their construction. The present results were combined with those of an earlier paper to yield what is believed to be a comprehensive summary map of the operational characteristics of optimised horizontal axis wind-turbines for the direct drive of water pumps.

NOMENCLATURE

AR	= Blade aspect ratio
C_p	= Power coefficient ≡ rotor power output/$\frac{1}{2}\rho U_\infty^3(\frac{\pi}{4}D^2)$
C_T	= Torque coefficient ≡ torque/$\frac{1}{2}\rho U_\infty^2(\frac{\pi}{4}D^2)(\frac{D}{4})$
D	= Diameter of rotor
U_∞	= Wind velocity
β	= Blade stagger angle (angle between blade surface and rotor center line)
λ	= Velocity ratio ≡ peripheral velocity of rotor/U_∞
λ_{Max}	= Maximum value of λ (i.e. λ at runaway)
Λ	= Value of λ for which C_p is a maximum
ρ	= Air density
σ	= Rotor solidity (see Fig. 2)
ϕ	= Sail-setting parameter (Cretian turbine - see Fig. 2)

INTRODUCTION

In recent years there has been a revival of interest in the use, primarily in developing nations, of simple horizontal axis wind-turbines for the direct drive of water pumps and other mechanical equipment. This has resulted in the development of new turbine designs (1,2), and attempts to adapt conventional, well established, concepts. Examples of the latter are classical, metal, multi-bladed turbines commonly employed, for stock watering duties primarily in North America and Australia (3); other examples are Cretian and simple slatted type turbines which are particularly easy to construct. One of the difficulties associated with the adaptation process is the lack of definitive performance data applicable to the various concepts. Recently, newly obtained performance data relating to classical multibladed turbines have become available; these results (4) agree, quite closely, with earlier information (5). However, so far as is known to the writer, no definitive, easily interpretted, experimentally obtained performance characteristics are available for either Cretian or slatted type turbines.

The objectives of the work described here are to present experimentally obtained performance characteristics for Cretian and slatted turbines and to compare these results with those for classical multibladed machines in addition to two new designs (1,2). It is, of course, essential that for this work to be meaningful the final comparisons should be made between optimised versions of each configuration. The focus of attention relates to small machines of approximately 10 to 13' (3 to 4m) rotor diameter.

TEST PROCEDURES

The Cretian turbine was tested, in model form, in an open-jet wind-tunnel at the University of Calgary. The wind-tunnel jet cross-section was 4.5' x 2.5' (1.37m x 0.76m). The model rotor was 20" (508mm) diameter and was located 12" (304mm) downstream from the jet entry into the enlarged working chamber. This location was established, on the basis of the known performance of a rotor used for calibration purposes, as the correct location, for the size of model tested, to eliminate either blockage problems due to too close an approach to the tunnel exit or jet-wake mixing influences due to excessive withdrawal of the model. A correction was incorporated to compensate for small velocity profile distortions at the jet-exit plane. Rotor speed was measured by means of a stroboscope. Torque measurements were carried out using a small prony brake attached to the turbine rotor shaft.

Due to the small size of the model and the relatively low wind velocity of approximately 13 ft/s (4 m/s) at which the wind-tunnel tests were carried out a Reynolds-number based correction

was applied to relate the results of the model tests to full scale units of 10 to 13' (3 to 4m) rotor diameter operating at a representative wind speed of 15 mile/h (7 m/s). A small additional correction was also incorporated, as explained later, to compensate for unavoidable geometric differences between the model and full scale Cretian turbines.

A single slatted type turbine, also of 20" (508 mm) rotor diameter was also built and similarly tested in the wind-tunnel. The results of this test were used to provide a correlation between modern wind-tunnel test methods and tests carried out approximately one hundred years ago on a comprehensive series of slatted rotors by Perry (6). Perry's tests were performed using a powered arm, orbiting in a horizontal plane, which moved a dynamometer equipped turbine rotor, mounted at the extremity of the arm, into air nominally at rest within a large test cell or enclosure. The uncertainties with Perry's tests, which tend to inhibit direct use of his results, relate to the opposing influences of a potential over-estimate of performance due to the orbitting motion of his [5' (1525 mm) diameter] turbine models and a performance underestimate due to the tendency of the model turbine to generate a circulatory movement of the air within the test enclosure.

The results of both the model tests and subsequently predicted full-scale performances were expressed in terms of power and torque coefficients, C_p and C_T respectively, presented as functions of velocity ratio λ. It has been shown elsewhere (4) that for the definitions of C_p and C_T employed;

$$C_T = \frac{2}{\lambda} C_p \qquad (1)$$

and when $\lambda = 0$;

$$C_T = 2\left(\frac{dC_p}{d\lambda}\right)_{(\lambda = 0)} \qquad (2)$$

These relationships were helpful in ensuring the consistency of the C_p and C_T curves.

CRETIAN TURBINE

The origins of the design of Cretian wind-turbines appears to be lost in antiquity. Accordingly there do not appear to be any definitive design rules available. The wind tunnel model, was therefore, based on relatively modern, metal framed, versions of the machine since these presumably suffer less from windage losses than more traditional forms with relatively thick wood spokes. The geometry of the frame of the wind-tunnel model unit is shown in Fig. 1. Figure 2 shows the planforms of the four sets of thin, plasticised-cloth sails tested. Each sail planform was tested using four lengths of the sail control line BC. The blade stagger angle, that is the angle at which the blade is set relative to the rotor axis, is, in effect, controlled by the sum of the total length AB, of the outer edge of the sail plus the control line length BC. The parameter ϕ employed in defining the sail setting is defined as the total length AC divided by the straight line length XY between adjacent spokes. Hence the minimum value of ϕ is unity and the larger the value of ϕ the smaller the blade stagger angle. The table in Fig. 2 lists the solidities of the four sets of sails employed.

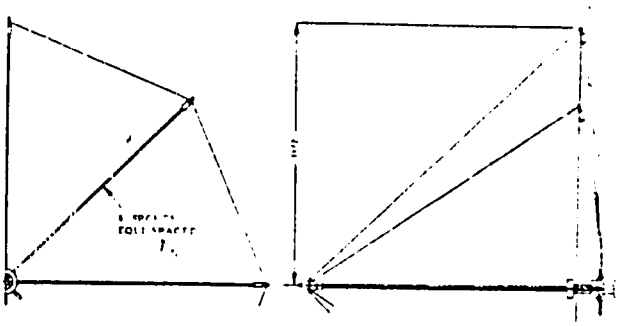

Fig. 1 Rotor Frame of Wind - Tunnel Model of Cretian Wind-Turbine.

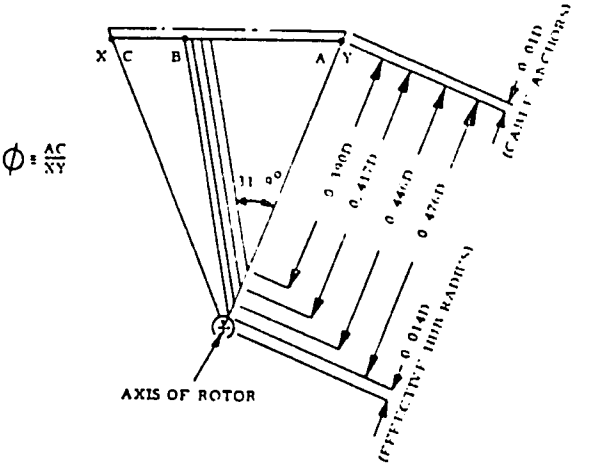

MAXIMUM DIMENSION OF SAIL	ROTOR SOLIDITY σ = $\frac{\Sigma \text{SAIL AREA}}{\text{ROTOR PROJECTED AREA}}$
0.476D	0.57
0.446D	0.50
0.417D	0.44
0.390D	0.38

Fig. 2 Sails of Model Cretian Wind-Turbine

It can be seen, therefore, that a total of sixteen configurations were tested and each configuration is identified uniquely by specifying both the solidity σ and the sail setting ϕ. The best result obtained is presented on the C_p and C_T versus λ planes in Fig. 3. The dotted curves of Fig. 3 represent the power and torque coefficients corrected to give the predicted performance of a full scale unit of 10 to 13' (3 to 4m) diameter operating in a wind of about 15 mile/h (7 m/s). The applied correction is made up of two approximately equal components. One portion of the correction was for the influence of Reynolds number and was based on a correction normally applied to a single stage of a reaction turbine (7). Since the wind turbine does not have any nozzle blades

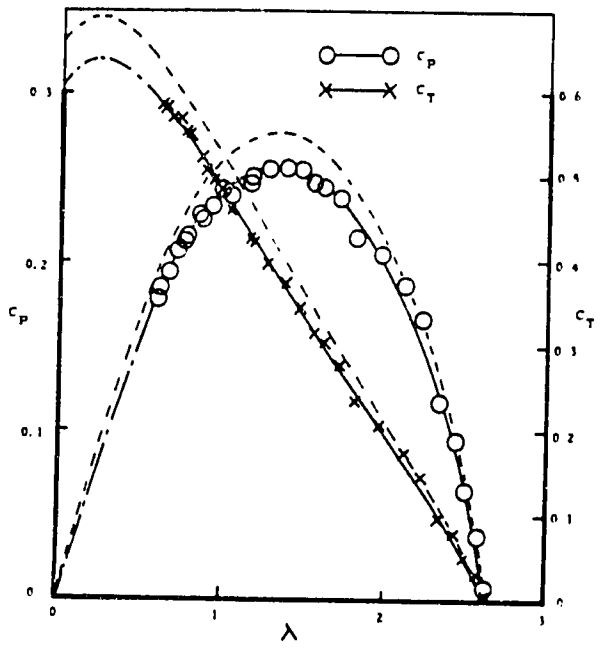

Fig. 3 Best Performance Characteristic of Model Cretian Wind-Turbine; Solidity $\sigma = 0.57$, $\phi = 1.06$. Estimated Full Scale Performance Shown Dotted.

only half the correction normally applicable to a full reaction stage was used. This correction procedure has been used previously to correct model test data for conventional multibladed turbines (4). The other correction factor relates to the incomplete use of the rotor disc projected area due to the outer edges of the sails being set in radially by 1% of the rotor diameter D (Fig. 2). Whilst this feature was virtually unavoidable in the model, it should be possible to eliminate this deficiency in a full scale machine.

The main trends apparent from the tests of the Cretian configurations are represented, by means of cross plotting, in Fig. 4, 5, and 6. It can be seen from these figures, which represent directly wind-tunnel test data and have not been corrected to full scale, that the configuration yielding the highest starting torque is not that which produces the highest power coefficient. Likewise it can also be seen that for each solidity, the highest runaway velocity ratio is, as might be expected, associated with the minimum possible value of ϕ. It is also apparent from Fig. 4 and 5 that performance increases with increasing solidity, σ, over the range investigated. Substantial increases in σ are relatively difficult to achieve in practice, in conjunction with values of ϕ only slightly greater than unity, due to the geometry of the system. Too large a value of AB (Fig. 2) results in the outer edge of each sail tending to curve such that there is an adverse influence on performance. There is evidence of such an effect in Fig. 4 for $\sigma = 0.57$, $\phi = 1.0$.

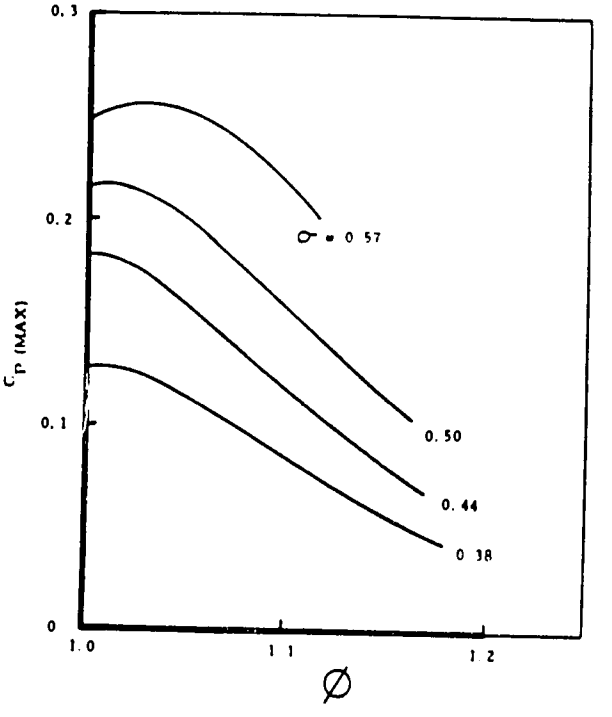

Fig. 4 Maximum Power Coefficient versus Sail Setting Parameter of Model Cretian Wind Turbines.

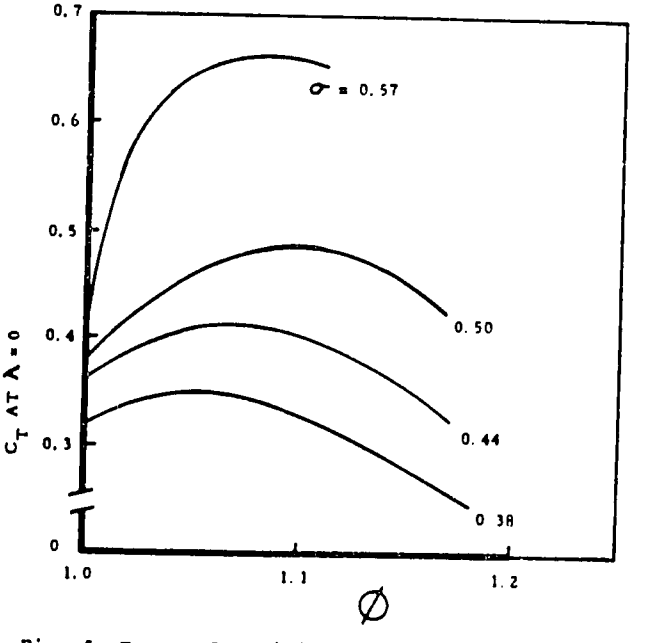

Fig. 5 Torque Coefficient at $\lambda = 0$ versus Sail Setting Parameter of Model Cretian Wind Turbines.

SLATTED TURBINE

Multibladed wind-turbines, generally constructed of wood, featuring flat-plate blade surfaces appear to have constituted the most common

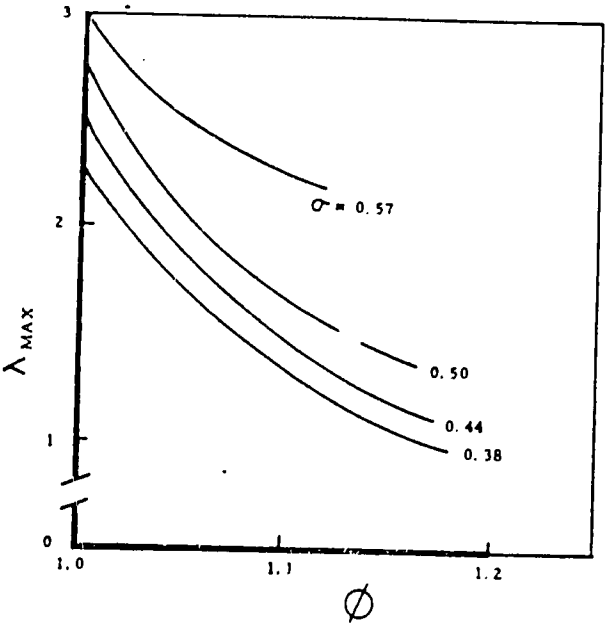

Fig. 6 Runaway Velocity Ratio versus Sail Setting Parameter of Model Cretian Wind-Turbines.

form of water-pumping turbine in North America up to about a century ago. This design was gradually displaced by the now classical multibladed machine, featuring cambered sheet metal blade surfaces, still in use today. The resurgence of interest in slatted turbines in developing nations appears to relate, primarily, to their ease of construction using indigneous materials. A detailed and comprehensive experimental study of the performance of slatted turbines, using the technique described previously, was carried out during 1882 and the following year by Thomas O. Perry on behalf of the United States Wind Engine and Pump Company of Batavia, Illinois. Due, it appears, to the proprietary nature of Perry's study the results were not published until 1899 (6). By this time there was, it seems, little interest in the bulk of Perry's results since attention had already been diverted from slatted to multibladed rotors of the now familiar type.

The best of Perry's slatted rotors for which full performance results are available is shown in Fig. 7. A 20" (508 mm) diameter model of this rotor was built and tested in the University of Calgary open jet wind tunnel. A comparison of the results obtained by Perry and those of the recent wind-tunnel tests is presented in Fig. 8. It can be seen from Fig. 8 that apart from a slight discrepancy at very low velocity ratios the two sets of results are virtually coincident. This implies that the previously referred to causes of error in Perry's tests largely cancel. However, it should be born in mind that the Reynolds number for Perry's tests was approximately three times that of the wind-tunnel model tests and hence, with a complete error cancellation, Perry's results should be somewhat superior to those obtained using the wind-tunnel. Nevertheless it appears that Perry's results can be treated as if they were all obtained

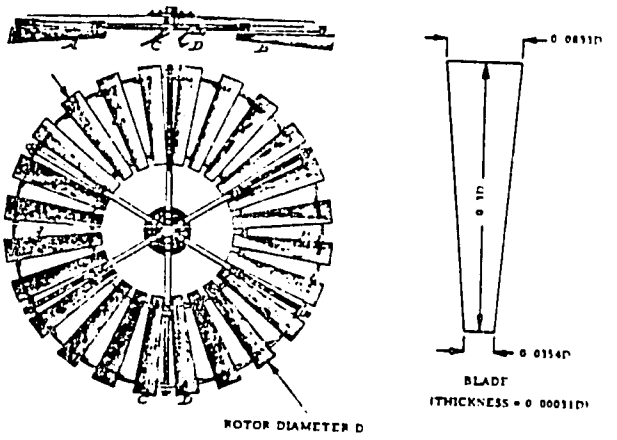

Fig. 7 Typical Slatted Rotor as Tested by Perry (Perry's Rotor No. 6, Ref. 6).

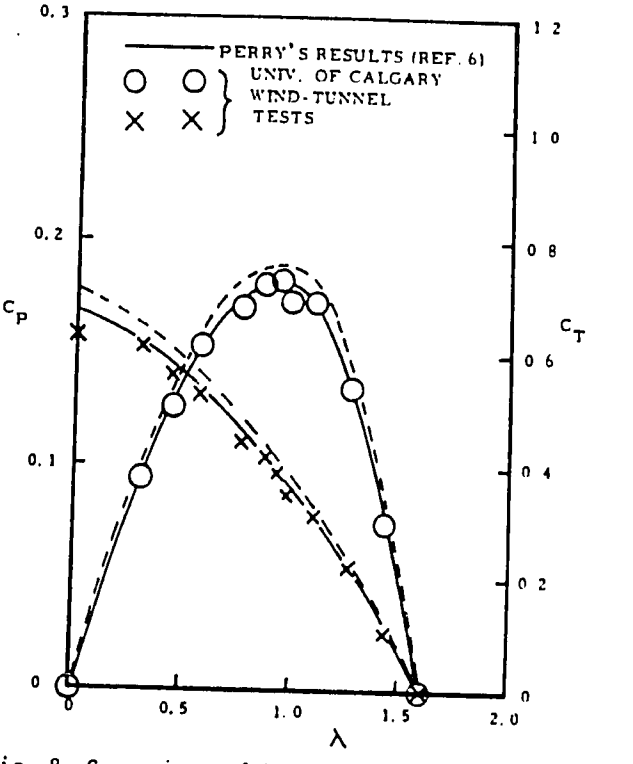

Fig. 8 Comparison of Results for Perry's Rotor No. 6 (σ = 0.544, 24 Blades, β = 60°) with Those for University of Calgary Replica.

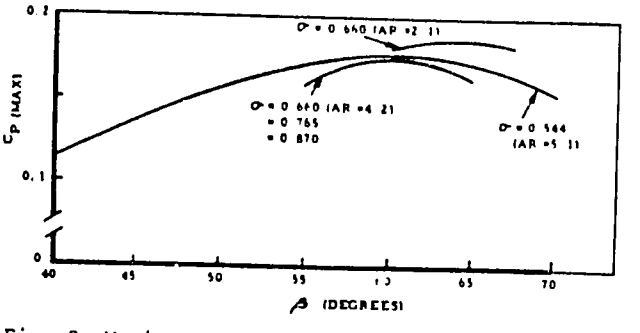

Fig. 9 Maximum Power Coefficient versus Blade Stagger Angle for Perry's Slatted Rotors.

from 20" (508 mm) diameter models tested in the University of Calgary open-jet wind-tunnel and corrected to yield a result applicable to 10 to 13' (3 to 4 mm) diameter rotors in a 15 mile/h (7 m/s) wind velocity exactly as for such models (7). Such a correction procedure accounts for the dotted curves appearing in Fig. 8.

Results obtained by Perry, without correction to full scale, are presented, in parametric form as a result of cross-plotting, in Fig. 9, 10 and 11. These curves, it should be pointed out, represent a summary of the results obtained from 29 configurations most of which have 24 blades. An interesting feature of Fig. 9 is that a slightly improved performance was obtained at a solidity, σ, of 0.660 by reducing the blade aspect ratio (AR) by a factor of 2. The blade aspect ratio reduction was achieved by using 12 blades each of which was twice the average chord of the 24 blades corresponding to twice the aspect ratio. Presumably the performance gain was due to a reduction in the blockage due to blade thickness dominating over the fundamental influences of aspect ratio; individual blade thickness was the same for both the 12 and 24 bladed rotors. It can also be seen from Fig. 10 that increasing rotor solidity has the expected effect of increasing starting torque.

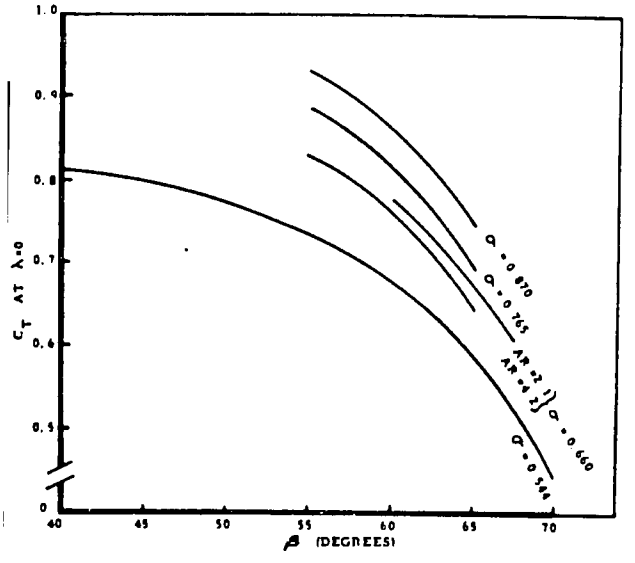

Fig. 10 Torque Coefficient at $\lambda = 0$ versus Blade Stagger Angle for Perry's Slatted Rotors.

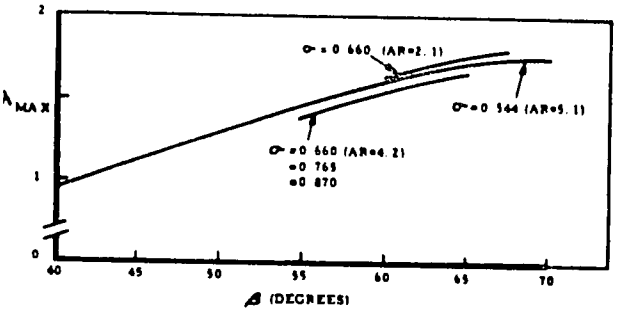

Fig. 11 Runaway Velocity Ratio versus Blade Stagger Angle for Perry's Slatted Rotors.

It can be noticed from Fig. 7 that the six timber spokes supporting Perry's rotor constitute a fairly substantial blockage in 6 of the 24 flow passages between the blades. Whilst for an all wood rotor Perry's construction, or something similar, appears to be essential a performance improvement could, it was thought, be obtained by the use of thinner metal spokes. A wind-tunnel test was conducted using a modified version of Perry's design which confirmed this expectation. The maximum power coefficient was increased by 28% by this means. However such a modification tends to defeat the advantages of an all wood construction.

PERFORMANCE COMPARISON

The performances of the best Cretian and slatted rotor configurations can be compared with each other, and with any other system, on the basis of power coefficient and torque coefficient provided account is taken of the differing velocity ratios of the units. Differences in velocity ratio can be accommodated by using, as an abscissa of the performance comparison curves the ratio, for each machine, of λ divided by λ_{max}. Hence the numerical value of this parameter ranges from zero to unity for all units. The influence of rotor speed on torque characteristics can also be accommodated by using ΛC_T in place of C_T where Λ is the value of λ for which C_p is a maximum. The ΛC_T parameter is, therefore, the torque obtained when the output torque is measured not at the rotor shaft but on an output shaft geared to the rotor shaft by frictionless gears. For a prescribed wind speed this ficticious output shaft runs at the same rotational speed for all units when each unit operates at its maximum power coefficient ie. at a velocity ratio $\lambda = \Lambda$.

Comparative performance curves for the Cretian and slatted rotors are presented on the C_p versus λ/λ_{max} and ΛC_T versus λ/λ_{max} planes in Fig. 12 and 13 respectively. Corresponding curves for another type of turbine, termed a delta-turbine, have been added to Fig. 12 and 13. The delta-turbine has previously been found to have one of the best overall performances of fixed-pitch water pumping windturbines which produce maximum torque at zero rotor speed in conjunction with a relatively high maximum power coefficient (4). It can be seen that both the Cretian and slatted rotors are less efficient, and produce lower torques, than the delta turbine (4). Curves have been added to Fig. 12 and 13 representing the performance of a Perry type optimized rotor modified for metal construction as distinct from wood.

By combining the results reported here with earlier information (4) it is possible to make a broader comparison of horizontal axis wind-turbines in the size range from 10 to 13' (3 to 4m) rotor diameter. For this comparison to be of most use to designers when selecting a rotor type, the relevant curves are presented on the $C_p \sim \lambda$ plane in the manner pioneered by Eldridge (5). Figure 14 is the $C_p \sim \lambda$ comparison chart from which diagram it can be seen that the Dutch designed SWD WEU-I-2 unit (1,4) gives the highest maximum C_p value. The next best value is due to the delta turbine (4). On a basis of starting torque, it can be shown that

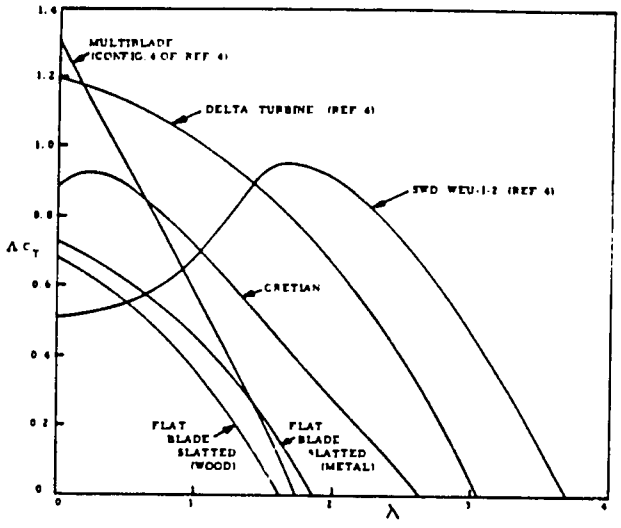

Fig. 15 Torque Characteristics Corresponding Fig. 14.

iv) a multibladed turbine, which is in effect a metal slatted turbine with cambered blades, gives a yet better performance

v) the delta-turbine gives the best results overall when attention is paid to both a high starting torque and a relatively high operational efficiency.

ACKNOWLEDGEMENTS

Tha author acknowledges the work of Ihor Kuzyk, a final year student in the Department of Mechanical Engineering, University of Calgary, who carried out the tests on the Cretian configurations. The writer is also grateful to Dan W. McKenzie of the U.S. Forest Service, San Dimas, California for drawing his attention to the work of Perry (6).

REFERENCES

1. Beurskens, H.J.M., Hageman, A.K., Hospers, G.D., Kragten, A. and Lysen, E.H., "Low Speed Water Pumping Windmills: Rotor Tests and Overall Performance", Proceedings, Third International Symposium on Wind Energy Systems, Paper K2, pp. 501-520, August 1980, (BHRA Fluid Engineering, Cranfield, Bedford, England).
2. Kentfield, J.A.C., "The Performance of Delta-Wing Bladed Wind-Turbines", Proceedings, 7th Australasian Hydraulics and Fluid Mechanics Conference, Brisbane, August 18-22, 1980 (Institution of Engineers of Australia, publication No. 80/4).
3. Fraenkel, P.L., "Food From Windmills", Intermediate Technology Publications Ltd., 9 King Street, London WC2E 8HN, England, Nov. 1975.
4. Kentfield, J.A.C., "A Performance Comparison of Various Wind-Turbine Types for Powering Water Pumps." Proceedings, 17th Intersociety Energy Conversion Engineering Conference, Los Angeles, 1982. IEEE Publications, pp. 2082-2088 (SAE Retrieval No. 829345).
5. Eldridge, F.R., "Wind Machines", Report Published by the Mitre Corporation for the National Sciences Foundation, Washington, D.C., 1975, pp. 55.
6. Perry, T.O., "Experiments With Windmills", United States Geological Survey, Government Printing Office, Washington, 1899.
7. Hawthorne, W.R. (Ed.), "Aeordynamics of Turbines and Compressors", (Vol. X, High Speed Aerodynamics and Jet Propulsion Series), Princeton University Press, Princeton, N.J., 1964, p. 481.